LUNG DISEASE IN THE CYSTIC FIBROSIS MUTANT MOUSE

Donald J. Davidson

Presented for the degree of PhD

University of Edinburgh

2000

Declaration

I declare that

a) this thesis has been composed by myself

b) that the work is my own, except where otherwise stated

Donald John Davidson

April 2000

Acknowledgements

I would like to thank my three supervisors, who have complemented each other perfectly. Thanks to David Porteous for gambling on a disillusioned medic and for his reassuring support, stimulation and gentle provocation, to Julia Dorin for her constant encouragement, positivity and nurturing, and to both of them for giving me a good enough reason (and a little push) to do my medical and surgical residencies. Thanks to John Govan for his infectious enthusiasm and confidence and to all three for their intellectual guidance and access to their combined wisdom.

Thanks to all those in the lab who have helped out with the work along the way: to Fiona for helping me make the primary culture system work, for several critical observations and for the introduction to Mars Bar profiteroles; to Gillian for collaborating all the way along and for being the ideal office mate in a variety of environments; to Gerry for helping with all the early mouse work and the Spanish wines; to Sheila Webb and the various tail-tippers for conscripting suitable wee participants for me; to Euan for being my immunohistochemical partner and a lesson in all things oblique; to Susannah for being an excellent summer student and overhauling my data analysis procedures; to Duncan for helping to start up the peptide studies (despite juggling in the hotel room); to David Sheppard for helping me to dabble in the mysterious art of electrophysiology; to Brendan for molecular assistance and Seattle hysteria; to Heather for regular advice, big smiles, big noise and manic energy; to Lorna for Reference Manager, reservations, envelopes, sellotape and for mothering us all; to Sheila Christie for keeping it all going, always making time and being good humoured when being repeatedly pestered; and to Kathy, Jane, Giorgia, Peter, Martin, John Maule, Julie, Paul, Stephanie, Barbie, Hazel, Chris, Mark, Ken, Tony and all the other West-wingers, old and new, for making it all such fun. Sorry to those I've forgotten to mention.

My thanks also go to all those in the HGU who weren't lucky enough to work in the West-wing, but helped me none the less: to Vince, Donald, Keith, Andy, Brendan and all the staff at the BRF and TU for taking such good care of the mice, for the top banter and for assisting me all the way; to Paul Perry for giving me the power to image and sorting it all out when I got in a mess; to Peter Teague for sharing his world of statistics; to Norman, Sandy and Douglas in Photography for all their assistance, often at short notice; to Siobhan in the Library for digging out the references and keeping an eye on pig hearts; to Al, John, Jenny and the rest of the Computing department for regular untangling, a superb service and the Mr Kipling memories; to Duncan and Len for constructing everything I came up with and for some cunning modifications, to the Admin department for keeping all the paperwork from us; to Stores for providing the ingredients; to Ruby and Adam for the Reception chat; to the HugeNuns for the challenge; and to Nick and the Social Committee for lots of fun, frustration and Unit cohesion.

A huge thank you to Wendy, Cathy, Alison, Jayne and Mike in Medical Microbiology for the bottles of bugs and all kinds of bacterial assistance over the years. Thanks also to my other collaborators: to Aurita, Phil, Mike, Joe, Jeff and Robert in Iowa for introducing me to airway primary cultures, electrophysiology, the big empty expanse in middle of the USA and (indirectly) the whirlpool bath; to John Findlay at King's Buildings for EM assistance and his bottomless repertoire of tales and jokes; to David Lamb for his help with the early histopathological assessments; to Bob, Kevin and Nicola at Albachem for successfully synthesising the peptides; to Michael, Burkhard, Ivo and Tomas in Hannover for sharing ideas and results, accents and sack races; to Bob, Johan, Inez and Lisa in Rotterdam for their suggestions, and the hospitality that made Rotterdam bearable; to Scott Randell at UNC for antibodies; and of course to the many mice, without whom this thesis would be rather slim.

Thanks to the Medical Research Council and the Cystic Fibrosis Trust for funding this research.

Thanks to my family and friends, particularly to Mum and Dad for always being there and supporting me in every way through Medical School. That MBChB has turned out to be useful. Who would have thought it. Finally, special thanks to Rebecca for all her love and support, for helping me survive my Residency, for help with the molecular biology and for saying "yes". Onward and upward, Vancouver here we come!

ABSTRACT

The discovery, in 1989, of the gene responsible for Cystic Fibrosis (CF), the cystic fibrosis transmembrane conductance regulator (*CFTR*), led to the development of mouse models of this disease. Such models were designed to facilitate the dissection of disease pathogenesis, to study the correlation between genotype and phenotype and to establish an invaluable resource for the development and evaluation of novel therapeutic agents. Fundamental to the success of such studies was the requirement that the mutant animals should develop the key phenotypic features of CF in humans. Initial characterisation of the first mouse models of CF demonstrated that they could be unequivocally distinguished from their wild type littermates and displayed many important disease features. However, the most important clinical consequence of CF, the development of chronic pulmonary infection with fibrotic lung damage, was not initially evident. In studies that preceded this thesis, we demonstrated an abnormal pulmonary phenotype in the Edinburgh CF mouse ($Cftr^{tm1Hgu}$ /$Cftr^{tm1Hgu}$), on an outbred MF1 background, in response to repeated exposure to CF related respiratory pathogens. These observations established this mouse as an important model system for studies aimed at elucidating the mechanisms involved in the development of CF lung disease. The aims of this thesis were 1) to further characterise lung disease in mouse models of cystic fibrosis, and 2) to study the mechanisms underlying the development of this disease.

Firstly, this thesis describes 1) the development and quantification of methods for the delivery of bacteria to the murine lung and 2) the analysis of the histopathological phenotype of mouse models of CF congenic on a C57Bl/6N background, in response to such techniques. These studies were performed using a clinical strain of *Staphylococcus aureus*, a pathogen that is characteristic of the early stages of lung infection in CF. The experiments addressed the null hypothesis that there was no difference between the

histopathological responses of 1) *Cftr*^{tm1Hgu} /*Cftr*^{tm1Hgu} mice or 2) *Cftr*^{tm1Hgu} /*Cftr*^{tm1Unc} compound heterozygote mice, and non-CF littermates. The results led to the following conclusions; a) mouse models of CF (*Cftr*^{tm1Hgu} /*Cftr*^{tm1Hgu} and *Cftr*^{tm1Hgu} / *Cftr*^{tm1Unc}) congenic on a C57Bl/6N background developed lung pathology in response to repeated exposure to nebulised *S. aureus,* b) significantly more severe pathology was observed in CF mice compared to non-CF littermate controls, c) the spectrum of disease observed in CF mice and non-CF littermates congenic on a C57Bl/6N background was narrowed in comparison to those on an outbred MF1 background, with wild type mice more severely affected, d) No difference was observed between the severity of disease in the *Cftr*^{tm1Hgu} /*Cftr*^{tm1Unc} mice in comparison to the *Cftr*^{tm1Hgu} /*Cftr*^{tm1Hgu} mice, implying that the reduction in background levels of wild type CFTR did not have a major influence upon the observed response to pathogen exposure, and e) assessment of the histopathology suggested an exaggerated response rather than abnormality in any one aspect of this response.

Until recently the mechanisms by which dysfunction of CFTR could lead to the development of characteristic CF lung pathology remained unclear. However, several compelling, and competing, hypotheses have been proposed, based largely on *in vitro* studies. This thesis also describes studies designed to complement the published research by utilising mouse models of CF and address the relevance of several of these theories in this model system.

It has been proposed that CFTR interacts directly with *P. aeruginosa* to internalise these bacteria into airway epithelial cells. It is postulated that this process plays a role in lung defence and is compromised in CF. This thesis describes preliminary *in vivo* studies addressing this mechanism in mouse models of CF. Although internalisation of *P. aeruginosa* was observed, no difference was demonstrated between *Cftr*^{tm1Hgu} /*Cftr*^{tm1Hgu} mice and non-CF littermates

Airway surface liquid (ASL) from primary cultures of human airway epithelial cells has been shown to display salt sensitive antibacterial activity, the dysfunction of which has been implicated in the pathogenesis of CF lung disease. Airway Beta Defensins have been demonstrated to constitute an important component of this defence system. This thesis describes studies to characterise mouse Beta Defensin-1 (mBD1) and contrast it with human Beta Defensin-1 (hBD1) and concludes that a) synthetic hBD1 and mBD1 both display salt-sensitive antibacterial activity, b) hBD1 may play a role in determining the spectrum of lung pathogens that characterise CF and the predilection of *P. aeruginosa* for the human CF lung, c) dysfunction of mBD1 in $Cftr^{tm1Hgu}$ /$Cftr^{tm1Hgu}$ mice may contribute to the lung phenotype observed in response to *S. aureus*, and d) the differences demonstrated between mBD1 and hBD1 may result in species specific profiles of bacterial susceptibility secondary to CFTR dysfunction. In order to complement these studies by performing analysis of native murine ASL this thesis describes the development and characterisation of a primary culture model of differentiated mouse tracheal epithelium, grown at air/ liquid interface. This model demonstrates confluent, polarised epithelium, with differentiation to produce ciliated and secretory cells, expression of *Cftr* and murine Beta Defensin genes and a characteristic electrophysiological profile.

Abbreviations used

5T	5-thymidine variant of the IVS8-T
7T	7-thymidine variant of the IVS8-T
9T	9-thymidine variant of the IVS8-T
°C	degrees centigrade
α_1AT	α_1-antitrypsin
µA	microamps
µCi	microcurie
µg	microgram
µl	microlitre
µm	micrometre
µM	micromole
aa	amino acid
Å	angstrom unit
A	adenine / amps
ABC	ATP-binding cassette
ADP	adenosine diphosphate
aGM_1	asialoganglioside 1
ASL	airway surface liquid
ATP	adenosine triphosphate
BAL	bronchoalveolar lavage
BALF	bronchoalveolar lavage fluid
B. cepacia	*Burkholderia cepacia*
Br^-	bromide ion
BSA	bovine serum albumin
C	cytosine
Ca^{2+}	calcium ion
CACC	Ca^{2+}-activated Cl^- currents
cAMP	cyclic adenosine monophosphate

CBAVD	congenital bilateral absence of the vas defrens
cDNA	complementary DNA
CF	cystic fibrosis
CFM1	CF modifier locus 1
CFTR	cystic fibrosis transmembrane conductance regulator
CFTR	cystic fibrosis transmembrane conductance regulator gene
Cftr	murine cystic fibrosis transmembrane conductance regulator gene
$Cftr^{tm3Bay}$	exon 2 replacement mouse model of CF, Baylor College of Medicine
$Cftr^{tm1Bay}$	exon 3 duplication mouse model of CF, Baylor College of Medicine
$Cftr^{tm1Cam}$	exon 10 replacement mouse model of CF, Cambridge University
$Cftr^{tm2Cam}$	ΔF508 mouse model of CF, Cambridge University
$Cftr^{tm1Eur}$	ΔF508 mouse model of CF, Erasmus University, Rotterdam
$Cftr^{tm1G551D}$	G551D mouse model of CF, University of Queensland, Australia
$Cftr^{tm1Hgu}$	exon 10 insertion mouse model of CF, Human Genetics Unit, Edinburgh
$Cftr^{tm2Hgu}$	G480C mouse model of CF, Human Genetics Unit, Edinburgh
$Cftr^{tm1Hsc}$	exon 1 replacement mouse model of CF, Hospital for Sick Children, Toronto
$Cftr^{tm1Kth}$	ΔF508 mouse model of CF, Kirk R. Thomas, University of Utah
$Cftr^{tm1Unc}$	exon 10 replacement mouse model of CF, University of North Carolina
cfu	colony forming units
Cl^-	chloride ion
CO_2	carbon dioxide

CPT-cAMP	8-(4-chlorophenylthio) adenosine 3′:5′-cyclic monophosphate
CPX	8-cyclopently-1,3-dipropylxanthine
DAPI	4,6-Diamidino-2-phenlyindole
dATP	deoxyadenosine triphosphate
dCTP	deoxycytosine triphosphate
Defb1	murine β-defensin-1 gene
Defb1	murine β-defensin-1
Defb2	murine β-defensin-2 gene
Defb2	murine β-defensin-2
Defcr	murine defensin gene cluster locus
DEPC	diethyl pyrocarbonate
dGTP	deoxyguanisine triphosphate
DHA	docosahexaenoic acid
DIOS	distal intestinal obstruction syndrome
DMEM	dulbecco's modified eagle medium
DMSO	dimethyl sulfoxide
DNA	deoxyribonucleic acid
dNTP	deoxynucleotide triphosphate
DTT	dithiothreitol
dTTP	deoxythymidine triphosphate
E. coli	*Escherichia coli*
EDTA	ethylenediaminetetraacetic acid
ELISA	enzyme linked immunoadsorbant assay
ENaC	amiloride sensitive epithelial sodium channel
ER	endoplasmic reticulum
ESR	erythrocyte sedementation rate
F_1	first generation offspring
F_2	second generation offspring, offspring of F_1 matings
FCS	foetal calf serum
FEV_1	forced expiratory volume in the first second

FITC	fluorescein isothiocyanate
g	relative centrifugal force / gram
G	guanine / gauge
GCH	goblet cell hyperplasia
GM_1	sialylated ganglioside 1
GSH	glutathione
GST	glutathione S-transferase
hBD-1	synthetic human beta defensin-1 peptide
HBD-1	human beta defensin-1
HBD-1	human beta defensin-1 gene
HBD-2	human beta defensin-2
HBD-2	human beta defensin-2 gene
HBE	human bronchial epithelial cell line
HBSS	Hank's balanced salt solution
HCO_3^-	bicarbonate
HEPES	N-2-hydroxyethylpiperazine-N'-2-ethanesulphonic acid
H. influenzae	*Haemophilus influenzae*
HNP	human neutrophil peptide
HNP	human neutrophil peptide gene
HPC	human placental collagen
Hprt	murine hypoxanthine phosphoribosyltransferase gene
HPLC	high performance liquid chromatography
I^-	iodide ion
IBMX	3-isobutyl-1-methyxanthine
IgG	immunoglobulin G
IL-6	interleukin-6
IL-8	interleukin-8
IL-10	interleukin-10
iNOS	inducible nitric oxide synthase
I_{sc}	short-circuit current
iu	international units

IVS8-T	intron 8 polypyrimidine tract
K^+	potassium ion
kb	kilobase
KC	chemokine-induced neutrophil chemoattractant KC
kDa	kiloDalton
L	litre
LAP	bovine lingual antimicrobial peptide
LAP	bovine lingual antimicrobial peptide gene
LPS	lipopolysaccharide
M	molar
Mb	mega-base
mBD-1	murine β-defensin-1
mBD-1	murine β-defensin-1 gene
mBD-3	murine β-defensin-3
mBD-3	murine β-defensin-3 gene
mBD-4	murine β-defensin-4
mBD-4	murine β-defensin-4 gene
MBL	mannose-binding lectin
MBL2	mannose-binding lectin gene
MDCK	Madin-Darby canine kidney cells
MEM	minimum essential media
MI	meconium ileus
MIP-2	macrophage inflammatory protein 2
mg	milligram
ml	millilitre
mm	millimetre
mM	millimolar
MMP	metalloproteinase
mRNA	messenger ribonucleic acid
MRSA	methicillin resistant *S. aureus*

MSD	membrane spanning domains
NBD	nucleotide binding domain
Na^+	sodium ion
NaCl	sodium chloride
NBF	neutral buffered formalin
NE	neutrophil elastase
NFκB	nuclear factor κB
ng	nanogram
NO	nitric oxide
oligo	oligonucleotide
ORCC	outwardly rectifying Cl^- channels
P. aeruginosa	*Pseudomonas aeruginosa*
PAS	periodic acid - schiff's stain
PBS	phosphate buffered saline
PCNA	proliferating cell nuclear antigen
PCR	polymerase chain reaction
PD	potential difference
PDC	poorly differentiated cells
$p(dN)_6$	random 6 base pair primers
PHA	pseudohypoaldosteronism
PI	pancreatic insufficiency
PKA	protein kinase A
PKC	protein kinase C
PNK	polynucleotide kinase
P_o	open probability
pS	pico-siemens
PS	pancreatic sufficiency
QTL	quantitative trait loci
R domain	regulatory domain
rhDNase I	recombinant human deoxyribonuclease I
RNA	ribonucleic acid

rpm	revolutions per minute
RSV	respiratory syncytial virus
RT	reverse transcriptase
RT-PCR	reverse transcriptase polymerase chain reaction
R_t	transepithelial resistance
S. aureus	*Staphylococcus aureus*
SCV	small colony variant
SD	standard deviation
SDS	sodium dodecyl sulphate
SEM	scanning electron microscopy
SLPI	secretory leukoprotease inhibitor
SP-A	surfactant protein A
SP-D	surfactant protein D
SPF	specified pathogen free
SSC	3 M sodium chloride/0.3 M sodium citrate
T	thymine
TAP	bovine tracheal antimicrobial peptide
TAP	bovine tracheal antimicrobial peptide gene
TBHQ	tert-Butylhydroquinone
TE	10 mM Tris.hydrochloric acid/1 M EDTA solution
TEM	transmission electron microscopy
TK	tyrosine kinase
T_m	melting temperature
TNF-α	tumour necrosis factor-α
Triton X-100	t-Octylphenoxypolyethoxyethanol
Tween	polyoxyethylenesorbitan
UTP	uridine triphosphate
UTR	untranslated region
UV	ultraviolet
V	volts
w/v	weight per volume

List of Tables

Chapter 1

Chapter 3

Chapter 4

Chapter 5

Chapter 6

Chapter 7

List of Figures

Chapter 1

Chapter 2

Chapter 3

Chapter 4

Chapter 5

Chapter 6

Chapter 7

List of Contents

Chapter 1

Introduction

Chapter 1: Introduction

1.1 Preface

In 1989 the gene responsible for Cystic Fibrosis (CF) was cloned and the predicted protein designated the cystic fibrosis transmembrane conductance regulator (CFTR). The ten years since that discovery have witnessed rapid progress in our understanding of this common genetic disorder. Progressively more detailed knowledge of the disease causing mutations, the gene expression patterns, the protein structure, its functions as an ion channel and as a conductance regulator, has allowed the development of reliable screening programmes, the creation of animal models and the design of novel therapeutic approaches. The biological basis of many aspects of the disease phenotype are becoming clearer, including recent significant advances in understanding the pathogenesis of the characteristic and ultimately fatal lung disease. While this great expansion of knowledge has started to bridge the gap between our understanding of the genetic defect and the well documented clinical sequelae, it has also served to demonstrate the mechanistic complexity of this "simple" single gene defect.

1.2 Cystic fibrosis – A clinical overview

1.2.1 Epidemiology

Cystic Fibrosis is the most common lethal autosomal recessive genetic disorder in Caucasian populations with a carrier frequency estimated at 1 in 29 and an incidence of about 1 in 3300 (National Institutes of Health

Developmental conference Statement on Genetic Testing for Cystic Fibrosis 1999). The disease also has a fairly high incidence amongst Hispanics but it is a rare disorder amongst native Africans and native Asians (see Table 1.1).

	Incidence Number / Total	Carrier Frequency Number / Total
Whites	1 / 3300	1 / 29
Hispanics	1 / 8000 - 9500	1 / 46
Ashkenazi Jews	1 / 3300	1 / 29
American Indians	1 / 1500 - 4000	1 / 19 – 1 / 32
African Americans	1 / 15300	1 / 60
Asian Americans	1 / 32100	1 / 90

TABLE 1.1 Incidence and carrier frequency of CF

The incidence and carrier frequency of CF in different ethnic populations in the USA, adapted from National Institutes of Health Developmental conference Statement on Genetic Testing for Cystic Fibrosis 1999.

1.2.2 Diagnosis

The diagnosis of CF was, for many years, made using the sweat test (Le Grys *et al* 1994, Quinton 1999). This protocol, designed to detect elevated sweat chloride levels in individuals with CF, was the gold standard for CF diagnosis, although false positives have been described in severe malnutrition, adrenal insufficiency and nephrogenic diabetes insipidus. However patients were identified with atypical presentations and intermediate sweat electrolyte levels in whom diagnosis of CF remained uncertain. An alternative diagnostic test is measurement of the nasal potential difference (Knowles *et al* 1981, Alton *et al* 1990). Alterations in

active ion transport across CF epithelia contribute to characteristic bioelectric profiles in CF individuals, which can be measured in the inferior nasal turbinates. This test has a high sensitivity, but may be influenced by the presence of nasal polyps, upper respiratory tract infections and previous nasal surgery. Since the cloning of the *CFTR* gene, a definitive diagnosis can now be offered to most patients by testing for the presence of mutations in CFTR. By combining detection of the most common mutations as appropriate for specific ethnic groups a mutation detection sensitivity of approaching 90% can be achieved in US whites and higher in some populations (National Institutes of Health Developmental conference Statement on Genetic Testing for Cystic Fibrosis 1999).

Criteria suggested for the clinical diagnosis of CF are shown in Table 1.2, requiring at least one criterion from class A and one from class B, with nasal potential difference measurements suggested as an additional tool where required (Kerem and Kerem 1995).

Class A
Typical pulmonary manifestations
Typical gastrointestinal manifestations
History of CF in the immediate family
Class B
Sweat chloride concentration > 60 mEq/L
Identification of two CFTR mutations

TABLE 1.2 Criteria for the diagnosis of CF
Adapted from Kerem and Kerem 1995.

The median age at diagnosis is 6 to 8 months. Almost two thirds of CF individuals are diagnosed before 1 year of age (National Institutes of

Health Developmental conference Statement on Genetic Testing for Cystic Fibrosis, 1999).

Screening for CF is performed using an assay of immunoreactive trypsinogen from a dried blood spot. At the present time, about 16% of neonates are screened for CF in the United Kingdom (Dodge 1999). Evidence of the value of such screening programmes remains controversial. One prospective controlled study in Wisconsin found that early diagnosis and treatment could prevent the decline in nutritional status that commonly affects CF children (Farrell *et al* 1997), while various health benefits have been reported using comparison with historical data (Dankert-Roelse and Te Meerman 1997). However, another prospective trial, carried out in Wales and the West Midlands, has found no evidence that screening *per se* has any major clinical benefit (Dodge 1999). Further studies are required to establish reliable data. However, many clinicians feel that the ability to institute specialised care and treatment early must be considered advantageous. This may prove particularly important in the future, given that the emphasis in much novel therapy development is on the prevention of disease progression rather than alleviation of symptoms.

1.2.3 Clinical manifestations and aetiology

CF is a multi-system disease with variable presentation. The classical phenotype is of salty sweat, pancreatic insufficiency, intestinal obstruction, male infertility and severe pulmonary disease.

These clinical manifestations reflect the tissue and cell specific expression pattern of *CFTR* (see section 1.3.7), being highly expressed in the sweat ducts, the pancreatic ducts, the digestive tract, the biliary ducts, the salivary glands, the reproductive organs and the airway submucosal glands.

Historically, this characteristic pathology has been ascribed primarily to the dysfunction of exocrine glands; producing viscid mucus, consequent mucus plugs and eventual organ destruction. However, since the cloning of *CFTR* it has become widely accepted that the fundamental defect in CF is not mucus production, but abnormalities of electrolyte transport in all affected epithelial tissues (reviewed in Quinton 1999). This defect results from the primary function of CFTR as a chloride ion channel and its secondary influences on other ion channels (see section 1.3.6).

In 1983, an abnormally high baseline transepithelial potential difference and anion impermeability was demonstrated in microperfused CF sweat ducts, when compared to those from non-CF subjects (Quinton 1983). This provided an explanation for the high salt content of CF sweat, in the form of a defect in ductal electrolyte absorption from the iso-osmotic fluid secreted in the acinar portion of the duct. It also demonstrated the presence of an electrolyte transport abnormality in the absence of morphological changes and independent of infection, inflammation or the effects of mucus. These studies thus provided the first description of the basic cellular defect that has now become recognised as the hallmark of the CF cell and underlies the abnormal electrophysiological profiles of affected tissues in CF. These bioelectrical abnormalities, reflecting alterations in the transport of chloride and sodium ions across the apical membrane of CF cells, have since been used extensively to characterise the electrolyte transport defects in affected organs in CF (reviewed in Anderson *et al* 1992).

Pancreatic lesions were amongst the first abnormalities to be documented in CF patients and prompted Andersen to use the term "cystic fibrosis of the pancreas" (Andersen 1938). Pancreatic insufficiency (PI) occurs in approximately 90% of patients with CF and shows a clear genotype/phenotype relationship (see section 1.3.4). Dysfunction is detectable at birth but the onset of signs of insufficiency is variable. Indeed, only 10% of residual pancreatic function is required to prevent malabsorption, with consequent malnutrition, steatorrhoea and failure to

thrive (Figarella and Carrere 1994). The typical pathogical features include mucus accumulation, ductal dilatation and obstruction with inspissated secretions, fibrosis and cyst formation. Progressive atrophy occurs with loss of acinar and ductal structures and the formation of scar tissue, separated only by isolated islets of Langerhans (Robbins and Kumar 1987). The explanation for this deterioration also lies in the dysfunction of fluid and electrolyte transport. The inhibition of fluid secretion in the pancreas results in abnormally concentrated macromolecules and a low volume output, with decreased HCO_3^- concentration. Consequently stagnation of proenzymes occurs with premature activation in the pancreatic ducts, causing progressive destruction (reviewed in Quinton 1999).

In addition to exocrine pancreatic insufficiency, approximately 50% of CF patients have impaired glucose tolerance, with overt diabetes occurring in roughly 10% (reviewed in Figarella and Carrere 1994). The incidence and prevalence of these conditions increases with age. Despite the fact that the pancreatic islands are relatively spared from the progressive fibrotic damage, this destructive process was considered to be responsible for the endocrine dysfunction. However, unlike the exocrine insufficiency, the endocrine dysfunction is unrelated to the CF genotype (Lanng *et al* 1991). It has, therefore, been suggested that it may not be a primary manifestation of CF.

The gastro-intestinal tract is also affected in CF (reviewed in Boat *et al* 1989). Meconium ileus, an obstruction of the small intestine with thick, dehydrated, mucoid material, occurs in 10-20% of CF individuals in the first few days of life and is virtually diagnostic. Its pathogenesis has been attributed to failure of enzyme secretion and the accumulation of undigested proteins *in utero*. However, an autopsy study of CF infants found no difference in the exocrine pancreas from those with or without meconium ileus, suggesting no relationship between pancreatic pathology and intestinal obstruction (Sturgess and Imrie 1981). This observation is supported by studies in mouse models of cystic fibrosis, in which intestinal obstruction occurs in the absence of pancreatic disease (see section 1.7.3).

Beyond the newborn period, the most common gastointestinal problem is distal intestinal obstruction syndrome (DIOS), occurring in 20% of patients. Similar to meconium ileus this is an obstruction of the terminal ileus with sticky, incompletely digested intestinal contents. With the exception of these intestinal obstructions, pathological changes in the intestinal tract are not prominent. Brunner's glands of the duodenum are hypertrophied, with ductal dilatation, mucus filled acini and an increased proportion of goblet cells. However there is little histopathological abnormality in the small intestinal mucosa, nor in the colon. Studies of the electrolyte abnormalities in the gut have demonstrated the increased sodium dependent glucose uptake and decreased secretory responses characteristic of the loss of CFTR chloride conductance (reviewed in Quinton 1999). It is these abnormalities that are considered to be fundamental to the intestinal manifestations in CF.

Hepatobiliary involvement may also occur in CF (reviewed in Boat *et al* 1989). Symptomatic biliary cirrhosis occurs in 2-5% of patients, but microscopic evidence of focal biliary cirrhosis is found in 25% of autopsies, with inspissation of secretions within the bile ducts, ductal dilatation, inflammation and fibrosis. Cholelithiasis is also observed, occurring in as many as 20% of CF patients.

Abnormalities of the genitourinary tract occur, presenting as azoospermia in over 95% of men with CF as a result of congenital bilateral absence of the vas deferens (CBAVD) (reviewed in Boat et al 1989). This tissue seems to be the most sensitive to CFTR dysfunction, with fibrotic, atrophic or absent vas deferens, epididymis and seminal vesicles. Only 2-3% of CF males are fertile, despite active spermatogenesis. Fertility in women with CF is higher at approximately 10%, but complicated by anovulation, secondary to poor nutrition or chronic lung infections. This low fertility rate may be attributable to the impediment to sperm caused by tenacious, cervical mucus, shown to be dehydrated and have abnormal electrolyte concentrations (reviewed in Boat et al 1989).

The most serious clinical manifestation is lung disease, which causes 90% of the morbidity in CF individuals and can severely compromised quality of life (National Institutes of Health Developmental conference Statement on Genetic Testing for Cystic Fibrosis 1999). Lung disease in CF is characterised by chronic microbial colonisation and repeated acute exacerbations of pulmonary infection, with distinctive bacterial flora, precipitating progressive, irreversible, inflammatory lung damage. Until recently the mechanism by which CFTR dysfunction could result in this pulmonary phenotype was not clear. However, recent studies have begun to bridge the gap between the development of airway disease and the genetic abnormality. Lung disease in CF will be considered in detail in section 1.4.

Since the cloning of the *CFTR* gene our understanding of the aetiology and cellular basis for the development of CF disease has progressed rapidly, incorporating the fundamental role of electrolyte transport abnormalities. However, this may not represent the whole picture. CFTR has been demonstrated to have functions other than its activity as a chloride channel, as discussed in section 1.3.6. In particular, a recent study has revived interest in the metabolism of essential fatty acids in CF (Freedman *et al* 1999). It suggests that a defect in lipid balance may occur as a direct consequence of CFTR dysfunction and play an important role in the expression of the disease.

1.2.4 Disease course and outcome

CF disease today has a very variable presentation and course. In some individuals serious gastro-intestinal problems and severe, early-onset pulmonary disease result in considerable morbidity, whereas others have relatively mild disease with presentation during adolescence and young adulthood. This variation appears to have both genetic and environmental

components and is discussed in later sections. As a result, outcomes vary from death due to complications of meconium ileus in the first few days of life or early death due to severe respiratory tract problems, through to mild, atypical symptoms in early adulthood and, rarely, a normal lifespan.

When first described in the 1930's (Anderson *et al* 1938), few CF children survived beyond 5 years. A combination of improved knowledge of the pathophysiology and recent advances in treatment has produced a dramatic improvement in prognosis. Median survival had increased to 18 years by 1976 and to 30 years by 1995 (National Institutes of Health Developmental conference Statement on Genetic Testing for Cystic Fibrosis 1999). However, there was little change in life expectancy between 1990 and 1995 and despite advances in therapy there remains no cure for CF.

1.2.5 Treatment

As our understanding of the molecular and biological basis of CF becomes more comprehensive, the goal of successful treatments becomes more accessible. New insights into the disease pathogenesis create opportunities for novel therapeutic interventions while also revealing the limitations of current treatments. Table 1.3 details the array of therapies now in use, or in development.

The major goals of traditional therapies have been to alleviate the pulmonary, gastrointestinal and pancreatic manifestations of the disease (reveiwed in Ramsay 1996).

Treatment of the airways has focused upon: 1) clearance of airway secretions, using chest physiotherapy with postural drainage, 2) antibiotic therapy; a) for the treatment of exacerbations of pulmonary infection, and b) as maintenance therapy designed to decrease bacterial colonisation, reduce the frequency of exacerbations and slow the disease progress, and 3) anti-

inflammatory drugs to minimise the inflammatory cascade and consequent lung damage. The value of bronchodilator therapy as an additional approach is more controversial, but is also considered. A more recent addition to therapy protocols is the use of inhaled purified, recombinant human deoxyribonuclease I (rhDNase I). This can be used to break down break down extracellular neutrophil DNA, reducing the viscoelasticity of sputum from CF patients and increasing mucus "clearability".

Treatment of the gastrointestinal and pancreatic systems has revolved around the use of pancreatic enzyme supplementation, to improve digestion, and high protein-energy diets with fat-soluble vitamins to maintain good nutrition.

Problems	Solutions	Treatments
Mutation of *CFTR*	♦ Provide normal gene ♦ Overcome stop mutations	♦ Gene therapy ♦ Aminoglycosides
Abnormal processing of CFTR	♦ Relocalisation	♦ Molecular chaperones
Defective CFTR	♦ Upregulate Function	♦ Pharmacological agents
Abnormal ion transport	♦ Increase chloride transport ♦ Block sodium uptake	♦ UTP ♦ Amiloride
Abnormal fatty acid balance	♦ Correct imbalance	♦ Fatty acid therapy
Thick obstructive mucus	♦ Decrease viscosity	♦ Mucolytics ♦ DNase
Impaired clearance	♦ Augment clearance	♦ Chest physiotherapy
Pulmonary infection	♦ Decrease bacterial load	♦ Antibiotics ♦ Salt-insensitive antimicrobial peptides
Pulmonary inflammation	♦ Diminish host reaction	♦ Anti-protease
Bronchiectasis	♦ Replace when irreversible damage	♦ Lung transplant

TABLE 1.3 Therapeutic approaches for CF lung disease

Adapted from Davidson and Porteous 1999.

The use of aggressive regimen incorporating these treatment mainstays has been responsible for the improvements in survival achieved thus far. However, novel approaches are required to make further increases in the life expectancy, while also aiming to improve quality of life rather than simply to alleviate symptoms. Thus, while there is a continuing need for the development of new antimicrobial agents, mucolytics and antiproteases, novel solutions are being sought in the new genetic knowledge (reviewed in Zeitlin 1999). These approaches include 1) the use of aminoglycosides to overcome stop mutations at the protein translational level, by suppressing termination, resulting in a full length CFTR, 2) relocating mutant CFTR to the apical surface by the modulation of chaperone protein associations, using butyrate compounds, or correcting the trafficking defect using chemical chaperones such as glycerol, 3) upregulating the function of correctly localised mutant CFTR, using compounds such as Genistein or CPX (8-cyclopently-1,3-dipropylxanthine), 4) compensatory regulation of alternative ion channels, by inhibiting sodium absorption using amiloride or stimulating chloride secretion through pathways that are not dependent upon cAMP, such as using UTP (Uridine triphosphate) to activate a P_2 purinergic receptor, 5) fatty acid replacement therapy with Docosahexaenoic acid (DHA) based product to address the apparent fatty acid imbalance, and 6) gene therapy, to directly replace the faulty gene. This final approach is possibly the most exciting novel therapy to have been borne from the new genetic knowledge, with the potential to correct all the downstream consequences that arise from CFTR dysfunction at once. However, initial enthusiasm has been tempered by a more realistic assessment of the many barriers to successful gene therapy, using both viral and non-viral based approaches, that have been revealed in the course of phase 1 trials (reviewed in Porteous and Innes 1999, Boucher 1999, and Welsh 1999). The problems faced in delivering gene therapy as a treatment for CF and some of the possible solutions are summarised in Table 1.4.

Further development of animal models and continuing basic research into the cellular and molecular biology of CF is essential for the analysis and optimisation of these novel therapies and to establish improved surrogate markers of clinical relevance.

Problems	Solutions
Inefficient gene delivery	♦ Improved vectors and delivery devices
Inflammatory response to vector	♦ Engineering and formulation of viral vectors and liposomes
Lack of cell specific targeting	♦ Viral subtypes ♦ Receptor mediated cell targeting
Transient expression	♦ Episomal maintenance ♦ Safe site integration ♦ Transfect stem cells
Non physiological expression	♦ Genomic context vectors ♦ Cell specific expression

TABLE 1.4 Challenges in gene therapy for CF
Adapted from Davidson and Porteous 1999.

1.3 The cystic fibrosis transmembrane conductance regulator

1.3.1 The cloning of the gene

The gene responsible for CF; the cystic fibrosis transmembrane conductance regulator (*CFTR*) gene, was cloned in 1989 (Rommens *et al* 1989, Riordan *et al* 1989, Kerem *et al* 1989). Located on the long arm of human chromosome 7, it was originally estimated to span over 250 kb, however, recent genomic sequencing indicates that it spans ~189kb (Ellsworth 2000). It contains 27 exons and encodes a 1480 residue transmembrane glycoprotein.

1.3.2 CFTR protein structure and function

The protein structure, proposed in 1989, was based upon comparison with members of the ATP-binding cassette (ABC) transporter family to which CFTR belongs (Riordan *et al* 1989). This model has proven to be remarkably accurate (Figure 1.1). CFTR consists of two repeated motifs, made up of six membrane spanning domains (MSD) and a nucleotide binding domain (NBD), separated by a regulatory domain (R domain).

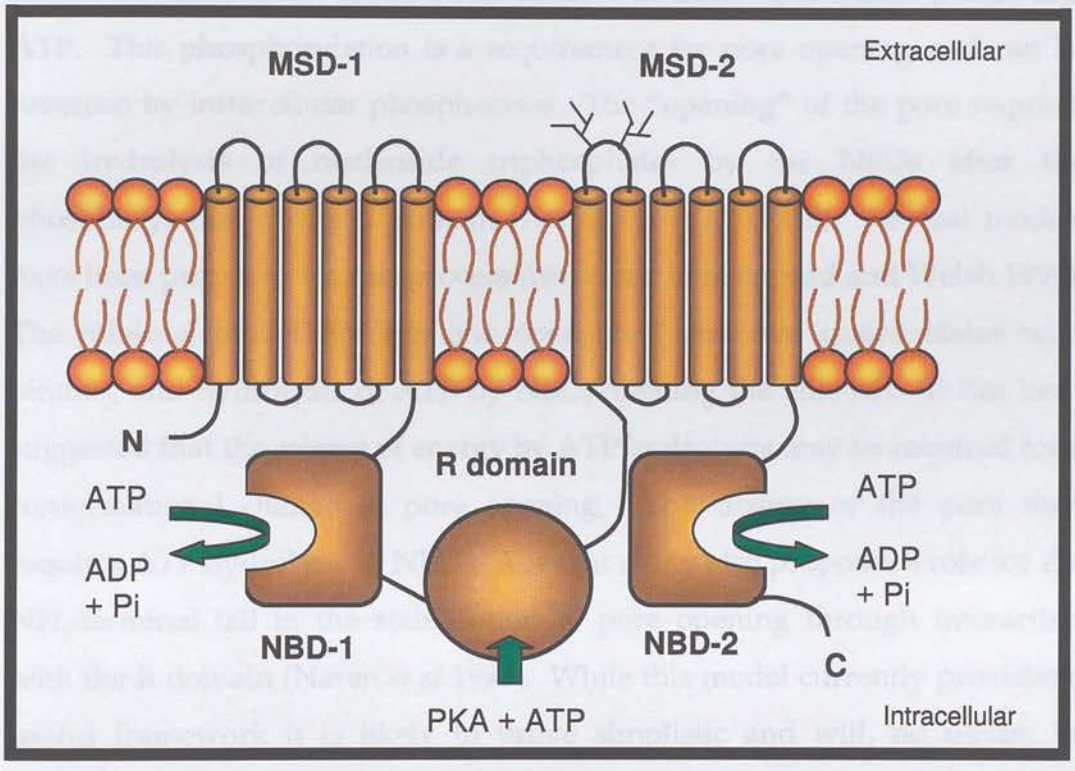

FIGURE 1 A model of the proposed structure of CFTR
Adapted from Sheppard and Welsh 1999.

Site directed mutagenesis studies targeting the membrane spanning domains (MSD) have been shown to alter the conduction and permeation

properties of CFTR, suggesting that these domains form a pore in the cell membrane. This pore is proposed to have a diameter of ~5.3-6 Å at its narrowest point, with larger vestibules on either side (reviewed in Sheppard and Welsh 1999). Studies suggest that this pore is kept "closed" by the R domain in its unphosphorylated state (reviewed in Gadsby and Nairn 1999). The R domain has 10 dibasic consensus phosphorylation sites, at least 5 of which are used *in vivo*. Phosphorylation at these sites, by cAMP dependent protein kinases (PKA and PKC), appears to have two effects; firstly permissive, perhaps releasing steric inhibition, and secondly stimulatory, facilitating interaction between the nucleotide binding domains (NBD) and ATP. This phosphorylation is a requirement for pore opening and can be reversed by intracellular phosphatases. The "opening" of the pore requires the hydrolysis of nucleoside triphosphates by the NBDs after the phosphorylation of the R domain (Anderson *et al* 1991b). Several models have been proposed for this process (reviewed in Sheppard and Welsh 1999). The minimal model predicts one open state and two closed states with binding and hydrolysis of ATP by NBD_1 opening the channel. It has been suggested that the release of energy by ATP hydrolysis may be required for a conformational change in pore opening. The closure of the pore then requires ATP hydrolysis at NBD_2. A recent study also proposes a role for the NH_2-terminal tail in the stabilisation of pore opening through interaction with the R domain (Naren *et al* 1999). While this model currently provides a useful framework it is likely to prove simplistic and will, no doubt, be revised further in the light of future discoveries. One area of current controversy affecting such models debates whether or not CFTR functions as a monomer. Biochemical data supports the view that CFTR functions as a monomer in the cell membrane, sedimented as a monomer using sucrose density gradients (Ostedgaard and Welsh 1992). However a recent study suggests that two CFTR molecules interact together to from a single pore (Zerhusen *et al* 1999). This could have important consequences for our

understanding and modelling of CF, particularly with regard to compound heterozygote and heterozygote status.

To confirm the function of CFTR as an apical membrane chloride channel, studies using recombinant CFTR were performed. The expression of CFTR was shown to generate cAMP-regulated chloride channels in cells that did not normally contain such channels or express endogenous CFTR (Anderson *et al* 1991a). Furthermore, the properties and regulation of these channels was shown to be similar to that of native CFTR in epithelial cells, with the following features; 1) a small single channel conductance (6-10 pS), 2) a linear current-voltage relationship, 3) selectivity for anions over cations, 4) an anion permeability sequence of $Br^- \geq Cl^- > I^-$, 5) activity regulated by cAMP-dependent phosphorylation and the hydrolysis of nucleoside triphosphates (reviewed in Welsh 1996). Mutation of specific residues in CFTR was shown to alter the ion selectivity of CFTR (Anderson *et al* 1991a). Finally, analysis of purified CFTR reconstituted in planar lipid bilayers demonstrated its function as a cAMP-regulated chloride ion channel protein with properties identical to those in native epithelium (Bear *et al* 1992).

Thus CFTR functions as a PKA- and ATP-regulated chloride channel, the gating processes of which involve the interaction of its cytosolic domains. In the absence of functional CFTR there is a failure of chloride ion transport at the sites of CFTR localisation.

1.3.3 Mutations in CFTR

Since the isolation of the *CFTR* gene there have been over 800 different mutations identified (National Institutes of Health Developmental conference Statement on Genetic Testing for Cystic Fibrosis 1999). Analysis of these reveal that about 50% are missense mutations, 20% are frame shift mutations caused by small insertions or deletions and 15% are nonsense

mutations. The remainder are splice site mutations and other variations (Kerem and Kerem 1996). There are several mutation hotspots with a high concentration of the more common mutations occurring in NBF_1 (reviewed in Tsui *et al* 1992). The most common of these is the ΔF508 mutation. This is a 3 base pair deletion, between 1652 and 1655 in exon 10, which removes phenylalanine 508 from NBD_1. It accounts for 70% of the mutant alleles in the caucasian population and for large portions of the alleles in other racial/ ethnic groups (Table 1.5). Only a handful of others are common (>1% of the total) but some of these are significantly enriched or depleted in specific ethnic populations. The vast majority of mutations are very rare. While these constitute a challenge to the clinical geneticist with respect to molecular diagnosis, they are also of considerable valuable in studies that seek to link protein structure to function and genotype to phenotype.

Group	% ΔF508	% common white alleles	% group specific alleles
Whites	70	13	-
Hispanics	46	11	-
Ashkenazi Jews	30	67	-
American Indians	0	25	69
African Americans	48	4	23

TABLE 1.5 CF mutations in specific ethnic groups

Adapted from National Institutes of Health Developmental conference Statement on Genetic Testing for Cystic Fibrosis 1999

Different mutations can cause different defects in the production and function of CFTR (see Figure 1.2).

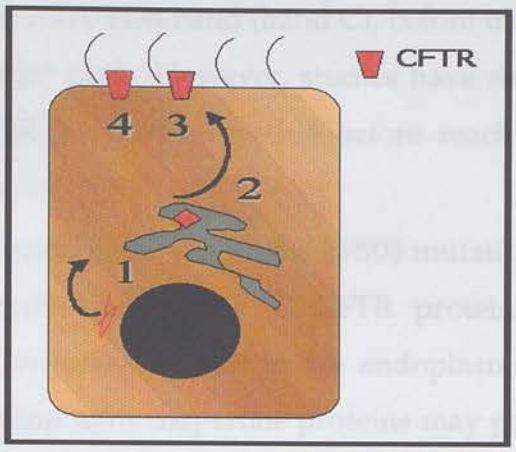

FIGURE 1.2 CFTR mutations classes 1 to 4

These mechanisms have been classified into five groups as described below (Welsh 1996):

Class 1 mutations:- Defective protein production.

The mutations in this group result in premature termination signals and protein truncation. Some cases, such as R553X, result in unstable mRNA and no detectable protein, in others unstable truncated proteins may be produced.

Class 2 mutations:- Defective protein processing.

These mutations have been shown to result in a failure to traffic CFTR to the correct cellular location. This group includes the most common mutation ΔF508 and the G480C mutation.

Studies have shown that CFTR progresses through several stages of glycosylation (Cheng *et al* 1990). This maturation can be observed by analysis of purified CFTR on an SDS-polyacrylamide gel. Nascent, non-glycosylated CFTR is observed as a 130 kDa band (band A), this is processed in the endoplasmic reticulum, to its core glycosylated form, detected as a 135 kDa band (band B). Wild type CFTR is then transported to the Golgi apparatus where it will undergo complex glycosylation resulting in mature

CFTR, observed as a 170 kDa band (band C), before transportation to the cell membrane and other sites. However, studies have shown that the majority of wild type CFTR becomes degraded before reaching the band C form (Cheng *et al* 1990).

In cells expressing CFTR with the ΔF508 mutation, band B protein fails to mature to produce any band C CFTR protein (Cheng *et al* 1990). Mechanisms are proposed to exist in the endoplasmic reticulum, whereby prolonged association with chaperone proteins may prevent the transport of mutant/misfolded/incorrectly complexed protein for further processing. The mutant protein is instead degraded in the endoplasmic reticulum by the ubiquitin-proteasome system (reviewed in Kopito 1999).

However, under permissive conditions *in vitro*, such as reduced temperature (Denning *et al* 1992), correct processing and localisation of mature protein can occur. Correction of the trafficking defect for class 2 mutations can allow the mutant CFTR to reach the apical membrane where it can demonstrate chloride channel function. This function can be comparable to wild type CFTR, in the case of G480C (Smit *et al* 1995), or, in the case of ΔF508, sub-optimally with between 30% (Denning *et al* 1992) and 100% (Li *et al* 1993) of normal wild type activity reported.

A considerable body of research supports this model for the dysfunction of CFTR containing class 2 mutations. However, the studies have been performed almost entirely in heterologous model systems and doubts exist about extrapolation to the *in vivo* situation. In a recent study immunohistohemical analysis was used to examine the localisation of both wild type CFTR and protein containing the ΔF508 mutation in tissue samples (Kälin *et al* 1999). The results suggested a tissue specific variability in the impact of this mutation on the expression and localisation of CFTR. Further studies are required to confirm and explain these findings

Class 3 mutations:- Defective Regulation

The mutations in this category, such as G551D, have less impact on the

processing and localisation of CFTR. Some of the mutant protein becomes correctly localised but defective regulation of chloride channel activity results in very little residual function. These proteins show little response to agonists under physiological conditions.

Class 4 mutations:- Defective Conduction

Mutations occurring in the putative membrane spanning domains, such as R117H and R334W, result in substantially reduced levels of ion transport, These mutant proteins are correctly processed, localised and regulated, but show reduced single channel conductance and a lower open state probability.

Class 5 mutations:- Reduced levels of normal RNA or protein

This category encompasses mutations that alter the quantity of normal mRNA and protein, such as the 5-thymidine (5T) variant of the intron 8 polypyrimidine tract (IVS8-T). This mutation results in alternative splicing of *CFTR* mRNA and gives rise to two transcripts; one normal and one with an in frame deletion of exon 9 (Chu *et al* 1992). The protein product of the latter is devoid of cAMP activated chloride conductance activity. The level of normal transcript has been shown to be tissue specific (Rave-Harel *et al* 1997) and to be dependent upon the associated IVS8-T. The 5T variant is associated with the lowest levels, these are increased with the 7T variant and highest with the 9T variant (Mak *et al* 1997).

In each class of mutation when the level of functional CFTR at the apical membrane of epithelial cells in CF patients falls below a critical level this results in the characteristic clinical abnormalities in the organs in which *CFTR* is expressed.

1.3.4 The genotype – phenotype relationship

Understanding the relationship between genotype and phenotype has obvious diagnostic and therapeutic implications. It can prove informative in determining the pathophysiology of the disease and the prospects for novel interventions. It is also critical in the design and interpretation of model systems

Mutations in *CFTR* are usually classified as either "mild" or "severe" dependent upon whether they confer pancreatic sufficiency (PS) or pancreatic insufficiency (PI).

Assessing the severity of mutations with reference to the classification described in section 1.3.3, those in classes 1 to 3 are generally "severe", while those in classes 4 and 5 tend to result in "mild" mutations (Durie *et al* 1999). The common ΔF508 mutation is classified as "severe", conferring pancreatic insufficiency. It is also associated with meconium ileus in approximately 10% of affected neonates. Although the G551D mutation is also "severe" and confers pancreatic insufficiency, it is observed to be associated with a much lower incidence of meconium ileus. R117H is a "mild" mutation, and is generally associated with pancreatic sufficiency. Despite these differences all three mutations are associated with infertility and lung disease. In contrast, the 5T mutation shows partial penetrance and a wide variability in disease expression. Individuals homozygous for the 5T allele have been documented to be asymptomatic despite expressing as little as 8% of normal CFTR in some tissues (Chu *et al* 1992). In other instances these individuals present with congenital bilateral absence of the vas deferens (CBAVD), but no other symptoms associated with CF.

This relatively clear relationship between genotype and phenotype demonstrated in the pancreas does not apply to all the affected systems (The Cystic Fibrosis Genotype-Phenotype Consortium 1993). In particular the severity of lung disease does not show a clear genotype correlation.

However, one study reported that ΔF508 heterozygotes with the second CF allele in the NBD-encoding exons has an increased risk of acquiring *P. aeruginosa* infection early in life (Kubesh *et al* 1993).

The relationship between genotype and phenotype is of course further complicated by compound heterozygosity and/or the presence of more than one mutation on the same allele. The presence of one "mild" allele will result in pancreatic sufficiency. Thus the "mild" allele appears to confer a dominant effect over the "severe" allele (Durie *et al* 1999). Individuals carrying the R117H allele are typically more severely affected if the R117H mutation is in *cis* with the 5T polymorphism as opposed to the 7T variant. This is probably because the associated IVS8-T will affect the quantity of already functionally impaired CFTR that is correctly spliced (Estivill *et al* 1996).

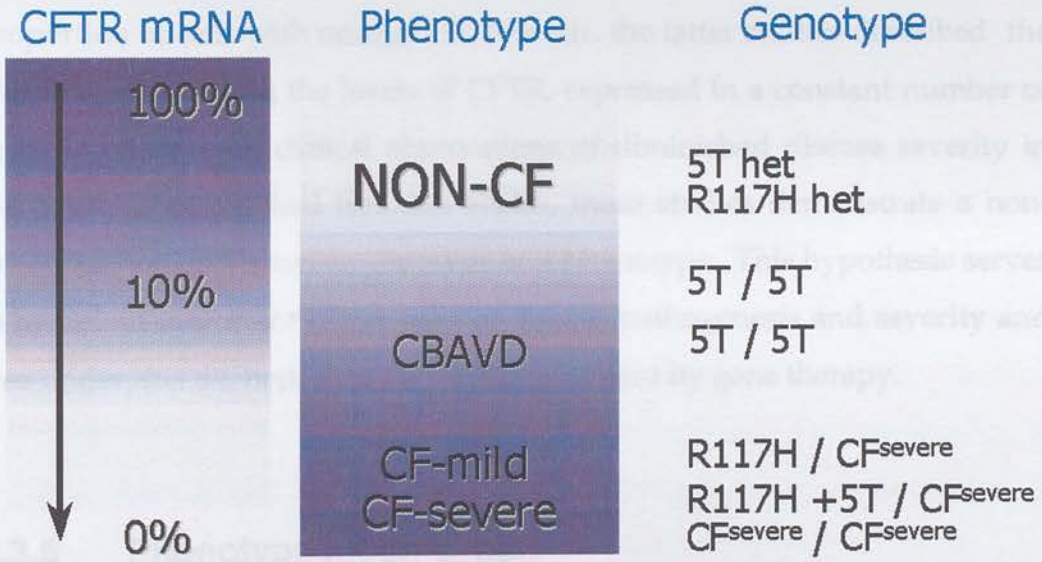

FIGURE 1.3 The effect of alterations in the quantity and quality of CFTR
Adapted from Estivill *et al* 1996.

Thus it is clear that the disease phenotype can be affected by alterations in both the quantity and the quality of CFTR (see Figure 1.3). Furthermore, the clinical characteristics of the disease may relate to the sensitivity of specific organs to CFTR dysfunction and tissue specific effects may impact upon the manifestation of identical mutations in different tissues.

The effects of alterations in the quantity of CFTR also help to address the important question of how much functional CFTR is required for therapeutic benefit. In studies using mixed epithelial cell monolayers of CF and non-CF cells, the results have suggested that functional CFTR is only required in approximately 10% of cells to restore chloride ion transport to normal (Johnson *et al* 1992). In contrast, the relationship between the proportion of CF cells and the level of sodium absorption is linear. Further work with transgenic CF mice (see section 1.7.3.1) broadly supports the non-linear relationship between CFTR levels and chloride transport *in vivo* (Dorin *et al* 1996). However, while the former studies examined variation in the proportion of cells with normal CFTR levels, the latter studies described the effects of variation in the levels of CFTR, expressed in a constant number of cells. Together with clinical observations of diminished disease severity in the presence of residual function alleles, these studies demonstrate a non-linear relationship between genotype and phenotype. This hypothesis serves to model an important component of disease pathogenesis and severity and also underpins the hopes for successful treatment by gene therapy.

1.3.5 Phenotype modification

While studies examining specific mutations and levels of functional CFTR can begin to explain some aspects of phenotype, this only provides a

partial explanation. The clinical phenotypes of individuals carrying identical mutations in CFTR can still demonstrate substantial variation.

CF is a single gene disorder in which all individuals inheriting two mutated alleles of the *CFTR* gene will manifest classical disease symptoms and pathology. This statement is broadly correct, although individuals with only class 5 mutations in both alleles (see section 1.3.3) may be diagnosed as having CBAVD rather than CF. Nevertheless, any disease process may be affected by environmental factors and by mutations in other genes that can impact upon related systems or processes. The latter influence is that of independently segregating phenotype modifier genes.

Mouse models of CF are a valuable resource in which to study these factors because of the ability to control both the environment and the genetic cross. In this manner it has been possible to compare the effect of specific CFTR mutations on different inbred strains and search for genetic modifiers of disease (see section 1.7.4). The first such modifier locus was identified in 1996, on the proximal region of mouse chromosome 7. This locus was shown to modify the onset and severity of intestinal pathology and survival (Rozmahel *et al* 1996). The region shows conserved synteny with human chromosome 19q13, and led to the detection of a modifier locus (CFM1), at 19q13.2, for meconium ileus but not pulmonary function (Zielenski *et al* 1999). It had been suggested that this modifier could take the form of a calcium dependent chloride channel that may be able to partially compensate for the absence of CFTR and alleviate the symptoms. However, no such candidate gene has yet been discovered at this locus. Further studies to establish genetic modifiers for pulmonary pathology in mouse models of CF are ongoing (see section 1.7.4) (Haston *et al* 1999, Innes and Dorin 1999).

A recent study investigating pulmonary phenotype modifiers in humans reported an association between mannose-binding lectin gene (*MBL2*) heterogeneity and the severity of lung disease and survival in CF (Garred *et al* 1999). Mutations in *MBL2*, and/or its promoter, result in decreased serum levels of MBL, a serum protein that forms part of the innate

immune defence (see section 1.6.2.5). These mutations are shown to correlate with life expectancy, the rate of pulmonary deterioration in CF individuals, (particularly in response to infection with *P. aeruginosa*) and perhaps susceptibility to *B. cepacia*.

Further insights may come from phenotype comparison of individuals with the same genotype and ethnic background in very different environments and from studies of CF twins with age matched siblings in similar environments and with the same *CFTR* genotype. A European study of this kind is currently underway (Bronsveld *et al* 1998).

Thus, independently segregating genes modify the effects of CFTR dysfunction in different tissues and are responsible for some of the phenotype variability observed. However, it is likely that environmental influences also play an important role in disease pathogenesis, particularly in the development of lung disease. A more thorough understanding of phenotype determinants will no doubt require the resolution of a complex series of interactions between specific mutation effects, genetic modifiers and environmental stimuli. Animal models of disease have great potential in the pursuit of this knowledge. However, in order to realise this potential, it is critical that the role of all of these phenotype determinants is appreciated and that consideration in given to the limitations of every model system.

1.3.6 Other roles for CFTR

Although the primary defect in CF is the failure of chloride transport, there is evidence that CFTR also acts as a conductance regulator, influencing the activity of other ion channels. It has been proposed that CFTR is involved in the regulation of ENaC activity, the function of outwardly rectifying Cl^- channels (ORCC) and the transport of ATP. In addition

intracellular CFTR has been proposed to influence exocytosis, endocytosis and the acidification of intracellular organelles.

In normal airway epithelium the dominant ion transport activity is the absorption of sodium ions by ENaC. The addition of amiloride will block this activity, with the remaining current being Cl^- secretion, induced by the resultant hyperpolarisation of the apical membrane and voltage clamping. It is worth noting, however, that *in vivo* (and in the absence of amiloride, under open-circuit conditions) the transepithelial gradient for Cl^- movement is absorptive. In CF epithelia there is an increase in the basal Na^+ absorption and a decrease in amiloride resistant current (Boucher 1994).

In vitro studies, using transfected Madin-Darby canine kidney (MDCK) cells (Stutts *et al* 1995) and lipid bilayers (Ismailov *et al* 1996), have demonstrated that CFTR can regulate the activity of ENaC in these systems. These studies have shown that in the absence of CFTR the basal rate of Na^+ transport by ENaC is enhanced and can be further stimulated by cAMP. However in the presence of wild type CFTR there is a decrease in the single channel open probability (P_o) of ENaC and an inhibitory effect with the addition of cAMP. A study utilising the yeast two hybrid system has suggested a direct protein interaction between the C-terminal end of the α-subunit of ENaC and a domain of wild type CFTR incorporating NBD_1 and the R domain may be critical for this interaction (Kunzelmann *et al* 1997). However, the underlying mechanism is unresolved.

In contrast to these studies, recent research using isolated sweat ducts demonstrated that ENaC activity was dependent upon, and increased with, the activity of CFTR (Reddy *et al* 1999). It has been suggested that the absorptive cells in the airway epithelium may behave in the same way as the sweat duct. However, because the airway epithelium contains both absorptive and secretory cells, the net effect of diminished absorptive transport and loss of secretory transport may appear as a net increase in sodium absorption in CF airways.

The role of ENaC and the transport of Na^+ ions may be of considerable significance in the pathogenesis of CF lung disease and will be seen to be fundamental to the hypotheses concerning the composition and function of the airway surface liquid (ASL) (see section 1.5.1).

CFTR has also been demonstrated to have a regulatory role in the activity of ORCC (reviewed in Schweibert *et al* 1999). The stimulation of ORCC requires the PKA- and ATP-dependent activation of CFTR and the transport of ATP across the cell membrane. This extracellular ATP then acts as an agonist, via purinergic receptors to stimulate ORCC activity. The release of extracellular ATP in the absence of active CFTR is not adequate for the activation of ORCC. Thus an additional role for CFTR involving direct interaction with ORCC is proposed. Whether the role of CFTR in the transport of ATP is direct, as an ATP channel, or indirect, as a regulator of ATP transport, is yet to be resolved. However, the results of various studies, including the demonstration that CFTR in lipid bilayers does not possess intrinsic ATP channel activity (Li *et al* 1996), suggest that CFTR plays an indirect role in this process. It has been suggested that CFTR may also influence the activity of Cl^- channels from the ClC family and Ca^+-dependent chloride channels. In this manner CFTR may promote the transport of Cl^- ions not only through its intrinsic Cl^- channel activity, but also through regulatory interactions with other apically localised ion channels.

The intracellular localisation of CFTR has been studied using immunological and functional approaches. While care must be taken over the interpretation of results where overexpression of CFTR and heterologous systems have been used, these suggest the presence of CFTR in the Golgi, ER and in sub-apical clathrin-coated vesicles (reviewed in Bradbury 1999). This is perhaps not surprising, given the requirement to traffic CFTR to the apical membrane. However, various studies suggest that CFTR is not simply in transit, but has functional significance at these sites.

In studies performed using CF and non-CF salivary glands, from both humans (McPherson *et al* 1986) and mouse models of CF (Mills *et al* 1995), a

failure of exocytosis was demonstrated in the CF tissues. This defect was manifest in the CF tissues as a decrease in mucin and amylase release in response to cAMP agonists, in comparison to non-CF samples. Further studies using cell lines have demonstrated that endocytosis and exocytosis are co-ordinately regulated by cAMP in the presence of functional CFTR, but not CFTR carrying clinical mutations. This effect on membrane recycling results in increased exocytosis and decreased endocytosis in response to raised levels of cAMP (Bradbury *et al* 1992).

These results have led to the hypothesis that CFTR may modulate the traffic of membrane vesicles. Furthermore, CFTR may regulate exocytic insertion of itself into the plasma membrane upon appropriate cellular stimulation, with recycling and endocytic retrieval after the removal of such stimuli. This hypothesis may be of significance to the pathogenesis of lung disease, with particular relevance to the possible internalisation of *P. aeruginosa* (see section 1.5.2.2) and the secretion of components of the innate lung defence (see section 1.6) by epithelial cells.

It has also been suggested that CFTR may be responsible for chloride transport across the membranes of intracellular organelles. Dysfunction of CFTR has been shown to result in defective acidification of these organelles (Barasch *et al* 1991). This has the potential to produce a myriad of secondary effects by altering the processing other glycoproteins in the Golgi apparatus, including the pattern of sulphation, sialylation and fucosylation. These changes could be of significance in the pathogenesis of CF lung disease, having the potential to create increased sites of adherence for respiratory pathogens (see section 1.5.2.1). However, more recent studies have produced conflicting results, finding no evidence of changes in organelle pH in CF cells (Seksek *et al* 1996, Chandy *et al* 1999).

These secondary defects serve to remind us of the complexities of the physiological processes in which CFTR is involved and the gaps in our knowledge. The role that these defects may play in disease pathogenesis remains unclear, but Na^+ hyperabsorption and the altered pattern of

glycoprotein sialylation have been proposed as fundamental to the development of lung disease in CF (see section 1.5).

1.3.7 Tissue specific localisation of CFTR

The expression pattern and localisation of CFTR in wild type tissues has been demonstrated to be both tissue and cell specific, using immunohistochemistry and *in situ* studies (reviewed in Cohn 1994).

The predominant site of CFTR in the eccrine sweat ducts has been shown to be the luminal reabsorptive duct cell. In these cells CFTR is localised primarily in the apical domain (Kartner *et al* 1992).

In the pancreas CFTR is observed at the highest levels in the apical region of the intralobular duct cells. It is also present at much lower levels in the cells lining the larger pancreatic ducts (Marino *et al* 1991).

Studies of the gastrointestinal tract have revealed that *CFTR* expression gradually decreases across both the proximal-to-distal axis and the crypt-villus axis. The highest levels have been shown to occur apically in the crypt enterocytes and submucosal glands (Brunner's glands) of the proximal small intestine (Strong *et al* 1994). High levels of CFTR have also been detected, with a punctate pattern throughout the cytoplasm, in a small subpopulation of enterocytes scattered throughout the villi, and in the secretory compartments of the goblet cells of the small intestine (Kälin *et al* 1999).

Expression of *CFTR* in the liver has been shown to occur primarily in the intrahepatic bile duct cells (Cohn 1999) and to be localised to the apical compartment.

Studies in the rat have demonstrated that the highest levels of CFTR in the reproductive system occur in the epithelial lining of the endometrium and in the seminiferous tubules. In the latter, this expression was shown to

be stage specific with respect to spermatogenesis (Trezise and Buchwald 1991).

Finally, the predominant site of *CFTR* expression in the lungs has been shown to be in the submucosal glands, with only low levels in the bronchial epithelium (Engelhardt *et al* 1992). Expression in the submucosal glands is at or near the apical membrane, uniform in the epithelia of the serous tubules, but observed in only a small subpopulation of non-ciliated epithelial cells in the collecting and ciliated ducts.

It is clear that the clinical manifestations reflect many of these observations, however the pattern of CFTR distribution also raises various questions, not least about the role of the submucosal glands in the development of CF lung disease.

1.4 Lung disease in cystic fibrosis

While the phenotypic analysis described in the previous section has provided a considerable amount of information about disease of the pancreas, vas deferens and digestive tract, the severity and course of pulmonary disease are not clearly predicted by the *CFTR* genotype.

Lung disease in CF is characterised by chronic microbial colonisation and repeated acute exacerbations of pulmonary infection, with a distinctive spectrum of pathogens. These episodes precipitate progressive, irreversible, inflammatory lung damage. Despite the recent advancement of various hypotheses the precise aetiology of CF lung disease is still relatively poorly understood.

1.4.1 Pathology of the CF lung

Clinical and pathological studies have clearly characterised end stage lung disease in cystic fibrosis and the most common sequence of events in its pathogenesis (reviewed in Pilewski and Frizzell 1999). The most prominent features being; excessive production of viscous mucopurulent secretions, airway obstruction and atelectasis, cytokine imbalance and a neutrophil dominated cellular response, resulting in severe bronchiectasis and respiratory failure.

The CF lung is macroscopically normal at birth, but studies have reported subtle histological abnormalities evident in the tracheal submucosal glands of CF foetuses (Ornoy *et al* 1987) and newborns (Esterly and Oppenheimer 1968). These studies describe hypertrophy and hyperplasia of the submucosal glands with inspissation of mucus secretions. However, another report suggested that similar pathology was evident in the submucosal glands of newborns that had died from other airways diseases, introducing questions about the relevance of these observations in CF (Oppenheimer 1981). Despite this report it does appear that mucus secretion is defective at an early stage in the pathogenesis of CF lung disease. More critical to our understanding of this process is whether or not this abnormality precedes infection.

The development of lung disease in young CF individuals is characterised by the onset of repeated bacterial infection. Studies of the clinical course suggest that this leads to airway inflammation and lung damage. However, studies in CF infants have raised the question of whether inflammation may, in fact, precede airway infection. In one study the analysis of bronchoalveolar lavage (BAL) samples from CF infants demonstrated pulmonary inflammation present very early in life and in the absence of bacterial colonisation (Khan *et al* 1995). In contrast, a subsequent, larger and more rigorous study failed to support the latter conclusion. In

this case the inflammatory profile of CF infants, that had no history of respiratory symptoms, no exposure to antibiotics and no BAL pathogens detected, was analysed. This was found to be significantly different from that of CF infants with evidence of pulmonary infection, but not to be significantly different from disease control subjects (Armstrong *et al* 1997). Furthermore, a longitudinal component to this study demonstrated resolution of inflammation following antibiotic treatment. This supports the hypothesis that infection plays a role in initiating and maintaining the airway inflammation that characterises CF lung disease.

The clinical course of CF lung disease is then characterised by a vicious cycle of infection, inflammation and airway damage, with complex interaction between pathogens, airway epithelial cells, cytokines and the immune system. Pulmonary secretions from CF patients contain an excessive neutrophil load and high levels of proinflammatory cytokines, including IL-8. These secretions also contain proteolytic enzymes produced by the neutrophils, such as elastase and cathepsin G, at sufficient levels to overwhelm the lungs anti-protease defence mechanisms (see section 1.6.2.3). Consequently these enzymes are capable of direct tissue injury, impeding bacterial clearance mechanisms and interfering with host immune mechanisms. In addition, the DNA from autolysing neutrophils aggregates into large fibrils with a consequent increase in the viscosity of the sputum. Mucus secretion may be stimulated both by the products of inflammatory cells and by bacterial endotoxins (reviewed in Shelhammer 1997). Furthermore, *P. aeruginosa* LPS has been demonstrated to profoundly upregulate transcription of the mucin gene *MUC2* in epithelial cells (Li *et al* 1997). The consequent hypersecretion of mucus from hypertrophied submucosal glands and hyperplastic goblet cells contributes to the viscous, mucopurulent pulmonary secretions that are so characteristic of CF.

Studies suggest that, aside from changes to the submucosal glands, the earliest lesions occur in the distal airways, with mucus obstruction of the bronchioles and inflammation of the bronchiolar walls (Esterly and

Oppenheimer 1968). Progression of the disease results in even more pronounced bronchiolitis and bronchitis, with goblet cell hyperplasia and metaplasia extending distally into the bronchioles and luminal obstruction with plugs of mucus and inflammatory infiltrate. Chronic colonisation with *P. aeruginosa* appears to accelerate this decline (see section 1.4.2.4) eventually leading to end stage lung disease, characterised by severe bronchopneumonia and bronchiectasis (Oppenheimer and Esterly 1975).

Post mortem examinations have made a considerable contribution to the characterisation of lung disease in CF, but are obviously restricted in a variety of ways. The main studies report either on predominantly end stage lung disease or observations from CF newborns that have died of meconium ileus. As a result of improved diagnosis and treatment the latter reports are rather older. It is obviously difficult to establish the relative roles of the many possible contributing factors, and the interplay between them, from these kinds of data. Nor is it possible to draw too many conclusions about the likely sequence of events. Theoretically, mouse models of CF provide a system with which to target these gaps in our knowledge. Such model systems may be manipulated to control all the factors contributing to phenotype development and allow characterisation, by histopathological or other means, at any timepoint required. In this manner these observations made in humans may provide the framework around which to construct a detailed explanation for the development of CF lung disease.

1.4.2 Microbiology of the CF lung

Lung disease is the major cause of morbidity and mortality in CF and is characterised by chronic microbial infection. The environment of the CF lung is unique, resulting in infection with a rather narrow spectrum of pathogens. This most commonly includes respiratory syncytial virus (RSV),

Staphylococcus aureus, *Haemophilus influenzae*, *Pseudomonas aeruginosa* and *Burkholderia cepacia*. In general, these occur in a similar sequence, with RSV infections and colonisation with *S. aureus* in infancy, followed by *H. influenzae* in early childhood, *P. aeruginosa* in later childhood to early adolescence and the highest incidence of *B. cepacia* in late teenage years (reviewed in Govan and Nelson 1992).

1.4.2.1 Viral infections

Infants with CF are typically subject to viral respiratory infections, most commonly with RSV, although disagreement exists as to whether such infections are more common in CF than in the general population. A longitudinal, observational study of an unselected cohort of CF infants identified in a screening programme examined the incidence of such infections in hospital admissions (Armstrong *et al* 1998). Almost 40% of the cohort were admitted to hospital for respiratory illness within the first year of life. Greater than 50% of these admissions were associated with viral infections, predominantly RSV. In those infants, the infections were self-limited, but the airway inflammatory responses were observed to be similar to the infants with bacterial infections. Furthermore, infants admitted with severe, or persistent, respiratory symptoms were found to be at increased risk of acquiring *P. aeruginosa* infection within the first five years of life.

Thus, it seems possible that early viral respiratory infections could be involved in establishing the vicious cycle of infection and inflammation that characterises the development of CF lung disease.

1.4.2.2 *Staphylococcus aureus*

The organism first recognised to cause chronic lung infection in the lungs of young CF individuals was *S. aureus* (Di Sant'Agnese and Anderson

1946). Colonisation with this bacteria once killed the majority of CF patients in infancy, but aggressive antibiotic therapy has enabled increased control over this infection in recent years.

S. aureus is a Gram-positive, non-motile, non-spore-forming, unencapsulated coccus. It is human commensal, commonly isolated from the anterior nares and the skin, but is also an important pyogenic organism. Approximately 30% of healthy people carry *S. aureus* in the nasopharynx, however, lower respiratory tract infection with *S. aureus* does not occur in the general population. It is characteristically the first bacteria to colonise the respiratory tract of CF individuals and is the predominant infection in the first two years of life (reviewed in Govan and Nelson 1992). No specifically CF-associated strains of *S. aureus* exist. The strain that is isolated from the lower airways of a CF individual is generally also carried in the nasopharynx and by non-CF family members (Tümmler and Kiewitz 1999).

S. aureus produces a variety of virulence factors including coagulase, leucocidin, protein A, catalase, hyaluronidase, haemolysins and exotoxins. However, the precise role of these factors in CF lung disease remains unclear.

The *S. aureus* strains isolated from CF sputum can be classified as three morphologically separate types; mucoid, non-motile and small colony variant (SCV). These vary with respect to the production of virulence factors and degree of antibiotic resistance (reviewed in Hutchison and Govan 1999). Mucin-binding capacity has also been shown to vary between strains, however all three colonial morphotypes have an affinity for human mucin (Tivier *et al* 1997).

A recent study examined the localisation of *S. aureus* in sections of infected bronchi and bronchioles of CF patients after lobectomy (Ulrich *et al* 1999). The bacteria detected were predominantly mucus bound, embedded, and uniformly distributed in the obstructing mucus plugs. Furthermore, utilising a cell ball model of respiratory epithelium, *S. aureus* was shown to adhere predominantly to the secreted mucus and not to the airway epithelial

cells. This mucus binding was not observed to be any greater in cell balls from CF patients than those from non-CF individuals. It was suggested that the binding of *S. aureus* to the mucus layer may in fact prevent contact with the epithelial cells, damage from bacterial toxins, invasion and systemic infection. It is possible that this mucin-binding capacity may enhance the ability of *S. aureus* to infect the CF airways as a result of impaired mucociliary clearance mechanisms (see section 1.5.1.1).

Despite the results of the cell ball studies described above, there is considerable *in vitro* evidence that *S. aureus* can bind strongly to specific bacterial receptors on the surface of airway epithelial cells (see section 1.5.2.1). These receptors are present at greater density on CF and regenerating airway epithelium, may be upregulated by bacterial products and can also act as receptors for *P. aeruginosa*. This hypothesis and studies detailing the affinity for mucus-binding need not be viewed as mutually exclusive. It is possible that epithelial cell adherence is a rare event, with serious consequences, which occurs with increased likelihood in CF. The role of epithelial damage and regeneration may also be critical, potentially increasing cell contact with bacteria and the number of receptors present on those epithelial cells.

Although the threat posed by *S. aureus* has diminished in the antibiotic era it may still play an important role in the initiation of CF lung disease and the creation of a unique environment that provides the opportunities for subsequent colonisation by other bacteria. Furthermore, it is unclear to what extent the extensive use of anti-staphylococcal chemotherapy has affected the spectrum of atypical pathogens that now characterise later stage lung disease in CF. Finally, as a consequence of the use and overuse of antibiotics in society, multi-drug resistance is becoming much more widespread. The emergence of methicillin resistant *S. aureus* (MRSA) is of considerable concern and has the potential to produce further re-evaluation of the threat posed by this organism in the future.

1.4.2.3 *Haemophilus influenzae*

Pulmonary infection with *Haemophilus influenzae* is common in young CF individuals, but the significance of this observation and the role of the organism in the development of CF lung pathology is controversial and its effect may be underrated. Many clinics do not routinely treat patients colonised with this organism, judging it to be almost commensal at low numbers (Hutchison and Govan 1999).

H. influenzae is a Gram-negative coccobacillus. The capsulated strains can cause diseases such as meningitis and osteomyelitis, while the non-capsulated strains are mainly responsible for exacerbations of chronic bronchitis and bronchiectasis in individuals with and without CF. The majority of isolates from CF patients are non-capsulated. CF individuals are often colonised with multiple strains of *H. influenzae*, with one predominant strain (Hutchison and Govan 1999).

H. influenzae infection can generally be well controlled with antibiotic therapy. However, as is the case for *S. aureus*, antibiotic resistance is also appearing in certain strains of this bacteria isolated from CF lungs.

1.4.2.4 *Pseudomonas aeruginosa*

After the first two years of life infection with the opportunistic pathogen *Pseudomonas aeruginosa* predominates. Evidence of infection in the lower airways occurs in a third of CF infants by the age of 5 years, (Grimwood *et al* 1997), rising to 90% of CF adults (Hutchison and Govan 1999). It remains unclear to what extent this organism is reliant upon previous infections and/or antibiotic therapies to alter the milieu of the CF lung and create an environment suited to its requirements.

P. aeruginosa is a Gram-negative, motile, non-sporing, non-capsulate bacillus that is widely distributed in water and soil. It is naturally resistant

to many antibacterial agents as a result of the relative impermeability of the OprF porin in the outer membrane, an active efflux system and the activity of β-lactamase (reviewed in Hancock 1998). *P. aeruginosa* is an opportunistic pathogen for plants and animals. Isolates produce numerous virulence factors including exotoxin A, exoenzyme S, elastase, alkaline protease, pyoverdin, haemolysins, lipopolysaccharide (LPS), pili and an unusual exopolysaccharide resembling the algae alginate (Gilligan 1991). In humans it can affect a variety of organs, such as infections of the eye, ear and burn wounds. It can also be the aetiological agent responsible for nosocomial pneumonia, causing disease primarily in immunocompromised individuals.

Infection with *P. aeruginosa* in CF is atypical in several key ways (Govan and Harris 1986); firstly, the host is immunocompetent in terms of cellular and humoral responses, secondly, the infection remains localised to the respiratory tract and finally, interaction between the host and pathogen results in a characteristic transformation of the bacteria. This transformation is from a classic non-mucoid to a mucoid colonial phenotype.

It has been suggested that initial asymptomatic, and often intermittent, colonisation of the upper respiratory tract occurs, preceding aspiration to the lower airways. Indeed, following lung transplantation in CF, colonisation of the new lungs occurs with the same strain of *P. aeruginosa* responsible for pre-transplant colonisation, suggesting a reservoir exists in the upper respiratory tract (Walter *et al* 1997).

Initial colonisation typically occurs with motile, planktonic *P. aeruginosa*. These bacteria have a non-mucoid colonial phenotype, smooth LPS and can be seen widely dispersed throughout the sputum. The distribution and frequency of strains seen in CF individuals matches that observed in other diseases and in the environment (Tümmler and Kiewitz 1999). Thus, colonisation may be possible with practically any strain. However, it seems likely that some strains have a greater propensity for the CF lung than others. In one study, two unrelated CF individuals were demonstrated to have become colonised with the same non-mucoid strain

after sharing a hydrotherapy pool, despite at least 5 other strains being present in the water (Nelson *et al* 1990). Interestingly, this strain was found to be highly mucinophilic, demonstrating chemotaxis and adhesion to CF mucin.

Early colonisation with non-mucoid strains may be eradicated, however, most individuals soon become colonised with a single strain of *P. aeruginosa* that remains throughout the patients lifetime (Römling *et al* 1994), despite the presence of anti-pseudomonal antibodies. Subsequent isolation of other strains is rare. Unrelated CF individuals are usually colonised with different strains, but siblings with CF tend to show colonisation with the same strain of *P. aeruginosa*, suggesting that cross-infection may occur if there is prolonged, close contact.

The transformation of *P. aeruginosa* in the CF lung is practically unique and almost diagnostic for the disease. This process results in colonisation with a non-motile, mucoid phenotype with rough LPS existing within a complex biofilm (reviewed in Govan and Deretic 1996). These strains lose their flagella and become LPS deficient (non-typable or polyagglutinating rough) with the loss of O side chains and increased susceptibility to human serum. Mutations in *mucA* gene, leading to inactivation, result in the constitutive expression of alginate biosynthesis genes (Martin *et al* 1993). It is the selection for these mutants in the CF lung that creates the mucoid phenotype. This process results in mucoid and non-mucoid organisms co-existing in the CF lung and in many cases a heterogeneous population of mucoid strains with different mutations in *mucA* (Boucher *et al* 1997). The environmental stimuli that provoke the conversion to mucoidy are as yet unclear. However, recent studies have suggested key roles for neutrophils and their oxygen radicals (Mathee *et al* 1999) and the dysfunction of naturally occurring antibacterial peptides (Singh *et al* 1999) (see section 1.6.1) in the creation of mucoid phenotypes. While all wild-type, non-mucoid strains of *P. aeruginosa* have the potential to undergo the transformation to mucoidy,

the only other natural niches known for the overtly mucoid form, outside of the CF lung, are in bronchiectasis and the rare occurrence in urinary tract infections (Boucher *et al* 1997).

The alginate produced by mucoid *P. aeruginosa* is an exopolysaccharide polymer made up of guluronic acid and mannuronic acid (reviewed in Govan and Deretic 1996). It confers further antibiotic resistance to the organism and an electrolyte-rich physical barrier to the host immune system, interfering with opsonic and non-opsonic mechanisms and quenching reactive oxygen intermediates. Alginate is the primary constituent of the biofilm, which supports the growth of these bacteria as microcolonies, adherent to the airway epithelium. These biofilms are complex "pillar" and "mushroom"-like structures with water channels between them, within which subgroups of bacteria may behave in quite diverse manners (Molin *et al* 1999). Bacteria within these biofilms may utilise a system known as quorum sensing to provide an index of population density, to regulate biofilm differentiation and integrity and the production of virulence factors. This is achieved with at least two cell-to-cell signalling systems communicating via the production of acylhomoserine lactone molecules (Davies *et al* 1998). Understanding these systems may establish novel approaches for therapeutic intervention.

While there is considerable variability in the time scale for the emergence of mucoid variants of *P. aeruginosa*, this process can occur in as little as three months after the initial colonisation (Govan and Deretic 1996). Subsequently, the forced expiratory volume in the first second (FEV_1), which is the single best predictor of mortality, will decline more quickly in these individuals. A recent study suggested that infection of CF individuals with mucoid *P. aeruginosa* was associated with both genotype and the level of opsonic antibodies specific for *P. aeruginosa* mucoid exopolysaccharide. However the only factor associated with the degree of functional impairment

of the lungs was the presence or absence of infection with mucoid strains (Parad *et al* 1999).

Thus lung colonisation with *P. aeruginosa* in CF involves a complex series of modifications from infection with a relatively innocuous strain through to the establishment of chronic infection with a mucoid organism and subsequent more rapid clinical deterioration. Despite considerable advances in the development of anti-pseudomonal therapy, it remains palliative and seldom, if ever, results in eradication of mucoid strains.

1.4.2.5 *Burkholderia cepacia*

Since the 1980s, infection with *Burkholderia cepacia* has become an increasing concern in CF and has led to policies within the CF community in an attempt to minimise cross infection.

B. cepacia was originally described as a plant pathogen, capable of causing the soft rot of onions (Burkholder 1950), and not considered to be pathogenic to humans. It is a Gram-negative, non-spore forming, aerobic, motile baccilus, found in soil, water and vegetation. It has an unusually large genome, with three replicons, a total DNA content of over 7 Mb and demonstrates considerable plasticity. Recent taxonomic studies have defined five distinct species within what is now referred to as the *B. cepacia* complex; genomovars I – V (Vandamme *et al* 1997). The majority of clinical strains are from genomovars II and III and show the greatest association with acute clinical decline. *B. cepacia* has been reported to produce a number of virulence determinants including haemolysin, protease, lipase, catalase and endotoxin, but the clinical significance of these observations is not yet clear (reviewed in Hutchison and Govan 1999). *B. cepacia* is notoriously resistant to antibiotics and disinfectants and no effective antimicrobial therapy is available. Indeed one study demonstrated the ability of this microbe to utilise Penicillin G as the sole source of carbon and energy (Beckman and

Lessie 1979). Furthermore, *B. cepacia* is resistant to killing by antimicrobial peptides (see section 1.6.1).

Strains of this multi-resistant organism constitute a threat both to CF individuals and also to those with Chronic Granulomatous disease (CGD). In individuals with CGD there is failure of oxidative killing by the phagocytic cells as a result of an inability to produce a respiratory burst (Sanders and Crystal 1997). This disease is characterised by recurrent infections, suppurative granulomas and infiltration of the viscera with pigmented, lipid-laden macrophages. It remains to be seen whether dysfunctional CFTR can also cause a defect in oxidative killing, although it has been suggested that inducible nitric oxide synthase (iNOS) associated antibacterial activity may be compromised in CF (see section 1.5.3.3).

The prevalence of *B. cepacia* infection in CF has risen from ~10% in 1971 (Isles *et al* 1984) to around current levels of ~20% (Hutchison and Govan 1999). However, localised rates can vary between 5% and 70%. The consequences of infection vary from asymptomatic colonisation through to *B. cepacia* "syndrome" in approximately 20% of cases. This "syndrome" is characterised by acute necrotising pneumonia with fever, septicaemia, leukocytosis and a raised erythrocyte sedementation rate (ESR) and is rapidly fatal. *B. cepacia* colonisation in CF reduces the average life expectancy by 50% (Hutchison and Govan 1999).

Studies have demonstrated that *B. cepacia* infection can occur by direct cross infection between patients (Govan *et al* 1993). This has led to segregation within CF clinics and communities in an attempt to prevent spread. This cross infection may occur via skin contact, aerosols and shared food or equipment, but probably occurs most easily by close and frequent social contact and by kissing. The transmissability of *B. cepacia* is strain dependent and outbreaks of infection have resulted from "epidemic strains", such as the notorious intercontinental ET/12 or Edinburgh-Toronto lineage (Govan and Deretic 1996). This isolate, and others responsible for epidemic spread, demonstrate considerable adhesion to respiratory mucin, associated

with giant cable pili (Sajjan *et al* 1995). The gene responsible for the cable pili has been identified as *cbl*. However, this is not present on all epidemic clones, suggesting the presence of other important virulence factors (Mahenthiralingham *et al* 2000).

As aggressive antimicrobial chemotherapy has dramatically reduced the impact of bacteria such as *S. aureus*, so unusual opportunistic pathogens not previously associated with human disease, such as *B. cepacia*, have arisen. It has been suggested that reducing the load of antibiotic sensitive bacteria creates a niche for highly resistant organisms to fill. Indeed the recent increase in the isolation of organisms such as *Alcaligenes xylosoxidans*, *Ralstonia pickettii* and *Stenotrophomonas maltophilia* may support this hypothesis (Hutchison *et al* 2000).

In this manner, the solution to one threat appears to be the catalyst for the onset of even greater problems. However, the basic underlying defect in CF remains the same. This reinforces the critical requirement for an improved understanding of disease pathogenesis. Why is the CF lung is so susceptible to infection, and why does it become colonised with these particular organisms?

1.5 The aetiology of CF lung disease

The lungs of CF neonates are macroscopically normal (see section 1.4.1), although the observation of submucosal gland abnormalities may be important. However, pulmonary infection and inflammation are evident from a very early age, with the isolation of RSV and *S. aureus* and raised levels of pro-inflammatory cytokines demonstrated (Armstrong *et al* 1998). Although some studies suggest that markers of inflammation are raised in advance of airway infection (Khan *et al* 1995), it is difficult to distinguish between cause and effect in CF humans. Regardless of this issue, this marks

the beginning of a series of insults that will eventually lead to bronchiectasis and death in the great majority if CF individuals. Despite considerable progress in the last few years, the precise mechanisms by which defective transepithelial Cl^- transport results in development of the characteristic pulmonary pathology remain poorly understood and the topic of considerable debate.

It has been proposed that *CFTR* mutations may cause a primary defect in lung function, which alters the lung environment. This alteration may be a point of no return, after which a self-perpetuating process begins and subsequent pathology need not result from a direct interaction with CFTR. This theory attempts to distinguish between CF *disease*, caused and perhaps maintained by CFTR dysfunction, and CF *lung disease*, a disease phase triggered by the former (Drittanti *et al* 1997). The alternative implies a direct role for mutant CFTR, or the absence of functional CFTR, throughout the disease process. In the former scenario, therapies designed to replace, or restore function to mutant CFTR may not be of significant value once CF *lung disease* was established. Thus, such models have significant bearing on the direction of future research and the emphasis in the design of novel therapies.

Whether CFTR dysfunction results in; 1) the creation of an abnormal lung environment which harbours, or fails to clear, infectious particles, or 2) an abnormal response to CF associated pathogens or impacted, dehydrated mucus, are questions that have been difficult to address. The dissection of the complex pathogenesis of this disease has suffered from the limitations imposed by restricted access to clinical material, a reliance on autopsy specimens with "end stage" lung disease and *in vitro* techniques. The development of improved primary culture models has facilitated novel approaches and a variety of interesting and at times conflicting hypotheses have arisen. Mouse models of CF provide an *in vivo* system in which to test out these hypotheses.

Two of the most prominent theories dealing with the fundamental defect in the CF lung have concentrated on the role and ionic composition of the airway surface liquid (ASL). These have become known as the "isotonic absorption/mucus dehydration" theory and the "hypotonic /defensin" theory. Other well established hypotheses examine the role of interactions between the epithelial cells and specific CF associated bacteria (see Figure 1.4). Further areas of research emphasise the importance of the submucosal glands, cytokines, nitric oxide (NO), antiproteases and the role of the cellular inflammatory response. These theories are not all mutually exclusive and it seems likely that they may help to explain different aspects of the disease process.

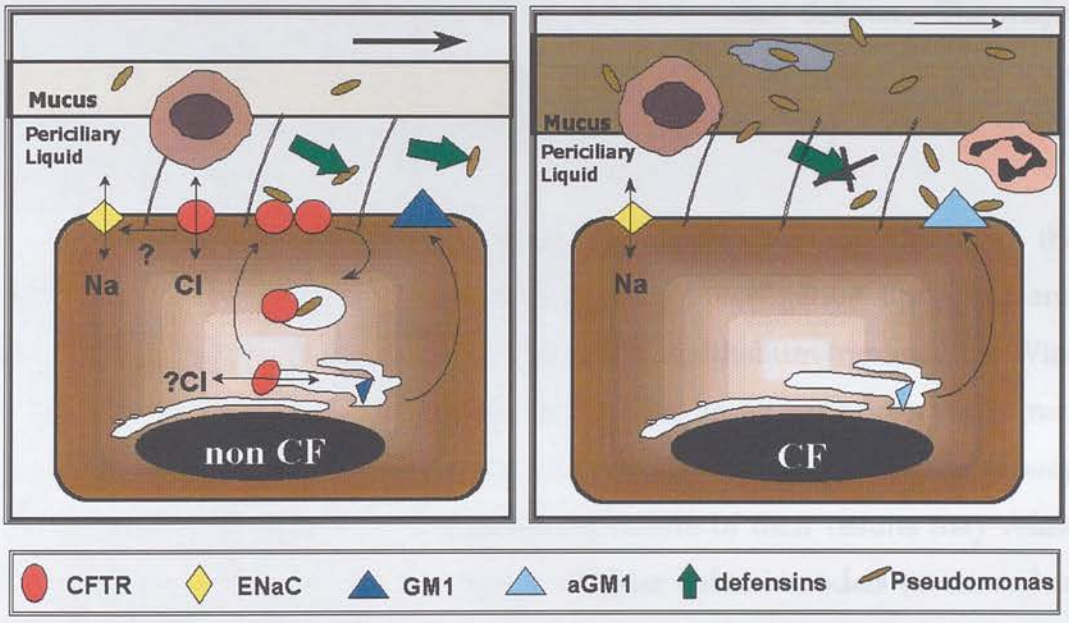

FIGURE 1.4 The pathogenesis of CF lung disease

Adapted from Davidson and Porteous 1998.

1.5.1 The airway surface liquid

The ASL is a thin layer of liquid, approximately 10 – 20 μm in depth, that covers the airway epithelium (reviewed in Pilewski and Frizzell 1999) and acts as the first line of lung defence. It is comprised of the periciliary liquid (or sol) layer, the minimum depth of which is proposed to be about 6 μm (the average cilia length), and mucus gel layer. The ASL contains mucins, proteins, lipids, peptides, ions and DNA. The upward movement of this liquid through the trachea is estimated to be 10–100 ml/day. The origin of the ASL is uncertain, as is the extent of the contribution made by the submucosal glands. It is proposed that the volume and/or ionic composition of the ASL is regulated by ion transport across the airway epithelium and that its composition plays a crucial role in airway host defence. The major active ion transport process across human airway epithelia is amiloride sensitive absorption of Na^+, with Cl^- acting as the major counter-anion (Knowles *et al* 1981).

Two major hypotheses linking the dysfunction of CFTR to the pathogenesis of CF lung disease have focused investigation upon salt and fluid absorption mechanisms across the airway epithelium (reviewed in Wine 1999). The studies upon which these theories are based have been performed predominantly using air/liquid interface primary cultures of human airway epithelium. The apparently contradictory nature of their results may relate to important differences in the nature of these culture models (reviewed in Guggino 1999).

1.5.1.1 The isotonic absorption/ mucus dehydration theory

In the traditional model for the development of CF lung disease, mucus hypersecretion and dehydration results in dysfunction of the normal

mucociliary clearance mechanisms. Bacterial infection and hyperviscous secretions result in the accumulation of mucus in the airways and airflow obstruction. Colonisation with CF associated pathogens occurs and persistent neutrophil influx contributes to an excessive and damaging inflammatory response and cytokine imbalance. Suppuration leads to ulcerative bronchitis and ultimately bronchiectasis. Recent studies have altered and clarified aspects of this model, proposing the "isotonic volume transport /mucus clearance" theory.

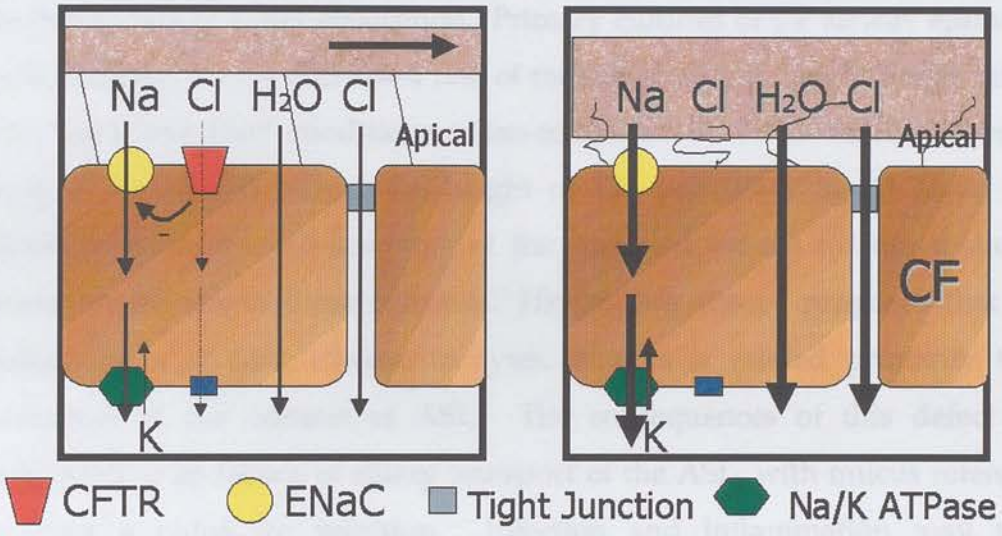

FIGURE 1.5 The Isotonic absorption / mucus dehydration theory
Adapted from Wine 1999.

This hypothesis proposes that the volume of ASL, in particular the periciliary liquid layer, is of critical importance and the result of a balance between secretion and absorption by the epithelium (see Figure 1.5). It proposes that the ASL is produced in the distal airways and removed proximally. The surface area of the distal airways is greater than that of the proximal airways, resulting in the need for volume absorption (Boucher 1994). Air/liquid interface primary cultures of airway epithelium were

utilised to demonstrate that the driving force for water absorption in the normal airways is the active, transcellular absorption of Na^+ (Matsui *et al* 1998). This is accompanied by the diffusion of Cl^- ions through tight junctions between the cells, followed by water, thus maintaining osmolarity. Consequently, this hypothesis predicts that the NaCl concentration of the ASL should be isotonic. This was demonstrated in the primary culture model, with the concentrations of Na^+ and Cl^- exceeding 100mM (Matsui *et al* 1998). According to this hypothesis, abnormally high Na^+ absorption, secondary to CFTR dysfunction (Stutts *et al* 1995), would result in an increased rate of water absorption. Primary cultures of CF airway epithelial cells demonstrated a decreased rate of reduction of ASL height under "thick film" and "thin film" conditions, when compared to non-CF cultures (Matsui *et al* 1998). Furthermore, the height of the periciliary liquid layer was observed to decrease below that of the cilia and induce rotational mucus transport defects in these cultures. Hence, this theory proposes that the pathogenesis of lung disease in cystic fibrosis is related primarily to a reduction in the volume of ASL. The consequences of this defect are suggested to be failure of ciliary transport of the ASL, with mucus retention creating a nidus for infection. Infection and inflammation may then upregulate mucus production and further exacerbate the defect (Li *et al* 1997).

One premise for this theory, requiring further examination is the need to absorb large volumes of fluid produced in the distal airways (reviewed in Pilewski and Frizzell 1999). Firstly, most distal airway cells are reported to be absorptive in nature, not secretory. Secondly, it may be that the mucus gel is moved proximally over the sol, with the latter acting as a stationary environment within which the cilia can beat. Furthermore, although studies on mucus from CF individuals suggest a spectrum of rheological abnormalities (Puchelle *et al* 1985), *in vivo* mucociliary clearance studies have been inconclusive (Yeates *et al* 1976, Regnis *et al* 1994). Finally, it is also worth noting that classical CF lung disease is not observed in individuals

with Primary Ciliary Dyskinesia Syndrome. This is a disorder of mucociliary clearance, which results in rhinitis and bronchitis and can lead to bronchiectasis, but generally causes a much less severe lung disease than CF (Afzelius 1997). However, in these individuals, mucus hydration, the volume of the periciliary layer and the cough reflex are all intact and may be able to compensate for the ciliary dysfunction to some extent.

1.5.1.2 The hypotonic / defensin theory

The second hypothesis proposes that the normal airway epithelium is capable of selectively absorbing salt, without water, to generate a hypotonic ASL (Zabner *et al* 1998) (see Figure 1.6). The theory describes the predominant mode of Cl^- transport as occurring transcellularly via chloride channels in the apical membrane and non-CFTR cAMP-activated Cl^- channels in the basolateral membrane (Uyekubo *et al* 1998), with concomitant Na^+ absorption through ENaC. This hypothesis predicts that the NaCl concentration in the ASL should be hypotonic, with the volume maintained constant by osmotic pressure from non-diffusable osmolytes capillary pressure from the cilia, or impermeability of the epithelium to water. CFTR has been demonstrated to be the major chloride channel regulating these ion effluxes. Hence this theory predicts that CFTR dysfunction would compromise the ability of the cells to absorb Cl^- ions from the ASL. This failure and the consequent impairment of Na^+ absorption would result in a raised salt concentration in the ASL of CF individuals. Studies utilising air/liquid interface primary cultures of airway epithelium have demonstrated that transcellular pathways for both Na^+ and Cl^- are required for normal fluid absorption. In non-CF epithelia, initial isotonic absorption, under "thick film" conditions, is followed by selective absorption of NaCl under "thin film" conditions. In the absence of CFTR this process cannot occur. A degree of Cl^- absorption occurs through the paracellular route,

however this is seen to plateau, having a Na^+ to Cl^- selectivity greater then 1. These studies estimate ASL Na^+ and Cl^- concentrations of 50 mM and 37 mM, respectively, in non-CF cultures and 100 mM and 90 mM, respectively, in CF (Zabner *et al* 1998). In both cases the same final depth of liquid was observed.

Studies have demonstrated that a hypotonic environment is required for the function of antibacterial agents within the ASL (Smith *et al* 1996). This antibacterial property of the ASL was demonstrated in studies utilising air/liquid interface primary cultures of normal airway epithelial cells, but found to be markedly reduced in the ASL from cultures of CF cells. Increasing the salt content of ASL isolated from non-CF cultures was shown to dramatically impair its antibacterial activity. Furthermore, this activity could be restored to ASL from CF cultures by decreasing the salt concentration. These results suggested that the components of the defence system are intact, but unable to function correctly in an environment of high levels of NaCl (Smith *et al* 1996). This led to speculation that CFTR dysfunction would alter the ionic environment of the CF lung, leading to impairment of the first line of lung defence against bacteria and viruses. This would predispose these individuals to infection and possibly precipitate a more pronounced compensatory response from other components of the defence system, affecting neutrophils, macrophages and cytokine production.

These studies have prompted further research to establish the key components of the innate lung defence system. These efforts have centred upon naturally occurring antimicrobial peptides; human β-defensins 1 and 2 (hBD1, (Goldman *et al* 1997), and hBD2, (Harder *et al* 1997), lysozyme and lactoferrin, (Travis *et al* 1999b) (see section 1.6).

Although this presents an attractive hypothesis, it is worth noting that individuals suffering from Pseudohypoaldosteronism (PHA) do not develop classical CF lung disease. In these individuals mutations in subunits of ENaC result in a salt-wasting disorder. Following the "hypotonic /

defensin" theory, a failure to produce hypotonic ASL might be anticipated in this condition. The systemic form results in elevated sweat sodium and chloride levels and chronic excessive secretion from the respiratory tract. However, despite predisposition to pulmonary infections and asthma like symptoms, they seldom develop bronchiectasis (Kerem *et al* 1997), nor the display the characteristic bacteriological profile of CF lung disease. Furthermore, this hypothesis offers no explanation for the susceptibility to pulmonary colonisation with *B. cepacia*, which has been demonstrated to be inherently resistant to cationic peptides (Hancock 1997).

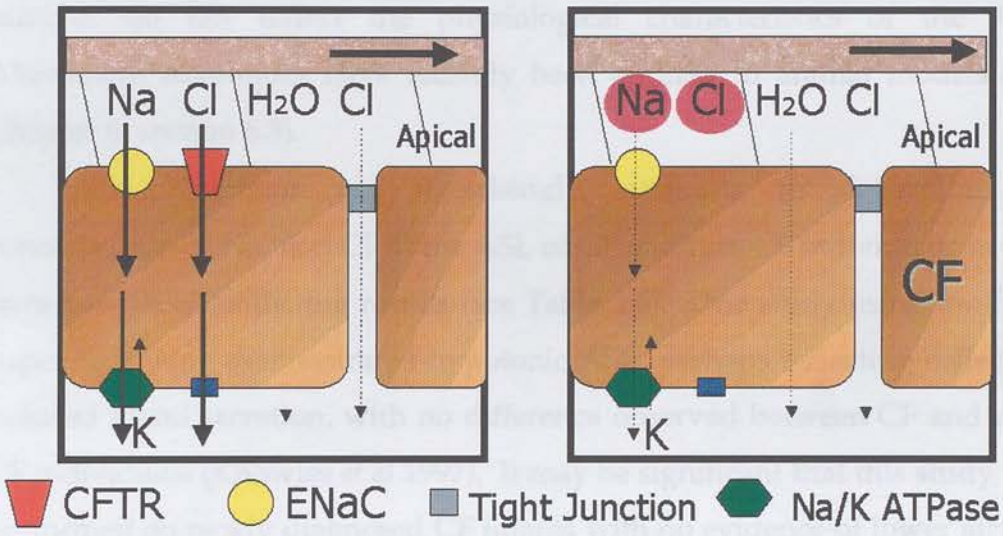

FIGURE 1.6 The Hypotonic/ defensin theory
Adapted from Wine 1999.

1.5.1.3 *In vivo* measurements of the ASL NaCl concentration

In view of these apparently contradictory hypotheses to explain CF pathogenesis, it is critical that the precise ASL composition is determined. However, the depth of this layer is so small in normal airways that ASL is difficult to sample *in vivo* without disturbing the underlying epithelium. In

addition, ASL is likely to be a complex mixture produced by the secretory cells of the surface epithelium, by the glands in the trachea and bronchi, and contributions from the bronchiolar and alveolar liquid. Thus, studies on isolated or cultured epithelium are not the ideal tools for analysing ASL composition.

The techniques used for ASL collection in humans have largely focused on the use of small pieces of filter paper to harvest the fluid (Joris and Quinton 1992, Knowles *et al* 1997). However the filter paper technique yields relatively large volumes of fluid compared to the amount of ASL present at the epithelial surface, raising the possibility that the collected samples do not reflect the physiological characteristics of the ASL. Alternative techniques have recently been applied to animal models (see Chapter 6, section 6.3).

Thus, perhaps not surprisingly, attempts to determine the concentration of Na^+ and Cl^- in the ASL of CF and non-CF individuals *in vivo* have provided conflicting results (see Table 1.6). One study using the filter paper technique demonstrated hypotonic ASL, perhaps reflecting collection induced gland secretion, with no difference observed between CF and non-CF individuals (Knowles *et al* 1997). It may be significant that this study was performed on newly diagnosed CF infants with no evidence of lower airway infection. Other studies have reported raised levels of NaCl in CF samples, using the filter paper technique (Joris *et al* 1993) or aspiration by a dry catheter (Gilljam *et al* 1989). The later was performed in older individuals with evidence of colonisation. Another study, using a nitrocellulose membrane to collect ASL, found no significant difference in Na^+ levels between CF and non-CF infants (Hull *et al* 1998). However, a significantly lower Cl^- concentration was recorded in CF infants with no evidence of inflammation than non-CF controls. This difference was not significant when studying CF infants with obvious signs of inflammation. No significant difference was observed when CF infants with and without inflammation were compared. A study utilising the bronchial xenograft model found a

small increase in the NaCl concentration in the ASL from CF cells, but a more significant hyperabsorption of NaCl and volume by the same xenografts (Zhang and Engelhardt 1999). The therapeutic consequences of the two theories discussed above are significantly different. Thus, the future development of techniques to provide accurate measurements and resolve this uncertainty is crucial.

		Knowles 1997			Joris 1993	Gilljam 1989	Hull 1998		Zhang 1999
Technique		Filter paper			Filter paper	Dry aspiration	Nitrocellulose membrane		xenograft
Site		N*	N	B	B	B	B	B	-
CF	Status	U			I	I	U	I	U
	n	9		9	3	10	5	7	27
	Mean age	27 y		14 m	**	24 y	3 m	2 y	-
	Na (mM)	95	110	80	121	NR	78	84	NR
	Cl (mM)	110	130	75	111	170	77	95	125
	K (mM)	20	30	25	22	5	NR	NR	NR
non CF	Status	U			U	I	U		U
	n	8		15	19	10	7		48
	Mean age	32 y		26 y	54 y	59 y	7 m		-
	Na (mM)	95	110	90	82	NR	85		NR
	Cl (mM)	110	125	90	84	85	108		114
	K (mM)	20	30	20	29	4	NR		NR

TABLE 1.6 Estimates of the ionic concentration of the ASL

Site: N = Nasal, B = Bronchial, Status: U = Uninfected, I = Infected, Mean age: y = years, m = months, * stimulated with chilli extract, ** 3 patients; aged 6 months, 16 years and 31 years.

1.5.2 Bacteria and epithelial cell interaction

The hypotheses describing abnormalities of the ASL both provide convincing theories to explain a generalised increase in susceptibility to infection. However, neither provides much explanation for the rather narrow spectrum of unusual pathogens that characterises CF lung disease. In contrast, the hypotheses concerned primarily with interaction between bacteria and epithelial cells specifically address the relevant bacteria. This area of research encompasses two main hypotheses; 1) the adherence of *P. aeruginosa* to asialylated glycoproteins (aGM_1) on the cell membrane and 2) the internalisation of *P. aeruginosa* by epithelial cells.

1.5.2.1 Bacterial adherence

The ability to rapidly remove, or kill, bacteria from the airways is crucial to lung defence. An increase in the number of epithelial receptors for the bacteria that characterise CF lung disease has been proposed. This has been suggested as a mechanism by which these pathogens may gain purchase within the airways and perhaps stimulate a destructive, pro-inflammatory response.

Studies utilising primary culture models of airway epithelium, have reported that *P. aeruginosa* adheres to CF cells significantly better than to controls.

Pilin have been demonstrated to be responsible for ~50% of *P. aeruginosa* binding. Pilin recognise and bind to the GalNAcβ1-4Gal sequence which is exposed in cell surface asialoganglioside 1 (aGM_1), but not in the sialylated forms of the glycolipid (GM_1) (Saiman and Prince 1993). Flow cytometric studies have demonstrated that a greater proportion of these glycolipids are asialylated in CF cells (Saiman and Prince 1993) than non-CF

cells. Thus receptors for *P. aeruginosa* are represented at higher levels in CF airway epithelia than controls, at the expense of the sialylated GM_1. The level of aGM_1 on CF cells has been found to be increased further in response to *P. aeruginosa* neuraminidase (Saiman and Prince 1993). Thus, this pathogen may be able to upregulate the expression of receptors for subsequent use and promote its adherence to the epithelial cells. The adherence of *P. aeruginosa* to CF cells can be blocked using both anti-aGM_1 antibodies and a broad spectrum neuraminidase inhibitor (Davies *et al* 1999).

In addition, this increased affinity for *P. aeruginosa* has also been observed in damaged and regenerating epithelial cells. During epithelial repair, particularly in CF, regenerating cells have been shown to display a further increase in the levels of aGM_1 (de Bentzmann *et al* 1996).

It has been proposed that the alteration in aGM_1 levels observed in CF cells may be a consequence of defective acidification of intracellular organelles, secondary to CFTR dysfunction (Barasch *et al* 1991). However, this mechanism has been questioned by more recent studies (see section 1.3.6). Regardless of the exact mechanism, further evidence for the role of CFTR in modulating the level of bacterial adherence comes from experiments utilising primary culture of respiratory epithelium from CF patients, before and after transfection with human *CFTR* gene therapy constructs (Davies *et al* 1997). The adherence of *P. aeruginosa* was found to be reduced in these studies following transfection of these cells.

It is worth noting that these observations are based largely upon studies using cells from ΔF508 homozygotes. One study, despite replicating these observations, reported no significant difference in *P. aeruginosa* adherence when using cells from patients with other CF mutations (Zar *et al* 1995). The adherence characteristics of immortalised CF cells were also reported to be different, demonstrating no significant difference from non-CF lines (Saiman *et al* 1992).

Interestingly, aGM_1 receptors are not specific for *P. aeruginosa.* Although bound *P. aeruginosa* could not be displaced by *E. coli*, it has been shown to be effectively displaced by *S. aureus* and *H. influenzae*. These two pathogens also reported to bind to aGM_1 receptors (Imundo *et al* 1995, Prince 1999).

Thus, this hypothesis suggests putative binding sites for CF related pathogens on airway epithelial cells, present in greater quantity on CF cells, particularly after injury, and further upregulated by bacterial exoproducts. Recent reports suggest that bacterial binding to aGM_1 is capable of triggering epithelial IL-8 expression, perhaps due to activation of Ca^{2+}-dependent kinases (Prince 1999). However, the full consequences of bacterial binding and their *in vivo* relevance are not yet clear.

It appears likely that these mechanisms may play an important role in the development of CF lung disease in the presence of increasing quantities of bacteria and lung damage. However, this theory fails to address the role of the mucus layer and ASL, which lie between the epithelial cells and pathogens entering the lung environment. As such, it may not represent the earliest defect manifest in CF lung disease. Furthermore, post mortem evidence reveals conflicting observations, with *P. aeruginosa* observed as microcolonies in an extracellular mucus layer, and rarely adherent to cells.

1.5.2.2 Bacterial internalisation

The interaction between epithelial cells and bacteria is also fundamental to another hypothesis, which suggests that airway epithelial cells may internalise *P. aeruginosa* as part of the host defence mechanism.

The key studies contributing to this hypothesis utilised a gentamicin-exclusion assay (see Chapter 2, section 2.8.1) to study the internalisation of *P. aeruginosa* into airway epithelial cells. In studies performed with cultured human airway epithelial cells, cells over-expressing normal CFTR were

demonstrated to internalise significantly more *P. aeruginosa* than non-expressing cells, or cells over-expressing ΔF508. The level of this bacterial internalisation was dependent upon the nature of the LPS of the bacterial strain selected, with those expressing a "rough" LPS phenotype less well ingested (Pier *et al* 1996). This LPS specificity was also demonstrated using a neonatal mouse model. In further studies, this internalisation was reported to be specifically blocked, both in cell lines and infected wild-type BALB/c mice, by pre-incubation with either a monoclonal antibody, directed against the first extracellular domain of CFTR, or with the peptide used to raise this antibody (Pier *et al* 1997). These results suggested that the first predicted extracellular loop (amino acids 108-117) of CFTR may act as a specific cellular receptor for the lipopolysaccharide core oligosaccharide of *P. aeruginosa*, resulting in bacterial ingestion. It is interesting to note that a deletion from the N-terminal to the fourth membrane spanning domain has been reported to have no effect on the ion channel properties of CFTR (Carroll *et al* 1995).

Immuno-localisation and electron microscopy studies were used to demonstrate a specific contact point between CFTR and *P. aeruginosa* at the cell surface and in the intracellular vesicles after internalisation. Furthermore, immuno-fluorescent detection of apical CFTR appeared to show enhanced apical expression after incubation with *P. aeruginosa* (Pier *et al* 1997). This suggests that the low level of CFTR expression on the apical surface of airway epithelial cells may be significantly upregulated, by unknown mechanisms, upon contact with *P. aeruginosa*. This CFTR may then form a point of adherence with the bacteria and consequently ingest the organism.

It is postulated that when exposed to low environmental levels of bacteria, focal internalisation and cell shedding might clear pathogens in this manner. This may be achieved by a minority of cells approaching desquamation. Indeed a similar mechanism has been reported, in which *P. aeruginosa* is internalised specifically by superficial exfoliating corneal cells

(Fleiszig *et al* 1995). Recent reports implicate a CFTR-regulated apoptotic mechanism as part of this clearance process (Pier *et al* 1999).

Thus, this hypothesis suggests that CFTR acts directly as a receptor for the internalisation of *P. aeruginosa* and that this constitutes a crucial lung defence mechanism that would be inoperative in the absence of functional CFTR. Such a mechanism may be impaired in the absence of apical CFTR or in the presence of correctly localised, but dysfunctional, protein.

However, the *in vivo* relevance of these observations is uncertain and this theory has been the subject of considerable scepticism. The definitive *in vitro* experiments were carried out using cell lines that over-expressed human CFTR and appear to require further induction of CFTR. Whether this induction is at the transcriptional, translational, post-translational or recycling level is not clear. In the small airways of the lung where infection is believed to initiate, CFTR expression is low. In addition, the monoclonal antibodies used in these studies have previously been reported to detect a cross-reacting protein (Walker *et al* 1995). In an earlier report, which observed the internalisation of *P. aeruginosa in vivo*, internalisation was seen mainly in those animals that developed severe pneumonia and was postulated as a route to more widespread infection (Tang *et al* 1995). This does not lend support to internalisation as a defence mechanism *in vivo*. Furthermore, the internalisation hypothesis would appear to conflict with the bacterial adherence theory, in which increased adherence is expected in CF cells, and does not explain why CF individuals are susceptible to infection with variety of other respiratory pathogens, not just *P. aeruginosa*. Finally, this theory also fails to address the issue of the mucus barrier, which protects the cells from the luminal contents.

The availability of mouse models of CF provides an ideal opportunity to test this hypothesis *in vivo* and establish the potential role of such a mechanism in the pathogenesis of CF lung disease.

1.5.3 Inflammatory mechanisms

The extensive study of airway inflammation in the CF lung has revealed a characteristic profile of cytokine and protease /anti-protease imbalance with an excessive infiltration of neutrophils. However, it remains unclear to what extent these are secondary to infection or the direct effects of CFTR dysfunction. The phagocytic function of neutrophils is normal and the humoral antibody responses are intact (reviewed in Konstan and Berger 1993), however opsonophagocytosis *in vivo* may be impaired by excess neutrophil elastase.

1.5.3.1 Cytokine imbalance

The inflammatory response is regulated by a complex balance between pro- and anti-inflammatory cytokines. The production of these proteins by epithelial and inflammatory cells in the CF lung has been the subject of considerable research. Excessive production of pro-inflammatory cytokines has been clearly demonstrated in the infected CF lung, however their role in the development of the disease is less clearly defined.

A study of BAL from CF patients, with mild, stable lung disease, and non-CF controls, reported increased levels of the pro-inflammatory cytokines IL-8, IL-6, tumour necrosis factor-α (TNF-α) and inhibitors of TNF-α activity (TNF soluble receptor fragments) in CF lavage fluid, in comparison to controls. A concomitant decrease in the level of IL-10 in CF individuals was also observed (Bonfield *et al* 1995), indeed this anti-inflammatory cytokine was undetectable in half of the CF samples. These observations were supported by immunohistochemical studies of macrophages extracted from the BAL samples. Further analysis, with fresh bronchial epithelial cells, demonstrated the same pattern of cytokine imbalance using

immunofluorescence and enzyme-linked immunoadsorbant assays (ELISA) (Bonfield *et al* 1999). Another study, examining sputum samples from CF individuals and controls, broadly supports these observations (Osika *et al* 1999). However, these reports differ significantly with regard to IL-6 levels, with the latter study reporting significantly less IL-6 in CF samples and re-evaluating the role of this cytokine to emphasise its anti-inflammatory functions.

In support of these observation, significantly increased levels of pro-inflammatory cytokines (TNF-α, IL-1β, IL-6, MIP-2 and KC) have been reported in BALF from $Cftr^{tm1Unc}/Cftr^{tm1Unc}$ mice after inoculation with *P. aeruginosa* laden agar beads, in comparison to wild type controls (van Heeckeren *et al* 1999). In addition, in contrast to wild type mice, the anti-inflammatory cytokine IL-10 was reported not to be measurable in $Cftr^{tm1Unc}/Cftr^{tm1Unc}$ mice.

These observations indicate that a characteristic profile of cytokine imbalance occurs in CF lung disease. Pro-inflammatory cytokines can cause cachexia, hyperglobulinaemia and airway infiltration with neutrophils (Bonfield *et al* 1995). TNF-α is capable of direct tissue injury and can increase the expression of IL-1, IL-6 and IL-8, while IL-8 is a potent chemoattractant and can stimulate neutrophils to release harmful lysosomal enzymes. IL-6 can stimulate B-cells and may lead to increased antibody production and local immune complex deposition. However, it may also induce the production of anti-inflammatory acute phase protein, C-reactive protein and α_1-antitrypsin (Osika *et al* 1999). IL-10 has been called the "cytokine synthesis inhibitory factor" (Bonfield *et al* 1995). This anti-inflammatory cytokine has been reported to decrease macrophage production of TNF-α, IL-1, IL-6 and IL-8.

Studies in IL-10-deficient transgenic mice have also provided interesting results. IL-10-deficient mice on a C57Bl/6J strain background have been found to have a significantly better bacterial clearance rate and

decreased levels of TNFα after exposure to aerosolised *P. aeruginosa* strain PAO1, but a significantly greater mortality in comparison to wild-type controls (Yu *et al* 1998). Those that survived demonstrated no difference in lung pathology in comparison to the wild-type controls. However, in response to repeated exposure, the IL-10-deficient mice developed significantly more severe, but qualitatively similar, lung pathology. This suggests that IL-10 may be important in suppressing lung inflammation in the continued presence of *P. aeruginosa*. Another study demonstrated significantly more severe pathology, weight loss and BAL neutrophil counts in IL-10-deficient mice, following the intratracheal instillation of agar beads laden with a clinical isolate of *P. aeruginosa*, than in wild-type controls (Chmiel *et al* 1999). However, no difference in overall survival rates of the animals, or the bacterial numbers in lung homogenates was observed. This was interpreted as evidence that in the absence of IL-10, increased inflammation led to excessive, injurious local responses to "chronic infection" with no more efficient bacterial killing.

Thus, the cytokine imbalance observed in CF would clearly be capable of conferring a profoundly pro-inflammatory phenotype and contributing to escalating inflammation. However, it is unclear whether this imbalance is secondary to infection in a compromised host or a direct effect of CFTR dysfunction, which precedes airway infection.

Studies in CF infants have suggested that inflammation and cytokine imbalance may constitute the primary event in the establishment of CF lung disease. BAL analysis demonstrated pulmonary inflammation to be present in a cohort of CF infants, in the absence of bacterial colonisation (Khan *et al* 1995). Furthermore, in two case studies, CF infants with recent onset respiratory infections were treated with antibiotic chemotherapy to clear the infection. In both cases typical cytokine imbalance, with raised levels of IL-6 and IL-8 and no detectable IL-10, was reported two months later, in the absence of infection (Bonfield *et al* 1999). However, another study

examining the inflammatory profile of CF infants, with no signs or history of pulmonary infection, reported no difference in comparison to non-CF control subjects (Armstrong *et al* 1997).

Thus a harmful cytokine imbalance is clearly evident in CF lung disease. This has been postulated to result primarily from a down regulation of the anti-inflammatory cytokine IL-10, leading to the persistent production of pro-inflammatory cytokines. However, it remains unclear whether this is a direct effect of CFTR dysfunction or whether infection plays a key role in initiating and maintaining the airway inflammation in CF. It seems unlikely that this issue can be easily resolved with human studies, in which there are obviously serious restrictions on the degree of manipulation and analysis acceptable. It may be that the continued use of mouse models can provide insights from which to extrapolate.

1.5.3.2 Protease – antiproteases

CF lung disease is characterised by an excessive influx of neutrophils, the products of which result in an imbalance between the levels of proteases and antiproteases in the airways (reviewed in Döring 1999).

Sputum samples from CF individuals with chronic lung inflammation may contain up to 10^9 neutrophils per ml. These neutrophils release powerful enzymes, stored in azurophilic granules, either in a fully active state (serine proteinases) or as pro-enzymes (metalloproteinases (MMP)). The serine proteinases include neutrophil elastase (NE), cathepsin G and proteinase 3. These display broad substrate specificity. NE is capable of direct injury to epithelial cells and cleaving antiproteases, immunoglobulins, complement and fibronectin. By cleaving the opsonic receptors on neutrophils and components of complement that act as ligands for these receptors, NE may interfere with opsonophagocytosis (Berger *et al* 1989). In addition NE may alter ciliary activity and mucociliary clearance, and

stimulate airway gland secretion. MMPs may be activated by NE and are specifically involved in the degradation of extracellular matrix. In CF further damage may result from bacterial MMPs, *P. aeruginosa* produces 3 known proteinases; elastase, alkaline proteinase and LasA.

In the non-CF lung damage from neutrophil proteases is prevented by protease inhibitors. The most abundant plasma protease inhibitor is α_1-antitrypsin (α_1AT), an acute phase protein produced by the liver in response to inflammation and IL-6. α_1AT may also be produced by the alveolar macrophages and epithelial cells and is upregulated by pro-inflammatory cytokines TNF-α, IL-1 and bacterial LPS. It inactivates NE quickly and irreversibly and is the major protective component of the alveoli. The major antiprotease in the upper airways is secretory leukoprotease inhibitor (SLPI), secreted by the epithelial cells and upregulated by defensins and α_1AT (van Wetering *et al* 2000). This protein has both antiprotease and antibacterial activity. In addition to SLPI, elafin, elastase-specific antiprotease, is also active in the airways (Simpson 1999).

Studies of the ASL from CF individuals have demonstrated an excess of NE elastase that overwhelms the antiprotease defences, even in young children (Birrer *et al* 1994). In almost all cases the NE-antiprotease balance was found to be in favour of NE, with free active NE present, despite normal local concentrations of SLPI and α_1AT.

Neutrophils also produce reactive oxygen species, which can produce direct tissue damage and inactivate antiproteases. In addition, reduced levels of glutathione (GSH) in the CF ASL have been reported. GSH may play an important role as an antioxidant in the lung, directly scavenging free radicals and acting as a co-substrate in the reduction of hydrogen peroxide (reviewed in Kelly 1999). Indeed, it has been suggested that CFTR may be permeable to GSH and involved in regulating its level in the ASL (Linsdell and Hanrahan 1998).

It is clear how this vicious cycle may contribute to the steady deterioration of lung function in CF. However, it is not yet evident whether this constitutes an abnormal reaction to infection or a disastrous compensatory response occurring as a consequence of failure of another component of the lung defence system. If a comparable phenotype were demonstrated in mouse models of CF, it would greatly assist in dissecting out the key components of this process.

1.5.3.3 The role of Nitric Oxide

Nitric oxide (NO) has also been implicated in the establishment of CF lung disease, as the result of a variety of studies (reviewed in Grasemann and Ratjen 1999).

NO appears to be involved in a wide range of processes; as a signal molecule inducing vasodilation and bronchodilation, as a powerful antimicrobial agent and suggested to have a role in the activity of ENaC channels. However, in excess NO causes inflammation and oxidative tissue damage through reactive intermediates. It is synthesised from L-arginine by constitutive and inducible isoforms of nitric oxide synthase. Expression of the latter form is initiated by inflammatory cytokines and bacterial products.

Increased levels of NO in exhaled breath have been reported in asthma and in patients with lung infections. However, despite chronic infection and inflammation, studies in CF individuals have demonstrated NO levels to be normal or low (Ho *et al* 1998). Although the source of NO in the lungs is not clear, inducible nitric oxide synthase (iNOS) has been reported to play a key role. iNOS expression has been demonstrated in the epithelial cells of the nose, trachea and bronchi (Kelley and Drumm 1998). However, although expression was found to be normal in the airway inflammatory cells, it was significantly decreased in the bronchial epithelial cells of CF lung specimens and CF cell lines (Meng, Q.-H. 1998). The

expression of iNOS has also been reported to be significantly reduced in mixed strain $Cftr^{tm1Kth}/Cftr^{tm1Kth}$ mice, homozygous for the ΔF508 mutation (Kelley and Drumm 1998). In addition, mice deficient in iNOS are more susceptible to infection with *Listeria monocytogenes* (MacMiking *et al* 1995), while wild type BALB/c mice treated with the iNOS inhibitor aminoguanidine are less able to clear a pulmonary dose of *P. aeruginosa* (Kelley and Drumm 1998). Thus, it has been suggested that iNOS related antimicrobial activity may be compromised in CF, resulting an in increased susceptibility to lung infection.

1.5.4 The role of the submucosal glands

The submucosal glands are found in the cartilaginous airways of the human respiratory tract, located in the submucosa, between the cartilage and the epithelium (reviewed in Pilewski and Frizzell 1999). It has been estimated that there are approximately 5000 glands in the adult human bronchial tree. The glands are tubuloacinar, with a duct opening onto and continuous with the airway epithelium. The glandular acini are composed of both mucous and serous cells, the secretions of which contribute to the ASL. The serous cells demonstrate the highest level of expression of CFTR in the airways (Engelhardt *et al* 1992) and secrete fluid containing a variety of antimicrobial agents, such as lysozyme, lactoferrin and β-defensins. The mucous cells are the major source of mucin in the airways. The most distal end of the gland is composed of serous acini (Meyrick *et al* 1969). Their secretions must pass through the mucus tubules, where the mucin, secreted by the mucous acini, may be hydrated and moved on. This mixture moves through the collecting ducts, to the ciliated ducts and finally onto the tracheal surface epithelium.

The role of CFTR in fluid secretion and/or ion reabsorption in the submucosal glands is not clear. Nor are the relative contributions of the surface epithelium and submucosal glands to the ASL. However, a recent study using porcine bronchi reported that fluid secretion was driven by CFTR and predominantly produced by the submucosal glands (Ballard *et al* 1999).

The earliest pathological findings in CF infants have been reported to be mucus inspissation, obstruction and dilatation of the submucosal glands newborns (Esterly and Oppenheimer 1968). It is it is clear that submucosal glands have the capacity to play a critical role in the development of CF lung disease. Inadequate hydration of the submucosal gland secretions could lead to the development of this pathology and contribute to a failure of mucociliary clearance mechanisms. Furthermore, failure of fluid and ion transport regulation in the production of ASL by the submucosal glands could contribute to dysfunction of salt sensitive antimicrobial components of the ASL. As a result the submucosal glands are now the focus of considerable attention, as studies aim to elucidate their role in the pathogenesis of CF lung disease.

The potentially critical role of the submucosal glands in the development of CF lung disease is important to consider in the interpretation and extrapolation of results from model systems. Despite frequent references to the contrary, submucosal glands are present in murine airways. However, unlike the human, these glands are predominantly localised in the most proximal part of the trachea and do not extend into the bronchi (Borthwick *et al* 1999). In the case of primary culture models of airway epithelium, no submucosal glands are present. This may affect the ability of these cultures to accurately reflect the *in vivo* situation in the airways.

1.6 The innate lung defence system

The adaptive immune system is relatively new in evolutionary terms and co-exists in higher animals with a more basic innate immune system (Ganz and Lehrer 1995). Recent studies have focused considerable attention upon the latter and in particular the role of antimicrobial peptides. Professional phagocytic cells ingest microbes into vacuoles and kill them using both oxidative mechanisms and antimicrobial peptides, stored within microbicidal organelles. Such antimicrobial peptides are also secreted by epithelial cells and constitute an initial barrier to infection. This innate immune system is not only the first line of defence, but may also determine the antigens to which the acquired immune system will respond and the nature of that response. The ASL contains a host of antimicrobial compounds, including defensins, cathelicidin, lysosyme, lactoferrin, SLPI and collectins (Ganz 1998).

The discovery that the ASL from primary cultures of airway epithelium displayed a salt-sensitive antibacterial activity (Smith *et al* 1996) prompted additional interest in the components of the innate lung defence system. The "hypotonic /defensin" theory proposes that CFTR dysfunction directly affects the ionic composition of the ASL, thus compromising the antimicrobial activity of the salt sensitive first line of lung defence. This protection breached, the organisms would have a better chance of colonising the lung. In addition it is possible that a compensatory response from other elements of the defence mechanism may occur, resulting in an increased neutrophil influx, the release of damaging elastase, cytokine imbalance and the triggering of inflammatory cascades, while cell - bacteria interactions may select for specific organisms.

The initial studies demonstrated that the antibacterial activity of the ASL was compromised by raised NaCl levels, that the antibacterial agent had a low molecular weight and that it was heat stable. However, the key

components of the innate lung defence involved were not identified. A subsequent report, utilising the bronchial xenograft model, confirmed the results of the earlier study and demonstrated restoration of antibacterial activity after adenoviral delivery of *CFTR* to the CF cells (Goldman *et al* 1997). This study implicated human β-defensin-1 (HBD-1), demonstrating expression throughout the airways and salt-sensitive antibacterial activity. Furthermore, the antibacterial properties of the ASL were reported to be largely abolished following the ablation of HBD-1 expression using antisense DNA. As a result of this report, considerable attention has been placed on the role of β defensins in CF. However, more recent results have suggested that while HBD-1 may play an important role it is unlikely to be wholly responsible for the CF lung phenotype and that there are many antibacterial components of the ASL worthy of investigation.

1.6.1 Defensins

Naturally occurring cationic peptides with broad spectrum antimicrobial activities have recently been discovered to contribute to the host defences of animals, insects and plants (reviewed in Lehrer and Ganz 1999, Huttner and Bevins 1999, Hancock 1997). These peptides are less than 100 amino acids (and generally < 35) and include defensins and cathelicidins.

1.6.1.1 Defensin structure

Defensins are small, 3-4 kDa peptides characterised by the presence of 6 cysteines, stabilised by disulphide bonds (reviewed in Ganz and Lehrer 1995). These peptides are cationic, due to the presence of the amino acids arginine and lysine. They are classified on the basis of the spacing and the

connectivity of their cysteines. In animals the two main types are α-defensins, in which the cysteines are linked 1-6, 2-4, 3-5, and β-defensins in which the cysteines are linked 1-5, 2-4, 3-6 (see Figure 1.7). Despite these differences defensins share a similar cationic β-sheet-rich amphipathic secondary structure, stabilised by the disulphide bridges. A hydrophobic region is spatially separated from the cationic region of the peptide (Ganz 1999). This structure is thought to be critical to the mechanism of action of these peptides and is conserved despite many naturally occurring amino acid substitutions within different defensins. A recent report suggested that the potency of antimicrobial peptides might correlate with the hydrophobicity gradient rather than the charge of the peptide (Travis *et al* 1999a).

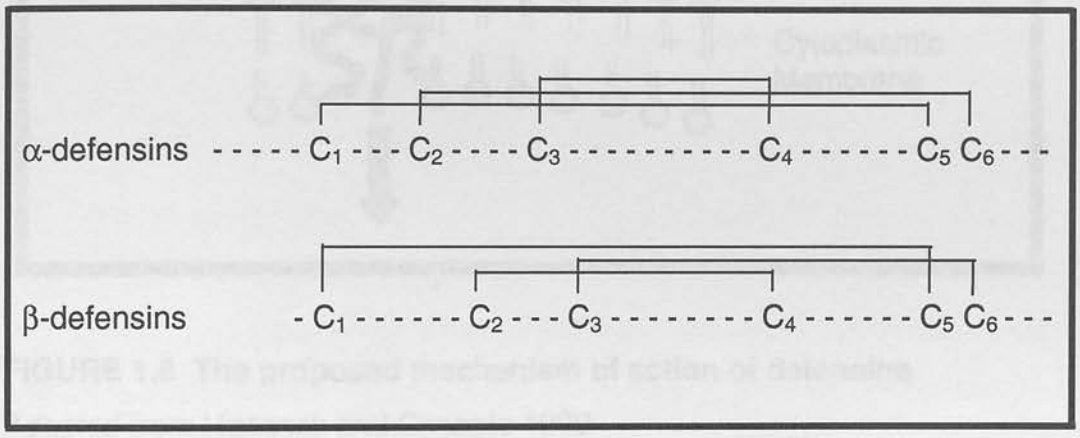

FIGURE 1.7 Defensin structure

The spacing and connectivity of cysteines in α- and β-defensins

1.6.1.2 Defensins – mode of action

The mode of activity of antibacterial peptides remains the subject of investigation. However, the current model suggests a 2 stage process in which peptides disrupt the membrane of the target cell then enter the cell

and interfere with its metabolic function in an as yet unspecificed manner (see Figure 1.8).

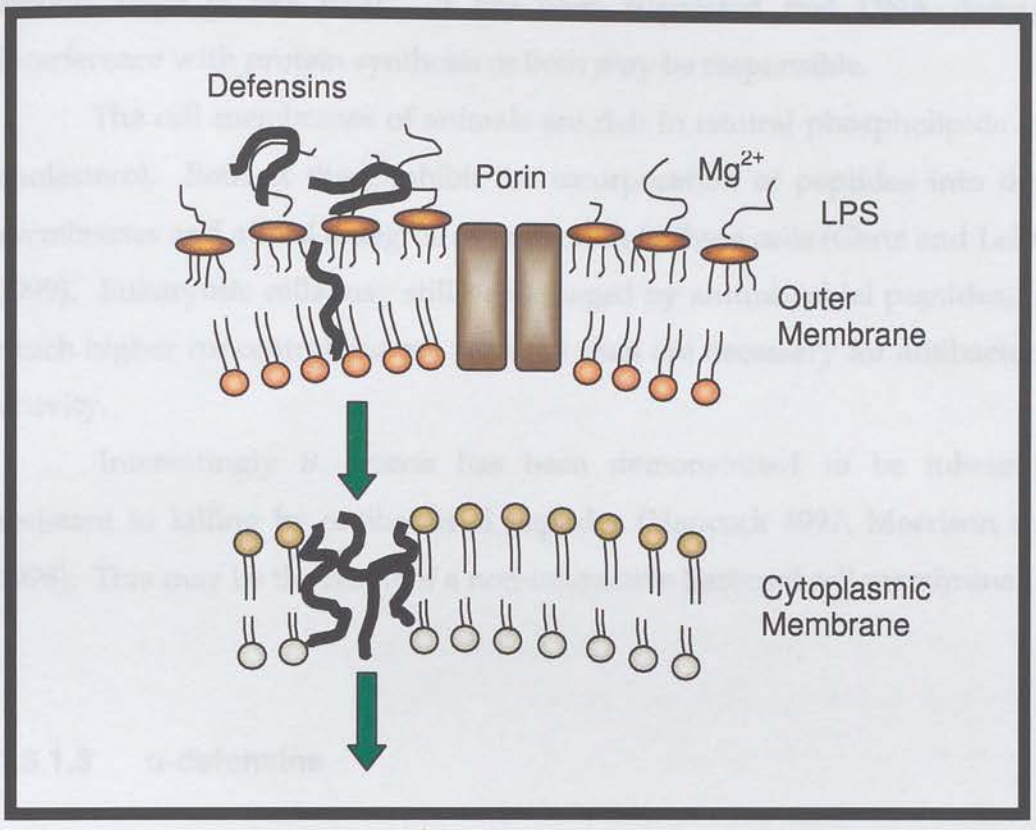

FIGURE 1.8 The proposed mechanism of action of defensins
Adapted from Hancock and Chapple 1999.

In the case of gram negative bacteria the peptides must breach both the outer and the cytoplasmic membranes. Only the latter is required for gram positive organisms. In the first stage, the positively charged peptides interact with the negatively charged divalent cation binding sites on the surface LPS, competitively displacing these ions. This disrupts the normal barrier of the outer membrane leading to self-promoted uptake (Hancock 1997). The peptides then insert into the cytoplasmic phospholipid membrane with the hydrophobic region in the membrane interior, while the cationic region interacts with the anionic phospholipid head groups. These peptides

are thought to assemble into multimeric pores, disrupting the membranes. However, at this stage the process is still reversible. Peptides subsequently enter the cell and produce irreversible damage. The mode of action of this second stage is less clear. It has been suggested that DNA damage, interference with protein synthesis or both may be responsible.

The cell membranes of animals are rich in neutral phospholipids and cholesterol. Both of these inhibit the incorporation of peptides into these membranes and afford a degree of protection to these cells (Ganz and Lehrer 1999). Eukaryotic cells may still be damaged by antimicrobial peptides, but much higher concentrations are required than are necessary for antibacterial activity.

Interestingly *B. cepacia* has been demonstrated to be inherently resistant to killing by antibacterial peptides (Hancock 1997, Morrison *et al* 1998). This may be the result of a non-interactive bacterial cell membrane.

1.6.1.3 α-defensins

The genes that encode for the α-defensins and the β-defensin families are clustered on chromosome 8p23 in humans (and the *Defcr* locus on proximal chromosome 8 in the mouse (Huttner *et al* 1997, Bals *et al* 1998a, Morrison *et al* 1998, Morrison *et al* 1999, Bals *et al* 1999)) and are thought to share common ancestry (Linzmeier *et al* 1999). However the two groups have evolved some major differences.

The α-defensins are initially synthesized as prepropeptides (Ganz and Lehrer 1995). These have a characteristic amino-terminal signal sequence for insertion into the endoplasmic reticulum, a propiece and the mature peptide at the carboxy-terminal. The propiece is anionic in nature and neutralises the cationic end of the peptide. This has been proposed as a mechanism to prevent spurious interactions with other proteins or the lipid

membrane and to facilitate folding. The α-defensins do not display antibacterial activity until cleavage has occurred to create the mature peptide (Valore *et al* 1994).

Once the mature peptide is formed, α-defensins have been reported to display broad spectrum antibacterial activity over the range of 1-100 μg/ml. This activity has been demonstrated against gram positive and gram negative bacteria, fungi and enveloped viruses, and to be inhibited by cations (reviewed in Ganz and Lehrer 1995). In addition, a host of other putative functions have been attributed to these peptides, including the induction of IL-8 and SLPI from epithelial cells, a role in the reduction of glutathione levels and the inhibition of cortisol secretion by the adrenal gland (reviewed in van Wetering *et al* 1999).

There are currently six α-defensins identified in humans (reviewed in van Wetering *et al* 1999). Human neutrophil peptides (HNP) 1–4 are found in the azurophilic granules of neutrophils. HNP1-3 make up 5-7% of total neutrophil protein and 30–50% of the protein content of the azurophilic granules, making them the most abundant neutrophil proteins. Neutrophils engulf microbes into vacuoles and kill them using either; oxygen dependent mechanisms, in which the respiratory burst produces superoxide anions, hydrogen peroxide and other oxidative metabolites, or antibacterial peptides. Thus HNPs are thought to act primarily at high concentrations in phagolysosomes. Human defensins (HD) 1 and 2 are found in the secretory granules of Paneth cells, where they are proposed to protect intestinal stem cells in the crypts from infection.

Although mice have been demonstrated to have an extended family of α defensins produced by Paneth cells in the intestine, called cryptidins, studies suggest that no α-defensins are present in murine neutrophils (Eisenhauer and Lehrer 1992). A recent study demonstrated that activation of cryptidins, by cleavage of the pro-region, was dependent upon matrilysin, a matrix metalloproteinase localised in the Paneth cells (Wilson *et al* 1999).

Matrilysin-deficient transgenic mice were found to have significantly impaired antimicrobial activity in studies of small intestinal extracts, isolated crypts stimulated with cholinergic agonists to produce Paneth cell degranulation and the gastrointestinal tract *in vivo*, using an oral infection model. In addition, the 50% lethal dose of *Salmonella typhimurium* for matrilysin-deficient transgenic mice was found to be a tenth of that for wild-type littermates. These studies demonstrate the important role of mature defensins in the murine gastrointestinal system.

1.6.1.4 β-defensins

The β-defensins were first described in cattle, with thirteen β-defensins expressed in bovine granulocytes and two in the bovine trachea (tracheal antimicrobial peptide (TAP) and lingual antimicrobial peptide (LAP)). Similar peptides have now been reported in a variety of other animals including humans and mice. The genes that encode for the β-defensin families are on chromosome 8p23 in humans and in the *Defcr* locus on proximal chromosome 8 in the mouse.

The β-defensins are also initially synthesised as prepropeptides. However, unlike the α-defensins, the cleavage of the propiece does not appear to be necessary for antimicrobial activity. Indeed, multiple isoforms of HBD-1 have been reported in kidney tissue and urine, with different amino terminal trunctations (Valore *et al* 1998). While the most common form (the 36 aa peptide) was the most potent and the least salt sensitive, all forms were reported to show differing profiles of antibacterial activity and salt sensitivity. These results imply that the proregion of β-defensins does not have an inhibitory role. In addition, this study synthesised defensins using a baculovirus system and demonstrated variation between cell lines in

the processing of HBD-1. This raisies the possibility that the post-translational modifications of defensins may occur in a cell specific manner.

In addition to their salt sensitive antibacterial activity, a recent report raised the possibility that, like α-defensins, the β-defensins may play a role as signalling molecules (Yang *et a*l 1999). This study reported that human β-defensins, in submicromolar concentrations, can attract memory T-cells and immature dendritic cells to the sites of infection, promoting adaptive immunity.

There are two β-defensins known in humans; HBD-1 and HBD-2. The dysfunction of the former has been suggested to play a critical role in the development of CF lung disease (Goldman *et al* 1997). HBD-1 was originally isolated from human blood filtrate as a 36 aa, 3.9 kDa peptide (Bensch *et al* 1995). The gene encoding HBD-1 (*HBD-1)* was cloned, located roughly 100–150 kb from *HNP-1* and shown to be over 7 kb. It has a large intron of 6962 bp and two exons (Liu *et al* 1997, McCray and Bentley 1997). The first exon is 128 bp and encodes the signal sequence and propiece, while the second exon is 234 bp and encodes the mature peptide. *HBD-1* expression has been demonstrated to be maximal in the urogenital tract and the kidney, but is also present in the trachea, submucosal glands, bronchus, nasal epithelium, salivary gland, pancreas, prostate, testes and small intestine (Zhao *et al* 1996, Goldman *et al* 1997, McCray and Bentley 1997) (see Table 1.7). No difference in the levels of expression have been observed in tissue from CF individuals when compared to non-CFs. It is not expressed prenatally, nor upregulated in response to inflammatory stimuli. hBD-1 synthetic peptides have been shown to display salt sensitive antimicrobial activity against *P. aeruginosa* (Goldman *et al* 1997, Morrison *et al* 1998, Singh *et al* 1998) in isolation, *in vitro.*

The second human β-defensin, HBD-2, was isolated from psoriatic human skin as a 41 aa peptide with 39% identity to HBD-1 at the amino acid level. It has been shown to have antibacterial activity against gram negative bacteria and *candida albicans* (Harder *et al* 1997) and to be approximately ten

times more potent than HBD-1 (Singh *et al* 1998). These studies have demonstrated that the salt sensitivity of this activity can be overcome by increasing the concentration of the peptide. The gene encoding HBD-2 (*HBD-2*) is smaller, at 1610 bp, with two exons (Bals *et al* 1998b, Liu *et al* 1998). The first exon is 81 bp and encodes the signal sequence. The second exon is 238 bp and encodes the mature peptide and a short segment of the propeptide. *HBD-2* is located approximately 100-600 kb centromeric of *HBD-1* on chromosome 8. The DNA sequence of *HBD-2* revealed four NFκB binding sites in the UTR. Such elements are not found in *HBD-1* but are observed in the *TAP* and *LAP* genes, which are upregulated in response to inflammatory stimuli (Russell *et al* 1996). This upregulation has also been demonstrated for *HBD-2* (Harder *et al* 1997, Bals *et al* 1998b, Liu *et al* 1998, Singh *et al* 1998). It is expressed in inflamed skin, but not in uninflamed skin. High levels have also been demonstrated in the respiratory tract, particularly in the epithelium of the proximal conducting airways and the serous tubules of the submucosal glands. *HBD-2* has also been reported in the urogenital tract, salivary gland and uterus (see Table 1.7). Expression has been observed in tissue from both CF and non-CFs individuals, but the concentration of HBD-2 in BAL collected from colonised CF individuals was found to be raised (Singh *et al* 1998).

Despite the reported absence of α-defensins in murine neutrophils, four murine β-defensin genes have been reported; *Defb1* (or *mBD-1*), *Defb2*, *mBD-3* and *mBD-4*. These genes are all localised to the *Defcr* locus on proximal chromosome 8 in the mouse, the conserved syntenic region of which is at chromosome 8p23 in humans. Aspects of the characterisation of mBD-1 peptide will be detailed in Chapter 6.

The first murine β-defensin gene (*Defb1* or *mBD-1*) was found by homology to *HBD-1* (Huttner *et al* 1997, Bals *et al* 1998a, Morrison *et al* 1998). *Defb1* has two exons and a 15 kb intron. The first exon encodes the signal sequence and part of the propiece, while the second encodes the rest of the

propiece and the mature peptide. The 204 bp open reading frame encodes a 69 aa prepropeptide, with 51% identity to HBD-1 and 36% identity to HBD-2. Constitutive *Defb1* expression has been shown in the epithelia of the proximal conducting airways, the kidney, tongue, heart and reproductive tract (see Table 1.7). It has also been shown to display salt-sensitive antibacterial activity against a range of microbes.

The gene for murine β-defensin-2 (*Defb2*) was recently identified, with exon /intron boundaries at the same site as *Defb1* (Morrison *et al* 1999). It encodes a 71 aa prepropeptide, with a 41% identity to mBD-1, a 34 % identity to HBD-1 and 30% identity to HBD-2. The DNA sequence did not reveal any relevant regulatory control elements in the UTR, however expression was shown to be upregulated in response to LPS. *Defb2* expression was demonstrated in the kidney and uterus and found to be induced in the trachea after exposure to pro-inflammatory stimuli (see Table 1.7).

The murine β-defensin-3 gene (*mBD-3*) demonstrates a similar intron/exon structure with a 1.7 kb intron and has an NFκB binding site in the 5′ UTR (Bals *et al* 1999). It encodes a 64 aa prepropeptide with 40% homology to HBD-2. Unlike all the other murine and human β-defensins, mBD-3 does not display identical spacing of the cysteine residues, with one less residue between cysteines 2 and 3. It is expressed at low levels in the lung, gastrointestinal tract, salivary gland and reproductive tract with induction observed in the airway epithelium and liver after lung instillation of *P. aeruginosa* (see Table 1.7). Baculovirus expressed mBD-3 has been demonstrated to have antibacterial activity against *E. coli* and *P. aeruginosa*, although salt sensitivity has not been described.

A further member of this gene family, *mBD-4*, was recently reported, encoding the mBD-4 β-defensin (Jia *et al* 1999). This peptide shares 45% identity with HBD-2. It is likely that further members of the family are still to be discovered within this gene cluster.

Tissue	*HBD-1*	*HBD-2*	*Defb1*	*Defb2*	*mBD-3*
Skin	+	++++*	NR	NR	NR
Lung	+	++++*	++	NR	++*
Trachea	+	++++*	++++	+*	++*
Gut	++	-	NR	NR	+
Salivary	+	-	NR	NR	+
Urogenital	++++	+	+	+	NR
Kidney	++++	-	++++	++	NR
Liver	+	-	++	NR	++*
Heart	NR	NR	+	+	NR

TABLE 1.7 Expression pattern of β-defensins in humans and mice.

+ expression, - no expression, NR - not reported, * in response to proinflammatory stimuli

The role of β-defensins in the development of CF lung disease remains uncertain. While one study implicates the dysfunction of HBD-1 as critical to the innate immune system, this is difficult to reconcile with the low concentrations estimated in the ASL (see Table 1.8). However, HBD-2 is upregulated in response to inflammatory stimuli, demonstrates ten times the potency of HBD-1, *in vitro*, and may be present at antibacterial concentrations in the ASL (Singh 1998). The defensin concentrations estimated in ASL may of course be inaccurate. The collection of the ASL *in vivo* has proved extremely challenging (see section 1.5.1.3) and the process of collection may significantly alter the composition of the collected fluid. In addition, it is possible that the charged nature of antimicrobial peptides may cause them to accumulate locally at epithelial surfaces or at the mucus interface and consequently distort attempts to quantify their concentration. These peptides may therefore be present at much greater concentrations localised within a particular phase of the ASL.

Establishing the roles of individual components of the ASL is complicated by synergistic interactions (Singh and Welsh 1997, Bals *et al* 1998b) as well as technical difficulties in the estimation of *in vivo* concentrations. This impact of synergy between all the antibacterial agents within the ASL has yet to be fully established, as have the signalling properties of defensins. The discovery of a homologous family of β-defensins in the mouse provides the opportunity to study the roles of these peptides in a murine model and the characterisation of defensin knockout mice may provide further illumination.

	Travis *et al* 1999b	Schnapp *et al* 1998	Singh *et al* 1998		Ganz 1998
	non-CF	non-CF	non-CF	CF	non-CF
Lysozyme	0.7 μg/ml	-	0.75 -10 μg/ml		2 -16 μg/ml
Lactoferrin	0.9 μg/ml	-	-	-	-
SLPI	0.1 - 2 μg/ml	-	-	-	-
HBD-1	-	-	≤ 2 ng/ml		0.2 – 2 ng/ml
HBD-2	-	-	0.1 -10 ng/ml	10 -100 ng/ml	
Cathelicidin LL37/hCAP-18	-	-	-	-	-
HD1-3	-	86 – 143 ng/ml	-	-	-

TABLE 1.8 Estimated concentrations of antibacterial components of ASL in BAL (estimated ~ 100 fold dilution of ASL)

1.6.2 Other antibacterial components of the ASL

The primary focus of research into the antibacterial properties of the ASL has concerned the role of defensins. However, these peptides are actually a fairly minor component of the ASL (see Table 1.8), which also contains, lysozyme, lactoferrin, SLPI, elafin, cathelicidin and collectins. All of these components have been proposed to have antibacterial activity and have the potential to be involved in the development of CF lung disease.

1.6.2.1 Lysozyme

Lysozyme is a component of both the phagocytic and secretory granules of neutrophils and is produced by macrophages and airway epithelial cells, particularly the serous cells of the submucosal glands. It is the most abundant antimicrobial protein found in BAL (Travis *et al* 1999b), at 0.7–10 μg/ml. It is a 14 kDa enzyme directed against peptidoglycan, a structurally important component of the bacterial cell wall. Lysozyme displays potent, salt sensitive antibacterial activity against many gram positive and gram negative organisms (Travis *et al* 1999b). However, reports suggest that lysozyme may only be bacteriostatic against *P. aeruginosa*, with these bacteria able to recover from this insult with time (Ganz 1998). It has been proposed that a "second hit" in the form of β-defensins may be required or that removal by mucociliary clearance might be expected prior to this recovery *in vivo*. Thus, while the role of lysozyme in CF airways may be directly compromised by a high salt environment, it may also be affected by defensin dysfunction and /or a mucociliary clearance defect.

1.6.2.2 Lactoferrin

Lactoferrin is another abundant antibacterial component of the ASL. It is an 80 kDa iron-binding protein, closely related to transferrin, present both in neutrophils and airway epithelial secretions. It inhibits bacterial growth by sequestering iron, but also has a direct, salt-sensitive, antimicrobial activity due to its amino terminal cationic fragment. It is less potent than lysozyme but is present in antibacterial concentrations in BAL (Travis *et al* 1999(b)). The direct antibacterial role of lactoferrin may be compromised in CF airways by a high salt environment.

1.6.2.3 Protease inhibitors

SLPI and elafin are antiproteases secreted by the airway epithelial cells (see section 1.5.3.2), both of which have been demonstrated to have antibacterial activity *in vitro*. In the case of SLPI, the carboxy-terminal domain acts as an inhibitor of NE and the amino terminal has modest antibacterial activity (Hiemstra *et al* 1996). This activity has been shown to display salt-sensitivity (Travis *et al* 1999b). The majority of the antibacterial activity of elafin also resides in the amino terminal domain, but it displays more potent activity than SLPI at all doses tested *in vitro* (Simpson *et al* 1999). In both cases, the full length molecule demonstrated greater antibacterial activity than either terminal fragment.

1.6.2.4 Cathelicidin

The cathelicidins are a large family of antimicrobial peptides with a conserved amino-terminal domain of roughly 100 aa and highly heterogeneous carboxy-terminal peptide sequences of 10-40 aa. In some

cathelicidins the full molecule displays antibacterial activity, whereas in other cases proteolytic cleavage of the active carboxy-terminal peptide is required. The only known human cathelicidin is hCAP-18, a 140 aa precursor to LL-37, the mature 37 aa peptide. LL-37/hCAP-18 has been demonstrated in neutrophil granules and is expressed in a wide range of tissues, highest in the bone marrow. In the lungs it is expressed by the airway epithelial cells, the serous and mucus cells of the submucosal glands and has been identified in BAL. Synthetic LL-37 has been shown to have broad spectrum, salt-sensitive antibacterial activity *in vitro* and to display synergy with lactoferrin (Bals *et al* 1998c). Thus, LL-37/CAP-18 may be compromised in a high salt ASL and also has the potential to play a role in the development of CF lung disease.

1.6.2.5 Collectins

The collectins are a family of polypeptides involved in mammalian host defences that includes surfactant proteins SP-A and SP-D and mannose binding lectin. They are the most abundant proteins found in lavages of the distal lung and constitute an important part of the innate lung defence system (Whitsett 1999).

SP-A and SP-D are produced by alveolar type II cells, the non-ciliated epithelial cells of the airways and by the submucosal glands. SP-A has been demonstrated to form multimeric structures and bind to bacteria and receptors on alveolar macrophages *in vitro*. It is also proposed to stimulate macrophage chemotaxis. SP-A knockout mice have been shown to display increased susceptibility to pulmonary infections with various pathogens, including *P. aeruginosa*, leading to airway inflammation, neutrophilic infiltrates and cytokine induction (LeVine *et al* 1998). In addition, alveolar macrophages from SP-A knockout mice displayed impaired phagocytosis of these pathogens. SP-D knockout mice have been reported to develop

progressive severe pulmonary emphysema and fibrosis from the age of three weeks with marked lung restructuring and accumulation of lymphocytes. These mice also display a failure of the respiratory burst in alveolar macrophages (Whitsett 1999).

The antibacterial activity of the collectins has not been proposed as salt sensitive in nature. However they may play an important role in the innate lung defence and as such dysfunction of these lectins would be expected to impact upon CF lung disease. Indeed, mutations in the *MBL* gene have recently been proposed as genetic modifiers of the CF lung disease phenotype (see section 1.3.5).

1.7 Mouse models of Cystic Fibrosis

1.7.1 The murine *Cftr* gene

The murine homologue of the human *CFTR* gene (*Cftr*) was isolated, on mouse chromosome 6, in 1991 (Tata *et al* 1991). The genomic region has recently been sequenced and comparative analysis performed with human *CFTR* (Ellsworth *et al* 2000). The *Cftr* gene spans ~152 kb, with all 27 exons highly similar to the human homologue at the sequence level. The intron and exon structure of the two homologues is mostly the same, with splice sites occurring at identical positions in both. The genomic sequence is reported to be highly conserved throughout, including large intronic segments, raising the possibility that they serve functionally important roles. The putative regulatory elements ~10 kb upstream of *CFTR* exon 1 are well conserved in *Cftr*. Interestingly, the polymorphic polyT tract located upstream of CFTR exon 9, implicated in Class 5 splicing defects (see section 1.3.3), is absent in murine *Cftr*.

The murine CFTR protein is very similar to the human (78% overall sequence identity at the amino acid level), particularly in the two nucleotide binding folds. The majority of known CF mutations occur in well conserved regions, suggesting conservation of function across species. The predicted mouse protein has a phenylalanine residue corresponding to that deleted in the common ΔF508 mutation, flanked by a 28 amino acid region identical to man. The putative first extracellular domain, implicated in the internalisation of *P. aeruginosa* (see section 1.5.2.2), is also well conserved with 13 of the 15 amino acids identical.

The degree of homology between human *CFTR* and mouse *Cftr* and the existence of the necessary molecular techniques made the development of mouse models of CF a viable proposition and established an array of novel investigative approaches in the study of CF.

1.7.2 Creation of mouse models of CF

The first mouse models of CF were created within three years of the isolation of the *CFTR* gene, using gene targeting in embryonic stem cells to disrupt the *Cftr* gene (Snouwaert *et al* 1992, Dorin *et al* 1992). A further twelve mouse models of CF have been reported since, with varying degrees of characterisation (Ratcliff *et al* 1993, O'Neal *et al* 1993, Colledge *et al* 1995, Hasty *et al* 1995, van Doorninck *et al* 1995, Zeiher *et al* 1995, Delaney *et al* 1996, Rozmahel *et al* 1996, Dickinson *et al* 1998, Merrill *et al* 1998). These models fall, broadly, into two categories; those designed to grossly disrupt *Cftr* and those that aim to model clinical mutations, such as ΔF508, G551D and G480C.

Mouse	Mutation	*Cftr* mRNA	Original Strain
Cftr^{tm1Unc} Snouwaert *et al* 1992	Exon 10 Replacement	No wild type mRNA detectable	C57Bl/6/129P2/OlaHsd BALB/c/129P2/OlaHsd B6D2/129P2/OlaHsd
Cftr^{tm1Hgu} Dorin *et al* 1992	Exon 10 Insertional	10% of normal levels of wild type mRNA	MF1/129P2/OlaHsd
Cftr^{tm1Cam} Ratcliff *et al* 1993	Exon 10 Replacement	No wild type mRNA detectable	MF1/129P2/OlaHsd C57Bl/6/129P2/OlaHsd
Cftr^{tm1Hsc} Rozmahel *et al* 1996	Exon 1 Replacement	No wild type mRNA detectable	CD1/(129X1/SvJ x 129S1/Sv-) and others
Cftr^{tm1Bay} O'Neal *et al* 1993	Exon 3 Insertional Duplication	<2% of normal levels of wild type mRNA	C57Bl/6/129S7/SvEvBrd
Cftr^{tm3Bay} Hasty *et al* 1995	Exon 2 Replacement	No wild type mRNA detectable	C57Bl/6/129S7/SvEvBrd
Cftr^{tm2Cam} Colledge *et al* 1995	ΔF508 Exon 10 Replacement	Mutant mRNA 30% of normal expression levels	C57Bl/6/129P2/OlaHsd
Cftr^{tm1Kth} Zeiher *et al* 1995	ΔF508 Exon 10 Replacement	Decrease in mutant mRNA levels in intestinal tract	C57Bl/6/129S6/SvEv
Cftr^{tm1Eur} Van Doorninck *et al* 1995	ΔF508 Exon 10 Insertional "Hit and Run"	Mutant mRNA expression at normal levels	FVB /129P2/OlaHsd
Cftr^{tm1G551D} Delaney *et al* 1996	G551D Exon 11 Replacement	Mutant mRNA 53% of normal expression levels	CD1/(129X1/SvJ x 129S1/Sv-)

TABLE 1.9 Mouse models of CF

The first mouse models were designed to be "knockouts", disrupting the *Cftr* gene to create absolute nulls, with no normal CFTR production. Different gene targeting strategies were used to create the various mouse models. The first strategy was a replacement gene targeting, designed to replace an exon of *Cftr* with disrupted homologous sequence. This method produced absolute nulls by replacing exon 10 (*Cftr*^{tm1Unc} (Snouwaert *et al* 1992), *Cftr*^{tm1Cam} (Ratcliff *et al* 1993)), exon 2 (*Cftr*^{tm3Bay} (Hasty *et al* 1995)) or exon 1

(*Cftr*^{tm1Hsc} (Rozmahel *et al* 1996)). In these mutants there is no mechanism for the production of wild type CFTR. The second strategy was replacement gene targeting, to generate duplication of exon sequences in either exon 10 (*Cftr*^{tm1Hgu} (Dorin *et al* 1992)) or exon 3 (*Cftr*^{tm1Bay} (O'Neal *et al* 1993)). The use of this strategy produced insertion into the target gene without loss of genomic sequence. Thus, in theory, these mutants retain the potential for reversion to wild type and the production of normal *Cftr* mRNA by various mechanisms. In the *Cftr*^{tm1Bay}/*Cftr*^{tm1Bay} mouse, duplication of the intact exon produced a frameshift and premature stop codon. In this mutant less than 1-2% of normal levels of wild type mRNA were reported and the phenotype was as severe as the other "null" mice. However, in the *Cftr*^{tm1Hgu}/*Cftr*^{tm1Hgu} mouse, in which there is introduction of an incomplete exon 10 running into plasmid sequence containing stop codons, exon skipping and aberrant splicing result in ~10% of normal levels of wild type mRNA expression (Dorin *et al* 1994). This has resulted in the description of this mutation as "residual function". The low level of normal CFTR may be responsible for significant phenotype differences observed between the *Cftr*^{tm1Hgu}/*Cftr*^{tm1Hgu} mouse and the absolute nulls (see section 1.7.3). However, human compound heterozygotes, such as R347P/ΔF508 or R117H/ΔF508, are predicted to retain approximately 15% and 7.5% of normal CFTR function respectively (Sheppard *et al* 1993). These individuals are still diagnosed as having CF and although pancreatic sufficient, can develop severe lung disease.

The second wave of mouse models of CF focused on accurately reproducing known clinical mutations. The replacement gene targeting strategy was used to created two models of the ΔF508 mutation (*Cftr*^{tm2Cam} (Colledge *et al* 1995)) and *Cftr*^{tm1Kth} (Zeiher *et al* 1995)) the G551D model (*Cftr*^{tm1G551D} (Delaney *et al* 1996)) and mouse models of the R117H and Y122X mutations (Merrill *et al* 1998). The other ΔF508 model (*Cftr*^{tm1Eur} (van Doorninck *et al* 1995)) and the G480C model (*Cftr*^{tm2Hgu} (Dickinson *et al* 1998) were created using a double homologous recombination ("Hit and Run")

procedure (Hasty *et al* 1991). This elegant technique produces a mutated exon without selection marker genes or plasmid sequences in the intronic structure of the gene. The presence of such intronic "debris" may be responsible for unwanted effects of transcriptional interference in the other models. In one study a mouse model containing only a neomycin resistance gene in intron 4 was established as a control line (Merrill *et al* 1998). Preliminary data suggested that this was sufficient to reduce the expression of wild-type *Cftr* mRNA to 10% of normal levels and produce an abnormal phenotype similar to other mouse models of CF (Merrill, personal communication).

1.7.3 Phenotype

The phenotypes of the different mouse models of CF bear most of the same hallmarks, however important differences have been observed. These phenotype variations have been shown to relate to the specific mutation, to environmental influences and to independently segregating modifier genes. The level of significance now attached to such phenotype modifiers was not evident during the initial characterisation of the many mouse models of CF. As a result, direct comparisons between the different models must be made with considerable care and with attention to the environmental conditions and background strain (see Table 1.9). The models in which the majority of significant studies have been performed are the $Cftr^{tm1Hgu}$, $Cftr^{tm1Unc}$ and $Cftr^{tm1Hsc}$, thus special attention will be paid to their characterisation.

1.7.3.1 Survival

	Mutation	Perinatal death	Adulthood	Body weight
Human	ΔF508	10% MI	20% DIOS	Impaired
Mouse	*Cftr*^{tm1Unc}	50% by day 7 40% death at weaning	<5% survival to adulthood	10 – 50% reduction
	Cftr^{tm1Hgu}	5% by day 7 2% death at weaning	90% survival to adulthood	No reduction
	Cftr^{tm1Cam}	80% by day 7 10% death at weaning	<5% survival to adulthood	50% reduction
	Cftr^{tm1Hsc}	55% by day 7 20% death at weaning	25% survival to adulthood	delayed
	Cftr^{tm1Bay}	40% by day 7 10% death at weaning	NR	70% reduction
	Cftr^{tm3Bay}	NR	40% survival at 1 month	reduced
	Cftr^{tm2Cam}	35% by day 16	<5% survival to adulthood	NR
	Cftr^{tm1Kth}	10% by day 7	40% survival to adulthood	50% reduction
	Cftr^{tm1Eur}	None	normal	20% reduction
	Cftr^{tm1G551D}	NR 67% survival at day 35 in SPF conditions 27% survival at day 35 in normal conditions		30 - 50% reduction

TABLE 1.10 Survival and body weight in mouse models of CF

Intestinal pathology and the resultant mortality appear to be the predominant hallmark of *Cftr* mutation in the mouse. The survival rates

reported in the initial characterisation of the different mouse models of CF vary from <5% in the *Cftr*^{tm1Unc}/*Cftr*^{tm1Unc} nulls, and similar rates in the majority of models, to ~90% in the *Cftr*^{tm1Hgu}/*Cftr*^{tm1Hgu} mice (see Table 1.10). The remaining 10% of *Cftr*^{tm1Hgu}/*Cftr*^{tm1Hgu} animals die around weaning as a result of intestinal obstruction, resembling meconium ileus. Interestingly, this is a similar proportion to the rate of meconium ileus in CF humans. The low level production of normal CFTR has been proposed to be the explanation for the significantly greater survival rate in the *Cftr*^{tm1Hgu}/*Cftr*^{tm1Hgu} mice. The results of a study addressing the relationship between the levels of intestinal *Cftr* mRNA, the electrophysiological profile and the survival rate, indicate that quite small corrections in gene activity can have marked electrophysiological and dramatic pathological consequences (Dorin *et al* 1996). The improved survival of the *Cftr*^{tm1Hgu}/*Cftr*^{tm1Hgu} mice provides obvious advantages for the study of large cohorts over longer time periods.

The mortality associated with intestinal disease has been reported to be manifest at two distinct periods; firstly within a few days of birth and secondly around the time of weaning to solid food (approximately 21 days). Study of the survival at these time points in the *Cftr*^{tm1Hsc}/*Cftr*^{tm1Hsc} mice, congenic on different inbred backgrounds revealed a modifier locus for intestinal phenotype in mouse models of CF (see section 1.7.4) (Rozmahel *et al* 1996). The high mortality at the time around weaning appears to result from the consumption of solid food, and the use of a liquid diet has been found to prolong the lifespan of *Cftr*^{tm1Unc}/*Cftr*^{tm1Unc} mice (Kent *et al* 1996). An alternative approach utilised the expression of human *CFTR* cDNA in the intestinal tract of these mice, under the control of the rat intestinal fatty acid-binding protein gene promoter. This has been demonstrated to correct the lethality of the intestinal defect in *Cftr*^{tm1Unc}/*Cftr*^{tm1Unc} mutant mice and lead to longer term survival, despite inappropriate cell-specific expression (Zhou *et al* 1994). However, concern persists about the confounding effects of CFTR

expression outwith the gastrointestinal system and follow-up studies have not been published.

These approaches prolong the survival of the *Cftr*^{tm1Unc}/*Cftr*^{tm1Unc} mice, providing increased cohort size and the potential for longer term study. However, it is important to appreciate that the minority of these null mutants survive, raising the possibility that some form of selection for less severely affected animals may occur. This is of particular importance where the mutation has not been bred to be congenic on an inbred strain. In addition, mice weaned on a liquid diet have been suggested to suffer the effects of malnutrition (Ip *et al* 1996) which may impact upon further phenotypic observations.

1.7.3.2 Intestinal disease

The most pronounced pathology in mouse models of CF has been reported in the gastrointestinal system. Variation between models has been reported in the specific pathology observed and the degree of severity. However, in most cases, characterisation of the mutant mice has revealed pathology similar to that initially reported for the *Cftr*^{tm1Unc}/*Cftr*^{tm1Unc} null mice (Snouwaert *et al* 1992). These observations include runting and failure to thrive, goblet cell hyperplasia, mucin accumulation, crypt dilation and intestinal obstruction (bearing similarity to meconium ileus), with resultant perforation, peritonitis and death. The *Cftr*^{tm1Hgu}/*Cftr*^{tm1Hgu} mice display a rather less severe phenotype, without runting or failure to thrive, however characteristic intestinal pathology is observed (Dorin *et al* 1992). Although characteristic pathology has been observed in the *Cftr*^{tm1G551D}/*Cftr*^{tm1G551D} mice, this model has been reported to display less mortality resulting from intestinal complications (Delaney *et al* 1996). It is interesting to note that compound heterozygote humans with G551D and ΔF508 mutations have a

lower incidence of meconium ileus than ΔF508 homozygotes (Hamosh *et al* 1992). The intestinal phenotype reported for the $Cftr^{tm1Eur}/Cftr^{tm1Eur}$ ΔF508 mouse is the least severe, with only a degree of runting and mild goblet cell hyperplasia observed (van Doorninck *et al* 1995). This is surprising in light of the phenotypes of other ΔF508 mouse models and CF individuals homozygous for ΔF508. The observations highlight the caution that must be used when interpreting the phenotype of mouse models of CF and the importance of clearly distinguishing between the different models and background strains utilised.

Studies characterising the electrophysiological profile of the intestines in mouse models of CF have found broadly similar phenotypes in the different models (Clarke *et al* 1992a, Dorin *et al* 1992, Ratcliff *et al* 1993, Clarke *et al* 1994, Colledge *et al* 1995, Hasty *et al* 1995, Smith *et al* 1995, van Doornick *et al* 1995, Zeiher *et al* 1995, Delaney *et al* 1996, Rozmahel *et al* 1996, Wilchanski *et al* 1996) (see Table 1.11). On the basis of this form of analysis mutant mice could be unequivocally distinguished from wild type littermates. Furthermore, these profiles closely model the electrophysiological phenotype in CF humans (reviewed in Grubb and Boucher 1999).

All of the mouse models of CF have been reported to display a significant decrease in the baseline potential difference (PD) and short-circuit current (I_{SC}) in the intestine. This is likely to be the result of a decreased rate of unstimulated chloride secretion. In addition, a complete absence, or a significant decrease, of cAMP-stimulated Cl^- secretion has also been reported in all of the models.

Mutation	Tissue	Baseline PD	cAMP-mediated Cl^- response	Ca^{2+}-related Cl^- response
CF Human	GI tract	←→ or ↑	↓	↓
Cftr^{tm1Unc}	jejunum caecum colon	↓	↓100%	↓
Cftr^{tm1Hgu}	jejunum	↓	↓65%	↓
	caecum	↓	↓65%	↓
Cftr^{tm1Cam}	caecum	↓	↓100%	NR
Cftr^{tm1Hsc}	rectum	NR	↓100%	↑
	* ileum	NR	↓100%	↑
Cftr^{tm1Bay}	ileum	←→	↓80%	NR
Cftr^{tm3Bay}	colon	NR	↓100%	↓
Cftr^{tm2Cam}	colon	↓	↓100%	↓
Cftr^{tm1Kth}	jejunum	←→	↓100%	NR
Cftr^{tmEur}	ileum	↓	↓66%	←→
Cftr^{tm1G551D}	jejunum	↓	↓99%	NR
	caecum	↓	↓95%	NR

TABLE 1.11 Intestinal electrophysiology in mouse models of CF

Comparison of the electrophysiological profiles of the intestinal epithelium in CF humans and mouse models of CF, on the original background strain. Increased (↑), decreased (↓) or preserved (←→) in comparison to non –CF controls. NR – Not reported. * Patch clamped isolated ileal crypt cells. See text for references.

While the "residual function" nature of the *Cftr*^{tm1Hgu} mutation may provide the explanation for the mild intestinal phenotype of the *Cftr*^{tm1Hgu}/*Cftr*^{tm1Hgu} mice (Dorin *et al* 1994), the improved survival rates of *Cftr*^{tm1G551D}/*Cftr*^{tm1G551D} mice and the mild nature of the intestinal disease in the *Cftr*^{tm1Eur}/*Cftr*^{tm1Eur} ΔF508 mice is less clear. Electrophysiological analysis of the intestines of *Cftr*^{tm1G551D}/*Cftr*^{tm1G551D} mice demonstrated a small Cl^- current, suggesting a low level of activity from the mutant CFTR (Delaney *et al* 1996), compatible with observations in G551D humans. It has been proposed that this may alleviate the severity of the phenotype. The *Cftr*^{tm1Eur}/*Cftr*^{tm1Eur} mice have also been shown to display a residual chloride permeability (van

Doorninck *et al* 1995), not observed in the intestinal tract of the other ΔF508 models. This may relate to the level of transcription from the targeted allele. Unlike the other ΔF508 models, the *Cftr*^{tm1Eur} mutation does not retain a selection cassette in the intron, with the capacity to impair transcription. In the presence of a greater amount of ΔF508 CFTR it is conceivable that a proportion may be correctly localised and display reduced function. Alternatively, or additionally, these phenotype observations may relate to the background strain used (see Table 1.9) or environmental conditions in different animal facilities. Indeed the survival rate of *Cftr*^{tm1Cam}/*Cftr*^{tm1Cam} mice has been reported to be much greater in Rotterdam than that reported in the literature for the same mice housed in Cambridge (van Doorninck *et al* 1995). This may relate to pathogen status of the facility, food, bedding or the founder mice sent to Rotterdam. The survival of *Cftr*^{tm1G551D}/*Cftr*^{tm1G551D} mice was also observed to be quite different when housed in a conventional non-SPF unit in comparison to an SPF facility (Delaney 1996).

1.7.3.3 Pancreatic disease

In CF disease in humans pancreatic insufficiency is a prominent manifestation of CFTR dysfunction. In contrast, pancreatic disease has not been convincingly demonstrated in most of the mouse models of CF. The only models in which any pancreatic disease has been observed are the absolute nulls. The initial characterisation of the *Cftr*^{tm1Unc}/*Cftr*^{tm1Unc} mice reported that 2 out of 5 mutant animals displayed a degree of acinar distention and the presence of eosinophilic material (Snouwaert *et al* 1992). While 5 out of 10 of the *Cftr*^{tm1Cam}/*Cftr*^{tm1Cam} mutants were reported to display dilatation and blockage of the small pancreatic ducts (Ratcliff *et al* 1993).

Subsequent studies have reached differing conclusions on the extent of pancreatic disease in these models. In one study, in which *Cftr*^{tm1Unc}/*Cftr*^{tm1Unc}

mice were weaned on a liquid diet, significant differences in pancreatic growth and specific enzyme activities were observed (Ip *et al* 1996). However, wild type controls showed similar, although less severe, abnormalities on this diet when compared to those on a solid diet. In conclusion, the abnormalities were suggested to be predominantly secondary to malnutrition. A further study, using a liquid elemental diet (Peptamen), reported luminal dilatation and the accumulation of zymogen granules at the apical pole of the ductal epithelial cells, in $Cftr^{tm1Unc}/Cftr^{tm1Unc}$ mice (DeLisle 1995). This phenotype has since been used, and corrected, in a study of the role of dietary fatty acids in CF. The role of the original diet in this phenotype may yet prove to be significant.

These observations suggest that there may be important differences between the human and murine pancreas with regard to the role of CFTR. Whereas high level expression of *CFTR* has been demonstrated in the human pancreas (Marino *et al* 1991), the level of expression of *Cftr* in the murine pancreas has been shown to be low (Snouwaert *et al* 1992). Furthermore, an alternative fluid secretory pathway which is activated by increases in intracellular calcium has been demonstrated in murine pancreatic cells (Gray *et al* 1995). These Ca^{2+}-activated Cl^- currents (CACC) can be observed in murine pancreatic duct cells which have no detectable CFTR. These CACC are a similar magnitude in mouse models of CF and wild type littermates, and are about 15 fold larger than CFTR currents. It appears likely that mouse models of CF do not develop significant pancreatic pathology, of the severity that occurs in the human disease, as a result of these physiological differences.

1.7.3.4 Reproductive Tissue

Most male patients with CF are infertile and a significant proportion of those with CVABD have class 5 mutations in CFTR, such as 5T (see section

1.3.3). These observations suggest that the male reproductive tract is particularly sensitive to CFTR dysfunction. High levels of expression of *Cftr* mRNA is reported in the murine testes and epididymis (Snouweart *et al* 1992). Female mice homozygous for the $Cftr^{tm1Unc}$, $Cftr^{tm1Cam}$ or $Cftr^{tm1G551D}$ mutations are infertile, while homozygote males have a reduced fertility. Both male and female mice homozygous for the $Cftr^{tm1Hgu}$ mutation are fertile, but have a reduced fertility, which is more pronounced in the females (Dorin, personal communication).

1.7.3.5 Lung disease

Lung disease is the primary concern for CF individuals, physicians and research scientists alike. Consequently, the value of mouse models of CF in dissecting the disease pathogenesis and developing novel therapies is largely dependent upon on the extent to which they mimic the lung disease seen in human CF patients.

Initial characterisation of the mouse models provided little indication of gross pulmonary abnormalities. These observations were greeted with some surprise. However, upon reflection, an expectation of mucus plugging, neutrophil accumulation and bronchiectasis in these mutant animals may be considered to be unrealistic. This is particularly true if bacterial interaction is required to initiate a cycle of infection and inflammation, given that most of these mutant animals were maintained in semi-sterile barrier facilities. Furthermore, the development of characteristic lung histopathology in CF individuals is a gradual process that occurs over years. The initial assessment of mouse models of CF was made after only a few weeks to months. Indeed, in the case of null mice, the vast majority died of gastrointestinal complications before a systematic assessment could be made. In this respect the prolonged survival of the $Cftr^{tm1Hgu}/Cftr^{tm1Hgu}$ mice proved to be particularly valuable.

Despite this apparent absence of pulmonary pathology, electrophysiological analysis of the mouse models of CF have been shown to clearly differentiate between mutants and wild type littermates (reviewed in Grubb and Boucher 1999). Studies have addressed both the bioelectric profile of the nasal epithelium (see Table 1.12) and that of the lower airways (see Table 1.13).

Mutation	Baseline PD	Amiloride response	cAMP-mediated Cl^- response	Ca^{2+}-related Cl^- response
CF Human	↑	↑	↓	←→
Cftr^{tm1Unc}	↑	↑	↓100%	↑
Cftr^{tm1Hgu}	↑	↑	↓70%	←→
Cftr^{tm1Cam}	↑	NR	NR	NR
Cftr^{tm1Hsc}	↑	↑	↓100%	↑
Cftr^{tm1Eur}	↑	↑	Response to Cl^- gradient	
Cftr^{tm1Kth}	↑	↑	↓100%	NR
Cftr^{tm1G551D}	↑	↑	↓100%	←→

TABLE 1.11 Nasal electrophysiology in mouse models of CF

Comparison of the electrophysiological profiles of the nasal epithelium in CF humans and mouse models of CF, on the original mixed genetic background strain. Increased (↑), decreased (↓) or preserved (←→) in comparison to non-CF controls. NR – Not reported. See text for references.

The analysis of the nasal epithelium has demonstrated hyperabsorption of Na^+ in all of the mouse models of CF for which the electrophysiological profile has been reported (Dorin *et al* 1992, Hyde *et al* 1993, Grubb *et al* 1994a, Smith *et al* 1995, van Doorninck *et al* 1995, Zeiher *et al* 1995, Delaney *et al* 1996, Rozmahel *et al* 1996, Wilschanski *et al* 1996) (see Table 1.12). This is manifest in a raised baseline PD and a significantly

greater decrease in PD in response to the ENaC inhibitor amiloride, than observed in wild type littermates. In addition a decrease, or absence, of cAMP-stimulated Cl^- conductance was observed in all the models tested, except for the $Cftr^{tm1Eur}/Cftr^{tm1Eur}$ mice. In the $Cftr^{tm1Eur}/Cftr^{tm1Eur}$ mice the response to a large chloride gradient was studied by substitution of chloride with gluconate in the apical solution and found to be quantitatively similar to non-CF controls (van Doorninck *et al* 1995). In these respects, the nasal epithelium in most of the murine models of CF accurately replicates the defects observed in the human airways. However, in contrast to human bioelectric profiles, the nasal mucosa of $Cftr^{tm1Unc}/Cftr^{tm1Unc}$ mice has been reported to display upregulation of the Ca^{2+}-mediated Cl^- secretory pathway, responsive to ionomycin and, to a lesser extent, forskolin (Grubb *et al* 1994a). Similar observations have not been observed in studies of the $Cftr^{tm1Hgu}$ mice (Smith *et al* 1995).

The analysis of the distal airways has proved to be more complex (see Table 1.13). In contrast to the human airways, studies in the mouse models of CF report no difference, or a reduction, in the amiloride-sensitive I_{sc} (Hyde *et al* 1993, O'Neal *et al* 1993, Grubb *et al* 1994b, Colledge *et al* 1995, Smith *et al* 1995, Delaney *et al* 1996). This suggests that the loss of CFTR does not result in the upregulation of ENaC in this tissue. The cAMP-stimulated Cl^- responses were mixed, while some showed no difference, others demonstrated a significant decrease. However, cAMP-stimulated Cl^- currents were still demonstrated in this tissue in all the mouse models of CF.

It has been proposed that an alternative Ca^{2+}-mediated Cl^- secretory pathway is dominant in the murine trachea and that this may be stimulated by forskolin (Grubb et al 1994b). It has been suggested that this pathway may be particularly dominant in the $Cftr^{tm1Unc}/Cftr^{tm1Unc}$ mice, but may be eliminated using pre-treatment with calcium agonists tert-Butylhydroquinone (TBHQ) and ionomycin (MacVinish *et al* 1997). Although this pathway was not found to be altered in the majority of the

mouse models of CF, it has been reported to upregulated in the *Cftr*^{tm2Cam}/*Cftr*^{tm2Cam} ΔF508 mice and *Cftr*^{tm1G551D}/*Cftr*^{tm1G551D} mice, when compared to wild-type littermate controls (Colledge *et al* 1996, Delaney *et al* 1996). More recent studies have demonstrated that the ion transport properties of the murine trachea are regulated by independently segregating modifier genes and show considerable variation between mouse strains (Farley *et al* 1998, Zapp and Drumm 1998) (see section 1.7.4).

Mutation	Baseline PD	Amiloride response	cAMP-mediated Cl^- response	Ca^{2+}-related Cl^- response
CF Human	↑ or ←→	↑	↓	←→
Cftr^{tm1Unc}	←→	←→	←→	←→
Cftr^{tm1Hgu}	↓	↓	↓ 60%	←→
Cftr^{tm1Cam}	↓	↓	↓ 75%	←→
Cftr^{tm1Bay}	←→	NR	** ↓ 70%	NR
Cftr^{tm2Cam}	←→	←→	*←→ to ↓ 60%	↑
Cftr^{tm1G551D}	←→	←→	↓ 60%	↑

TABLE 1.13 Tracheal electrophysiology in mouse models of CF

Comparison of the electrophysiological profiles of the tracheal epithelium in CF humans and mouse models of CF, on the original mixed genetic background strains. Increased (↑), decreased (↓) or preserved (←→) in comparison to non–CF controls. NR – Not reported. * Greatest decrease observed in the youngest mice. ** Studied in cultured foetal tracheal cells. See text for references.

As a consequence of these electrophysiological profiles it has been suggested that the murine trachea may not be the ideal model for the human airways. Nevertheless, the mouse models of CF do display electrophysiological abnormalities as a result of *Cftr* mutation. Thus, any

resultant pathology is of interest, interpreted in the context of knowledge of both the similarities and the differences between humans and mice.

Additional concerns have been raised about the cellular composition of the murine airways and the distribution of submucosal glands. The human airways are composed primarily of ciliated cells, whereas the murine airways are predominantly composed of Clara cells (Pack *et al* 1980). It has been suggested that for this reason the murine airways may be a better model of the human bronchioles than the large airways. Despite reports to the contrary, mice do have submucosal glands in the airways. However, unlike the human, these glands are predominantly localised in the most proximal part of the trachea and do not extend into the bronchi (Borthwick *et al* 1999). Furthermore, the distribution pattern of these glands is affected both by strain background (see section 1.7.4) and *Cftr* mutation (Innes and Dorin 1999).

The first observations relating to abnormal phenotype in a mouse model of CF were made in the $Cftr^{tm1Hgu}/Cftr^{tm1Hgu}$ mice. In initial studies of outbred MF1/129 $Cftr^{tm1Hgu}/Cftr^{tm1Hgu}$ mice no gross lung disease was observed at birth, or in animals born and raised in isolator conditions (Davidson *et al* 1995). However, histopathological evidence of pulmonary pathology was noted in mice reared in normal (non-specified pathogen free (SPF)) animal house conditions. Although no significant difference existed between the genotypes, there was a trend towards worse pathology in the CF mutant mice. Subsequent studies on $Cftr^{tm1Hgu}/Cftr^{tm1Hgu}$ mice provided additional indications of an abnormal lung phenotype in untreated mice.

An evaluation of the cytokine levels in BAL from untreated MF1/129 $Cftr^{tm1Hgu}/Cftr^{tm1Hgu}$ mice revealed significantly increased levels of the pro-inflammatory cytokine TNF-α in the mutant mice in comparison to non-CF littermates (Morrison 1999b). Interestingly this was only demonstrated in studies of animals maintained in standard, non-SPF conditions. In the animals maintained in a full barrier, SPF facility the levels of TNF-α were

significantly lower in both mutant and non-CF mice, with no significant difference between the genotypes observed. This suggests that an abnormal lung phenotype may not be manifest without exposure to pathogens.

Further histological analysis of untreated MF1/129 *Cftr*^{tm1Hgu}/*Cftr*^{tm1Hgu} mice revealed a significant increase in the number of inflammatory cells (predominantly lymphocytes) present in the lamina propria, in comparison to non-CF littermates (Zahm *et al* 1997). In addition, the mucociliary transport of inert particles *in vivo* was demonstrated to be significantly impaired in the *Cftr*^{tm1Hgu}/*Cftr*^{tm1Hgu} mice in comparison to non-CF littermates. Although a significant decrease in particle transport rate was observed, no difference in the ciliary beat frequency was noted (Zahm *et al* 1997). A subsequent study, using embedded, cultured lung slices from mice with the *Cftr*^{tm1Unc} mutation, partially backcrossed onto the C57Bl/6 background, repeated these observations (Cowley *et al* 1997a). In addition this study reported that ciliary beat frequency could be increased by infection with *P. aeruginosa*, whereas particle transport rate was dependent upon both infection and CF status.

Studies performed by myself and colleagues at the Human Genetics Unit prior to this thesis, demonstrated that the MF1/129 *Cftr*^{tm1Hgu}/*Cftr*^{tm1Hgu} mice displayed an abnormal lung phenotype in response to aerosolised, CF associated bacteria (Davidson *et al* 1995). Utilising nebulisation techniques (see Chapter 3) aerosolised bacteria were delivered to the lungs of cohorts of mutant and non-CF mice. Bacteriological and histological analysis was performed to establish the clearance of these pathogens and the histopathological response to repeated exposure. These studies demonstrated significantly impaired airway clearance of aerosolised *S. aureus* and *B. cepacia* in the mutant mice, in comparison to non-CF littermates. Furthermore, the MF1/129 *Cftr*^{tm1Hgu}/*Cftr*^{tm1Hgu} mice developed significantly more severe, pathogen specific, lung pathology after repeated exposure to these bacteria, in comparison to non-CF littermate controls. The spectrum of

abnormal pathology included lymphocytic aggregates, goblet cell hyperplasia (GCH) and metaplasia, mucus retention, bronchiolitis, pneumonia and oedema.

These initial studies provided the first demonstration of an abnormal pulmonary phenotype, other than electrophysiological profiles, in a mouse secondary to *Cftr* mutation. Consequently this provided the opportunity to investigate disease pathogenesis in a model system for CF, to interrupt the process at defined stages, with appropriate controls, in defined and manipulated genotypic and environmental conditions. The aims of this thesis were to further characterise the pulmonary phenotype and to examine the factors contributing to its development. These studies and the relevant contemporary studies in other mouse models of CF will be discussed in the following chapters.

1.7.4 Phenotype modification

Mouse models of CF provide a valuable resource in which to assess the role of CFTR and dissect the initiating and potentiating factors in disease pathogenesis. In addition, they provide an ideal resource in which to establish the contribution of independently segregating modifier genes to CF phenotype.

The greatest advantage of mouse models for such studies is the ability to control both the environment and the genetic background. Strains of laboratory mice have been specifically inbred over generations to establish inbred strains. Within such strains all the mice are practically 100% genetically identical. Repeated backcrossing of mouse models of CF with chosen inbred strains has been performed. The resultant offspring are considered to be certified congenic after 10 backcross generations and 99.9% inbred. The study of congenic inbred mouse mutants of CF should result in a

more homogeneous phenotype than that observed in an outbred strain, in which many genetic differences exist between littermates. In addition it decreases the potential pitfall of phenotype influencing genes co-segregating with the *Cftr* mutation in a proportion of the outbred mice. Different mutations of *Cftr* have been established on the same genetic background. In these animals the only genetic difference should be the nature of the mutation in *Cftr*. This allows the direct comparison of mutations and the elucidation of mutation specific effects upon phenotype. In addition, the same *Cftr* mutations have been established on different inbred lines. This has introduced the possibility of comparing the effects of genetic differences between various inbred strains and facilitated the search for independently segregating genetic modifiers of disease.

The first modifier locus was identified on the proximal region of mouse chromosome 7 (Rozmahel *et al* 1996). The $Cftr^{tm1Hsc}/Cftr^{tm1Hsc}$ mouse was originally studied on a mixed outbred CD1/129 background and classified into three categories dependent upon survival. The original founder mouse was then bred with a selection of different inbred strains to produce F_1 heterozygotes. These were then bred together to produce F_2 animals, homozygous for the mutation with different genetic backgrounds. Analysis of these mice demonstrated long term survival, beyond weaning, in a proportion of the mutant mice on some backgrounds, but not others. A genome scan was then performed with polymorphic DNA markers to identify potential modifier loci. It has been suggested that a gene encoding a Ca^{+}-activated Cl^{-} channel may be responsible, however, to date the gene responsible has not been reported. As a direct consequence of this study a genetic modifier locus for meconium ileus in humans has been identified on the syntenic region on human chromosome 19.

The $Cftr^{tm1Hgu}$ and $Cftr^{tm1Unc}$ mutations have been inbred to congenic on the C57Bl/6 strain (Dorin *et al* 1997, Kent *et al* 1997). The inbred C57Bl/6 $Cftr^{tm1Unc}/Cftr^{tm1Unc}$ mice demonstrate only 6% survival at day 20, despite weaning onto a liquid diet, while mice with the $Cftr^{tm1Unc}/Cftr^{tm1Unc}$ continue to

show high rates of survival. Initial analysis of the phenotype of the inbred C57Bl/6 *Cftr*^{tm1Unc}/*Cftr*^{tm1Unc} mice, reported a host of pulmonary abnormalities. However, aspects of the methodology relating to the evaluation by light microscopy and pulmonary function tests, were inappropriate and many of these original observations have not been substantiated by future analysis (Haston, personal communication). Nevertheless quantitative trait loci (QTL) analysis based on alveolar thickening and collagen deposition in the inbred C57Bl/6 *Cftr*^{tm1Unc}/*Cftr*^{tm1Unc}, relative to inbred BALB/c *Cftr*^{tm1Unc}/*Cftr*^{tm1Unc} mice has identified one locus meeting the criteria for suggestive linkage (Haston *et al* 1999). In addition, increased lung neutrophil counts and myeloperoxidase levels in inbred *Cftr*^{tm1Unc}/*Cftr*^{tm1Unc} mice are being assessed on different strain backgrounds.

Studies of the *Cftr*^{tm1Hgu}/*Cftr*^{tm1Hgu} mice have demonstrated that the distribution of submucosal glands in the murine trachea is determined both by the *Cftr* genotype and the genetic background (Innes and Dorin 1999). In *Cftr*^{tm1Hgu}/*Cftr*^{tm1Hgu} mice, both inbred and outbred, the submucosal glands have been observed to extend more distally than in wild-type littermate controls. Utilising recombinant inbred strains two putative loci associated with this phenotype have been identified, on mouse chromosomes 9 and 10. The region on chromosome 9 includes several genes, of which one candidate may be the gene encoding Glutathione S-transferase (GST).

Analysis of inbred mouse strains has also revealed strain specific variation in the electrophysiological properties of the murine airway epithelium (Farley *et al* 1998, Zapp and Drumm 1998). These studies demonstrate the existence of genetic modifiers that determine the ion transport profile of both the nasal and tracheal epithelium. Furthermore, these studies raise the possibility of independent genetic factors determining the expression and/or function of CFTR in these tissues. The tracheal forskolin response is reported to consist of two main components. Pre-treatment with calcium agonists has been used to reveal the cAMP-mediated Cl^- secretion (MacVinish *et al* 1997). This approach abolished the forskolin

stimulated response in C57Bl/6 mice but not in BALB/c mice. This suggests that only the latter strain of mouse had an appreciable level of CFTR activity in the trachea and that the major mode of chloride transport in the former was via Ca^{2+}-activated channels. This demonstrates that other genetic influences may modify phenotype and may be important in the interpretation of the electrophysiological profiles of different mouse models of CF, on different background strains (see section 1.7.3.5). Furthermore, it suggests that tracheae of BALB/c mice are more likely to display an abnormal phenotype as a result of *Cftr* mutation than are C57Bl/6 mice. These studies intend to map the genetic modifier responsible for these phenotype variations.

While it is possible that genetic modifiers for lung disease in mouse models of CF may have no relevance in the human disease process, the first example shows that in some cases they may reveal biologically relevant mechanisms in both mouse and man. It is hoped that these discoveries may provide insight into the pathogenesis of CF and even reveal possible targets for novel therapies.

1.8 Aims of this thesis

The initial demonstration of abnormal pulmonary phenotypes in *Cftr*^{tm1Hgu}/*Cftr*^{tm1Hgu} mice established these animal as an important model for the development of lung disease in CF. However, the original studies were performed using outbred mice and displayed a broad spectrum of pathology in response to pathogens. This thesis aimed to-

a) establish reliable bacterial exposure techniques by evaluating and quantifying methods of bacterial delivery to the murine lung.

b) assess the relative roles of genetic strain background, residual CFTR function and environmental influences upon the variability of pulmonary phenotype observed in outbred *Cftr*^{tm1Hgu}/*Cftr*^{tm1Hgu} mice in response to repeated bacterial exposure. This was addressed by assessment of the pulmonary phenotype of mouse models of CF in response to repeated exposure to *Staphylococcus aureus*, using:

   1) *Cftr*^{tm1Hgu}/*Cftr*^{tm1Hgu} mice inbred onto the C57Bl/6 background to assess the phenotype of this mutation on an inbred strain

   2) *Cftr*^{tm1Hgu}/*Cftr*^{tm1Unc} compound heterozygote mice, inbred onto the C57Bl/6 background, to assess the effect of decreasing the level of normal CFTR

c) address the factors contributing to the development of an abnormal pulmonary phenotype in the *Cftr*^{tm1Hgu}/*Cftr*^{tm1Hgu} mice assessing both the similarities and the differences between the

human and murine lungs. The relevance of current theories for the pathogenesis of CF lung disease in humans was examined by:

1) studying the role of internalisation of bacteria by murine epithelial cells

2) studying and comparing the antibacterial profile of human and murine β-defensins

d) establish and characterise an air/liquid interface primary culture model of murine tracheal epithelial cells

Chapter 2

Materials and Methods

Chapter 2: Materials and Methods

2.1 Animals

All wild type mice used were supplied by Charles Rivers UK Ltd., Margate, UK. All mouse models of CF were bred in house with assistance from Dr Julia Dorin and Dr Sheila Webb, MRC Human Genetics Unit, Edinburgh. Mice were used at various ages for different studies as specified in the details for individual experiments. Where non-CF littermate controls were used, cohorts were age and weight matched. With the exception of mice used for primary culture studies, animals were housed in the Biomedical Research Facility, Western General Hospital, Edinburgh and maintained under standard conditions. These conditions were not specified pathogen free (SPF). For primary culture studies C57Bl/6N mice of both sexes were used, aged 5 – 7 weeks and maintained in the Transgenic Unit, Evans Building, Western General Hospital, Edinburgh, under SPF conditions. Routine health screening was performed by Harlan UK Ltd., Blackthorn, Bicester, Oxon., UK. All experimental work complied with the UK Animal (Scientific Procedures) Act 1986.

2.2 Genotype analysis of mouse models of CF

A breeding colony of mouse models of CF was maintained in the Biomedical Research Facility, Western General Hospital, Edinburgh. Anaesthetised mice were ear clipped for identification and tail tipped for

genotyping with the assistance of Vincent Ranaldi, Biomedical Research Facility, Western General Hospital, Edinburgh. Genotyping was performed as described below. Mice were also supplied from an alternative breeding colony maintained by Dr Julia Dorin and Dr Sheila Webb, MRC Human Genetics Unit, Edinburgh. These mice were genotyped by Dr Sheila Webb, MRC Human Genetics Unit, Edinburgh.

2.2.1 Preparation of total genomic DNA from tail tips

Tail tips were incubated overnight at 50°C in 500 ml of Quick Lysis Buffer (100 mM Tris HCl pH 8.5, 5 mM EDTA, 200 mM NaCl, 0.2% SDS) containing 50 µg of Proteinase K (Boehringer Mannheim UK, Lewes, East Sussex, UK). The samples were then vortexed vigorously and centrifuged for 10 minutes at 15 000 rpm. The resultant supernatants were added to 0.5 ml of 100 % ethanol and the precipitated DNA spooled onto glass rods. The DNA was washed with 70 % ethanol and then air-dried for 5 minutes, after which it was resuspended in 50 µl of TE (10 mM Tris HCl, 0.1 mM EDTA, pH 4.0).

2.2.2 Restriction enzyme digestion of DNA

Genomic DNA was digested overnight at 37 °C with 0.67 u/µl Xba I and 0.67 u/µl Sal I restriction enzymes (both supplied, with buffer by Boehringer Mannheim UK, Lewes, East Sussex, UK) in 1x Buffer H with 3.34 mM spermidine. Digestions were analysed for completeness by gel electrophoresis.

2.2.3 Agarose gel electrophoresis

DNA molecules were separated according to their size on horizontal agarose gels. The percentage of agarose used to make the gel depended on the size range of the DNA molecules to be resolved. Digested genomic or plasmid DNA was commonly run at 0.7–1% w/v agarose gels, whereas smaller fragments, such as most PCR products, were run on 1-2% agarose gels. The agarose was dissolved and cast in TAE buffer (0.04 M Tris-base; 0.001 M EDTA, 0.02 M Na Acetate, pH to 8.2 with glacial acetic acid) which was also used as the running buffer. Ethidium bromide (5 μg/100ml) was added directly to the molten agarose. 1x loading buffer (10x DNA loading buffer: 20% Ficoll (Pharmacia Biotech, St. Albans, UK), 100 mM EDTA, Orange G (Sigma-Aldrich Co. Ltd, Poole, Dorset, UK)) was added to the DNA prior to loading the sample on the gel. Gels were run in electrophoresis apparatus (Biosciences Services) at 20-100 V depending upon the resolution and run-time required.

200-500 ng of the appropriate size marker was used per gel;

a) λ DNA digested with HindIII (Boehringer Mannheim UK, Lewes, East Sussex, UK)
b) ΦX 174 digested with HaeIII (Boehringer Mannheim UK, Lewes, East Sussex, UK)

The sizes of the bands given by these markers is listed below:

λ HindIII (bp)	ΦX 174 HaeIII (bp)
23,130	1,353
9,416	1,078
6,632	872
4,361	603
2,322	310
2,027	281
564	271
125	234
	194
	118
	72

2.2.4 Southern blot transfer of DNA

DNA fragments were separated by agarose gel electrophoresis, visualised under a mid-range UV transilluminator and photographed, next to a ruler to allow for future sizing of DNA fragments, using a video copy processor. The gel was soaked in Denaturing Buffer (0.5 M NaOH, 1.5 M NaCl) for 30 minutes and then in Neutralisation Buffer (0.5 M Tris, 1.5 M NaCl, pH 5.5) for 10 minutes. The gel was then placed in water until ready to blot. A large strip of chromatography paper (17 Chr; Whatman International Ltd., Maidstone, UK) was soaked in 20 x SSC (3 M NaCl, 0.3 M Na citrate) and placed on a glass plate, so that the ends of the paper were in a reservoir of 20 x SSC, forming a wick. A piece of chromatography paper (3 MM Chr; Whatman International Ltd., Maidstone, UK) was then cut, slightly larger than the size of the gel, soaked in 20 x SSC and placed on top of the wick. The gel was placed upside down on top of the wet chromatography paper and a piece of Hybond-N nylon transfer membrane (Amersham Pharmacia Biotech UK Ltd, Little Chalfont, Buckinghamshire, UK), soaked in 2 x SSC (0.3 M NaCl, 0.03 M Na citrate) placed directly onto the surface of the gel to cover the entire surface of the gel, excluding any trapped air bubbles. Two pieces of 3MM chromatography paper, pre-soaked in 2 x SSC, were placed on top of the membrane. Areas of exposed wick were covered in Saran wrap (Dow Chemical Company). A weighted stack of paper towels was placed on top to draw the fluid through the gel and transfer the DNA to the membrane by capillary transfer. Gels were blotted overnight. The membrane was rinsed in 2 x SSC, fixed by baking at 80°C for 20 minutes and then stratalinked by exposure to 1200 µJoules of UV irradiation (Stratalinker 1800, Stratagene). Membranes were stored between two sheets of 3MM chromatography paper at room temperature.

2.2.5 Radioactive hybridisation

2.2.5.1 Preparation of radioactively labelled DNA probes

Labelled probes from double stranded DNA were made by the random priming method (Feinberg and Vogelstein 1983). The labelling reaction involves random priming from hexanucleotides and then polymerisation along the DNA strand catalysed by the Klenow fragment of *E. coli* polymerase I. The reaction mix includes dATP, dTTP, dGTP and radiolabelled [α-^{32}P]-dCTP so that radioactivity is incorporated into the newly synthesised strand. Approximately 50 ng of purified DNA in a total volume of 12 µl was boiled for 10 min to ensure denaturation, cooled rapidly to prevent reannealing of the strands, and spun down. The denatured DNA was then labelled using 4 µl of High Prime (Boehringer Mannheim UK, Lewes, East Sussex, UK) and 30 µCi [α-^{32}P] dCTP (Amersham International P.L.C., Amersham, Bucks.). The reaction was incubated at 37 °C for 30 minutes. Incorporation was estimated by washing a small amount of the probe on a GF/B circular filter (Whatman International Ltd., Maidstone, UK) with trichloroacetic acid (TCA) to remove unincorporated material, and the probe used if the incorporation was 50% or above. The probe was stripped by boiling for 10 min with 1 mg sonicated salmon sperm and 1 mg mouse genomic DNA followed by incubation at 68 °C for 45 minutes. The probe was then added to the prehybridised filters.

2.2.5.2 Hybridisation of radioactive DNA probes

Under a solution of 2 x SSC, the filters were placed between two slightly larger sheets of gauze, with up to 3 layers of filters. Air bubbles trapped between the filters and gauze were expelled, the layers were rolled

up together, transferred to hybridisation bottles (Hybaid Ltd., Ashford, Middlesex, UK) and unrolled onto the surface of the bottle. Filters were pre-hybridised at 68 °C for a minimum of 1 hour in rotating hybridisation bottles with 20 ml Hybridisation Solution (6 x SSC, 10% Dextran sulphate, 0.5% SDS, 0.1% BSA, 0.1% Ficoll, 0.1% polyvinylpyrrolidone, 0.1% disodium pyrophosphate). After pre-hybridisation, radiolabelled probe (see section 2.2.5.1) was added directly to the solution and the blots hybridised overnight at 68 °C. Filters were washed with 2 x SSC/0.1% SDS at 68 °C for 15 minutes and then 0.2 x SSC/0.1% SDS at 68 °C for 15 minutes monitoring the background radiation with a Geiger counter.

The filters were exposed to Kodak X-OMAT AR film at –70 °C in light-tight cassettes containing intensifying screens, for a length of time dependent upon the intensity of the radiolabelled probe (several minutes to days). The film was developed in a RGII (Fugi) automatic x-ray film processor.

Wild type mice were identified by a hybridising fragment of ~ 6 kb between Xba I restriction sites in introns 9 and 10, whereas a smaller hybridising fragment of ~ 5 kb, between the Xba I restriction site in intron 10 and a Sal I restriction site introduce by the insertional mutation, was diagnostic for the *Cftr*^{tm1Hgu} mutation.

To remove the radioactive probes from the filters, they were placed in a metal tray containing water at 100 °C. The heat was immediately removed from the tray and the contents allowed to cool.

2.3 Preparation of bacteria

Bacteria were provided by Professor John Govan and prepared by Wendy Hannant, Dr Cathy Doherty or Dr Jayne Hughes, Department of Medical Microbiology, University of Edinburgh. The bacterial strains used were; *Staphylococcus aureus* CF clinical isolate C1705, *Pseudomonas aeruginosa*

CF clinical isolate J1385 and strain PAO1, *Escherichia coli* clinical isolate J2408 and *Burkholderia cepacia* CF clinical isolate J2315. *Pseudomonas aeruginosa* CF clinical isolate J1385 has been documented to have preferentially infected several CF individuals, despite exposure to other strains simultaneously in a jacuzzi, and be particularly mucinophilic (Nelson *et al* 1990). *Burkholderia cepacia* CF clinical isolate J2315, is the virulent Edinburgh-Toronto epidemic strain ET/12 (Govan and Deretic 1996).

An aliquot of the appropriate strain was recovered from storage, in 10% w/v skimmed milk at –70 °C, thawed and streaked on the appropriate media. This was incubated at 37 °C overnight (or for 48 hours for *B. cepacia*). Nutrient broth (25 g/L, 0.5% w/v Yeast extract; Oxoid Ltd., Basingstoke, Hampshire, UK) was inoculated with a few colonies and incubated at 37 °C overnight in an orbital incubator. The bacterial suspension was centrifuged at 3000x g for 10 minutes and the supernatant removed. The bacterial pellet was resuspended in 0.85% saline and standardised using a spectrophotometer (CamLab) at OD_{590}, to a density previously determined to correspond to ~ 10^9 cfu/ml.

The following media were used: *S. aureus* was grown on Blood agar (39 g/L Columbia base agar (Oxoid Ltd., Basingstoke, Hampshire, UK), 5% defibrinated horse blood (E & O Laboratories Ltd., Burnhouse, Bonnybridge, Scotland) added after autoclaving and cooling), *P. aeruginosa* was grown on Pseudomonas isolation agar (45 g/L, 2% glycerol; Difco Laboratories Ltd., West Molesey, Surrey, UK), *E. coli* was grown on MacConkey agar (44.5 g/L; Mast Diagnostics, Mast Group Ltd., Bootle, Merseyside, UK), *B. cepacia* was grown on Cepacia medium (32.5 g/L, Ticarcillin 100mg/L, Polymixin B 300,000 u/L; Mast Diagnostics, Mast Group Ltd., Bootle, Merseyside, UK).

2.4 Construction of bacterial delivery apparatus

Murine nebuliser apparatus designs were adapted from an original design by Professor David Porteous, Medical Genetics Section, Department of Medical Sciences, University of Edinburgh (formerly MRC Human Genetics Unit, Edinburgh) (see Figure 3.1). The apparatus was constructed with the assistance of Duncan Fletcher and Leonard Hay, MRC Human Genetics Unit, Edinburgh. The apparatus was constructed in house from perspex (see Figure 3.2). The individual tubes within which each mouse was positioned were adapted from 50 ml catheter tip syringes (Terumo, Surgicon Ltd., Brighouse, W. Yorks., UK).

Tracheal intubation catheters were constructed in house by Duncan Fletcher and Leonard Hay, MRC Human Genetics Unit, Edinburgh. These were adapted spinal needles (25G x 3.5"; Terumo, Surgicon Ltd., Brighouse, W. Yorks., UK), shortened to 6 cm, blunted and with a 30° bend positioned 1 cm from the end. Intubation frames were also constructed in house by Duncan Fletcher and Leonard Hay, MRC Human Genetics Unit, Edinburgh, based on a previously published design (Ho and Furst 1973).

2.5 Bacterial delivery methods

2.5.1 Nebulisation

Mice were maintained in HEPA air filtered isolator cabinets for the duration of the experiment and caged in groups of mixed genotype. Exposed and unexposed control mice were housed in separate cages within the same isolator unit. Where mouse models of CF were analysed, groups of mutant mice and non-CF littermates, of comparable age and weight, were

exposed to bacteria in parallel. A maximum of six mice, of < 30g body weight, were restrained in radially arranged tubes in nebulisation apparatus (see section 2.4). Each animal was placed in a separate tube, with a cone shape for the mouse's nose open into the main chamber at one end and the other end obstructed with a rubber bung, greased with Vaseline. A carrier gas mixture of 95% O_2 and 5% CO_2 (BOC gases, Guildford, Surrey, UK), regulated via an XR600 oxygen regulator (Oxylitre Ltd., Manchester, UK) was passed through a sidestream nebuliser (System-22 Optimist®, Medic-Aid, Pagham, Sussex, UK), containing the bacterial suspension or PBS, at a rate of 12 L/minute. The addition of a baffle (a kind gift from Dr Peter Middleton, Ion Transport Laboratory, National Heart and Lung Institute, London) was used to reduce the air particle size. The aerosolised solution was circulated in the main chamber from which the mice were breathing and vented from the delivery chamber to be purged twice through Virkon disinfectant (Antec International Ltd., Sudbury, Suffolk, UK).

The standard exposure protocol for the assessment of the bacterial delivery profile of the apparatus was the nebulisation of ~ 4 ml of bacterial suspension over 5 minutes, either with or without the baffle. Mice were removed from the apparatus and immediately sacrificed by lethal intraperitoneal injection of 20 mg of sodium phenobarbitone (Euthatal, Rhone Merieux) and processed as described in section 2.6.

The standard exposure protocol for the repeated exposure studies comprised the nebulisation of ~ 4 ml of bacterial suspension over 5 minutes, with the baffle followed by the nebulisation of ~ 4 ml of bacterial suspension over 5 minutes without the baffle. Treated animals were then returned to standard cages within the isolator. This protocol was repeated on a daily basis, 5 days a week, for 4 weeks. On the final day of exposures, 4 previously unexposed mice were also exposed, after which all the animals were given 24 hours clearance time. Mice were sacrificed by lethal intraperitoneal injection of 20 mg of sodium phenobarbitone (Euthatal, Rhone Merieux) and processed as described in section 2.7. In some cases, unexposed mice,

maintained in the same isolator as the exposed mice but not actively exposed to bacteria, were also sacrificed and studied.

A glass impinger was used to assess the viability of nebulised bacteria. The nebuliser outlet was connected directly to the inlet of the impinger via plastic tubing and the nebulised solution was bubbled through PBS to collect the bacteria. The resultant suspension was analysed using standard bacteriological methods.

2.5.2 Direct intratracheal instillation

Adult mice were anaesthetised with an intraperitoneal injection of Avertin (4.4 mM 2-2-2-tribromoethanol, 2.5% 2-methyl-2-butanol, in distilled water), using 200 µl per 10 g body weight. Anaesthesia was induced within 1 minute and lasted for approximately 45 minutes. The instillation was performed using a non-surgical, intratracheal instillation method adapted from a published technique (Ho and Furst 1973). The anaesthetised mouse was placed with its upper teeth hooked over a wire at the top of the support frame (see Figure 3.4) with a spring pushing the thorax forward to position the pharynx, larynx and trachea in a vertical straight line. The lower jaw was held open with a loop of thread around the lower teeth and weighted. The airway was illuminated externally using a swan neck fibre optic lamp placed against the mid sternum. The tongue was moved to one side and an intubation catheter (see section 2.4) was inserted between the vocal folds at the base of the larynx and passed into the clearly illuminated tracheal lumen. With the catheter held steady, 20 µl of bacterial suspension or 5% methylene blue dye in PBS was placed in a well at the proximal end of the catheter. A 1ml syringe was then attached to the end of the catheter and the solution gently instilled into the trachea with 200 µl of air. The animal was maintained in an upright position for 2 minutes after instillation to allow the

fluid to drain into the respiratory tree. Mice were sacrificed by lethal intraperitoneal injection of 20 mg of sodium phenobarbitone (Euthatal, Rhone Merieux) and processed as described in section 2.6 or 2.8.

2.6 Microbiological assessment of murine tissue

2.6.1 Bacteriological assessment of murine lungs

Animals were sacrificed by lethal intraperitoneal injection of 20 mg of sodium phenobarbitone (Euthatal, Rhone Merieux). The lungs and trachea were removed together into 1 ml PBS at room temperature. In some instances the trachea and proximal primary bronchi were separated from the lung lobes and processed in a separate 1 ml aliquot of PBS. The tissue was homogenised (Omni International homogeniser, Camlab Ltd., Cambridge, UK) in the PBS, using a separate, sterile homogeniser head for each sample. Homogenisation was performed in a Class II laminar flow hood. Serial ten-fold dilutions of the homogenates were performed in PBS and 100 µl aliquots were plated out on appropriate agar (see section 2.3). Plates were incubated at 37 °C overnight (or for 48 hours for *B. cepacia*), the resultant colony forming units were counted and extrapolated to provide the cfu count for the neat sample.

2.6.2 Bacteriological assessment of murine stomach

Animals were sacrificed by lethal intraperitoneal injection of 20 mg of sodium phenobarbitone (Euthatal, Rhone Merieux). The stomach and oesophagus were removed together to 1 ml PBS at room temperature. Tissue was processed in an identical manner to murine lungs (see section 2.6.1).

2.6.3 Virological assessment

Animals were anaesthetised with Hypnorm/Hypnovel (4:2:1 mix of distilled water: Hypnorm (Roche, Welwyn Garden City, UK): Hypnovel (Janssen Pharmaceutical Ltd., Gove, Oxford, UK); 10 µl/g of body weight). Tail tip venesection was performed for the collection of a ~1.5 ml blood sample. Animals were sacrificed by lethal intraperitoneal injection of 20 mg of sodium phenobarbitone (Euthatal, Rhone Merieux). Blood samples were centrifuged at 7000x g and the serum was tested using a Murine ImmunoComb™ kit (Orgenics Ltd., Charles River UK Ltd., Margate, UK) in accordance with the manufacturers instructions.

2.7 Histological assessment of murine lungs

2.7.1 Preparation of murine lungs for wax sectioning

The thorax was opened to clearly reveal the lung fields and an intravenous catheter (24G x ¾"; Terumo, Surgicon Ltd., Brighouse, W. Yorks., UK) was passed into the proximal trachea, just below the thyroid cartilage. The needle was removed from the catheter and a length of surgical suture was tied around the trachea to secure the plastic catheter sheath in position. The lungs were then gently inflated *in situ* by passing ~ 1 ml fixative through the catheter. The catheter was removed and the surgical suture simultaneously tightened to occlude the proximal trachea. The lungs were then removed and placed in fixative.

Tissues were fixed in either: a) 10% Neutral Buffered Formalin (10% formaldehyde, 0.15 M NaH_2PO_4, 0.1 M sodium hydroxide) at room

temperature for at least 4 hours, or b) 50% Acetone, 50% Methanol mix, at room temperature for 20 minutes to 1 hour.

The fixed tissues were then placed in a Tissue-Tek Vacuum Infiltration Processor 4621 (Bayer Diagnostics, Newbury, Berkshire, UK) and processed through a programme that consisted of the following steps:

1. PBS	- 1 hour at 40 °C
2. 30% ethanol	- 1 hour at 40 °C
3. 50% ethanol	- 1 hour at 40 °C
4. 70% ethanol	- ≥ 1 hour at 40 °C
5. 85% ethanol	- 1 hour at 40 °C
6. 95% ethanol	- 1 hour at 40 °C
7. 100% ethanol	- 1 hour at 40 °C
8. 100% ethanol	- 1 hour at 40 °C
9. xylene	- 1 hour at 40 °C
10. xylene	- 1 hour at 40 °C
11. paraffin wax	- 1 hour at 60 °C
12. paraffin wax	- 1 hour at 60 °C
13. paraffin wax	- 1 hour at 60 °C
14. paraffin wax	- 1 hour at 60 °C

The lungs were then divided into three portions to separately process the trachea, the large single left lobe and the smaller right lobes. The tissues were then placed in metal moulds, covered with molten paraffin wax and a plastic Tissue-Tek cassette (Bayer Diagnostics, Newbury, Berkshire, UK). The wax was allowed to cool and solidify on ice and the paraffin wax block containing the tissue was removed from the mould ready for sectioning.

Paraffin wax blocks were sectioned on a Reichert-Jung 2030 microtome using disposable blades. The large left lobe was orientated and sectioned in such a manner as to section through the length of the major

bronchus as shown in Figure 2.1. Representative sections were cut anterior to, posterior to and through the major bronchus. Sections were cut at 3-5 μm and floated out on water at 40 °C. The sections were then mounted onto glass slides and left to dry at room temperature. Glass slides had been previously coated with Vectabond™ (Vector Laboratories Ltd., Orton Southgate, Peterborough, UK) according to the manufacturer's instructions. Sections were stored at room temperature.

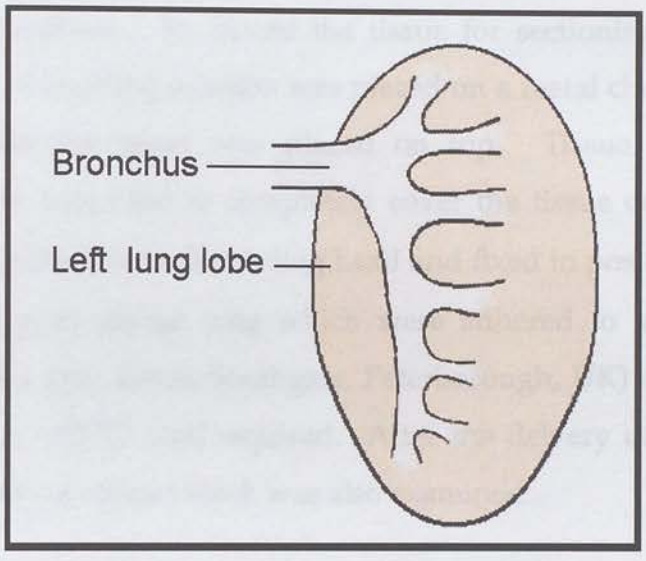

FIGURE 2.1 LUNG SECTIONING

The large left lung lobe was orientated and sectioned through the length of the major bronchus.

2.7.2 Preparation of murine lungs for cryostat sectioning

The thorax was opened to clearly reveal the lung fields and an intravenous catheter (24G x ¾"; Terumo, Surgicon Ltd., Brighouse, W. Yorks., UK) was passed into the proximal trachea, just below the thyroid cartilage. The needle was removed from the catheter and a length of surgical

suture was tied around the trachea to secure the plastic catheter sheath in position. A 25% Tissue Tek O.C.T. embedding solution (Agar Scientific, Stansted, Essex, UK) in PBS solution was gently passed into the lungs via a cannula. Tissues were placed in a plastic tube and then placed directly into liquid nitrogen. Samples were stored at -70 °C.

Samples were sectioned on a Cryostat CM3000 (Leica, Milton Keynes, UK). The temperature controls on the cryostat were set as follows: chamber -40 °C, cutting head -25 °C. The tissue was removed from the liquid nitrogen and placed in the cryostat chamber for at least an hour allowing the tissue temperature to equilibrate. To mount the tissue for sectioning a drop of Tissue Tek O.C.T. embedding solution was placed on a metal chuck and just before solidification the tissue was placed on top. Tissue Tek O.C.T. embedding solution was used to completely cover the tissue on the chuck which was then mounted onto the cutting head and fixed in position. 10 µm sections were cut from mouse lung which were adhered to Vectabond™ (Vector Laboratories Ltd., Orton Southgate, Peterborough, UK) coated glass slides and stored at –70 °C until required. After the delvery of methylene blue dye the partially sectioned block was also examined.

2.7.3 Rehydration of paraffin wax embedded sections

Paraffin wax embedded tissue section slides were incubated at 60 °C for 30 minutes to melt the wax and then processed manually through the following steps at room temperature :

1) xylene - 10 minutes
2) xylene - 10 minutes
3) 100% ethanol - 5 minutes
4) 100% ethanol - 5 minutes

5) 90% ethanol - 5 minutes
6) 70% ethanol - 5 minutes
7) 50% ethanol - 5 minutes
8) 30% ethanol - 5 minutes
9) distilled water - 5 minutes

2.7.4 Periodic Acid Schiff staining of tissue sections

This staining technique was used to visualise mucin containing cells which stain a bright magenta colour. Tissue section slides were rehydrated, through xylene and an ethanol series, to distilled water (see section 2.7.3) and then stained by immersion in the following solutions at room temperature, unless otherwise specified:

1) 1% α-Amylase solution in distilled water - 1 hour at 37 °C
2) wash well in running water - 2 minutes
3) 1% Periodic Acid - 5 minutes
4) wash well in running water - 2 minutes
5) Schiff reagent - 10 minutes
6) wash well in running water - 10 minutes

The following counter stain was then performed:

1) Haematoxylin - 5 minutes
2) wash well in running water - 2 minutes
3) acid alcohol (1% HCl in 70% ethanol) - 10 seconds
4) wash well in running water - 2 minutes
5) saturated lithium carbonate - 10 seconds
6) wash well in running water - 2 minutes

The slides were then dehydrated and mounted as described in section 2.7.6. α-Amylase, Periodic Acid, Schiff reagent and Haematoxylin were all supplied by Sigma-Aldrich Company Ltd., Poole, Dorset, UK.

2.7.5 Haematoxylin and Eosin staining of tissue sections

This staining technique was used to examine basic tissue morphology. Tissue section slides were rehydrated through xylene and an ethanol series to distilled water (see section 2.7.3) and then stained by immersion in the following solutions:

1) Haematoxylin	- 5 minutes
2) wash well in running water	- 2 minutes
3) acid alcohol (1% HCl in 70% ethanol)	- 10 seconds
4) wash well in running water	- 2 minutes
5) saturated lithium carbonate	- 10 seconds
6) wash well in running water	- 2 minutes
7) Eosin solution	- 2 minutes
8) wash in water	- 30 seconds
9) 100% ethanol	- 15 seconds
10) 100% ethanol	- 1 minute

The slides were then dehydrated and mounted as described in section 2.7.6. Haematoxylin and Eosin were supplied by Sigma-Aldrich Company Ltd., Poole, Dorset, UK. Eosin solution consisted of 3 parts of 1 % aqueous eosin to 1 part of 1% ethanol/0.05% acetic acid.

2.7.6 Dehydration and mounting of tissue sections

Following staining, tissue section slides were dehydrated as follows:

1) 30% ethanol - 2 minutes
2) 50% ethanol - 2 minutes
3) 70% ethanol - 2 minutes
4) 90% ethanol - 2 minutes
5) 100% ethanol - 5 minutes
6) 100% ethanol - 5 minutes
7) xylene - 5 minutes
8) xylene - 5 minutes

Once the xylene had evaporated a small amount of DPX mountant (BDH Laboratory Supplies, Poole, Dorset, UK) was added to the slide and a coverslip gently placed over the tissue section ensuring no air bubbles were trapped. The slides were left to air dry overnight.

2.7.7 Bright field microscopy and image capture

Brightfield imaging of tissue sections was performed on an Ortholux microscope (Leitz Wetzlar, Germany). Images were captured on slide film using a Wild Photoautomat MPS45 and Wild MP55 camera (Wild, Heerbrugg, Switzerland). Slide images were developed and transferred to digital format by Norman Davidson, Sandy Bruce and Douglas Stuart, MRC Human Genetics Unit, Edinburgh. Adobe photoshop software (Adobe Systems Incorporated, Mountain View, CA, USA) was used for the annotation of images.

2.7.8 Assessment of lung pathology

Sections of wax embedded murine lungs were stained using a Periodic acid Schiff stain and analysed by bright field light microscopy. Three representative sections of the large left lobe, cut anterior to, posterior to and through the major bronchus, and 3 sections through the right lobes from each animal were examined and scored blinded to genotype and treatment protocols. Samples were assessed on the basis of 5 features, graded on a scale of 1 to 5 on the basis of specified criteria (see Chapter 4 Table 4.1 and Figures 4.1a and 4.1b). Assessment of lung histopathology was performed twice, using these criteria, and the scores ranked before the study was unblinded. Duplicate blinded analyses of the total score were compared using a weighted Kappa measure of agreement (see section 2.12). Two-sample T-tests and Kruskal-Wallis tests were used to test for significance, with assistance from Peter Teague, MRC Human Genetics Unit.

2.7.9 Peroxidase Immunohistochemistry

Paraffin wax embedded tissue section slides were rehydrated to distilled water as described in section 2.7.3, but without prior heat treatment to melt the wax. The first two xylene immersions were performed for 30 minutes. Cryostat sections were prepared by fixing tissue sections in acetone for 10 min at –20 °C and then air dried. The region of interest was delineated by marking a ring around the tissue section with a wax PAP pen (Agar Scientific Ltd., Stansted, Essex, UK). Slides were then immersed sequentially in the following solutions, at room temperature unless otherwise stated:

1) Peroxo-block (Zymed Laboratories Inc., San Francisco, CA, USA) was used to block endogenous peroxidase activity:

paraffin wax sections - 2 minutes

cryostat sections - 45 seconds

2) wash 3 times with PBS - 10 minutes

3) Blocking solution and Avidin block - 20 minutes

(Blocking solution : 2% normal animal serum from the species that the secondary antibody was raised in, 0.2% Tween (Polyoxyethylenesorbitan), 2% w/v BSA, 7% Glycerol)

4 drops per ml of Avidin solution from a Biotin/Avidin Blocking kit (Vector Laboratories Ltd., Orton Southgate, Peterborough, UK) was added to the Blocking solution to block non specific binding of Biotin/Avidin system components, according to the manufacturer's instructions.

4) gently remove blocking solution

5) Primary antibody and Biotin block - 60 minutes

Primary antibody was diluted to the appropriate concentration in Blocking solution (see step 3).

4 drops per ml of Biotin solution from a Biotin/Avidin Blocking kit (Vector Laboratories Ltd., Orton Southgate, Peterborough, UK) was added to the diluted primary antibody to block non specific binding of Biotin/Avidin system components, according to the manufacturer's instructions.

6) wash 3 times with PBS - 10 minutes

7) Secondary antibody - 30 minutes

The biotinylated secondary antibody was diluted to the appropriate concentration in Blocking solution (see step 3).

8) wash 3 times with PBS - 10 minutes

9) Avidin : Biotinylated peroxidase Complex - 30 minutes

Avidin : Biotinylated peroxidase Complex (Vector Elite ABC Kit, Vector Laboratories Ltd., Orton Southgate, Peterborough, UK) was prepared 30 minutes before use, according to the manufacturer's instructions.

10) wash 3 times with PBS - 10 minutes

11) Peroxidase substrate - 5 minutes

VIP Peroxidase substrate (Vector Laboratories Ltd., Orton Southgate, Peterborough, UK), was prepared following the manufacturers instructions.

12) wash with running water - 5 minutes

13) dehydrate and mount as described in section 2.7.5

When a primary antibody raised in mouse was used on mouse tissue an additional 20 minute blocking stage was performed before step 3, using Blocking solution (see step 3) with 1% unlabelled anti-mouse IgG, raised in sheep (SO20-220) and 1% unlabelled anti-mouse immunoglobulins, raised in sheep (SO21-220), both supplied by the Scottish Antibody Production Unit, Law Hospital, Carluke, Scotland.

Monoclonal anti-Protein A antibody (P2921) was supplied by Sigma-Aldrich Company Ltd., Poole, Dorset, biotinylated anti-mouse IgG (H & L) antibody (BA-9200) and goat serum (S-1000) were supplied by Vector Laboratories Ltd., Orton Southgate, Peterborough, UK.

2.8 Assessment of bacterial internalisation

2.8.1 Gentamicin exclusion assay

Adult mice (3-6 months old) were anaesthetised with an intraperitoneal injection of Avertin (4.4 mM 2-2-2-tribromoethanol, 2.5% 2-methyl-2-butanol, in distilled water), using 200 µl per 10 g body weight. Tracheal intubation and direct intratracheal instillation of bacteria were performed as described in section 2.5.2. Mice were inoculated with suspensions of fresh, overnight cultures of *P. aeruginosa* CF clinical isolate J1385. After an incubation period of two hours, the mice were sacrificed by lethal intraperitoneal injection of 20 mg of sodium phenobarbitone (Euthatal,

Rhone Merieux). The lungs and tracheae were removed and finely chopped in a petri dish, using a scalpel blade. The chopped lung tissue was transferred to 5 ml Dissociation solution (100 µg/ml Dispase I (neutral protease) (Boehringer Mannheim UK, Lewes, East Sussex, UK), 300 u/ml Collagenase Type XI (Sigma-Aldrich Company Ltd., Poole, Dorset, UK) in PBS), prewarmed to 37 °C. The petri dish was rinsed with the same solution. The suspension was incubated at 37 °C for 20 minutes in an incubator shaker, before being vigorously agitated by repeated aspiration and expulsion with a sterile fine tip pastette (Alpha Laboratories Ltd., Eastleigh, Hampshire, UK) for 30 seconds. The suspension was incubated at 37 °C for a further 20 minutes, followed by vigorous agitation as before, after which it was centrifuged at 1000x g for 15 minutes at room temperature. The supernatant was removed and the pellet was resuspended in 5 ml of 2.5 µg/ml Trypsin solution (Sigma-Aldrich Company Ltd., Poole, Dorset, UK) in PBS at room temperature. This suspension was vigorously agitated as before, incubated at room temperature for 30 minutes and then vigorously agitated again. The suspension was centrifuged at 1000x g for 15 minutes at room temperature. The supernatant was removed and the pellet was resuspended in 10 ml Hank's Balanced Salt Solution (HBSS) without calcium, magnesium or Phenol red (GIBCO BRL, Life Technologies Ltd., Paisley, Scotland), at room temperature. The resultant single cell suspension was then split into a 6 ml Aliquot A and a 4 ml Aliquot B as illustrated in Chapter 5, Figure 5.1. Aliquot A was homogenised using an Omni homogeniser, with replaceable heads, (CamLab Ltd., Cambridge, UK) after which Triton X-100 (t-Octylphenoxypolyethoxyethanol; Sigma-Aldrich Company Ltd., Poole, Dorset, UK) was added to a final concentration of 0.5% and vortexed to lyse all the cells and release any internalised bacteria. Duplicate tenfold serial dilutions were performed from Aliquot A, using HBSS, and plated on Pseudomonas Isolation agar (45 g/L, 2% glycerol; Difco Laboratories Ltd., West Molesey, Surrey, UK). This sample (Sample 1) indicated the total

number of bacteria delivered. Gentamicin (Sigma-Aldrich Company Ltd., Poole, Dorset, UK) was added to the remains of Aliquot A and the whole of Aliquot B to a final concentration of 250 μg/ml and incubated for 1 hour at 37 °C in an incubator shaker. This killed the extracellular bacteria, but not intracellular (Pier *et al* 1997). The samples were centrifuged at 1000x g for 15 minutes at room temperature, the supernatant was removed and the pellet was resuspended in 10 ml HBSS. This was repeated three times to wash off the gentmicin and finally resuspended in the original volume. The samples were homogenised, after which Triton X-100 was added to a final concentration of 0.5% and vortexed to lyse all the cells and release any internalised bacteria. Duplicate tenfold serial dilutions of samples from the gentamicin treated Aliquot A (Control 1) and Aliquot B (Sample 2) were performed in HBSS and plated on agar. Sample 2 indicates the number of bacteria surviving the gentamicin treatment and is proposed to represent the internalised bacteria, released by cell lysis. Control 1 confirms the bactericidal activity of gentamicin on all the exposed bacteria and should not contain any viable organisms. A dilution of the original bacterial suspension (1% of the total dose delivered to the mice) was added to the remains of the gentamicin treated Aliquot A after washing. Duplicate tenfold serial dilutions were performed in HBSS and plated on agar (Control 2). Control 2 confirms that the washing steps are sufficient to remove the gentamicin and thus that any internalised bacteria released by cell lysis will not be subject to the effects of this aminoglycoside antibiotic. In addition, the lungs and trachea of an untreated mouse were removed, homogenised, treated with 0.5% Triton X-100 and a dose of bacteria equal to that delivered to the live mice added. Duplicate tenfold serial dilutions of samples were performed in HBSS and plated on agar (Control 3). Control 3 evaluates any antibacterial activity of the homogenised, lysed cellular material. Plates were incubated overnight at 37 °C, the resultant colony forming units (cfu) were counted and extrapolated to provide the cfu counts for the neat suspensions.

2.8.2 Gentamicin sensitivity assay

P. aeruginosa CF clinical isolate J1385 was recovered from storage at –70 °C, thawed and streak on Pseudomonas isolation agar (45 g/L, 2% glycerol; Difco Laboratories Ltd., West Molesey, Surrey, UK). This was incubated at 37 °C overnight. Nutrient broth (25 g/L, 0.5% w/v Yeast extract; Oxoid Ltd., Basingstoke, Hampshire, UK) was inoculated with a few colonies and incubated at 37 °C overnight in an orbital incubator. 100 µl aliquots of this fresh bacterial suspension were added to 10 ml volumes of Nutient broth containing gentamicin (Sigma-Aldrich Company Ltd., Poole, Dorset, UK) at final concentrations of 0 mg/ml, 1 mg/ml, 10 mg/ml, 100 mg/ml, 250 mg/ml and 500 mg/ml and incubated at 37 °C overnight in an orbital incubator. Pseudomonas isolation agar plates were inoculated using a multiplate inoculator, with each sample. The presence or absence of bacterial growth was examined at each concentration of gentamicin to establish minimum bactericidal concentration levels.

2.8.3 Visualisation of single cell suspension

100 µl samples of enzymatically dissociated murine lung cells, from various stages in the protocol described in section 2.8.1, were used to make air-dried samples by cytospin (Shandon Scientific). Glass slides were precoated with Vectabond (Vector Laboratories Ltd., Orton Southgate, Peterborough, UK) according to the manufacturer's instructions. The air-dried samples were fixed and stained with Diff-Quik ® (Dade, Garridor Ltd., Abingdon, Oxfordshire, UK) according to the manufacturer's instructions.

2.9 Assessment of synthetic defensin peptides

2.9.1 Synthesis of synthetic defensin peptides

Synthetic defensin peptides (hBD-1 and mBD-1) were designed to represent the mature portion of the prepropeptides of HBD-1 and Defb-1 respectively. The peptides were purchased from and synthesised by Albachem Ltd., King's Buildings, Edinburgh, UK, as described below.

hBD-1 was synthesised from Fmoc-Lys(Boc) loaded Wang resin (0.25 mM), and mBD-1 was synthesised from Fmoc-Ser loaded Wang resin (0.48 mM). 1 mM of the amino acids was single coupled via HOCt/DIC, with the exception of His, which was coupled with 3 mM HOCt. The hBD-1 peptide was cleaved from the resin by stirring in EDT (0.25 ml), thioanisole (0.5 ml), water (0.5 ml) and phenol (0.75 g) for 2 minutes, then adding TFA (9.5 ml) and stirring for 4 hours at room temperature. The resin was removed by filtration into ether from which the peptide was precipitated, washed with ether and applied to a Vydac C18 column (flow rate 5 ml/minute, 5 ml loop, 10–50% B over 28 minutes). mBD-1 peptide was cleaved from the resin by stirring in EDT (0.25 ml) and water (0.5 ml) for 2 minutes before adding TFA (9.5 ml). The mixture was stirred at room temperature under nitrogen for 2 hours before being filtered into ether from which the cleaved peptide was precipitated, washed with ether, taken into aqueous acetonitrile and lyophilised. The peptide was then applied to a Vydac C18 column (flow rate 8 ml/minute, 5 ml loop, 10-90% B, 40 minutes). The purified peptides were analysed by RP HPLC (Vydac C18, 5 min loop), R_t = 17 minutes, which, in both cases resulted in a single peak, and MALDI TOF MS analysis showed the correct molecular weight for hBD-1 and mBD-1.

The peptides were lyophilised, weighed and then applied to a Vydac C18 analytical HPLC column with the absorbance set at 214 nm and 280 nm to confirm the weight of the peptide. Equal quantities of each peptide were

analysed and their UV absorbance measured. Both had similar profiles on HPLC and the peak heights were almost identical, confirming the accurate balance measurements. On this basis the peptides were divided into 100 µg aliquots by dissolving in a known volume of water and dividing appropriately. The peptide aliquots were then lyophilised and stored at –20 °C.

2.9.2 Functional analysis of synthetic defensin peptides

Fresh, overnight cultures of bacteria were prepared as described in section 2.3 and supplied in 0.85% saline at ~ 1 x 10^9 colony forming units per ml. Immediately prior to use, 1 ml aliquots of bacterial suspension were centrifuged at 1000x g for 10 minutes at room temperature and resuspended in 10 ml of 10 mM Phosphate buffer (8 mM K_2HPO_4, 2 mM KH_2PO_4, 5.6 mM D-Glucose) containing either 0 mM, 30 mM, 60 mM, 90 mM, 120 mM or 150 mM NaCl (buffer pH 7.60 at 0mM NaCl, pH 7.40 at 30 mM NaCl, pH 7.33 at 60 mM NaCl, pH 7.27 at 90 mM NaCl, pH 7.23 at 120 mM NaCl and pH 7.20 at 150 mM NaCl). A 1 in 50 dilution of the bacterial suspension was performed in the same buffer providing a suspension of ~ 2 x 10^6 cfu per ml. Two sets of duplicate 500 µl reactions were prepared containing 50 µl of either 10 mM Phosphate buffer alone or 10x stock of synthetic peptide (0.5 mg/ml to give a final concentration of 0.05 mg/ml unless otherwise stated) rehydrated in 10 mM Phosphate buffer, 47.5 µl of 10 x stock of NaCl in 10mM Phosphate buffer (0 mM, 300 mM, 600 mM, 900 mM, 1.2 M or 1.5 M NaCl) and 377.5 µl of 10mM Phosphate buffer, to which 25 µl of bacterial suspension (~ 5 x 10^4 cfu) in the appropriate salt concentration was added. These reactions were incubated for 30 minutes at 37 °C, after which duplicate sets of serial tenfold dilutions were prepared from each sample, in 10 mM Phosphate buffer with the appropriate concentration of NaCl. 100 µl samples

were plated out on the appropriate agar (see section 2.3), incubated at 37 °C for 24 hours (48 hours for *B. cepacia*), colony counts were performed and extrapolated to provide the cfu count for the neat sample. The anti-microbial activity of the peptide was compared against buffer alone, to control for the effects on the bacteria of varying the NaCl environment. These studies were repeated to ensure the validity of results, reproducing the salt-sensitive antibacterial profile on a minimum of two separate occasions for each set of conditions.

The optimisation of this method was performed with the assistance of Dr Duncan Borthwick, MRC Human Genetics Unit, Edinburgh, UK. The analysis of the antibacterial activity of synthetic peptides against *B. cepacia* was performed with assistance from Dr Alison Maxwell, Department of Medical Microbiology, University of Edinburgh, UK. Repeated confirmatory studies were performed with the assistance of Susannah MacLean, MRC Human Genetics Unit, Edinburgh, UK.

2.9.3 Statistical analysis of synthetic defensin peptides

Assessment of the appropriate statistical methodologies and analysis of the initial studies was performed by Peter Teague, MRC Human Genetics Unit, Edinburgh.

The bacteriological studies of the synthetic defensin peptides produced results in the form of colony forming unit counts, with duplicate reactions and duplicate dilutions providing four values for each point. These data were observed to have a Poisson distribution (with a number of rare events within a fixed area), thus a square root transformation was performed to allow valid statistical analysis. Applying this transformation stabilised the group variances within but not between each study, thus each experiment's data set was analysed by analysis of variance separately. Analysis of

variance was performed and standard errors for the group means were derived from the mean square error in the analysis of variance. The minimum standard distance could now be calculated for 5%, 1% and 0.1% significance levels. In repeated experiments it was observed that significance at the 0.1% level was reliably repeatable, whereas significance at the 5% level was frequently unrepeatable. Analysis of the significance of differences between peptide and control samples was performed using the minimum standard distance and illustrated graphically, plotting the NaCl concentrations against cfu means under square root transformation, with group standard errors.

The standard means of the colony forming unit counts were used to calculate the quantity of bacteria surviving in the peptide treated samples as a percentage of the counts from the buffer only samples, to control for the effects of changes in NaCl concentration alone. These percentages were expressed as "percentage killing", an variance for this ratio was calculated as:-

$$\text{Var}(\text{meanP}/\text{meanB}) = \frac{(\text{meanB})^2 \times \text{var}(\text{meanP}) + (\text{meanP})^2 \times \text{var}(\text{meanB})}{(\text{meanB})^4}$$

Where P is the peptide sample, B is the buffer only control and Var is the variance. This was used to calculate standard errors and the data was displayed graphically.

2.10 Primary culture of murine tracheal epithelium

2.10.1 Animals

All mice used for primary culture experiments were specified pathogen free. C57Bl/6N mice of both sexes were used, aged 5–7 weeks (Charles Rivers UK Ltd., Margate, UK). All experimental work complied

with the UK Animal (Scientific Procedures) Act 1986. Animals were killed by asphyxiation with CO_2.

2.10.2 Isolation and culture of tracheal epithelial cells

On day 1 the mice were killed by asphyxiation with CO_2, doused with 70% ethanol and tracheae excised, severed at the proximal surface of the thyroid cartilage and at the bifurcation of the bronchi. The thyroid glands and other adherent tissues were removed from the superolateral surfaces (while retaining the underlying proximal tracheae). Tracheae were cut open lengthways, washed in PBS and transferred to Collection Media (see section 2.10.3), pre-warmed to 37 °C. Batches of eight tracheae were transferred to 20 ml of pre-warmed Dissociation Media, containing Pronase and DNase (see section 2.10.3) and incubated at 37 °C for 60 minutes. To stop digestion, 5 ml of sterile foetal calf serum was added before tracheae were gently agitated to dissociate epithelial cells. This was achieved by lightly inverting the suspension 12 times. The suspension was not shaken vigorously. The tracheal "husks" were removed from the suspension and gently washed in 10 ml of Culture Media (see section 2.10.3) by lightly inverting the suspension 12 times, as before. The resultant cell suspensions were pooled and centrifuged at 120x g for 5 minutes at room temperature. After removing supernatants, the pellets were resuspended and washed in 10 ml of Culture Media, centrifuged at 120x g for 5 minutes and resuspended in 5 ml of Culture Media. This suspension was incubated at 37 °C for 2 hours on a 100 mm culture dish (Premaria ™ (Falcon 3803); Becton Dickinson UK Ltd, Oxford, UK) to remove contaminating non-epithelial cells. After this incubation, the media was collected with a fine pastette to collect the unattached cells, centrifuged at 120x g for 5 minutes and resuspended in Culture Media (200 µl of for every two tracheae used). Viable cell counts

were performed using a 50:50 dilution of cell suspension and 1% Trypan Blue (Sigma-Aldrich Company Ltd., Poole, Dorset, UK), utilising a haemocytometer. The number of stained and unstained (viable) cells was counted in two grids, under an inverted light microscope, with the total number of viable cells estimated as 2 x mean viable cell count x 10^4/ml. The dissociated cells from two tracheae (~ 4 x 10^5 cells) were seeded onto one tissue culture insert semi-permeable support membrane (Costar Transwell-clear ™ (3470), tissue culture treated polyester membrane 24 well plate inserts, 0.4 µm pore; Corning Costar, High Wycombe, UK) in 200 µl of Culture Media, with 600 µl outside the insert. To pre-coat these inserts with Type VI, Acid Soluble, Human Placental Collagen (HPC) (C-7521; Sigma-Aldrich Company Ltd., Poole, Dorset, UK), 100 µl of collagen solution (0.5 mg ml^{-1} HPC in distilled water with 0.2% glacial acetic acid) was added to the semi-permeable membrane, air dried overnight and then washed twice with PBS before use. The cells were incubated at 37 °C, in 6% CO_2 in a humidified WTC Binder incubator (Philip Harris, Ashby de la Zouch, Leicestershire, UK) for 3 days. On day 4 the media on the apical surface of the cultured cells was removed, along with any non-adherent cells and debris, and the media on the outside of the insert (bathing the basolateral surface) was replaced with 600 µl USG Media (see section 2.10.3). Once the cells had reached confluency the apical surface of the insert appeared dry, this normally occurred from day 4 onwards. The media bathing the basolateral surface was replaced twice weekly. The primary cultures were maintained in this manner and retained an air interface for as long as the culture remained viable (up to 80 days).

The preparation of primary cultures of murine tracheal epithelia was performed with the assistance of Fiona Kilanowski, MRC Human Genetics Unit, Edinburgh, UK.

2.10.3 Media formulations

COLLECTION MEDIA

1:1 mix of Dulbecco's Modified Eagle Medium (DMEM) (1966-029; GIBCO BRL, Life Technologies Ltd, Paisley, UK) and HAM'S F-12 (21765-029, GIBCO BRL Life Technologies Ltd, Paisley, UK) media containing 100 iu/ml Penicillin / 100 µg/ml Streptomycin (Sigma-Aldrich Company Ltd., Poole, Dorset, UK).

DISSOCIATION MEDIA

Calcium- and Magnesium-free Minimum Essential Media (MEM) (44 mM $NaHCO_3$, 54 mM KCl, 110 mM NaCl, 0.9 mM NaH_2PO_4, 0.25 µM FeN_3O_9, 1 µM Na Pyruvate, 42 µM Phenol Red, pH 7.5), 60 iu/ml Penicillin / 60 µg/ml Streptomycin, 1.4 mg/ml Pronase (165121; Boehringer Mannheim UK, Lewes, East Sussex, UK), 0.1 mg/ml DNAse (DN-25; Sigma-Aldrich Company Ltd., Poole, Dorset, UK).

CULTURE MEDIA

1:1 mixture of DMEM and HAM'S F-12 media containing 100 iu/ml Penicillin / 100 µg/ml Streptomycin, 5% FCS and 120 iu/L Insulin (Nova Human Actrapid NOV100M; AAH Pharmaceuticals, Glasgow, UK).

USG MEDIA

1:1 mixture of DMEM and HAM'S F-12 media containing 100 iu/ml Penicillin / 100 µg/ml Streptomycin and 2% Ultroser-G serum substitute (15950-017; GIBCO BRL, Life Technologies Ltd, Paisley, UK).

2.10.4 Electron Microscopy

Scanning (SEM) and transmission (TEM) electron microscopy were performed on primary cultures of murine tracheal epithelia and tracheal specimens.

2.10.4.1 Scanning electron microscopy

For SEM, specimens were prepared in the following manner:

1) wash with PBS x 5	- 20 minutes
2) fix in 2.5% Glutaraldehyde in PBS	- 30 minutes
3) wash with PBS x 3	- 10 minutes
4) fix with 1% Osmium Tetroxide in PBS	
cultured cells	- 45 minutes
tissue samples	- 90 minutes
5) wash with PBS x 3	- 5 minutes
6) wash with distilled water	- 5 minutes
7) 50% ethanol	- 15 minutes
8) 70% ethanol	- 15 minutes
9) 95% ethanol	- 30 minutes
10) 100% ethanol	- 30 minutes
10) dry 100% ethanol	- 30 minutes
11) hexamethyldisilazane	- 20 minutes
12) hexamethyldisilazane	- 20 minutes
13) air dry overnight	

Primary culture specimens were then cut from the plastic insert and both these and tracheal specimens were mounted on stubs using carbon adhesive discs and silver dag (Agar Scientific Ltd., Stansted, UK) and sputter

coated. This final preparatory step was performed by John Findlay, Biological Sciences E.M. Facility, King's Buildings, University of Edinburgh.

Specimens were viewed using a Cambridge S250 scanning electron microscope at the Biological Sciences E.M. Facility, King's Buildings, University of Edinburgh. Images were recorded on Kodak Tmax 100 film.

To assess quantitatively the different cell populations present, morphometric analyses were performed on SEM images, using primary cultures of murine tracheal epithelium at day 4, 8, 14 and 28 after seeding and tracheal specimens from 5 week old mice. This was accomplished by counting the number of ciliated and non-ciliated cells in ≥ 4 fields of 100 cells and ≥ 2 specimens for each time point.

2.10.4.2 Transmission electron microscopy

Preparation of TEM specimens was performed by John Findlay, Biological Sciences E.M. Facility, King's Buildings, University of Edinburgh.

For TEM, specimens were fixed as for SEM (see section 2.10.4.1). After dehydration specimens were infiltrated with Spurrs resin by means of Propylene oxide in the following manner:

1) Ethanol : Propylene oxide: Spurrs resin 3 : 1 : 0 - 30 minutes
2) Ethanol : Propylene oxide: Spurrs resin 2 : 1 : 0 - 30 minutes
3) Ethanol : Propylene oxide: Spurrs resin 1 : 1 : 0 - 30 minutes
4) Ethanol : Propylene oxide: Spurrs resin 1 : 2 : 0 - 30 minutes
5) Ethanol : Propylene oxide: Spurrs resin 0 : 3 : 1 - 1 hour
6) Ethanol : Propylene oxide: Spurrs resin 0 : 1 : 1 - 2 hours
7) Ethanol : Propylene oxide: Spurrs resin 0 : 1 : 2 - 2 hours
8) Ethanol : Propylene oxide: Spurrs resin 0 : 0 : 1 - 4 hours
9) Ethanol : Propylene oxide: Spurrs resin 0 : 0 : 1 - overnight

Serial sections were cut on a Lecia UCT Ultramicrotome at 80 - 110 nm.

Sections were viewed on a Philips CM120 Biotwin microscope at the Biological Sciences E.M. Facility, King's Buildings, University of Edinburgh. TEM plates were Kodak SO 163.

TEM sections were used to provide additional information about the ultrastructure of primary cultures of murine tracheal epithelium and the morphology of cell types present. Analysis of TEM sections was not performed quantitatively.

2.10.5 Histochemistry

Primary culture membranes were washed in PBS and fixed with 50% acetone : 50% methanol for 5 minutes, while still in intact tissue culture inserts. The semi-permeable membrane with attached cells was cut from the plastic frame before staining. To indicate the presence of goblet cells a standard Periodic Acid Schiff stain was performed (see section 2.7.4), but without the use of α-amylase. Cells were viewed without counter staining or counter stained with Haematoxylin (see section 2.7.4). Cells were viewed on an Olympus CK-2 inverted microscope. Images were captured on slide film using a Wild Photoautomat MPS45 and Wild MP55 camera (Wild, Heerbrugg, Switzerland). Slide images were developed and transferred to digital format by Norman Davidson, Sandy Bruce and Douglas Stuart, MRC Human Genetics Unit, Edinburgh. Adobe photoshop software (Adobe Systems Incorporated, Mountain View, CA, USA) was used for the annotation of images.

2.10.6 Fluorescence Immunohistochemistry

Primary cultures of murine tracheal epithelia and tracheal sections were characterised using antibodies to different cytokeratins, vimentin and α-smooth muscle actin. This assessment was performed using the following antibodies; a mouse monoclonal anti-human pan cytokeratin (C-2562; Sigma-Aldrich Company Ltd.) (1:100 dilution), mouse monoclonal anti-human α-smooth muscle actin (A-254; Sigma-Aldrich Company Ltd.) (1:400 dilution), mouse monoclonal anti-human vimentin (V-6630; Sigma-Aldrich Company Ltd.) (1:40 dilution), mouse monoclonal anti-Proliferating Cell Nuclear Antigen (PCNA) (P-8825; Sigma-Aldrich Company Ltd.) (1:2000 dilution) and rabbit anti-mouse cytokeratin 14 (K14) and rabbit anti-mouse cytokeratin 18 (K18). K14 and K18 were a kind gift from Dr Scott Randell, University of North Carolina Cystic Fibrosis Centre, Chapel Hill, North Carolina, USA. K14 and K18 were raised in rabbits immunised with peptide sequences present in the mouse homologues of human cytokeratin 14 and 18 (K14 – CGKWSTHEQVLRTKN-COOH, K18 – CGRWSETNDTRVLRH-COOH), conjugated to maleimide-activated ovalbumin or bovine serum albumin (Pierce, Rockford, IL, USA) and affinity purified on peptides linked to maleimide-activated Sepharose (Pierce). Negative controls were performed omitting the primary antibodies.

Tissues were fixed in 50% acetone : 50% methanol, processed to paraffin wax blocks and cut to 4 μm sections by microtome (see section 2.7.1). Paraffin wax embedded tissue section slides were rehydrated to distilled water as described in section 2.7.3, but without prior heat treatment to melt the wax. The first two xylene immersions were performed for 30 minutes. The region of interest was delineated by marking a ring around the tissue section with a wax PAP pen (Agar Scientific Ltd., Stansted, Essex, UK). Tissue sections were then processed as described below, at room temperature, unless otherwise stated.

Primary culture specimens were washed 3 times PBS, fixed in 50% acetone : 50% methanol for 5 minutes, washed 3 times in PBS again and cut from the culture insert. Specimens were processed as described below, at room temperature, unless otherwise stated, in wells of a 96 well tissue culture plate :

1) wash with PBS - 5 minutes
2) Blocking solution - 20 minutes
   (Blocking solution : 2% normal animal serum from the species that the secondary antibody was raised in, 0.2% Tween (Polyoxyethylenesobitan), 2% w/v BSA, 7% Glycerol)
3) gently remove blocking solution
4) Primary antibody - 60 minutes
   Primary antibody was diluted to the appropriate concentration in Blocking solution (see step 2).
5) wash 3 times with PBS - 10 minutes
6) Secondary antibody - 30 minutes
   The Fluorescein Isothiocyanate (FITC) secondary antibody was diluted to the appropriate concentration in Blocking solution (see step 2).
7) wash 3 times with PBS - 10 minutes
8) mount in Vectashield™ (H-1000; Vector Laboratories Ltd., Peterborough, UK) containing 3.75 µg/ml DAPI (4,6-Diamidino-2-phenlyindole) nuclear stain.

Stained segments of tissue culture insert with attached cells were mounted in Vectashield™ (H-1000; Vector Laboratories Ltd., Peterborough, UK) on glass slides, taking care that the cells faced upwards. Slides had been precoated with Vectabond Reagant (Vector Laboratories Ltd., Peterborough, UK) according to the manufacturer's instructions. A glass coverslip was overlayed and the edges were sealed with clear nail varnish.

When a primary antibody raised in mouse was used on mouse tissue an additional 20 minute blocking stage was performed before step 2, using Blocking solution with 1% unlabelled anti-mouse IgG, raised in sheep (SO20-220) and 1% unlabelled anti-mouse immunoglobulins, raised in sheep (SO21-220) , both supplied by the Scottish Antibody Production Unit, Law Hospital, Carluke, Scotland. This additional step was followed by washing with PBS, as in step 5 above.

FITC labelled sheep anti-mouse IgG (S121-201) and FITC labelled donkey anti-rabbit (S076-201), sheep serum and donkey serum were supplied by the Scottish Antibody Production Unit, Carluke, UK. Secondary antibodies were used diluted 1:100 in Blocking solution (see step 2 above).

Specimens were viewed using an Axioplan 2 microscope (Carl Ziess Ltd., Welwyn Garden City, UK). Images were acquired using a Pentamax Digital Camera (Princeton Instruments, Marlow, UK). In house capture routine scripts and IPLab Scientific Image Processing software, Version 3.1.1c (Signal Analytics, Vienna, VA, USA) were used to process images and standardise the representation of fluorescence levels between specimens.

To quantify immunohistochemical data, morphometric analyses were performed using primary cultures of murine tracheal epithelia at day 4, 8, 14 and 28 after seeding. The number of cells staining positive per 100 nuclei was counted in 3 fields per sample ($n \geq 2$ at each time point). Analyses of sections of tracheal specimens were also performed ($n \geq 3$ specimens for each antibody). The cell density was assessed by counting the number of nuclei in 3 fields of view at 630x magnification ($n = 4$ at each time point).

2.10.7 Preparation of RNA

All RNA preparations were performed in a double HEPA filter hood (MedicalAir Technology, Manchester) using RNase, DNase free plugged tips.

Primary cultures of murine tracheal epithelia were washed once with PBS, after which 100 µl RNAzol B (Biogenesis Ltd., Poole, UK) was added and moved up and down a few times to ensure that all the cells were completely lysed. Samples were transferred to a fresh screwcap eppendorf tube on ice. 10 µl chloroform was added to each sample and shaken vigorously (not vortexed) for 15 seconds, followed by a 5 minute incubation on ice. The samples were then centrifuged at 10000x g for 15 minutes at 4 °C and the top layer transferred to a fresh screwcap eppendorf tube on ice. The RNA was precipitated by the addition of 45 µl isopropanol (with or without 4 µl glycogen (10 mg/ml stock)) and incubated for at least 15 minutes on ice. The samples were then centrifuged at 10000 x g for 15 minutes at 4 °C and the resulting RNA pellet washed, by vortexing with 75 % ethanol (in DEPC (diethyl pyrocarbonate) treated water) and dried. The RNA was resuspended in 10 µl DEPC treated water and stored at – 70 °C. The quantity and quality of the RNA preparation was assessed by spectrophotometry, assessing the ratio of values at 260 nm and 280 nm.

2.10.8 Preparation of cDNA

All cDNA preparations were performed in a double HEPA filter hood (Medical Air Technology, Manchester, UK) using RNase, DNase free plugged tips. First strand cDNA synthesis was performed from RNA samples using Ready-To-Go® You-Prime First-Strand Beads (Amersham Pharmacia Biotech, St. Albans, UK) as described by the manufacturers. A 2 µg sample of total RNA was diluted to 25 µl in DEPC treated water and denatured by incubation at 65 °C for 10 minutes, before being placed on ice. The sample was transferred to a tube of First-Strand Reaction Mix Beads, but not mixed. 0.2 µg of random hexamer ($pd(N)_6$; Pharmacia Biotech, St. Albans, UK) was added as the chosen primer with DEPC

treated water to make the volume up to 33 µl. This was left at room temperature for 1 minute to allow primer annealing. The sample was then gentley vortexed and briefly spun down in a microfuge to collect the contents at the bottom of the tube, before being incubated at 37 °C for 60 minutes. 5 µl samples were then used in a standard PCR amplification reactions (see section 2.10.9) or stored at – 20 °C. An identical control reaction was performed using First-Strand Reaction Mix Beads in DEPC water that had been incubated at 95 °C for 5 minutes to heat inactivate the Murine Leukaemia virus (M-MuLV) reverse transcriptase to verify for RNA amplification. A minus RNA control was also included to assay for contamination.

2.10.9 Amplification of DNA by polymerase chain reaction

All PCR reactions were performed in a double HEPA filter hood (Medical Air Technology, Manchester, UK) using Rnase, DNase free plugged tips.

Specific DNA sequences were amplified using published methodology (Saiki *et al* 1988). The specificity is provided by oligonucleotide primers complementary to the 5′ ends of the two strands of sequence to be amplified. These primers anneal to the template DNA strand and direct amplification by a thermostable polymerase.

A 50 µl reaction containing up to 1 µg of genomic DNA or 1 ng of plasmid, 5 µl 10 x PCR buffer (P), 5 µl 25 mM $MgCl_2$, 1 µl of 50 x dNTP mix (10 mM of each nucleotide; Advanced Biotechnologies Ltd., Epsom, Surrey, UK) and 100 ng of each primer was prepared in a 0.5 ml thin-walled PCR tube (Advanced Biotechnologies Ltd., Epsom, Surrey, UK). 2.5 units of thermostable *AmpliTaq* DNA polymerase (Perkin Elmer, Roche Molecular Systems Inc., New Jersey, USA) were added to the mixture which was then

overlayed with 50 µl mineral oil (Sigma-Aldrich Company Ltd., Poole, Dorset, UK).

Thermal cycling was controlled by a programmable heating block (OmniGene; Hybaid Ltd., Ashford, Middlesex, UK). Three-step temperature cycling conditions varied, depending on the primers used and length of amplification. The first step was a high temperature step (92 – 94 °C) to denature the template DNA, usually 1-3 minutes in the first cycle, 10-30 seconds thereafter. This was followed by a reduction in temperature to allow the primers to anneal to the template. The annealing temperature is critical in determining the success of the reaction and is dependent upon the structure of the primer. Annealing temperatures were set at ~ 5°C below the primer melting temperatures (T_m). Annealing steps were 30-90 seconds long. Finally the temperature was increased to 72 °C to permit the extension from the primers by the polymerase. The extension time is also critical, with longer products needing longer extension times (~ 2 minute per kb of sequence). Multiple cycles of these steps result in exponential amplification of the desired sequence. The basic programme was 30 cycles of denaturation, annealing and extension steps.

10 µl of the reaction was visualised by electrophoresis on 1–2% agarose gels (see section 2.2.3).

The gene expression profile of primary cultures of murine tracheal epithelia was investigated using cDNA prepared from the primary culture cells as template for intron spanning PCR reactions. A minus DNA negative control and a positive control using the appropriate plasmd DNA were included in each experiment.

Oligonucleotide primers were purchased from Genosys Biotechnologies Inc. Primers were generally chosen to be between 18 and 24 nucleotides in length, with a T_m between 50 °C and 70 °C. Only a 2 nucleotide internal match was allowed if it involved the 3′ end and where possible the A + T : C + G ratio was near 50%.

Gene	Primer name	Primer Sequence (5' – 3')	T_m
Cftr	9AI (exon 9)	5'-AGCAATGGTGACAGAAAACATTCC-3'	68 °C
	11B (exon 11)	5'-CTTGCTAAAGAAATCCTTGCACGC-3'	70 °C
Hprt	5'HP (exon 3)	5'-CTGTAGATTTTATCAGACTGAAGAG-3'	68 °C
	3'HP (exon 8)	5'-GTCAAGGGCATATCCAACAACAAAG-3'	72 °C
Defb1	def1	5'-CCAGCTGCCCATCTAATACC-3'	72 °C
	def2	5'-AATCCATCGCTCGTCCTTTA-3'	63 °C
Defb2	DR5'new	5'-GCCATGAGGACTCTCTGCTC-3'	64 °C
	DR3'new	5'-TGTCACTTGACTTCCATGTGC-3'	64 °C

2.10.10 Radioactively labelled oligonucleotide probes

DNA oligonucleotides were used as probes following radiolabelling using the T4 polynucleotide kinase enzyme, which catalyses the transfer of the terminal phosphate of [γ-^{32} P] ATP to the 5'-hydroxy termini.

Labelled probes from oligonucleotides 15-25 bp in length were made by end-labelling. Approximately 50 ng of oligonucleotide DNA was labelled in a total volume of 20 µl containing 2 µl of 10 x PNK buffer (50 mM Tris HCl pH 8.5, 10 mM $MgCl_2$, 5 mM DTT), 10 units of polynucleotide kinase (Boehringer Mannheim UK, Lewes, East Sussex, UK), and 30 mCi [γ-^{32} P] ATP (Boehringer Mannheim UK, Lewes, East Sussex, UK). The reaction was incubated at 37 °C for 1 hr and then added directly to the prehybridised filters.

Filters were pre-hybridised at 7-10 °C below the T_m for the oligonucleotide for a minimum of 1 hr in rotating hybridisation bottles with 20-50 ml oligo hybridisation buffer (6 x SSC, 0.5% SDS, 0.1% BSA, 0.1% Ficoll, 0.1% polyvinylpyrrolidone, 0.1% disodium pyrophosphate) and 1 mg sonicated salmon sperm. After pre-hybridisation, radiolabelled oligo probe was added directly to the solution and the blots hybridised for 4 hours at a

temperature of 7-10 °C lower than the oligo T_m. Filters were then washed with 4 x SSC/0.1 % SDS for 15 minutes followed by a second wash of 2 x SSC/0.1 % if required. The filters were exposed to Kodak X-OMAT AR film at –70 °C in cassettes containing intensifying screens.

Defb-2 PCR products were not visible on a stained agarose gel after 34 cycles of PCR but were detectable by hybridisation with a *Defb-2* internal oligonucleotide probe, with the sequence TGATCAGTCAACGGG.

2.10.11 Pro-inflammatory stimulation of primary cultures

Total RNA was prepared from primary cultures of murine tracheal epithelium with or without exposure to pro-inflammatory stimuli. A 20 µl volume of either 80 µg of lipopolysaccharide from *E.Coli* (serotype O26:B6; Sigma-Aldrich Company Ltd., Poole, Dorset, UK) in PBS, or ~ 2 x 10^5 cfu of *P. aeruginosa* CF clinical strain J1385 in PBS was gently added to the apical surface of the primary cultures. Untreated controls were simultaneously exposed to PBS alone. Primary cultures were incubated for 30 minutes at 37 °C in a humidified WTC Binder incubator (Philip Harris, Ashby de la Zouch, Leicestershire, UK), after which they were washed with PBS and processed as described in section 2.10.7.

2.10.12 Transepithelial resistance measurement

To monitor the transepithelial resistance (R_t) of cultured murine tracheal epithelia, an EVOM™ epithelial voltohmmeter (World Precision Instruments, Stevenage, UK) was used, after the addition and equilibration of 200 µl of USG Media (see section 2.10.3), pre-warmed to 37 °C, to the apical surface. The longer end of the probe was inserted into

the media surrounding the tissue culture insert, while the shorter end was inserted into the insert, taking care not to touch the culture cell layer. R_t was monitored at day 4, 8, 14 and 28 after seeding. The same technique was used to monitored R_t on HBE cell line cultures (see section 2.11).

2.10.13 Ussing chamber analysis

Electrophysiological analysis of primary cultures of murine tracheal epithelia was performed using modified Ussing chamber apparatus (Jim's Instruments Manufacturing Corp, Iowa City, IA, USA), a Physiological Instruments VCCMC2 Dual Channel Voltage-Current Clamp (ADInstuments Ltd., Hastings, UK), a MacLab/4s recorder and Chart for Macintosh (version 3) data acquisition and analysis software (both supplied by ADInstruments Ltd., Hastings, UK).

The circulating waterbath supplying the modified Ussing chambers was started and the equipment was given 1 hour to equilibrate at 37 °C. A "dummy" culture insert was mounted in the modified Ussing chamber and both the apical and basolateral surfaces bathed with a physiological solution containing: 140 mM NaCl, 5 mM KCl, 0.36 mM K_2HPO_4, 0.44 mM KH_2PO_4, 1.3 mM $CaCl_2$, 0.5 mM $MgCl_2$, 10 mM N-2-hydroxyethylpiperazine-N'-2-ethanesulphonic acid (HEPES), 4.2 mM $NaHCO_3$ and 5 mM D-glucose, titrated to pH 7.2 with Tris. This solution was constantly gassed with 95% CO_2, 5% O_2. The voltage (ELEC/CV; ADInstuments Ltd., Hastings, UK) and current (Ag/AgCl) electrode pairs were connected to the apical and basolateral solutions by polyethylene tubing (PE160; Garridor Ltd., Oxfordshire, UK) filled with 3 M KCl - 3% w/v Noble Agar (A5431; Sigma-Aldrich Company Ltd). The Voltage-current clamp was switched on and given at least 10 minutes to warm up.

The voltage was measured under open circuit conditions and this asymmetry voltage between the voltage measuring electrodes was offset so that the voltage reads 0.0. The fluid resistance compensation button was then used to measure the current and verify that ~ 60-68 μA was registered, indicating that the resistance of the current passing bridges or electrodes was not excessive.

Primary cultures of murine tracheal epithelia were then mounted in the modified Ussing chambers, being careful not to change the positions of the electrode tips, and the transepithelial voltage was clamped at 0 mV. I_{sc} was recorded continuously using the MacLab/4s recorder, R_t was monitored by 10 mV voltage steps (duration 0.1 second, period 10 seconds) and calculated using Ohm's Law. A positive I_{sc} value represented a flow of positive charge from luminal (apical) to basolateral solution (anions moving in the opposite direction).

To investigate the electrophysiological characteristics of primary cultures of murine tracheal epithelia, the following agents were sequentially added: a) amiloride (10 μM) to the apical reservoir to inhibit the epithelial Na^+ channel (ENaC), b) cAMP agonists (10 μM forskolin, 100 μM 3-isobutyl-1-methyxanthine (IBMX) and 500 μM 8-(4-chlorophenylthio) adenosine 3′:5′-cyclic monophosphate (CPT-cAMP)) to the apical reservoir to activate the cystic fibrosis transmembrane conductance regulator (CFTR) Cl^- channel, and c) bumetanide (100 μM) to the basolateral reservoir to inhibit the Na^+, K^+, $2Cl^-$ co-transporter and hence, transepithelial Cl^- secretion. Each reservoir contained both the test drug and the previously studied drugs within the sequence. The addition of each agent was performed only after stablilisation of I_{sc}. This protocol was performed on primary cultures of murine airway epithelium at day 28 after seeding (n = 6).

Amiloride hydrochloride (A7410), bumetanide (B3023), CPT-cAMP (C3912), forskolin (F6886), HEPES (H7523) and IBMX (I7018) were all

supplied by Sigma-Aldrich Company Ltd., Poole, Dorset, UK. All other chemicals were of reagant grade.

CPT-cAMP and Amiloride were dissolved in distilled water, forskolin and bumetanide in dimethyl sulfoxide (DMSO) and IBMX in ethanol. Stock solutions were stored at –20 °C and diluted in the physiological solution to achieve final concentrations immediately before use.

2.11 Cell culture

Human Bronchial Epithelium (HBE) cells lines were seeded at a density of 4 x 10^5 cells per insert, on tissue culture insert semi-permeable support membranes (Costar Transwell-clear™ (3470), tissue culture treated polyester membrane 24 well plate inserts, 0.4 µm pore; Corning Costar, High Wycombe, UK) in 200 µl of media, with 600 µl outside the insert. To pre-coat these inserts with Type VI, Acid Soluble, Human Placental Collagen (HPC) (C-7521; Sigma-Aldrich Company Ltd., Poole, Dorset, UK), 100 µl of collagen solution (0.5 mg ml^{-1} HPC in distilled water with 0.2% glacial acetic acid) was added to the semi-permeable membrane, air dried overnight and then washed twice with PBS before use. Alternatively inserts were previously incubated overnight at 37 °C with Minimal Essential Medium (MEM) containing 0.1 mg/ml (w/v) BSA, 0.1 mg/ml (w/v) Fibronectin (33016-023; GIBCO BRL, Life Technologies Ltd, Paisley, UK) and 0.05 mg/ml (w/v) mouse collagen IV (33018-011; GIBCO BRL, Life Technologies Ltd, Paisley, UK). Cells were cultured in MEM with Earle's salts and L-glutamine (31095-029; GIBCO BRL, Life Technologies Ltd, Paisley, UK) containing 10% FCS, 1% non-essential amino acids and 100 iu/ml Penicillin / 100 µg/ml Streptomycin (Sigma-Aldrich Company Ltd., Poole, Dorset, UK). The cells were incubated at

37 °C, in 6% CO_2 in a humidified WTC Binder incubator (Philip Harris, Ashby de la Zouch, Leicestershire, UK). Cells reached confluency after approximately 7 days but were unable to maintain an air-liquid interface. Transepithelial resistance measurements were stable from day 7 onwards (see section 2.10.12).

2.12 Statistical analysis

Calculations of means, standard deviations, Student's T tests and Kruskal-Wallis tests were performed using Minitab 12.23 software (Minitab Inc.) or Microsoft Excel 97 software (Microsoft Corporation). Differences were considered statistically significant when $P < 0.05$. Duplicate blinded analyses of the total score for severity of murine lung histopathology (see section 2.7.8) were compared using a weighted Kappa measure of agreement. This was performed by distributing the scores between 10 categories equally spaced across the range and comparing the observed frequencies of exact agreements and levels of disagreements with the derived expected numbers. Advice on statistical analysis was provided by Peter Teague, MRC Human Genetics Unit, Edinburgh. Statistical analysis of the antibacterial activity of synthetic defensin peptides is described in section 2.9.3.

Chapter 3

Bacterial delivery systems

Chapter 3: Bacterial delivery systems

3.1 Introduction

Initial studies using the *Cftr*^{tm1Hgu}/*Cftr*^{tm1Hgu} mice demonstrated that no gross lung phenotype was evident when the mice were born and maintained in sterile conditions (Davidson *et al* 1995). However, abnormalities were observed when these animals were challenged with CF related respiratory pathogens (see Chapter 1, section 1.7.3.5).

These preliminary studies were performed using a relatively crude nebulisation chamber. The bacterial delivery profile of this apparatus had not been quantitatively determined, examined for reproducibility, or analysed in terms of its anatomical distribution pattern. In addition, concerns had been raised about the possibility that nebulisation may shear bacterial pili. This would have particular significance in the delivery of *P. aeruginosa*. The adherence of pili to aGM_1 receptors has been suggested to play an important part in the predilection of this bacteria for the CF lung (see Chapter 1, section 1.5.2.1). Consequently, techniques and apparatus suitable for clearly quantified, reproducible bacterial delivery, with and without nebulisation, to defined regions of the pulmonary system were assessed and developed.

A variety of modifications of two primary approaches were assessed. Firstly, adaptation of the mouse nebuliser apparatus, initially developed by Prof. David Porteous in the MRC Human Genetics Unit, Edinburgh. Secondly, the development of direct intratracheal instillation techniques.

3.2 Mouse nebuliser apparatus

3.2.1 Design

The nebuliser apparatus developed for the preliminary studies was a relatively crude device. The results of these bacterial exposure experiments revealed significant differences between the *Cftr*^{tm1Hgu}/*Cftr*^{tm1Hgu} mice and their non-CF littermates, but with a broad spectrum and considerable overlap observed in the phenotypes of the two groups of mice. One possible reason for this may have been flaws with the delivery system. Consequently the original design was reassessed for further studies.

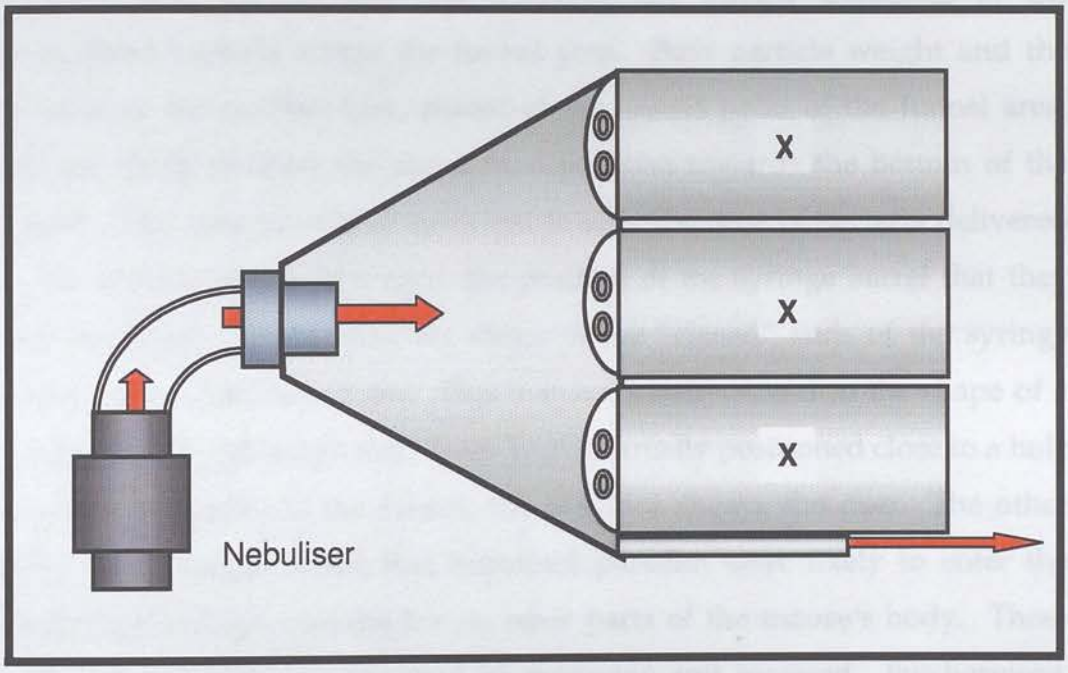

FIGURE 3.1 Nebuliser design #1

The original mouse nebuliser design. Mice are placed in the syringe barrels indicated by **X**. The red arrows indicate the flow of nebulised bacterial suspension.

The original apparatus (Nebuliser #1) consisted of a Sidestream nebuliser feeding directly into a plastic funnel via a plastic tube with a right angled bend (see figure 3.1). The wide end of the funnel was attached to six 50 ml plastic syringe barrels, with the "closed" ends facing into the funnel and each punctured with 5 holes. All the surrounding gaps were sealed with the exception of one outflow tube. Mice were placed, head first, into each of the syringe barrels with the syringe plunger used to prevent them from turning around or leaving the tube. A bacterial suspension was then nebulised into the funnel area from which the mice would breath.

This design appeared to have a variety of theoretical and practical weaknesses. The bacteria were delivered, by carrier gas, at a flow rate of 12 litres per minute, directly into a right angled tube, about 7 cm from the nebuliser head. It seemed likely that this had the potential to damage the bacteria, alter particle size and influence the airflow dynamics of the aerosolised bacteria within the funnel area. Both particle weight and the position of the outflow tube, placed at the lowest point of the funnel area, seemed likely to draw the aerosolised particles towards the bottom of the funnel. This may have been sufficient to alter the dose of bacteria delivered to the animals, dependent upon the position of the syringe barrel that they each occupied. In addition, the shape of the "closed" ends of the syringe barrels was a flattened dome. This was not ideally suited to the shape of a mouse's head. Although their noses were normally positioned close to a hole connecting directly to the funnel, this was not always the case. The other holes in the barrel meant that nebulised particles were likely to enter the barrel and perhaps coat the fur on other parts of the mouse's body. These bacteria would later be removed by grooming and ingested. Furthermore, the cluster of syringe barrels made it difficult to monitor the status of all the mice during the course of the experiment, particularly the one in the middle, in case of signs of distress. Finally, the material from which the syringe barrels was constructed was rather too easily chewed. The numerous holes

at the end of the barrel gave the mice easy purchase to rapidly destroy the apparatus.

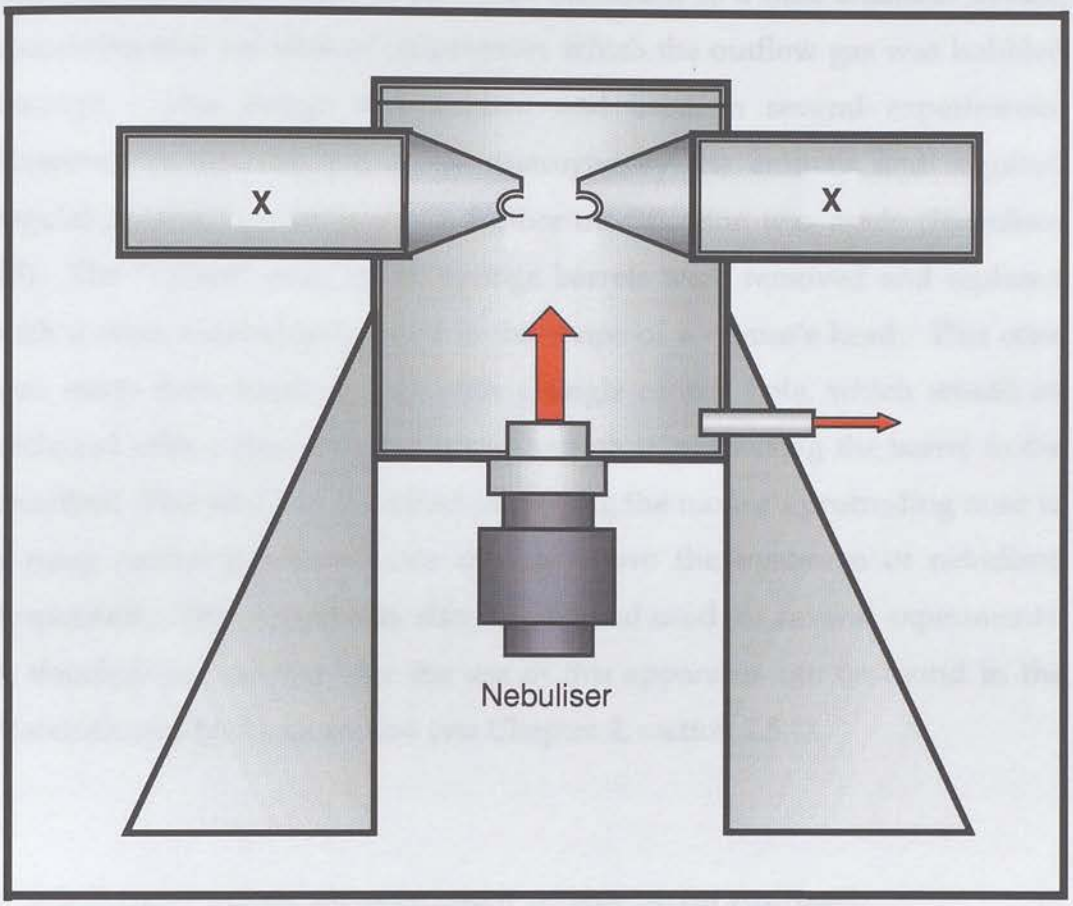

FIGURE 3.2 Nebuliser design #2 and #3

The radial multi-nebuliser, models #2 and #3. Mice are placed in the syringe barrels indicated by **X**. The red arrows indicate the flow of nebulised bacterial suspension.

The nebulisation apparatus was redesigned (Nebuliser #2) to address these concerns and constructed by Duncan Fletcher at the MRC Human Genetics Unit, Edinburgh (see figure 3.2). The new design allowed direct entry of the nebulised bacterial suspension into a cylinder, at point

equidistant from 6 radially arranged 50 ml syringe barrels. Flow was directed up toward these barrels with the outflow at the base of the cylinder venting the chamber as the particles descended again. To address additional safety concerns, the outflow pipe was connected to a dual chamber device, containing two volumes of disinfectant, which the outflow gas was bubbled through. This design was studied and used in several experiments. However, it was still too easily destroyed by the animals and required regular repairs. Consequently a further modification was made (Nebuliser #3). The "closed" ends of the syringe barrels were removed and replaced with a cone, more closely fitted to the shape of a mouse's head. This cone was made from hard perspex with a single central hole, which would be occluded with a mouse's nose stuck through it, connecting the barrel to the chamber. This also had the effect of moving the mouse's protruding nose to a more central position, more directly above the upstream of nebulised suspension. This design was also studied and used for several experiments. A detailed methodology for the use of this apparatus can be found in the Materials and Methods section (see Chapter 2, section 2.5.1).

3.2.2 Quantitative assessment of bacterial delivery

Quantitative assessment of the mouse nebulisation apparatus was conducted using groups of 4–6 non-CF mice on a mixed outbred MF1/129 strain background. A standard protocol was followed as described in Materials and Methods (see Chapter 2, section 2.5.1 and 2.6.1). Briefly, mice were restrained in the nebuliser apparatus while 4 ml of bacterial suspension was nebulised into the chamber over a period of 5 minutes. The initial quantitative studies were performed using a well characterised *B. cepacia* CF clinical isolate J2315, on the basis that the viability of this organism might be less impaired in the lung environment during tissue processing than other

bacteria. Subsequent studies were performed using *S. aureus* CF clinical isolate C1705. Bacterial suspensions, prepared from fresh overnight cultures, were supplied by Wendy Hannant and Cathy Doherty, Medical Microbiology department, University of Edinburgh (see Chapter 2, section 2.3). Animals were sacrificed immediately after the nebulisation period, the lungs were removed and homogenised in PBS, either with or without the trachea. In the latter scenario, the trachea and primary bronchi were processed separately from the lungs to establish the level of deposition in the largest airways (see section 3.2.3). Dilutions of the homogenates were plated out on appropriate agar and the resultant colony forming units counted.

The bacterial deposition established in the murine lungs using these nebuliser delivery systems was compared to previously published particle inhalability curves for small laboratory animals (Ménache *et al* 1995). The respiratory minute volume for the mice was calculated according to the Guyton formula (Raabe *et al* 1988): respiratory minute volume (ml) = 2.1 x (weight (g))$^{0.75}$. The mean body weight of the mice used in these studies was 22 g, providing an estimated respiratory minute volume of ~ 20 ml. The inhaled dose was estimated as the concentration of bacteria per ml x length of exposure x respiratory minute volume and corrected for inhalability according to the particle size. The inhalability size varies between species. In small laboratory animals ~ 95% inhalability is predicted for particles < 0.7 μm diameter, with ~ 45% inhalability predicted for 10 μm diameter particles (Ménache *et al* 1995). At a carrier gas flow of 12 litres per minute the sidestream nebuliser has been demonstrated to create particles of approximately 1.9 μm (Alton *et al* 1993). The addition of a "baffle" decreased particle size to 1.7 μm. In mice, inhalability of ~ 85% and ~ 90% would be expected for particles of 1.9 μm and 1.7 μm respectively (Ménache *et al* 1995). These corrections were applied to estimate inhaled dose.

The lung deposition efficiency is dependent upon particle size and increases as a function of particle size when normalised for inhalability

(Ménache *et al* 1995). If all particles are inhalable then as the size increases so the percentage of inhaled particles deposited in the lungs approaches 100%. However, above an optimum size, some particles are not inhalable and the lung deposition will decrease. Although smaller particles have a higher inhalability, the deposition rate of the smallest particles is low. For mice the optimum particle size has been estimated to be between 1 μm and 3.5 μm. The deposition efficiency calculated is a function of particle size and represents the pulmonary deposition as a percentage of the estimated inhale dose. For particle sizes of 1.9 μm and 1.7 μm deposition efficiencies of ~ 50% and ~ 40% would be expected on the basis of previous studies using monodispersed aerosols of fused aluminosilicate particles labelled with ^{169} Ytterbium (Ménache *et al* 1995).

3.2.2.1 Nebuliser #2

The modified Nebuliser #2 apparatus was used to assess the delivery of *B. cepacia*, as shown in Tables 3.1 and 3.2. The concentration of the bacterial suspension was estimated using spectrophotometery and showed some variation between experiments, thus study results are not pooled. The total lung delivery of viable bacteria using this system is reasonably reproducible, with a maximum 6 fold variation observed between mice. This variation did not correlate with the position in the apparatus occupied by the mouse, or with the weight of the animal. The mean number of viable bacteria recovered from the lungs of each mouse was 3.3×10^4 ($\pm 1.9 \times 10^4$) in the first experiment and 5.6×10^4 ($\pm 1.6 \times 10^4$) in the second experiment detailed below. This constituted a lung deposition efficiency of 0.77% and 0.66% respectively.

Experiment 1	Total cfu count Lung and airways	Total cfu count stomach and oesophagus
Mouse A	2.2×10^4	4.6×10^3
Mouse B	3.9×10^4	1.1×10^3
Mouse C	5.5×10^4	1.6×10^3
Mouse D	1.3×10^4	1.8×10^3
Mean	**3.3×10^4**	**2.3×10^3**
SD	1.9×10^4	1.6×10^3
Estimated total nebulised dose	**3.0×10^9** in 60 L	
Estimated inhaled dose	**4.3×10^6**	
Deposition efficiency	**0.8 %**	

TABLE 3.1 Nebuliser #2 – bacterial delivery profile 1

Quantification of the bacterial delivery profile of Nebuliser #2, using *B. cepacia*.

Experiment 2	Total cfu count Lung and airways	Cfu count Lung	cfu count Large airways
Mouse A	7.7×10^4	7.5×10^4	1.6×10^3
Mouse B	3.3×10^4	3.3×10^4	-
Mouse C	5.5×10^4	5.4×10^4	1.1×10^3
Mouse D	5.1×10^4	5.1×10^4	-
Mouse E	6.2×10^4	6.2×10^4	-
Mean	**5.6×10^4**	-	-
SD	1.6×10^4	-	-
Estimated total nebulised dose	**6.3×10^9** in 60 L		
Estimated inhaled dose	**8.5×10^6**		
Deposition efficiency	**0.7 %**		

TABLE 3.2 Nebuliser #2 – bacterial delivery profile 2

Quantification of the bacterial delivery profile of Nebuliser #2, using *B. cepacia*.

These studies were repeated using *S. aureus*. A representative experiment is shown in Table 3.3. The total lung delivery of viable bacteria is similar to that demonstrated for *B. cepacia*. The mean number of viable

bacteria recovered from the lungs of each mouse was 7.1×10^4 ($\pm 0.8 \times 10^4$). This constituted a lung deposition efficiency of 1.4% .

Experiment 3	Total cfu - Lung and airways
Mouse A	7.2×10^4
Mouse B	8.1×10^4
Mouse C	6.1×10^4
Mouse D	6.9×10^4
Mean	**7.1×10^4**
SD	0.8×10^4
Estimated total nebulised dose	**3.6×10^9** in 60 L
Estimated inhaled dose	**5.1×10^6**
Deposition efficiency	**1.4 %**

TABLE 3.3 Nebuliser #2 – bacterial delivery profile 3

Quantification of the bacterial delivery profile of Nebuliser #2, using *S. aureus*

These studies demonstrate that Nebuliser #2 provided a reasonably reproducible delivery of bacteria to the lungs, with a range of approximately 1×10^4 - 1×10^5 cfu per mouse, and deposition efficiency of 0.7-1.4%. This apparatus was used for repeated nebulisation studies (see Chapter 4).

On the basis of previous studies, deposition efficiencies of ~ 50% would be expected for 1.9 μm diameter particles (Ménache *et al* 1995). Thus, the deposition efficiency established for Nebuliser #2 is only ~ 2% of the anticipated level. This is likely to relate to chamber design and the viability of the bacteria. The assessment of bacterial delivery will only indicate the number of viable organisms in the lung and a considerable proportion of the bacteria may be killed by innate lung defences in the tissue processing period. In addition, damage to bacteria as a result of the nebulisation process cannot be ruled out. To assess the impact of nebulisation upon the viability of *S. aureus*, the nebulised suspension was passed directly into PBS in a glass impinger, dilutions were plated and colony counts performed. In repeated

studies the number of viable bacteria collected was found to be ~10% of the total number of bacteria nebulised. This suggests that a large proportion of the bacteria nebulised may be killed by this process, although it is possible that this technique may have failed to collect all of the nebulised organisms. Thus the low deposition efficiency, in comparison to the published studies, is likely to be the result of chamber design and bacterial death, both in the murine lungs and as a result of the nebulisation process. The effect of the "baffle" upon bacterial viability was not quantified.

The similarity in the proportion of bacteria delivered to the mouse lungs whether *S. aureus* or *B. cepacia* was used suggests that this delivery profile is likely to be independent of the bacteria used. However, quantitative assessment should still be repeated before the use of other bacteria with this delivery system.

3.2.2.2 Nebuliser #3

Nebuliser #3 was constructed to survive the attentions of its experimental occupants more effectively, but also altered the position of the mouse's nose with respect to the chamber inlet. Consequently, similar quantitative studies were performed using this design. It was found to increase the dose received per mouse. A representative study is detailed in Table 3.4.

The original repeated exposure studies using mouse models of CF, were performed using a standard protocol comprising two periods of nebulisation, 5 minutes with and 5 minutes without the addition of a "baffle" to alter particle size. At a carrier gas flow of 12 litres per minute the sidestream nebuliser created particles of approximately 1.9 μm. The addition of the "baffle" to this nebuliser decreased particle size to 1.7 μm (Alton *et al* 1993). This was proposed to increase delivery to the smaller airways. The

studies described here also examined the impact of the baffle upon bacterial delivery.

	Protocol	Total cfu count Lung and large airways
Estimated total dose nebulised in 5 min	-	**8×10^9 in 60 L**
Mouse A	5 minutes exposure without the "baffle"	1.5×10^6
Mouse B		1.6×10^6
Mouse C		1.5×10^6
Mean		**1.5×10^6**
SD		0.1×10^6
Estimated inhaled dose		**1.1×10^7**
Deposition efficiency		**13.6 %**
Mouse D	5 minutes exposure without the "baffle" and 5 minutes exposure with the "baffle"	1.0×10^6
Mouse E		2.3×10^6
Mouse F		1.9×10^6
Mean		**1.7×10^6**
SD		0.7×10^6
Estimated inhaled dose		**2.3×10^7**
Deposition efficiency		**7.4%**
Mouse G	5 minutes exposure with the "baffle"	5.3×10^5
Mouse H		6.3×10^5
Mouse I		5.7×10^5
mean		**5.8×10^5**
SD		0.5×10^5
Estimated inhaled dose		**1.2×10^7**
Deposition efficiency		**4.8%**

TABLE 3.4 Nebuliser #3 – bacterial delivery profile

Quantification of the bacterial delivery profile of Nebuliser #3, using *S. aureus*, with and without the addition of a nebuliser "baffle".

The mean number of viable organisms recovered from the lungs of each mouse was 1.5×10^6 ($\pm$ 0.05×10^6) when the protocol detail above for

Nebuliser #2 (without the "baffle") was used. This constituted a lung deposition efficiency of 13.6%. The addition of the "baffle" significantly reduced the mean number of viable bacteria recovered from the lungs of each mouse to 5.8×10^5 ($\pm 0.5 \times 10^5$) ($p = 0.004$). This constituted a lung deposition efficiency of 4.8% of the estimated total number of bacteria nebulised into the chamber. Analysis using a protocol of 5 minutes with the "baffle" and 5 minutes without, confirmed these data, with the quantity of viable bacteria being approximately equal to the sum of the other two protocols performed independently (see Table 3.4). This apparatus was also used for repeated nebulisation studies (see Chapter 4).

These studies demonstrate that Nebuliser #3 provided a reproducible delivery of bacteria to the lungs, with a range of approximately 1×10^6 - 2×10^6 cfu per mouse, and a deposition efficiency of 13.6%. Although this is still lower than the 50% deposition efficiency expected for 1.9 μm particles (Ménache *et al* 1995), it is considerably higher than the efficiency achieved with Nebuliser #2. This difference demonstrates the importance of chamber design. The remaining difference between the deposition efficiency expected and that observed is likely to relate to bacterial death, contrasting with the use of inert radioactive particles in the published study.

As anticipated, the smaller particles produced by the addition of the "baffle" decreased the deposition efficiency from 13.6% to 4.8%. Although 40% deposition efficiency might be expected for 1.7 μm particles (Ménache *et al* 1995), the previously discussed explanations apply.

3.2.2.3 Nebuliser #1

Finally, to allow direct comparison to be made between studies performed using the original nebulisation apparatus and those with the new design, the old apparatus was assessed in the same manner (without the "baffle"), using *S. aureus* (see Table 3.5).

	Total cfu count Lungs and airways
Mouse A	1.8×10^5
Mouse B	1.5×10^5
Mouse C	1.1×10^5
Mouse D	1.6×10^5
Mouse E	1.0×10^5
Mouse F	1.2×10^5
Mean	**1.4×10^5**
SD	0.3×10^5

Estimated Total nebulised dose	**2.3×10^9** in 60 L
Estimated inhaled dose	**3.2×10^6**
Deposition efficiency	**4.4%**

TABLE 3.5 Nebuliser #1 – bacterial delivery profile

Quantification of the bacterial delivery profile of Nebuliser #1, using *S. aureus*.

As a result of damage by experimental animals during previous studies, the equipment could not be restored to full function and the results of this experiment should be viewed only as a general indication of the level of bacterial delivery in previous studies. However, the delivery profile seems to be broadly comparable with results using the other nebuliser designs and indeed, probably better then a dose delivered using Nebuliser #2.

3.2.3 Bacterial distribution profile

In order to evaluate the distribution of nebulised bacteria, specimens from the studies described above (see section 3.2.2.1) were divided before processing. The trachea and primary bronchi were detached from the lungs

and processed separately. In addition, the stomach and oesophagus were dissected from the same animals and also processed in an identical manner.

These studies demonstrated that approximately 2% of the bacteria delivered to the lungs was located in the largest airways immediately after nebulisation (n = 2, Table 3.2). The other 98% was in the smaller airways and the alveolar spaces. The dose located in the oesophagus and stomach at this time point was found to be approximately 10 fold smaller than the lung dose (see representative experiment in Table 3.1).

In addition to these quantitative studies, lungs from mice exposed to *S. aureus* in these experiments were fixed with 10% NBF and processed to paraffin wax blocks (n = 6, see Chapter 2, section 2.7.1). Sections cut from these specimens were subjected to immunohistochemical analysis, using an antibody to *S. aureus* protein A (see Chapter 2, section 2.7.9). These studies demonstrated the presence of *S. aureus* in the alveolar spaces, following delivery by nebulisation (see Figure 3.3).

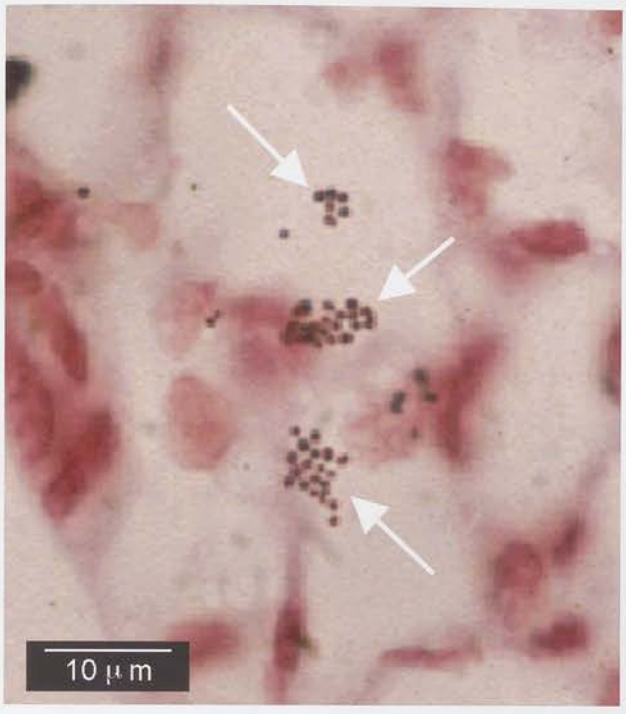

FIGURE 3.3 Delivery of *Staphylococcus aureus* to the peripheral airways

A light microscopic image of mouse alveoli, demonstrating the presence of *S. aureus* in the alveolar spaces. Clusters of bacteria are indicated by white arrows.

3.3 Intratracheal Instillation

An alternative delivery system was also sought that did not involve nebulisation of the bacteria and was capable of high dose delivery. To meet these requirements methods of direct intratracheal instillation were assessed.

The most commonly used method involves an incision in the neck of the mouse, separation of the submandibular glands and puncture of the trachea. This technique was rejected on the basis that it created a wound site, which could become infected, unnecessary trauma and could result in severe inflammation secondary only to the method of bacterial delivery. In addition, this technique was not amenable to repeat dosing, using the same mouse over a short time period.

An alternative technique was employed, optimising a previously described non-surgical method (Ho and Furst 1973). This is described in detail in Materials and Methods (see Chapter 2, section 2.5.2). Briefly, an anaesthetised mouse was placed in a specially constructed frame to appropriately configure the position of its head and thorax (see figure 3.4). A bright light was placed against the xiphisternum and the tongue extended, revealing illumination of the tracheal lumen. An adapted spinal needle was passed into the tracheal and 25 µl of bacterial suspension delivered, followed through by a small volume of air. This technique required a considerable amount of practice, but once mastered proved to be a quick and effective method for the delivery of concentrated bacterial suspensions.

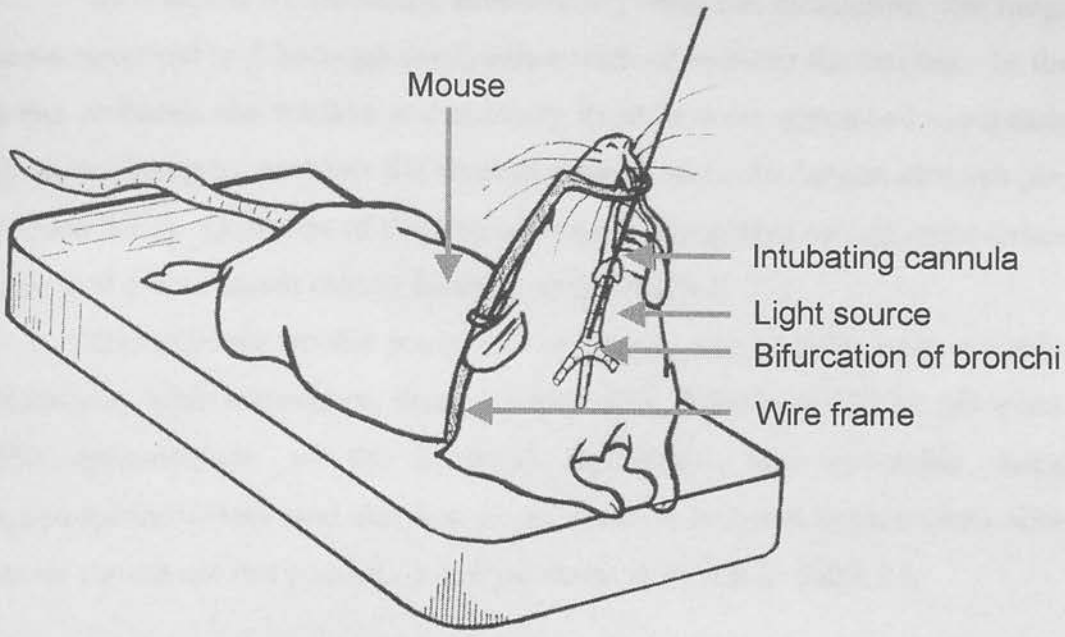

FIGURE 3.4 Direct Intratracheal instillation

3.3.1 Quantitative assessment of bacterial delivery

Quantitative assessment of this non-surgical, direct intratracheal instillation technique was performed using groups of 6 non-CF mice on a mixed outbred MF1/129 strain background. A standard protocol was followed, as described in Materials and Methods (see Chapter 2, sections 2.5.2 and 2.6.1). For the purpose of initial quantification, mice were exposed to *B. cepacia* CF clinical isolate J2315, on the basis that the viability of this organism might be less impaired in the lung environment during tissue processing than other bacteria. Subsequent studies were performed using non-mucoid *P. aeruginosa* CF clinical isolate J1385. Bacterial suspensions, prepared from fresh, overnight cultures, were supplied by Wendy Hannant and Cathy Doherty, Medical Microbiology department, University of Edinburgh (see Chapter 2, section 2.3).

Animals were sacrificed immediately after the instillation, the lungs were removed and homogenised, either with or without the trachea. In the latter scenario, the trachea and primary bronchi were processed separately from the lungs to establish the level of deposition in the largest airways (see section 3.3.2). Dilutions of the homogenates were plated out on appropriate agar and the resultant colony forming units counted.

The delivery profile using this technique was initially very variable. However, with experience, more reproducible delivery could be achieved. The concentration of the bacterial suspension was estimated using spectrophotometery and showed some variation between experiments, thus study results are not pooled. A typical result is shown in Table 3.6.

	Total cfu count Lungs and airways	cfu count Lungs	cfu count Large airways
Mouse A	1.7×10^7	-	1.7×10^7
Mouse B	1.1×10^7	-	1.1×10^7
Mouse C	1.4×10^7	-	1.4×10^7
Mouse D	1.4×10^7	-	1.4×10^7
Mouse E	9.3×10^6	8.0×10^6	1.3×10^6
Mouse F	6.8×10^6	6.1×10^6	0.7×10^6
Mean	**1.2×10^7**	-	-
SD	3.4×10^6	-	-

Estimated total dose instilled	**3.6×10^7**
% recovery of total dose instilled	**33.3%**

TABLE 3.6 Direct intratracheal instillation – bacterial delivery profile 1

Delivery of *B. cepacia* to the lungs of a cohort of non-CF MF1 mice by direct intratracheal instillation.

The number of bacteria instilled was assessed by delivery of an identical volume of bacterial suspension directly into PBS via the intubating cannula. The instillation of 3.6×10^7 cfu of *B. cepacia* into the airways, resulted

in recovery of 1.2×10^7 ($\pm 3.4 \times 10^7$) cfu by removal and homogenisation of the lungs, with a range of 20-50% of the delivered dose being recovered.

The subsequent analysis of this delivery technique using *P. aeruginosa* demonstrated a very similar delivery profile (see Table 3.7).

	Total cfu count
Lung and airway homogenate Mouse A	1.6×10^7
Lung and airway homogenate Mouse A	1.6×10^7
Lung and airway homogenate Mouse A	1.3×10^7
Lung and airway homogenate Mouse A	1.2×10^7
Mean	**1.4×10^7**
SD	0.2×10^7

Estimated total dose instilled	**2.5×10^7**
% recovery of total dose instilled	**56%**

TABLE 3.7 Direct intratracheal instillation – bacterial delivery profile 2

Delivery of *P.aeruginosa* to the lungs of a cohort of non-CF MF1 mice by direct intratracheal instillation.

Delivery of bacteria by direct intratracheal instillation resulted in the death of approximately 1 in 20 of the experimental animals. This was increased if volumes greater than 25 µl were instilled.

3.3.2 Bacterial distribution profile

In order to evaluate the distribution of bacteria delivered by intratracheal instillation, some specimens from the studies described above (see section 3.3.1) were divided before processing. The trachea and primary bronchi were detached from the lungs and processed separately. In addition, the stomach and oesophagus were dissected from the same animals and also processed in an identical manner.

This assessment demonstrated that approximately 10% of the bacteria recovered from the lungs were present in the largest airways immediately after nebulisation (see Table 3.6). The other 90% were in the smaller airways and the alveolar spaces. After a successful delivery, homogenates of the stomach and oesophagus were found to contain less than 1% of the dose found in the lungs.

The total number of cfu recovered from the lungs and upper gastrointestinal tract was rarely found to exceed 60% of the estimated dose instilled. The quantity of bacteria lost in the nasopharynx and mouth remains unquantified, but seems unlikely to constitute such a large proportion. It is likely that the remaining bacteria are killed or removed by the lung defences during the dissection period or perhaps destroyed during the processing of the lung homogenate.

In addition to these quantitative studies, intratracheal instillation of 5% methylene blue dye was performed using exactly the same protocol to visualise the pattern of distribution of instilled solution in the lung fields (see figure 3.5). The lungs were immediately removed, examined and then frozen in liquid nitrogen to prepare for cryosection (see Chapter 2, section 2.7.2). Both gross specimens and partially sectioned frozen blocks demonstrated homogeneous blue staining in the trachea and the large airways of all the lung lobes. This staining was observed to extend to the alveolar spaces with a more patchy distribution pattern noted.

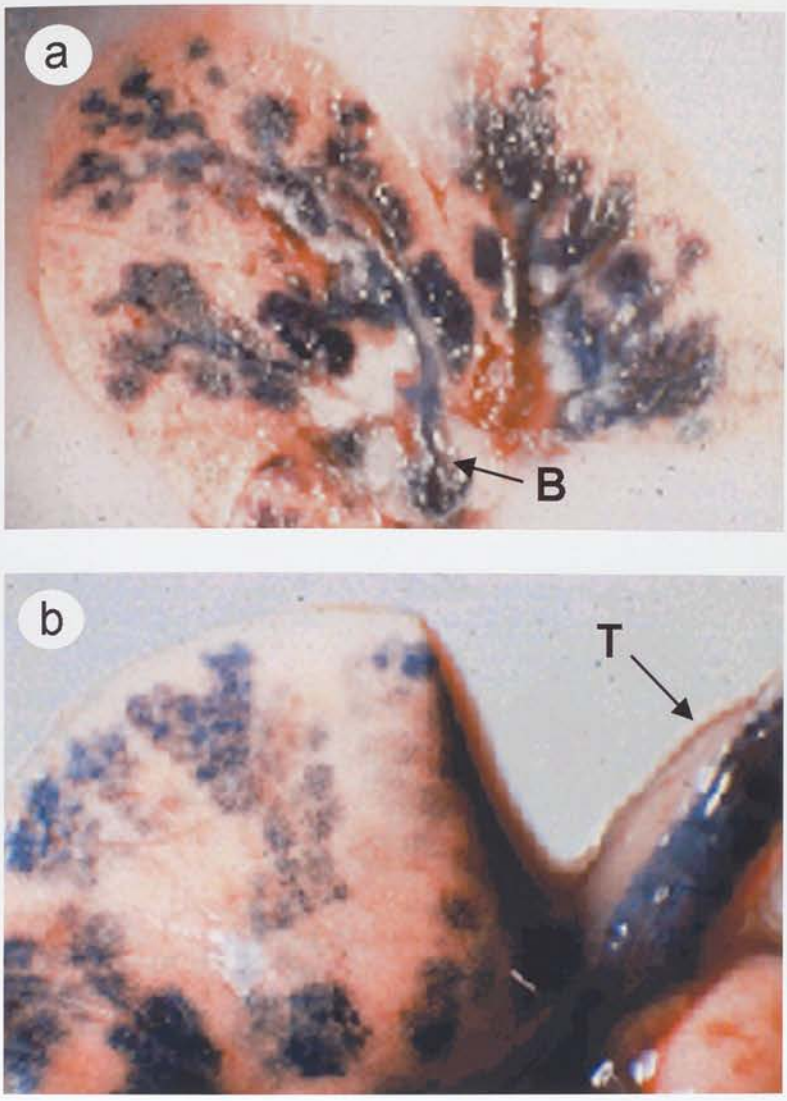

FIGURE 3.5 Distribution pattern of direct intratracheal instillation

Methylene blue dye was instilled into the mouse lungs by direct intratracheal instillation. The distribution pattern was observed in a) specimens prepared as frozen blocks for cryosectioning and partially sectioned, and b) gross specimens. Trachea (T) and primary bronchus (B) are indicated.

3.4 Discussion

The assessment of the pulmonary phenotype of mouse models of CF in response to pathogen exposure, requires well-defined and reproducible bacterial delivery protocols. These techniques should be judged according to the following criteria; a) a well quantified and clearly reproducible delivery profile, b) a defined distribution of bacterial delivery within the host systems and minimal delivery outwith the lung, c) the option to repeat the delivery to the same animals within a short time frame and / or regularly over a longer period, d) minimal invasiveness, resulting in as little stress to the experimental mice as possible, e) the introduction of the bacteria to the host system should reproduce biologically natural phenomenon where ever possible, f) minimal mortality as a result of the technique g) minimal bacterial damage, and h) technically "user friendly" with high "throughput".

The delivery of bacteria to murine lungs using the radial multi-nebuliser provides a well quantified, clearly reproducible delivery, low dosage to areas outwith the lung and maximal, homogenous distribution throughout the airways and lung parenchyma. However, the quantity of bacteria delivered is dependent upon the specific nebuliser design used and altered by the presence of the "baffle". It can be easily repeated within a short time frame or regularly over a longer period of time. It is minimally invasive and appears to cause little stress, mice enter the syringe barrels without coercion after just a couple of sessions. The delivery of bacteria by inhalation of aerosolised particles is clearly a reasonably natural methodology, although the dose delivered may not be. Experimental mortality is low, the technique is easy and can be applied to large numbers of mice in a short period of time. The major reservation about this technique is the consequences of nebulisation for the viability and normal functioning of the bacteria. Nevertheless, it clearly satisfies the majority of the criteria applied. Although the deposition efficiency was found to be lower than

previously reported (Ménache *et al* 1995) this is likely to relate to a) the use of particle inhalation curves from pooled data using rabbits, guinea pigs, rats and hamsters as well as mice in the published study b) the specific chamber design and nebuliser used, and c) the use of inert radioactive particles in the published study, as opposed to bacteria, susceptible to killing by the nebulisation process and innate lung defences. Ultimately, for the purposes of these studies, the critical outcome is reproducible quantification of the delivery profiles of the apparatus used.

The non-surgical direct intratracheal instillation of bacteria is a rather more demanding and labour intensive method of delivery that requires some training. However, once the technique has been mastered, it can provide well quantified, fairly reproducible, high dose delivery to the lung, with minimal delivery outwith the lung. A homogenous distribution is observed in the large airways, with a more patchy distribution in the lung parenchyma. Delivery can be repeated within a short time frame, but is probably not suited to regularly dosing over a longer period of time. It is relatively non-invasive, however, anaesthetic is required and abrasion to the tracheal epithelium and pharynx may occur. The delivery of bacteria in a liquid bolus is clearly a less natural technique and the bolus alone may upset lung homeostasis. Experimental mortality is more common than by nebulisation, but is still relatively low in the hands of an experienced technician. This method is more time consuming and consequently cannot be applied to such large numbers of mice. However delivery using this technique should not affect bacterial viability or result in bacterial damage. Although this technique does not fulfil the criteria as fully as nebulisation, the ability to deliver high doses of bacteria, without concern about bacterial damage, is important for certain experimental protocols.

An alternative approach to bacterial delivery that was rejected without analysis was the use of agar beads. This approach has been adopted by several groups (van Heeckeren *et al* 1997, Gosselin *et al* 1998) in the study of mouse models of CF (see Chapter 4, section 4.7). This method is relatively

demanding and labour intensive. It cannot provide particularly well quantified, or reproducible bacterial delivery as a result of several key problems; a) beads of bacteria encased in agar will become lodged in airways, dependent upon their size, b) random breakdown of beads will result in the release of large numbers of bacteria capable of rapid proliferation, c) attempts to quantify the numbers of bacteria will be distorted by agar, preventing unreleased bacteria from growing as individual colonies in culture, instead producing one large colony forming unit. This technique will result in minimal delivery outwith the lung, but a patchy distribution in the airways and lung parenchyma. Repeat delivery could be performed, although given that the intention of this technique is to establish a chronic colonisation, this is less significant. The method is relatively non-invasive, but clearly results in a particularly artificial scenario. The presence of the agar is intended to replicate the effect of *P. aeruginosa* alginate and produce microcolonies and chronic infection. However, agar is not the same as alginate and chronic infection with mucoid strains does not occur instantaneously. This process occurs over time in humans with CF, with colonisation by non-mucoid strains occurring, usually after infections with other organisms, followed by a series of phenotypic changes within the CF lung environment (see Chapter 1, section 1.4.2.4). The agar bead technique completely bypasses this process to establish a chronic retention model in an environment that has not been subjected to the classical early events in CF lung disease pathogenesis. As such, it is very unlikely to reveal any significant data about the development of CF lung disease. In addition, it remains unclear whether it can be considered a valid model of chronic mucoid infection, having simply superimposed retention of bacteria, in an artificial medium, on an otherwise unaffected lung. For these reasons, this technique was not evaluated.

demanding and labour intensive. It cannot provide particularly well quantified, or reproducible bacterial delivery as a result of several key problems; a) beads of bacteria encased in agar will become lodged in airways, dependent upon their size, b) random breakdown of beads will result in the release of large numbers of bacteria capable of rapid proliferation, c) attempts to quantify the numbers of bacteria will be distorted by agar, preventing unreleased bacteria from growing as individual colonies in culture, instead producing one large colony forming unit. This technique will result in minimal delivery outwith the lung, but a patchy distribution in the airways and lung parenchyma. Repeat delivery could be performed, although given that the intention of this technique is to establish a chronic colonisation, this is less significant. The method is relatively non-invasive, but clearly results in a particularly artificial scenario. The presence of the agar is intended to replicate the effect of *P. aeruginosa* alginate and produce microcolonies and chronic infection. However, agar is not the same as alginate and chronic infection with mucoid strains does not occur instantaneously. This process occurs over time in humans with CF, with colonisation by non-mucoid strains occurring, usually after infections with other organisms, followed by a series of phenotypic changes within the CF lung environment (see Chapter 1, section 1.4.2.4). The agar bead technique completely bypasses this process to establish a chronic retention model in an environment that has not been subjected to the classical early events in CF lung disease pathogenesis. As such, it is very unlikely to reveal any significant data about the development of CF lung disease. In addition, it remains unclear whether it can be considered a valid model of chronic mucoid infection, having simply superimposed retention of bacteria, in an artificial medium, on an otherwise unaffected lung. For these reasons, this technique was not evaluated.

Chapter 4

Repeated bacterial exposure studies

Chapter 4: Repeated bacterial exposure studies

4.1 Introduction

Initial studies using the *Cftr*^{tm1Hgu}/*Cftr*^{tm1Hgu} mice demonstrated that no gross lung pathology was evident when the mice were born and maintained in sterile conditions. However, abnormalities were observed when these animals were exposed to aerosolised CF related respiratory pathogens (Davidson *et al* 1995). The abnormal pulmonary phenotype observed in response to bacteria consisted of a clearance defect and the development of more pronounced lung pathology, in comparison to wild type littermates. The studies addressing both components of this phenotype demonstrated considerable variation between individual mice. Comparisons made on the basis of genotype showed broad overlapping spectrums. Thus, while the differences between *Cftr*^{tm1Hgu}/*Cftr*^{tm1Hgu} mice and their non-CF littermates were statistically significant, the extent of the variation prevented further development as a model for therapy testing or the analysis of phenotype modifier loci.

The most likely sources of the variable phenotype observed in these studies were considered to be; a) genetic influences: 1) the use of a mouse model of CF on an outbred MF1/129 background strain, 2) variation in the degree of residual function in individual *Cftr*^{tm1Hgu}/*Cftr*^{tm1Hgu} mice, and b) environmental influences: differences in the extent of prior, or co-existing, lung infection. Experimental strategies were adopted to minimise and address the significance of these factors.

A mouse breeding programme was initiated to repeatedly backcross the outbred mice onto three inbred stains (C57Bl6/N, BALB/c and FVB). This work was performed by Dr Julia Dorin and Dr Sheila Webb, at the MRC

Human Genetics Unit, Edinburgh, and established lines of inbred mice congenic for the *Cftr*^{tm1Hgu} mutation. The degree of genetic similarity of the animals within the same inbred line removes the influence of independently segregating genetic modifiers and would be expected to result in a more homogeneous phenotype. The C57Bl6 strain has previously been reported to be more susceptible to lung disease (Gosselin *et al* 1995, Stevenson *et al* 1995) and was therefore chosen for further bacterial exposure studies.

The variation in the degree of residual function in individual *Cftr*^{tm1Hgu}/*Cftr*^{tm1Hgu} mice has the potential to impact upon the severity of their phenotype. The presence of low levels of wild type CFTR in *Cftr*^{tm1Hgu}/*Cftr*^{tm1Hgu} mice appears to afford them protection from the severe gastrointestinal disease associated with most of the other mouse models of CF (see Chapter 1, sections 1.7.3.1 and 1.7.3.2). This factor would ideally be assessed using quantitative RT-PCR to examine the precise levels of normal *Cftr* mRNA produced in the lungs of each mouse studied. However, to date, the quantitation of message levels in lung tissues from *Cftr*^{tm1Hgu}/*Cftr*^{tm1Hgu} mice, has not been possible. Consequently an alternative approach was adopted. *Cftr*^{tm1Hgu}/*Cftr*^{tm1Hgu} mice have been estimated to express ~10% of wild type levels of *Cftr* mRNA (Dorin *et al* 1994), whereas *Cftr*^{tm1Unc}/*Cftr*^{tm1Unc} mice are absolute nulls (Snouwaert *et al* 1992). Thus *Cftr*^{tm1Hgu}/*Cftr*^{tm1Unc} compound heterozygote mice would be expected to express ~5% of wild type levels of *Cftr* mRNA. Analysis of the pulmonary phenotype of *Cftr*^{tm1Hgu}/*Cftr*^{tm1Unc} compound heterozygote mice, inbred onto a C57Bl/6N background was therefore performed to address the effect of varying the degree of residual CFTR function.

Histological analysis was previously performed on lungs from *Cftr*^{tm1Hgu}/*Cftr*^{tm1Hgu} mice, and non-CF littermates, maintained under standard, non-SPF animal facility conditions (Davidson *et al* 1995). In contrast to animals born and raised in isolators, this study demonstrated pathological changes associated with lung infection and inflammation, with a trend towards more frequent and severe pathology in the *Cftr*^{tm1Hgu}/*Cftr*^{tm1Hgu} mice.

These observations included bronchiolitis, pneumonia, goblet cell hyperplasia and metaplasia, mucus retention, perivascular and peribronchiolar lymphoid aggregates and aspiration pneumonia. The differences between genotypes were not statistically significant, but indicated the presence of lung pathology in animals maintained under these conditions, in the absence of experimental bacterial exposure. Thus in a cohort of mice selected for study, differences between individual mice may exist in the extent of prior, or co-existing, lung infection. It was not practical to breed sufficient numbers of mice for bacterial exposure studies under isolator conditions. Hence, the animals used in the subsequent studies were all raised under standard, non-SPF animal facility conditions.

4.2 Bacterial Delivery

The repeated bacterial exposure studies were performed using the radial nebuliser designs described in Chapter 3, section 3.2. (Nebulisers #2 and #3). The specific protocols used are described in Materials and Methods (see Chapter 2, sections 2.5.1 and 2.7) and the key points are highlighted in the following sections. Nebuliser #2 was characterised and used to replace, and theoretically improve upon, the damaged Nebuliser #1. Damage to Nebuliser #2 necessitated its replacement and led to the production of Nebuliser #3. This was used for subsequent studies and characterised retrospectively, at which stage the considerable difference in delivery profile was established. This difference in the dose delivered by the two nebuliser designs creates significant difficulties in interexperimental comparisons and will be discussed.

The previous studies using $Cftr^{tm1Hgu}/Cftr^{tm1Hgu}$ mice on a mixed outbred MF1/129 background strain had demonstrated abnormalities in the response to nebulised *S. aureus* and *B. cepacia*. On the basis that *S. aureus* is the bacteria

most commonly associated with early stage lung disease in CF children (Hutchison *et al* 1999), this bacteria was used for subsequent studies. *S. aureus* CF clinical isolate C1705 was supplied by Professor John Govan and prepared by Wendy Hannant and Cathy Doherty at the Department of Medical Microbiology, University of Edinburgh (see Chapter 2, section 2.3).

4.3 Histopathological analysis

The previous study served to indicate the predominant histopathological features associated with repeated exposure of the murine lung to aerosolised *S. aureus* and the range of severity observed. In order to minimise the subjective nature of assessment of the outcomes of subsequent experiments and eliminate bias, a scoring system was established based upon these original studies. Five main features were selected; a) Bronchiolitis, b) Pneumonia, c) Goblet cell hyperplasia and metaplasia, d) Mucus retention and e) Perivascular and peribronchiolar lymphoid aggregates. These features were graded on a scale of 1 to 5 on the basis of specified criteria (see Table 4.1 and Figures 4.1a and 4.1b). Assessment of lung histopathology was performed twice, in blinded fashion, using these criteria. The scores thus established were assessed using a weighted Kappa measure of agreement to assess variability between the duplicate analyses. The preparation of tissue samples is described in the Materials and Methods (see Chapter 2, section 2.7).

BRONCHIOLITIS	
Score	**Interpretation**
1	excess inflammatory cells in some bronchi cross sections
2	excess inflammatory cells in smaller airways, clusters of cells in many bronchi
3	numerous cells in many smaller airways
4	numerous cells in most smaller airways, inflammatory exudate and occasional "plugs" obstructing airway
5	"plugs" of inflammatory cells and exudate obstructing many airways

PNEUMONIA	
Score	**Interpretation**
1	patchy excess of alveolar and interstitial inflammatory cells,
2	more widespread, cells in most alveoli, patches with numerous cells per airspace
3	several cells in most alveoli +/- small areas of consolidation
4	widespread numerous cells in almost all alveoli in all lobes / several patches consolidation
5	large areas / whole lobes consolidated

GOBLET CELL HYPERPLASIA & METAPLASIA	
Score	**Interpretation**
1	confined to trachea / primary bronchi
2	extensive in trachea / primary bronchi, extending into small bronchi/ large bronchioles
3	extensive in small bronchi, extending into smaller bronchioles
4	extending into terminal bronchioles / >50% of epithelial cells in some large airways
5	numerous in terminal and into respiratory bronchioles / majority of epithelial cells in majority of larger airways

MUCUS RETENTION	
Score	**Interpretation**
1	occasional strands in larger airways
2	strands in many large airways & into bronchioles, or occasional strands with larger masses
3	numerous strands in smaller airways +/- larger masses
4	numerous strands and large masses mixed with inflammatory cells
5	areas of obstruction by large masses of mucus

LYMPHOID AGGREGATE	
Score	**Interpretation**
1	minimal presence
2	lymphoid aggregation around most vessels and some airways
3	most vessels partially to fully cuffed, most airways partially cuffed
4	massive cuffing many vessels, many airways fully cuffed
5	most vessels and airways fully cuffed with massive lymphoid aggregates

TABLE 4.1 Criteria for histopathological assessment

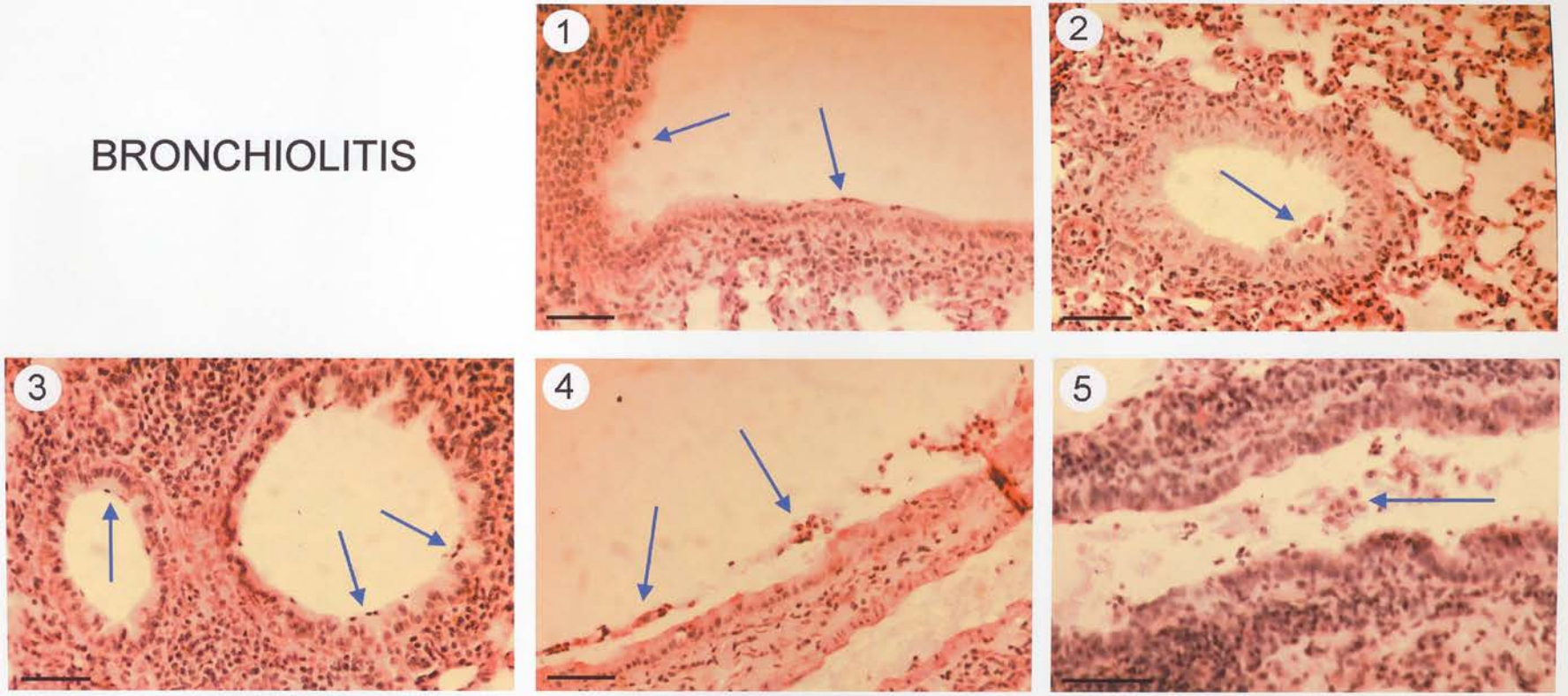

FIGURE 4.1a Criteria for histopathological assessment - Bronchiolitis

Light micrographs of PAS stained murine lung sections, taken from the studies detailed in Chapter 4 to provide a pictorial representation of the criteria described in Table 4.1. Scores 1-5 for Bronchiolitis are demonstrated. Inflammatory cells are indicated with blue arrows. The black bar represents 25 μm.

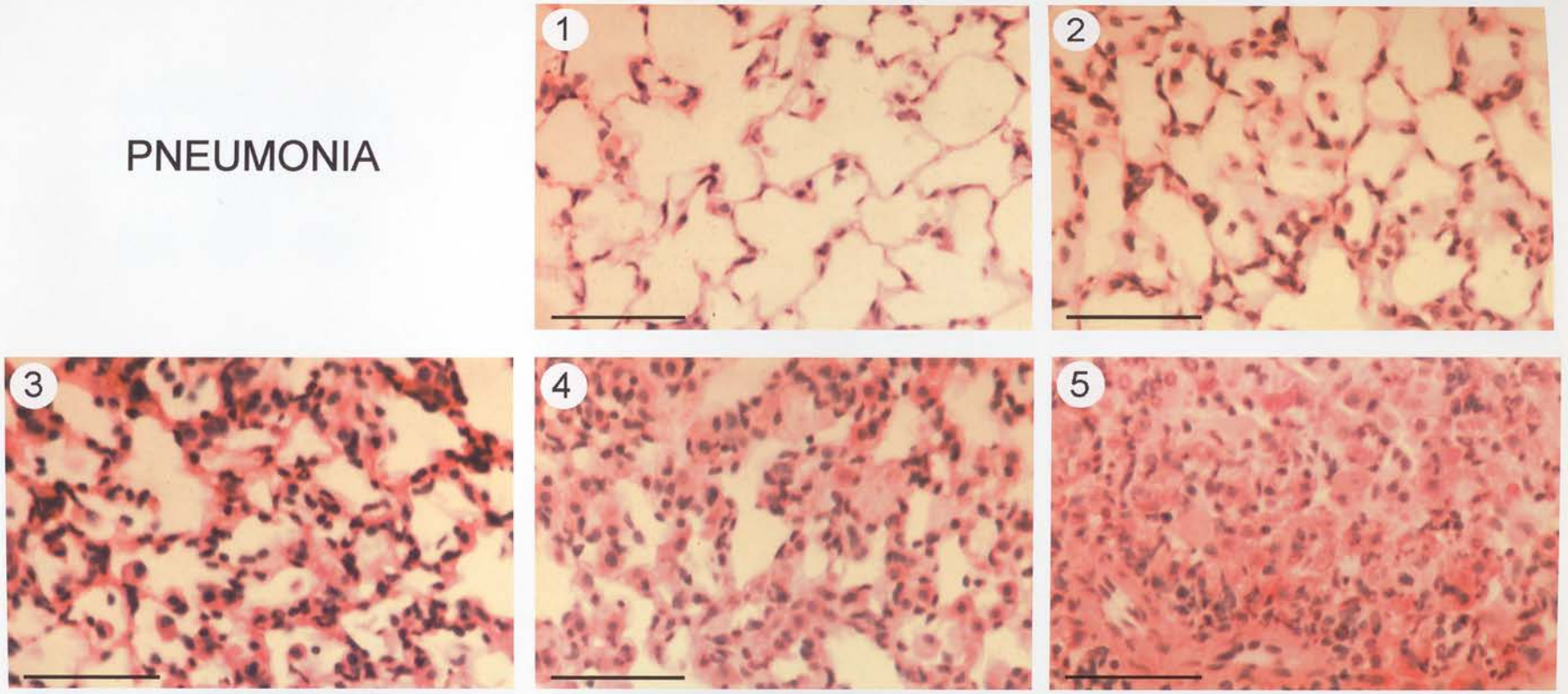

FIGURE 4.1b Criteria for histopathological assessment - Pneumonia

Light micrographs of PAS stained murine lung sections, taken from the studies detailed in Chapter 4 to provide a pictorial representation of the criteria described in Table 4.1. Scores 1-5 for Pneumonia are demonstrated. The black bar represents 25 μm.

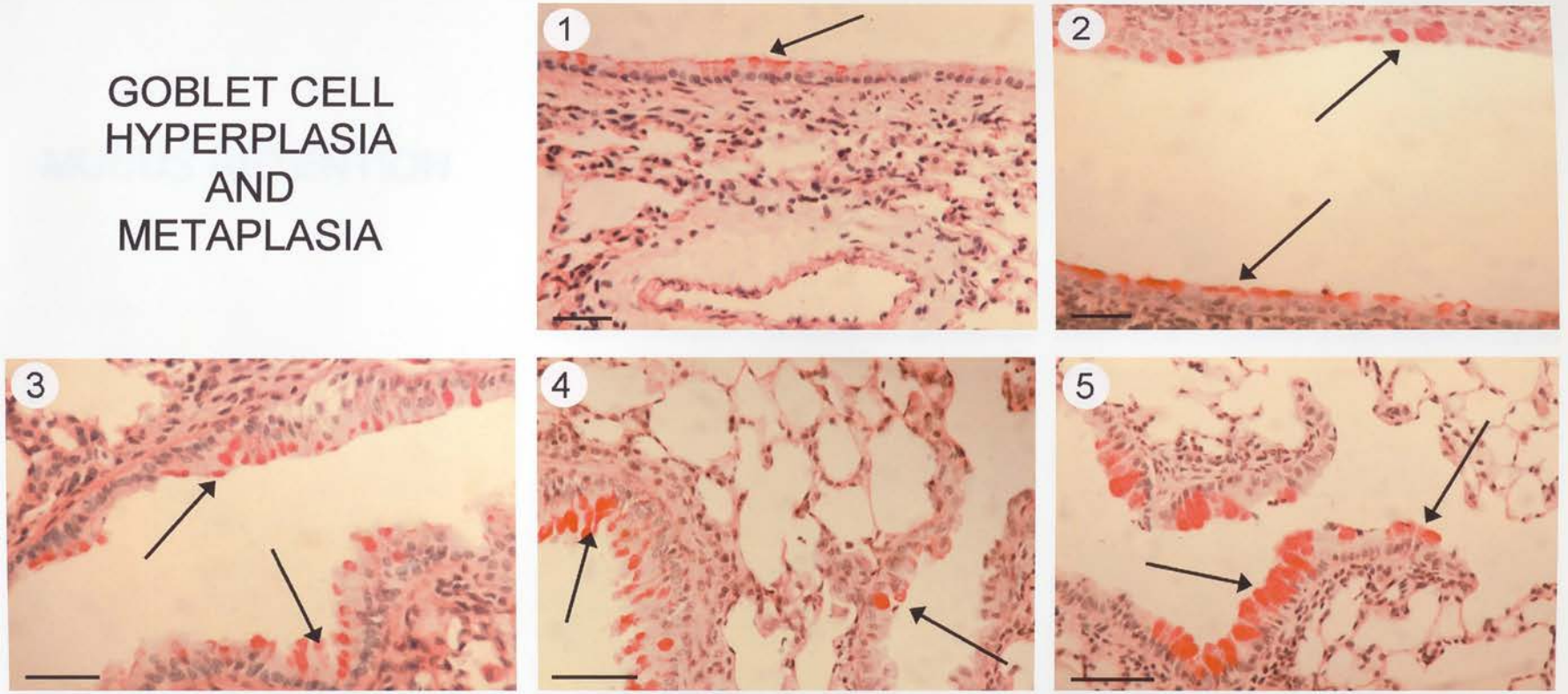

FIGURE 4.1c Criteria for histopathological assessment – Goblet cell hyperplasia and metaplasia

Light micrographs of PAS stained murine lung sections, taken from the studies detailed in Chapter 4 to provide a pictorial representation of the criteria described in Table 4.1. Scores 1-5 for Goblet cell hyperplasia and metaplasia are demonstrated. PAS positive goblet cells are indicated by black arrows. The black bar represents 25 μm.

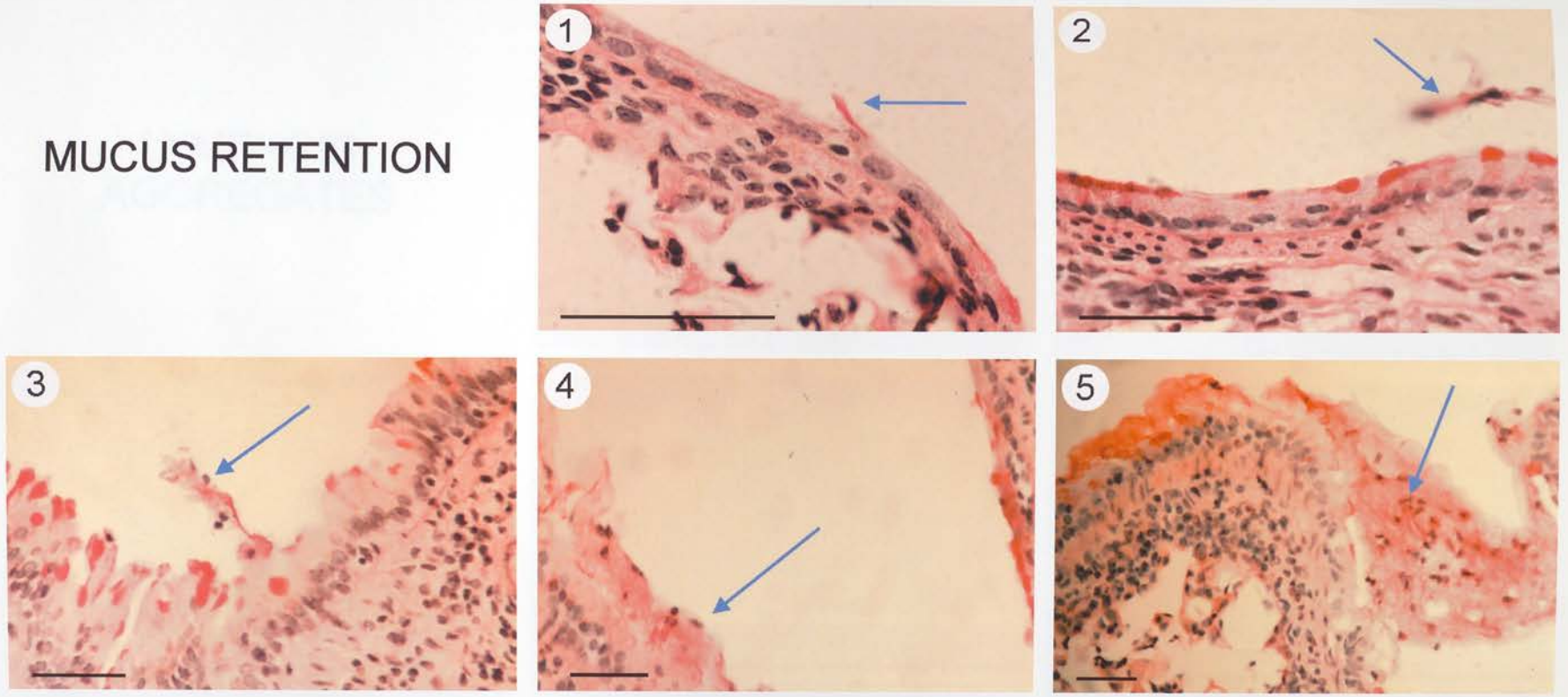

FIGURE 4.1d Criteria for histopathological assessment – Mucus retention

Light micrographs of PAS stained murine lung sections, taken from the studies detailed in Chapter 4 to provide a pictorial representation of the criteria described in Table 4.1. Scores 1-5 for Mucus retention are demonstrated. Mucus is indicated by blue arrows. The black bar represents 25 μm.

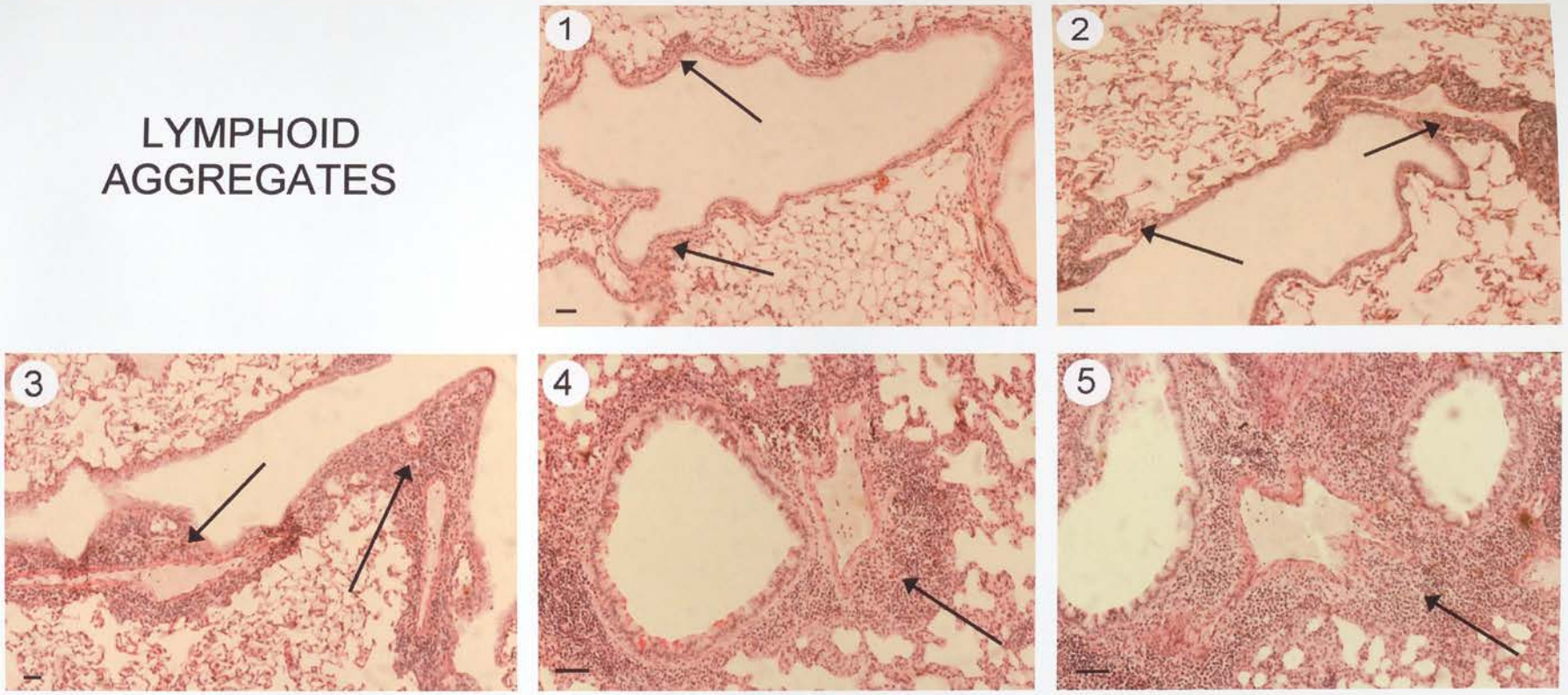

FIGURE 4.1e Criteria for histopathological assessment – Lymphoid aggregates

Light micrographs of PAS stained murine lung sections, taken from the studies detailed in Chapter 4 to provide a pictorial representation of the criteria described in Table 4.1. Scores 1-5 for Lymphoid aggregates are demonstrated. Perivascular and peribronchiolar lymphoid agggregates are indicated by black arrows. The black bar represents 25 μm.

4.4 Repeated bacterial exposure of inbred mice

To assess the effect of the *Cftr*^{tm1Hgu} mutation backcrossed onto a C57Bl6/N background strain, a cohort of age matched *Cftr*^{tm1Hgu}/*Cftr*^{tm1Hgu} mice and non-CF littermates was selected from backcross generation n = 8. This cohort consisted of 10 *Cftr*^{tm1Hgu}/*Cftr*^{tm1Hgu} mice and 12 non-CF mice (6 wild type mice and 6 heterozygotes). The mice were all 2 - 3 months old and were raised in standard, non-SPF conditions. All but 4 of the mice (see below) were exposed to *S. aureus* by repeated nebulisation, in a radial multi-nebuliser (Nebuliser #2; see Chapter 3, section 3.2.2.1). The daily protocol used was 5 minutes with the baffle followed by 5 minutes without the baffle. This was repeated 5 days a week, for 4 weeks. No animals died during this period. The dose of bacteria delivered was estimated to be approximately 5 x 10^4 cfu/mouse/day. On the final day of bacterial exposures the 4 previously unexposed members of the cohort (2 *Cftr*^{tm1Hgu}/*Cftr*^{tm1Hgu} mice and 2 heterozygotes) were also exposed, after which all the animals were given 24 hours clearance time. The lungs and tracheae were removed, inflated, fixed, processed, sectioned at defined sites and stained with PAS as described in the Materials and Methods (see Chapter 2, section 2.7).

A total of 6 section profiles were studied per mouse and scored blinded as described in section 4.3. This analysis was performed in duplicate. A weighted Kappa value of 0.93 was calculated demonstrating excellent agreement between the duplicate analyses. The scores generated for histopathological features were ranked, individually for each feature and using the total score (sum of the scores for all 5 features), before the study was unblinded. These scores are displayed graphically in Figures 4.2 and 4.3.

Previous assessment of untreated mice (11 *Cftr*^{tm1Hgu}/*Cftr*^{tm1Hgu} mice, 7 heterozygotes and 8 wild types) indicated a mean total score of 1.8 ± 3.2.

Consequently a total score of 5 is taken to indicate the upper limit expected for an untreated mouse (as indicated on Figure 4.2).

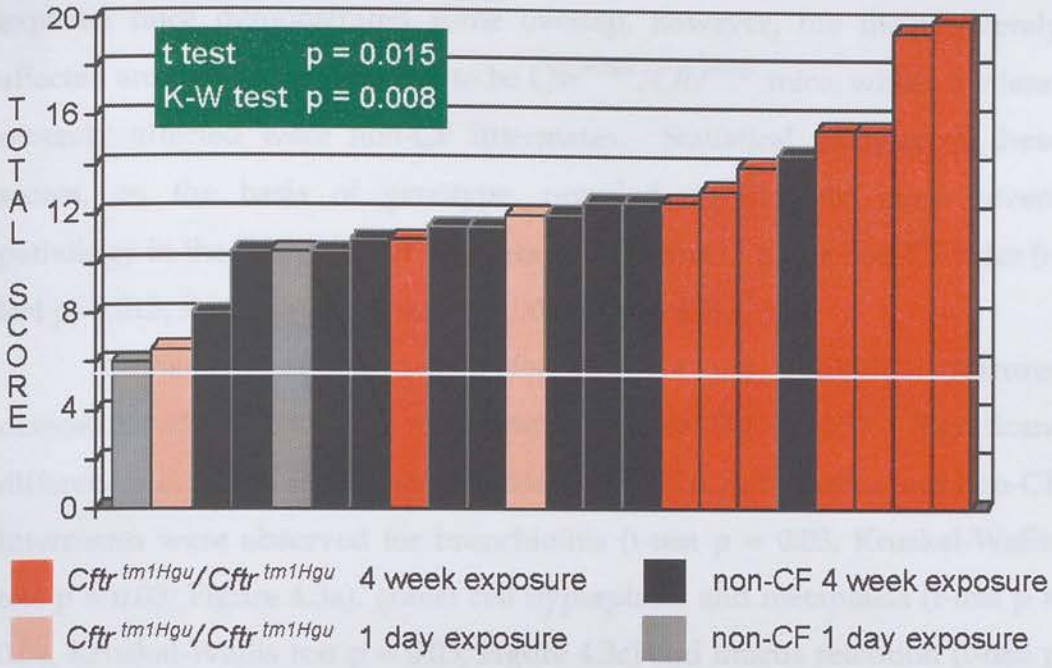

FIGURE 4.2 Repeated bacterial exposure of inbred mice- Total histopathology score.

The severity of pathology was ranked according to the total score (sum of the five features assessed). Each column represents an individual mouse. The genotype and level of exposure to bacteria are indicated. The white line indicates the upper limit for untreated mice.

The total scores for each of the 4 week exposed mice were raised above 5, regardless of genotype (Figure 4.2). The total scores for each of the 1 day exposed mice were also raised above 5 (although two were only marginally raised). Statistical analysis of the total scores for each mouse, on the basis of bacterial exposure, demonstrated significantly more severe pathology in the 4 week exposed mice in comparison to the one day exposed control mice, regardless of genotype (t-test $p < 0.001$, Kruskal-Wallis test $p < 0.001$). However, although the two least affected animals were both one day

exposed controls (1 *Cftr*^{tm1Hgu}/*Cftr*^{tm1Hgu} mouse and 1 non-CF mouse), the other two controls were as severely affected as most of the non-CF mice.

The ranked assessment of the total scores for each of the 4 week exposed mice demonstrated some overlap, however, the most severely affected animals were observed to be *Cftr*^{tm1Hgu}/*Cftr*^{tm1Hgu} mice, whilst the least severely affected were non-CF littermates. Statistical analysis of these scores, on the basis of genotype, revealed significantly more severe pathology in the *Cftr*^{tm1Hgu}/*Cftr*^{tm1Hgu} mice in comparison to the non-CF mice (t-test p=0.015, Kruskal-Wallis test p=0.008; Figure 4.2).

Assessment of the scores for each of the individual features demonstrated considerably more variation (see Figure 4.3). Significant differences between the 4 week exposed *Cftr*^{tm1Hgu}/*Cftr*^{tm1Hgu} mice and non-CF littermates were observed for bronchiolitis (t-test p = 0.03, Kruskal-Wallis test p = 0.03; Figure 4.3a), goblet cell hyperplasia and metaplasia (t-test p = 0.04, Kruskal-Wallis test p = 0.03; Figure 4.3c) and mucus retention (t-test p = 0.03, Kruskal-Wallis test p = 0.03; Figure 4.3d). However none of these features distinguished between genotypes as successfully as the total score. In addition, the individual animals having the highest scores for each of these features were not always the same animals. Nevertheless, as the total score increased, each of the component scores tended to do the same (Figure 4.3f). No significant difference was observed for pneumonia (t-test p = 0.20, Kruskal-Wallis test p = 0.18; Figure 4.3b) or lymphoid aggregates (t-test p = 0.10, Kruskal-Wallis test p = 0.15; Figure 4.3e).

Interestingly, although the one day exposed mice were clearly observed to have the lowest scores for pneumonia and lymphoid aggregates, this was less clear cut for the other features. Indeed, one of most severe examples of goblet cell hyperplasia and metaplasia was observed in one of the control mice.

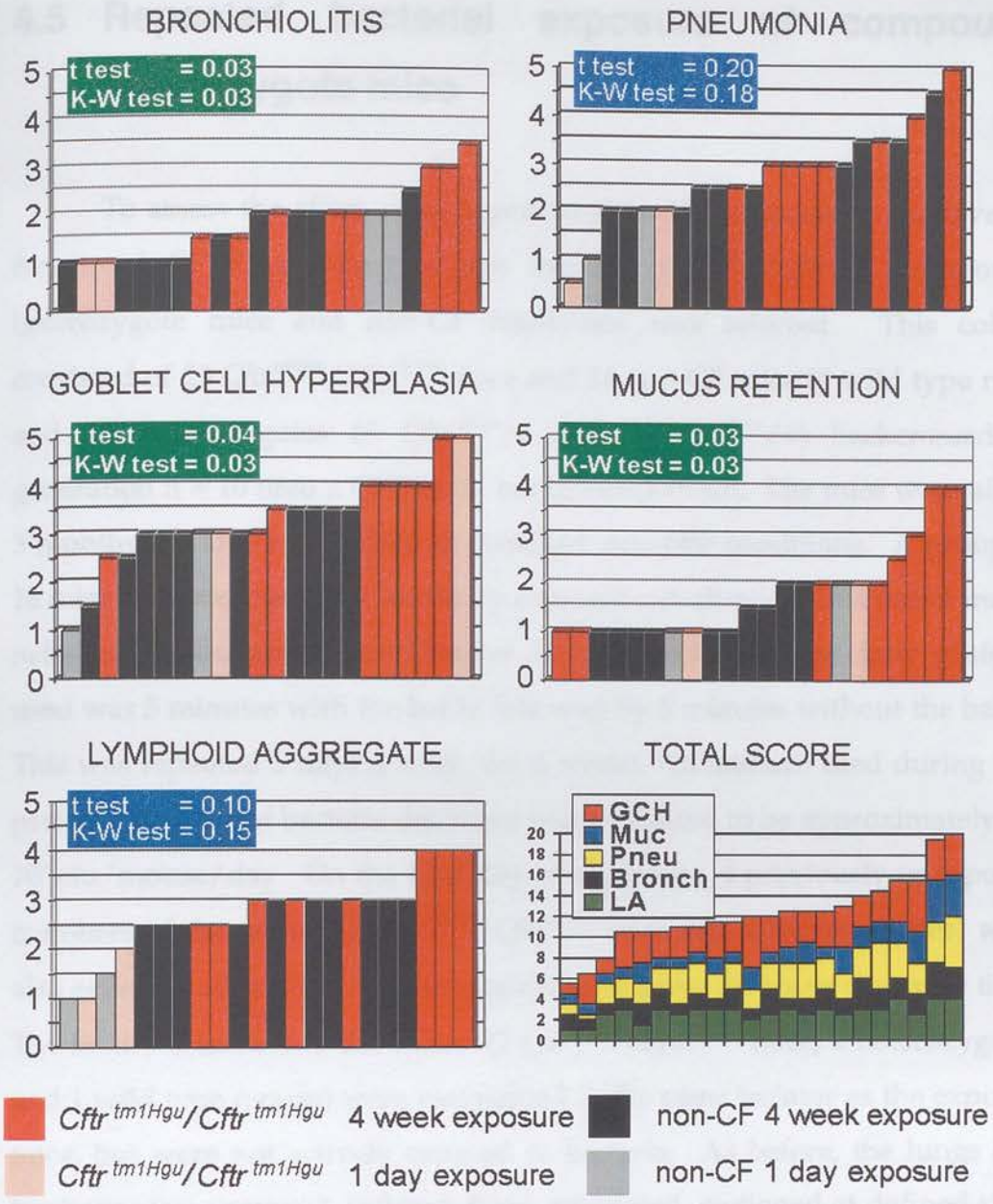

FIGURE 4.3 Repeated bacterial exposure of inbred mice- Component histopathology scores

The severity of pathology for each of the five features assessed was ranked; a) bronchiolitis, b) pneumonia, c) goblet cell hyperplasia and metaplasia, d) lymphoid aggregate. Each column represents an individual mouse. The genotype and level of exposure to bacteria are indicated The white line indicates the upper limit for untreated mice. f) represents the total score colour coded to demonstrate the value of each of its component parts.

4.5 Repeated bacterial exposure of compound heterozygote mice

To assess the effect of an approximately 50% decrease in the level of functional CFTR, a cohort of age matched *Cftr*^{tm1Hgu}/*Cftr*^{tm1Unc} compound heterozygote mice and non-CF littermates was selected. This cohort consisted of 13 *Cftr*^{tm1Hgu}/*Cftr*^{tm1Unc} mice and 14 non-CF mice (4 wild type mice and 10 heterozygotes (5 *Cftr*^{tm1Hgu}/+ and 5 *Cftr*^{tm1Unc}/+) backcrossed to generation n = 10 onto a C57Bl6/N background strain. The mice were all 2 - 3 months old and were raised in standard, non-SPF conditions. A group of 18 mice were exposed to *S. aureus* by repeated nebulisation, in a radial multi-nebuliser (Nebuliser #3; see Chapter 3, section 3.2.2.2). The daily protocol used was 5 minutes with the baffle followed by 5 minutes without the baffle. This was repeated 5 days a week, for 4 weeks. No animals died during this period. The dose of bacteria delivered was estimated to be approximately 2 x 10^6 cfu/mouse/day. On the final day of exposures, 4 previously unexposed members of the cohort (2 *Cftr*^{tm1Hgu}/*Cftr*^{tm1Hgu} mice and 2 heterozygotes) were also exposed, after which all the animals were given 24 hours clearance time. The final 5 members of the cohort (2 *Cftr*^{tm1Hgu}/*Cftr*^{tm1Hgu} mice, 2 heterozygotes and 1 wild type mouse) were maintained in the same isolator as the exposed mice, but were not actively exposed to bacteria. As before, the lungs and tracheae were removed, inflated, fixed, processed, sectioned at defined sites, stained with PAS and scored blinded in duplicate. A weighted Kappa value of 0.93 was calculated demonstrating excellent agreement between the duplicate analyses. The scores are displayed graphically in Figures 4.4 and 4.5.

The total scores for each of the 4 week exposed mice were raised above 5, regardless of genotype (Figure 4.4). The total scores for each of the 1 day exposed mice were also ≥ 5, whereas all but one of the unexposed mice had a total score of less than 5. Statistical analysis of the total scores for

each mouse, on the basis of bacterial exposure, demonstrated significantly more severe pathology in the 4 week exposed mice in comparison to the pooled control mice, regardless of genotype (t-test $p < 0.001$, Kruskal-Wallis test $p < 0.001$). In this study, all the control mice were clearly less severely affected than the exposed mice on the basis of total score.

The ranked assessment of the total scores for each of the 4 week exposed mice demonstrated some overlap, as before. However, the most severely affected animals were observed to be $Cftr^{tm1Hgu}/Cftr^{tm1Unc}$ mice, whilst the least severely affected were non-CF littermates. Statistical analysis of these scores, on the basis of genotype, revealed significantly more severe pathology in the $Cftr^{tm1Hgu}/Cftr^{tm1Unc}$ mice in comparison to the non-CF mice (t-test $p = 0.009$, Kruskal-Wallis test $p = 0.017$; Figure 4.4).

Assessment of the scores for each of the individual features was observed to demonstrate considerably more variation (see Figure 4.5), as was observed with $Cftr^{tm1Hgu}/Cftr^{tm1Hgu}$ mice. In this study significant differences between the 4 week exposed $Cftr^{tm1Hgu}/Cftr^{tm1Unc}$ mice and non-CF littermates were observed for pneumonia (t-test $p = 0.01$, Kruskal-Wallis test $p = 0.02$; Figure 4.5b) and mucus retention (t-test $p = 0.02$, Kruskal-Wallis test $p = 0.02$; Figure 4.5d). However, the total score more effectively distinguished between genotypes than any of its component parts when assessed alone. As noted in the previous study, although the highest scores for individual features did not occur in the same animals, as the total score increased, so each of its component scores tended to do likewise (Figure 4.5f). No significant difference was observed for bronchiolitis (t-test $p = 0.10$, Kruskal-Wallis test $p = 0.10$; Figure 4.5a), goblet cell hyperplasia and metaplasia (t-test $p = 0.08$, Kruskal-Wallis test $p = 0.07$; Figure 4.5c) or lymphoid aggregates (t-test $p = 0.36$, Kruskal-Wallis test $p = 0.34$; Figure 4.5e).

Interestingly, although the control mice were clearly observed to have the lowest scores for lymphoid aggregates, bronchiolitis and pneumonia, this was less clear cut for mucus retention. As in the previous

study, one of most severe examples of goblet cell hyperplasia and metaplasia was observed in a control mouse, in this case an untreated control.

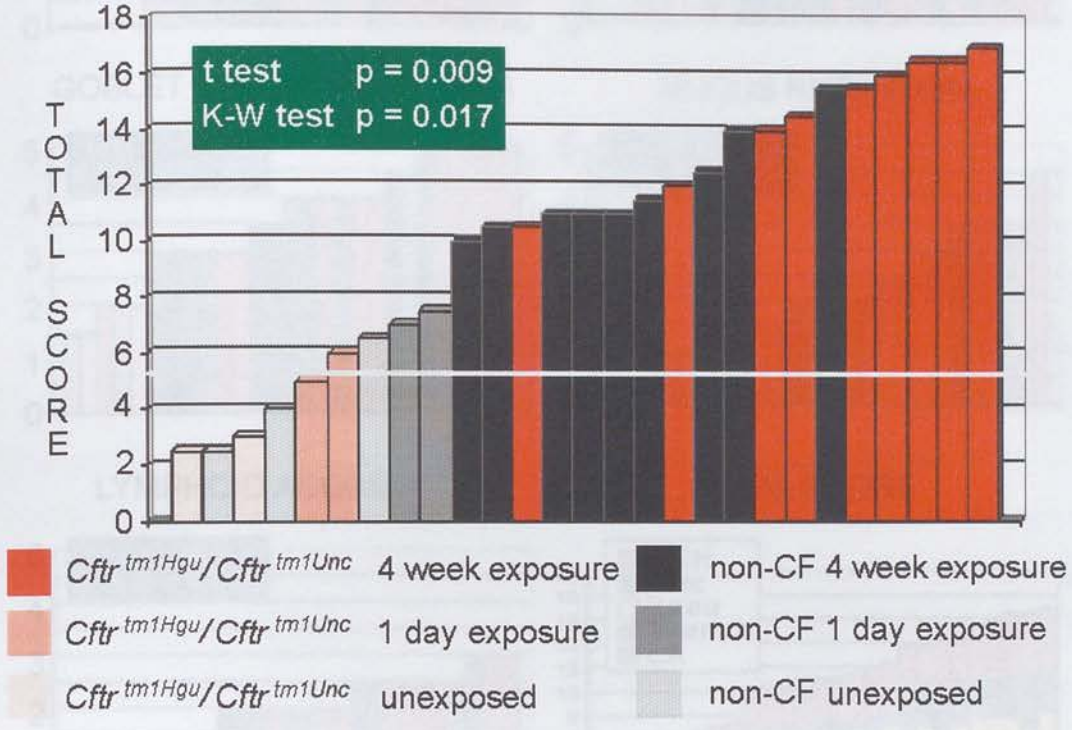

FIGURE 4.4 Repeated bacterial exposure of compound heterozygote mice- Total histopathology score

The severity of pathology was ranked according to the total score (sum of the five features assessed). Each column represents an individual mouse. The genotype and level of exposure to bacteria are indicated. The white line indicates the upper limit previously established for untreated mice.

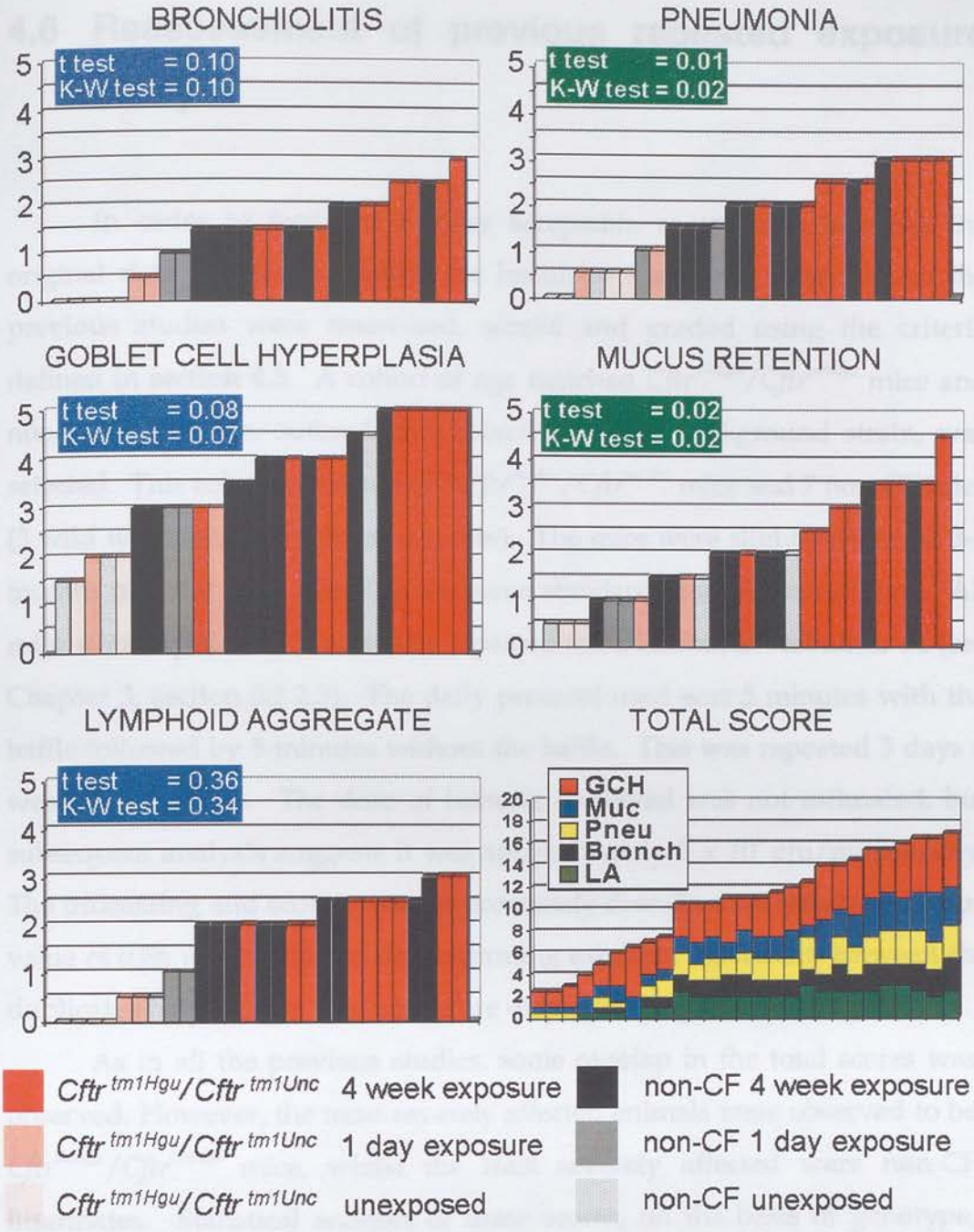

FIGURE 4.5 Repeated bacterial exposure of compound heterozygote mice- Component histopathology scores.

The severity of pathology for each of the five features assessed was ranked; a) bronchiolitis, b) pneumonia, c) goblet cell hyperplasia and metaplasia, d) lymphoid aggregate. Each column represents an individual mouse. The genotype and level of exposure to bacteria are indicated. The white line indicates the upper limit previously established for untreated mice. f) represents the total score colour coded to demonstrate the value of each of its component parts.

4.6 Reassessment of previous repeated exposure study

In order to facilitate a more acceptable comparison between the original data and these studies, the histology specimens from one of the previous studies were reassessed, scored and graded using the criteria defined in section 4.3. A cohort of age matched *Cftr*^{tm1Hgu}/*Cftr*^{tm1Hgu} mice and non-CF littermates, outbred on a mixed MF1/129 background strain, was selected. This cohort consisted of 5 *Cftr*^{tm1Hgu}/*Cftr*^{tm1Unc} mice and 7 non-CF mice (3 wild type mice and 4 heterozygotes). The mice were slightly older, at 3-5 months old, but were raised in the same standard, non-SPF conditions. All mice were exposed to *S. aureus* by repeated nebulisation, in Nebuliser #1 (see Chapter 3, section 3.2.2.3). The daily protocol used was 5 minutes with the baffle followed by 5 minutes without the baffle. This was repeated 5 days a week, for 4 weeks. The dose of bacteria delivered was not estimated, but subsequent analysis suggests it was approximately 2×10^5 cfu/mouse/day. The processing and scoring was as previously described. A weighted Kappa value of 0.86 was calculated demonstrating excellent agreement between the duplicate analyses. The total scores are displayed graphically in Figure 4.6.

As in all the previous studies, some overlap in the total scores was observed. However, the most severely affected animals were observed to be *Cftr*^{tm1Hgu}/*Cftr*^{tm1Hgu} mice, whilst the least severely affected were non-CF littermates. Statistical analysis of these scores, on the basis of genotype, revealed significantly more severe pathology in the *Cftr*^{tm1Hgu}/*Cftr*^{tm1Hgu} mice in comparison to the non-CF mice (t-test $p = 0.01$, Kruskal-Wallis test $p = 0.02$; Figure 4.6). The component scores were not analysed separately due to the small cohort size in this study.

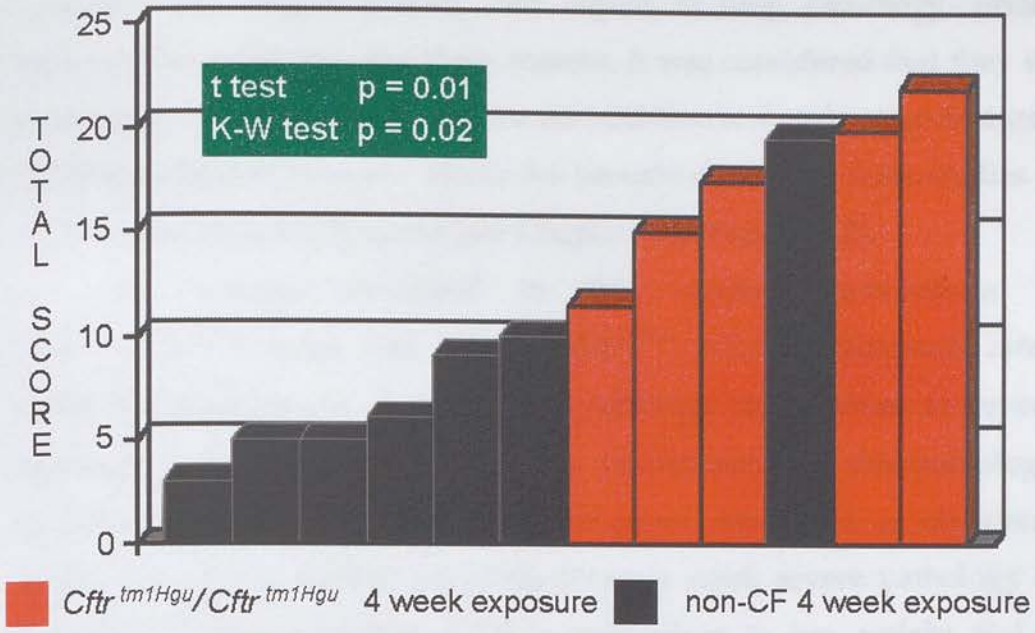

FIGURE 4.6 Repeated bacterial exposure outbred mice- Total histopathology score

The severity of pathology was ranked according to the total score (sum of the five features assessed). Each column represents an individual mouse. The genotype and level of exposure to bacteria are indicated.

4.7 Discussion

Previous studies demonstrated that *Cftr*^{tm1Hgu}/*Cftr*^{tm1Hgu} mice on a mixed outbred MF1/129 background strain were impaired in their ability to clear aerosolised *S. aureus* from their lungs (Davidson *et al* 1995). This is likely to be the causative factor in the increased severity of lung pathology subsequently seen in these mice in response to a repeated insult.

The repeated exposure studies described in this chapter were performed to examine the sources of variation in the lung phenotype observed in *Cftr*^{tm1Hgu}/*Cftr*^{tm1Hgu} mice in response to bacteria. The mutant animals were young, unlikely to have experienced repeated previous lung

infections and largely normal with regard to lung pathology, prior to experimental exposure. For these reasons, it was considered that they were most likely to constitute a model for the initiation and early stage features of CF lung disease in humans. Hence the bacteria chosen for these studies was a CF clinical isolate of *S. aureus* (see Chapter 1, section 1.4.2.2).

The studies described in this chapter demonstrate that *Cftr*^{tm1Hgu}/*Cftr*^{tm1Hgu} mice and *Cftr*^{tm1Hgu}/*Cftr*^{tm1Unc} mice, backcrossed onto a C57Bl/6N background develop lung pathology in response to repeated exposure to aerosolised *S. aureus*. The characteristics of this pathology is similar to that observed in the outbred mice. Moreover, as observed in studies using the outbred mice, significantly more severe pathology was observed in mouse models of CF in comparison to age, weight and sex-matched, non-CF littermate controls.

Unfortunately direct comparisons between the previous studies and the experiments described in this chapter are complicated by the significant differences in the nebulisation apparatus used, and hence the level of bacteria delivered (see Chapter 3, section 3.2). Estimates of the bacterial delivery profiles of the three nebulisers used suggested that the doses, in cfu/mouse/day, were; ~2 x 10^5 in the original studies, ~5 x 10^4 in the repeat bacterial exposure of inbred mice (Expt. 4.4) and ~2 x 10^6 in the repeat bacterial exposure of compound heterozygote mice (Expt. 4.5). This represents as much as a 40 fold difference and is a significant concern in the context of interexperimental comparison. Nevertheless, with this caveat in mind, comparisons may still be made.

The two studies with the most pronounced difference in bacterial dose are Expt. 4.4 and Expt. 4.5. In both of these studies the mouse models of CF were compared to groups of non-CF littermates, of the same age, backcrossed onto a C57Bl/6N background strain. Thus, valid comparison can be made between these control groups to assess the impact of the bacterial dose. Analysis of these studies resulted in an average total score for 4 week exposed non-CF mice of 11.5 ± 1.7 (n = 10) in Expt. 4.4 and 11.9 ± 1.8

(n = 9) in Expt. 4.5. These scores are not significantly different (p = 0.59), demonstrating that the increased dose of bacteria did not affect the severity of pulmonary histopathology in non-CF mice. Furthermore, analysis of the mouse models of CF in all three studies resulted in average total scores of 17.0 ± 4.3 (n = 5) in the original study, 15.1 ± 3.2 (n = 8) in Expt. 4.4 and 14.7 ± 2.2 (n = 9) in Expt. 4.5. Statistical analysis by t-test indicates no significant difference between the original study and either Expt. 4.4 or Expt. 4.5 (p = 0.43 and p = 0.32 respectively) or between Expt. 4.4 and Expt. 4.5 (p = 0.77). This indicates that regardless of any of the differences between these studies there was no significant difference in the severity of pathology in the mouse models. These results suggest that direct comparisons can be made between these studies, despite the quantitative differences in the levels of bacterial exposure.

Establishment of the *Cftr*^{tm1Hgu} mutation congenic on inbred lines will have reduced the genetic variation between mutant animals. This was intended to decrease the degree of variation in the lung phenotype in response to bacterial exposure and the degree of overlap between the phenotypes of mouse models of CF and non-CF littermates.

The spectrum of disease observed in response to bacterial exposure, in *Cftr*^{tm1Hgu}/*Cftr*^{tm1Hgu} and non-CF mice backcrossed onto the C57Bl/6N strain does indeed seem to have been reduced (see Figure 4.2) in comparison to outbred mice (see Figure 4.6). The range of total scores in the 4 week exposed inbred mice of all genotypes is between 8 and 20 (mean 13.1 ± 3.1, n = 18) in Expt. 4.4, in comparison to a range of 3 to 22 (mean 11.9 ± 6.6, n = 12) in the outbred mice in the original study. Although, the range and SD are decreased in the inbred mice, there is no significant difference between the mean total scores (p = 0.56).

When analysis is performed on the basis of genotype, there is a significant difference between the *Cftr*^{tm1Hgu}/*Cftr*^{tm1Hgu} and non-CF mice in both the original study and Expt.4.4. The level of significance is not increased in the inbred animals (p = 0.01 for the original studies, p = 0.015 for Expt. 4.4).

In addition, there is no significant difference between the total scores for the *Cftr*^{tm1Hgu}/*Cftr*^{tm1Hgu} in the two studies, 17.0 ± 4.3 (n = 5) in the original study and 15.1 ± 3.2 (n = 8) in Expt.4.4 (p = 0.43). The most obvious difference between the two experiments is the response of the non-CF mice to repeated bacterial exposure. The mean total score for the mixed, outbred MF1/129 non-CF mice in the original study was 5.6 ± 2.2 (n = 7), whereas in Expt. 4.4, the inbred C57Bl/6N non-CF mice had a mean total score of 11.5 ± 1.7 (n = 10). This difference is despite a lower estimated dose of bacteria in the latter study. However, the difference is not significant (p = 0.18). This non-significance is the result of one severely affected non-CF outlier in the original study with a score of 19.5 (95% higher than the next most severely affected non-CF mouse in this study). It is possible that the lung disease observed in this animal was pre-existing and not the result of the experimental procedure. Dixon's gap test (Bliss 1967) was applied to assess the validity of rejecting this mouse as an outlier. The difference between the suspected outlier and the next closest value, as a proportion of the range of the sample (for n = 7 non-CF mice), including the suspect variate, was found to exceed the normal expectation at $p < 0.05$. Thus, failure to omit the discordant observation would bias the rest of the sample. After removal of this outlier, significantly more severe histopathology (p = 0.003) is demonstrated in the inbred C57Bl/6N non-CF mice in comparison to the mixed, outbred MF1/129 non-CF mice.

Thus the spectrum of disease observed in response to bacterial exposure is narrowed in the C57Bl/6N mice in comparison to the mixed, outbred background strain. However, overlap still exists between the *Cftr*^{tm1Hgu}/*Cftr*^{tm1Hgu} mice and non-CF littermates. Indeed, the predominant effect appears to be an increased severity of disease in the wild type inbred mice. This is perhaps not surprising, given that C57Bl/6 mice have previously been reported to showed increased susceptibility to lung disease (Gosselin *et al* 1995, Stevenson *et al* 1995). However, this predisposition would appear to have no additional effect on the severity of lung disease in

Cftr^{tm1Hgu}/*Cftr*^{tm1Hgu} mice. This may indicate that the defect in the defence system of the C57Bl/6N strain is a component part of the defect arising secondary to the *Cftr*^{tm1Hgu} mutation. Alternatively it may be unrelated, but non-additive in its effect.

Interestingly, a recent study demonstrated that C57Bl/6N wild type mice had a low tracheal forskolin response and that this was largely abolished by pretreatment with ionomycin and TBHQ, to reduce the calcium linked contribution (Farley *et al* 1998). This suggests that there is little functional CFTR present in the tracheae of these mice and that wild type C57Bl/6N mice may have a natural "CF-like" defect in the trachea. This is compatible with the observation of the repeated bacterial exposure studies. However, the basis for this functional defect is unclear. This defect does not extend to the nose (Farley *et al* 1998) and the effect in the smaller airways is unquantified. Furthermore, in contrast to these electrophysiological results, semi-quantitative RT-PCR indicates normal expression of *Cftr* in the tracheae of C57Bl/6N mice, although the primary source may be the submucosal glands rather than the tracheal epithelium (Innes, personal communication). Finally, the pulmonary phenotype in response to bacterial exposure is significantly different in wild type mice in comparison to *Cftr*^{tm1Hgu}/*Cftr*^{tm1Hgu} littermates. This indicates that the level of CFTR function must still be greater in the wild type mice, at least in the lower airways, or that functions of CFTR other than those assessed by electrophysiological techniques must vary between the wild type mice and *Cftr*^{tm1Hgu}/*Cftr*^{tm1Hgu} littermates.

The *Cftr*^{tm1Unc} mutation has also been backcrossed to become congenic on a C57Bl/6 inbred background. However, in this case C57Bl/6J was used, as opposed to C57Bl/6N. *Cftr*^{tm1Unc}/*Cftr*^{tm1Unc} mice on the original mixed strain background did not demonstrate any abnormal pulmonary histopathology (Grubb and Boucher 1999). In contrast, the inbred *Cftr*^{tm1Unc}/*Cftr*^{tm1Unc} mice demonstrated significantly more severe lung disease in comparison to wild type mice and compared to those on a mixed background (Kent *et al* 1997). However, the only two primary characteristics of the reported phenotype

that have survived closer scrutiny are an increased deposition of collagen in the alveolar interstitium and a moderate increase in the neutrophils present in the lungs (Haston, personal communication). The observation of abnormal lung pathology in *Cftr*^{tm1Unc}/*Cftr*^{tm1Unc} mice congenic on a C57Bl/6J strain, but not the original mixed strain, has been attributed to a failure to activate an alternative Ca^{2+}-dependent Cl^- channel in inbred mice. Whereas upregulation of this channel is seen in the nasal epithelium of mixed strain *Cftr*^{tm1Unc}/*Cftr*^{tm1Unc} mice (Grubb *et al* 1994a), it was not observed in those congenic on a C57Bl/6J strain (Kent *et al* 1997). However, these studies are not extended to the lower airways in the inbred mice. The differences in the pathology observed in the inbred *Cftr*^{tm1Unc}/*Cftr*^{tm1Unc} mice and the inbred *Cftr*^{tm1Hgu}/*Cftr*^{tm1Hgu} mice may be attributable to the use of different C57Bl/6 inbred strains.

The second possible component of phenotype variation addressed was the role of residual CFTR function in the mouse models of CF. The repeated bacterial exposure of *Cftr*^{tm1Hgu}/*Cftr*^{tm1Unc} compound heterozygote mice was performed to establish the effect of a ~ 50% decrease in the background level of normal *Cftr* expression, in comparison to *Cftr*^{tm1Hgu}/*Cftr*^{tm1Hgu} mice on the same inbred background. No difference was observed between the severity of disease observed as a result of this modification, when Expt. 4.5 (see Figure 4.4) is compared to Expt. 4.4 (see Figure 4.2).

There was no significant difference between the mean total scores for the 4 week exposed mice of all genotypes ($p = 0.81$), comparing Expt. 4.5 (13.3 ± 2.4, $n = 18$) and Expt. 4.4 (13.1 ± 3.1, $n = 18$). Analysis on the basis of genotype demonstrated no significant difference ($p = 0.77$) between the mean total scores of the *Cftr*^{tm1Hgu}/*Cftr*^{tm1Unc} mice (Expt. 4.5; 14.7 ± 2.2, $n = 9$) and the *Cftr*^{tm1Hgu}/*Cftr*^{tm1Hgu} mice (Expt. 4.4; 15.1 ± 3.2, $n = 8$). It also demonstrated no significant difference ($p = 0.59$) between the mean total scores of the non-CF mice in Expt. 4.5 (11.9 ± 1.8, $n = 9$) and Expt. 4.4 (11.5 ± 1.7, $n = 10$). As described for the previous studies, a significant difference between mouse

models of CF (in this case *Cftr*^{tm1Hgu}/*Cftr*^{tm1Unc} mice) and non-CF littermates was observed ($p = 0.009$).

Thus, *Cftr*^{tm1Hgu}/*Cftr*^{tm1Unc} compound heterozygote mice did not demonstrate a significantly more severe pulmonary phenotype than *Cftr*^{tm1Hgu}/*Cftr*^{tm1Hgu} mice, backcrossed onto the same inbred background. This is despite a higher estimated dose of bacterial exposure and an expected reduction in normal levels of wild type *Cftr* expression from ~ 10% to ~ 5%. This observation suggests that an abnormal pulmonary phenotype may be manifest when the level of functional CFTR falls below a minimum threshold level, but will not be exacerbated by further decreases. This is supported by observations in human disease patterns. CF individuals with residual function mutations and splice mutations are termed "mild" with reference to their pancreatic disease, and may have less severe intestinal pathology, however, this does not relate to their lung disease (see Chapter 1, sections 1.3.3 and 1.3.4). The severity of pulmonary disease in such patients may still be severe (The Cystic Fibrosis Genotype-Phenotype Consortium 1993).

However, as discussed above, the function of normal CFTR in the tracheae of C57Bl/6N mice may be disrupted and may not correlate with the level of expression of *Cftr*. Thus, it is possible that the use of this strain of mouse may undermine the basis of this study. The extent to which this effect might be manifest in the lower airways is unclear.

The experimental design incorporated two types of control animals; 1 day exposure controls and untreated controls. The severity of lung disease, as assessed by mean total scores, in the 4 week exposed mice was significantly higher than the control mice in both experiments (Expt. 4.4; $p < 0.001$, Expt. 4.5; $p < 0.001$). The animals with the lowest total scores were always controls and the total scores for untreated mice were well below the score for the least severely affected 4 week exposed mouse (see Figure 4.4). However, some of the 1 day exposed mice had total scores similar to those of less severely affected, predominantly non-CF mice (see Figure 4.2). This suggests that there was no cumulative effect on the lung pathology in these

less severely affected repeatedly exposed mice. However, closer inspection of the individual component scores reveals a slightly more complex picture. As anticipated, the 1 day exposed mice show little evidence of perivascular and peribronchiolar lymphoid aggregates, or of pneumonia, suggesting that these develop in response to repeated bacterial exposure. The other components are more variable, particularly the level of goblet cell hyperplasia and metaplasia observed. Indeed, two of the mice with the highest scores for this feature were control animals, one of which was untreated.

These observations indicate that after just one exposure to *S. aureus*, mice can develop features of lung disease comparable to the less severely affected repeated exposure mice. In addition, features of lung disease may be pre-existing in some of the mice prior to the onset of experimental bacterial exposure. The latter consideration however, may complicate the assessment of these studies. It is possible that prior abnormal responses to lung infections may exacerbate the response of mouse models of CF to experimental bacterial exposure and precipitate more pronounced differences between these animals and non-CF littermates.

The cause of this pre-existing pathology is not clear. The lung homogenates from 8 randomly selected $Cftr^{tm1Hgu}/Cftr^{tm1Hgu}$ mice (n = 4) and non-CF mice (n = 4) failed to demonstrate the presence of any significant numbers of bacteria in the lower airways. Furthermore, the regular microbiological analysis of sentinel mice from the colony, performed routinely in the animal facility, did not show evidence of significant bacterial infection. However, these screens did occasionally indicate the presence of murine viruses. Serological testing for Sendai virus, Coronavirus and Murine Pulmonis was performed on randomly selected $Cftr^{tm1Hgu}/Cftr^{tm1Hgu}$ mice (n = 10) and non-CF mice (n = 5) using a Murine ImmunoCom kit. This test was strongly positive for Coronavirus in 6/10 $Cftr^{tm1Hgu}/Cftr^{tm1Hgu}$ mice and 2/5 non-CF mice, but negative for the two other viruses tested. When this test was repeated using $Cftr^{tm1Hgu}/Cftr^{tm1Hgu}$ mice (n = 5) and non-CF mice (n =

5), born and raised in isolator conditions, no positive results were obtained. This indicates one possible causative factor for the presence of abnormal lung histopathology in animals raised in standard conditions but not in those raised in isolators. However, a positive result for the presence of Coronavirus was found not to correlate with the presence of abnormal histopathology. Although viral infection was not found in the mice born and raised in isolator conditions, it was not practical to breed sufficient numbers of mice for bacterial exposure studies in this manner.

In the period following these studies, access to a new SPF barrier facility has become available. Gillian Morrison (MRC Human Genetics Unit, Edinburgh) has performed studies on the cytokine levels in BAL from mice raised in this facility and those from the original standard, non-SPF, animal facility. These studies have demonstrated a significantly raised level of BAL TNF-α in *Cftr*^{tm1Hgu}/*Cftr*^{tm1Hgu} mice in comparison to non-CF littermates, but only in animals maintained in the non SPF facility (Morrison 1999). In addition, the levels of BAL TNF-α were observed to be higher in animals from this facility than those from the SPF facility, regardless of genotype. This suggests increased inflammatory stimulus in the mouse models of CF from non-SPF conditions, secondary to background levels of microbes present in that facility, but not in SPF conditions. This would be compatible with a failure to clear or kill inspired microbes as effectively as non-CF littermates and supports the previous studies performed on the *Cftr*^{tm1Hgu}/*Cftr*^{tm1Hgu} mice on a mixed, outbred MF1 strain background (Davidson *et al* 1995).

In conclusion, the variability observed in the original studies using outbred mice is likely to be related to independently segregating genes in the outbred strain and variation in the degree of pre-existing lung pathology in the mice. Differences between individual *Cftr*^{tm1Hgu}/*Cftr*^{tm1Hgu} mice in the level of residual CFTR function are less likely to have had a significant effect. The use of inbred strains, from SPF facilities, should enhance the prospects of more clearly defined lung phenotypes in *Cftr*^{tm1Hgu}/*Cftr*^{tm1Hgu} mice.

The occurrence of a histopathological pulmonary phenotype in mice, secondary to mutation in *Cftr*, is important confirmation that mouse models of CF may be of value in dissecting the pathogenesis of CF lung disease. However, important considerations remain with regard to the mechanisms underlying the development of more severe pulmonary pathology in response to *S. aureus* in the mutant mice, the specific nature of this pathology and the response to other CF associated pathogens, particularly *P. aeruginosa*.

In a previous control study, a cohort of 10 mixed, outbred MF1/129 mice (5 $Cftr^{tm1Hgu}/Cftr^{tm1Hgu}$ mice, 2 heterozygotes and 3 wild type mice), 2 – 4 months old, from non-SPF conditions, were selected. These mice were exposed to nebulised PBS (the carrier vehicle for bacteria in the other studies) alone, for 4 weeks, using the same protocol as described for the other studies. In this experiment, no significant pathology was observed above expected background levels (total score ≤ 5). This indicates that this technique itself does not induce pathology.

It is possible that a large proportion of the bacteria nebulised in these studies are killed by this procedure, as suggested in Chapter 3, section 3.2.2.1. This may result in the delivery of a large number of dead bacteria to the mouse lungs, in addition to the dose of viable microbes. It is not clear to what extend the pathology observed related to the dead bacteria as well as the viable organisms. However, in previous studies using mixed, outbred $Cftr^{tm1Hgu}/Cftr^{tm1Hgu}$ mice, the specific histopathological consequences of repeated exposure to *B. cepacia* were different to those observed in response to *S. aureus* (Davidson *et al* 1995). Whereas bronchiolitis predominated in the $Cftr^{tm1Hgu}/Cftr^{tm1Hgu}$ mice exposed to *S. aureus*, pneumonia was more frequently observed after repeated exposure to *B. cepacia*. This pathogen specific response supports a primary role for the viable bacteria in the establishment of the pulmonary pathology observed.

Histopathological assessment of the lungs of mice repeatedly exposed to *S. aureus* revealed a significant difference between the mouse models of CF

and non-CF controls. This was consistently demonstrated when assessment was performed using the total score, but not for the scores assigned to the 5 features from which it was comprised. Thus, the total score assigned for severity of pathology was more closely correlated with genotype than any individual component part of that score. This suggests an exaggerated normal response in these mice, rather than abnormality in any one aspect of this response. This is compatible with a general impairment of the antimicrobial properties of the murine tracheal ASL, a mucocilary clearance defect or any other mechanism that would have resulted in the prolonged presence of bacteria in the lungs of mouse models of CF. To further dissect the mechanisms underlying the pathogenesis of the lung pathology observed, alternative approaches were required. Studies aimed at addressing some of these issues are described in the remaining chapters of this thesis.

The specific lung histopathology described in the mouse models of CF bear many similarities to CF lung disease, including bronchiolitis, goblet cell hyperplasia and metaplasia and mucus retention (see Chapter 1, section 1.4.1). However, there are equally striking differences. In contrast to CF individuals, the mouse models of CF do not display bronchiectasis, or a dramatic neutrophil accumulation in the lungs.

The absence of bronchiectasis in mouse models of CF is likely to be attributable to the relatively short life span of mice, in comparison to humans. The classical end stage CF lung disease is the end result of repeated cycles of infection and inflammation over many years (see Chapter 1 section 1.4). This difference may also be a consequence of the relatively sterile conditions in which most experimental animals are maintained. Even the mice described in this chapter are experimentally exposed to bacteria only briefly and over just 4 weeks.

The relative absence of an accumulation of neutrophils in the lungs of mouse models of CF repeatedly exposed to pathogens, when compared to CF humans, is more perplexing. The *Cftr*^{tm1Unc}/*Cftr*^{tm1Unc} mice, congenic on a

C57Bl/6J strain background, were reported to have a significantly raised number of neutrophils in the lung, in comparison to wild type mice, as observed by TEM (Kent *et al* 1997). This increase was only moderate (2–4 fold), although these mice had not been experimentally exposed to bacteria. An increase of similar proportions in the number of interstitial macrophages and fibroblasts was also noted.

The failure of the *Cftr*^{tm1Hgu}/*Cftr*^{tm1Hgu} mice to respond to bacterial exposure with a dramatic neutrophilia may been ascribed to the nature of the infectious stimulus. The experiments described in this chapter address only the histopathological response to repeated bacterial exposure and provide no evidence of chronic infection with *S. aureus* in these mice. To have provided this additional information would have required homogenisation of a defined portion of the mouse lung, to be plated on agar and assessed by counting the resultant colonies. However, previous studies had demonstrated that such infections were frequently lobar in nature. As a result, the loss of a portion of the lung for such analysis could have produced misleading histopathological assessment and unrepresentative bacteriological analysis. Our previous studies have demonstrated that the ability of *Cftr*^{tm1Hgu}/*Cftr*^{tm1Hgu} mice to clear aerosolised *S. aureus* from their lungs is significantly compromised in comparison to non-CF littermates (Davidson *et al* 1995). However, regardless of genotype, all the mice were able to clear, or kill, the vast majority of bacteria delivered to their lungs. Thus, it is possible that chronic infection is not established as a result of repeated exposure protocols and that the phenotype described is a cumulative response to delayed clearance, or killing, of bacteria. In the presence of a chronic infection, the neutrophil accumulation anticipated might be precipitated. In a model purported to simulate chronic lung infection with mucoid *P. aeruginosa*, this bacteria was delivered to the lungs of *Cftr*^{tm1Unc}/*Cftr*^{tm1Unc} mice encased in agar beads (see below). A severe, neutrophil dominated endobronchial inflammation was reported in these mice (van Heeckeren *et al* 1997, Gosselin *et al* 1998). However, this was a

focal response, limited to the parenchyma around the individual beads. Furthermore, there was no difference between the lung histopathology or the neutrophil counts observed in the *Cftr*^{tm1Unc}/*Cftr*^{tm1Unc} mice and those observed in the non-CF controls.

Thus, differences are observed between the lung disease evident in mouse models of CF, under the experimental conditions evaluated to date, and classical human CF lung disease. This should perhaps not be surprising given the numerous differences between them. These include differences in the electrophysiological properties of the airways (see Chapter 1, section 1.7.3.5), lifespan and exposure to environmental risk factors, as discussed above. In addition, there are significant differences in lung anatomy and the cellular composition of the airway epithelium. Human lungs consist of two lobes on one side and three on the other, with submucosal glands present throughout the cartilaginous airways. The epithelium of the proximal airways is predominantly comprised of ciliated cells, goblet cells and basal cells, whereas the most numerous cells lining the distal airways are ciliated cells and Clara cells (Ross and Reith 1985). Murine lungs consist of 4 lobes on one side and one lobe on the other, with submucosal glands confined largely to the proximal trachea (Borthwick *et al* 1999). The airways are predominately comprised of ciliated cells and Clara cells at all levels, with few goblet cells present (Pack *et al* 1980, Pack *et al* 1981). Thus, murine airways are more similar to human bronchioles rather than proximal airways. This may prove to be beneficial, with disease of the distal airways being characteristic of early stage CF lung disease in humans.

It has been suggested that the relative absence of goblet cells and the lack of submucosal glands beyond the proximal trachea in mouse models of CF may prevent the development of classical CF lung disease. However, some of the first signs of abnormal pathology in CF individuals occurs in the bronchioles, distal to the submucosal glands. In addition, the studies described in this chapter clearly demonstrate both goblet cell hyperplasia and metaplasia and mucus retention in mice exposed to bacteria. Another

study, using mixed background *Cftr*^{tm1Unc}/*Cftr*^{tm1Unc} mice, was designed to address this concern (Cressman *et al* 1998). Allergic airways disease was induced in these mice, using chicken ovalbumin. This produced an identical pattern of goblet cell hyperplasia and metaplasia and lymphocytic aggregates in both the *Cftr*^{tm1Unc}/*Cftr*^{tm1Unc} mice and non-CF controls. These mice were then challenged with *P. aeruginosa* or *S. aureus* followed by *P. aeruginosa*. No difference was observed in the bacterial clearance profiles of the *Cftr*^{tm1Unc}/*Cftr*^{tm1Unc} mice in comparison to the non-CF controls. This suggested that increased mucus production was not sufficient to impair bacterial clearance in the *Cftr*^{tm1Unc}/*Cftr*^{tm1Unc} mice. However, the effective hydration of the excess mucus, as a result of a predominantly Ca^{2+}-dependent Cl^- pathway in the tracheae of mixed background *Cftr*^{tm1Unc}/*Cftr*^{tm1Unc} mice may be responsible for these observations.

The intrinsic differences between CF mice and CF humans should not be viewed too negatively. While such distinctions may prevent mouse models of CF from accurately reproducing all aspects of CF lung disease in humans, the differences may prove as illuminating as the similarities. Furthermore, many of the features discussed above have also been demonstrated to vary between different strains of mice (see Chapter 1, section 1.7.4). These contrasting phenotypes are an important strength of mouse models. Taken together these approaches may be capable of establishing the critical factors in the development of CF lung disease in humans. Rather than pursue the development of all aspects of classical human CF lung disease in mouse models, it is equally valid and informative to study lung disease in mouse models of CF in its own right. In this manner the consequence of *Cftr* mutation in the mouse lung is addressed and the underlying mechanisms evaluated. Extrapolation to human disease processes can then be performed, recognising both the similarities and the differences between mice and humans.

The final important issue to address is the response of mouse models of CF to exposure to bacteria other than *S. aureus*. It is unclear whether CF

infants would be abnormally susceptible to organisms such as *P. aeruginosa* and *B. cepacia* in the absence of previous infections with respiratory viruses and organisms such as *S. aureus* and *H. influenzae* (see Chapter 1, section 1.4.2). Nonetheless, studies have been performed to address the response of mouse models of CF to these important organisms.

Previously reported studies demonstrated than $Cftr^{tm1Hgu}/Cftr^{tm1Hgu}$ mice, on a mixed, outbred MF1/129 strain background, demonstrated an impaired ability to clear aerosolised *B. cepacia* from their lungs, in comparison to non-CF littermates (Davidson *et al* 1995). In addition, they developed significantly more severe lung pathology in response to repeated exposure to this organism. This phenotype was similar to that described after repeated exposure to *S. aureus*. However, in contrast, pneumonia was a predominant component of the response to *B. cepacia*. This demonstrated a pathogen specific component to the responses observed in these studies.

The study of *P. aeruginosa* in mouse models of CF is complicated by a variety of factors. The most important of these is the phenotypic alterations that this organism undergoes over the course of chronic infection of the lungs of CF individuals (see Chapter 1, section 1.4.2.4). Although the initial infections in CF individuals are with planktonic strains, the rapid deterioration of the CF lung occurs after transformation of these bacteria and colonisation with these mucoid *P. aeruginosa* (Govan and Deretic 1996). Thus, it is unclear whether the most revealing studies will arise from challenging mouse models of CF with non-mucoid *P. aeruginosa*, to evaluate predisposition to infection, or modelling colonisation with mucoid strains in the absence of previous rounds of infection. The ideal study would of course demonstrate increased susceptibility to infection with non-mucoid *P. aeruginosa*, followed by the emergence of mucoid strains within the mouse lung and colonisation. In addition, the significance of previous infections with other organisms and the consequent antibacterial chemotherapy received, in priming the CF lung for *P. aeruginosa* infection in unclear. Given

these complicating factors, it is perhaps not surprising that the chronic *P. aeruginosa* infections observed in CF lung disease have not been successfully modelled in CF mice to date.

A series of studies were performed using *Cftr*^{tm1Hgu}/*Cftr*^{tm1Hgu} mice inbred on a mixed MF1/129 strain background, and wild type controls. These mice were repeatedly exposed to mucoid or non-mucoid clinical isolates of *P. aeruginosa*, both with and without prior exposure to RSV (Larbig *et al* 1998). The delivery of bacteria was performed both by nebulisation and direct instillation, using techniques similar to those described in Chapter 3. No significant difference was observed between the clearance profiles or the pulmonary histopathology of the *Cftr*^{tm1Hgu}/*Cftr*^{tm1Hgu} mice and the non-CF controls, under any of these conditions. This is in sharp contrast to the results observed using *S. aureus* and *B. cepacia* and suggests that *Cftr*^{tm1Hgu}/*Cftr*^{tm1Hgu} mice do not show increased susceptibility to infection with this organism. However, an alternative explanation must be considered relating to the establishment of inbred mixed background mice. Lines of inbred mice were established from founder *Cftr*^{tm1Hgu}/*Cftr*^{tm1Hgu} mice on a mixed outbred MF1/129 strain background. It is conceivable that this process selected for the most fertile mice, potentially those afforded the most protection from the *Cftr*^{tm1Hgu} mutation by independently segregating modifier genes. As a result the progeny of these inbred lines may be less severely affected than the majority of the original outbred mice. Indeed, a recent electrophysiological study of these mice appears to indicate that the CF phenotype has been lost (Tümmler, personal communication).

In a more recent study the clearance of a clinical isolate of *P. aeruginosa* was assessed in *Cftr*^{tm1Kth}/*Cftr*^{tm1Kth} mice (carrying the ΔF508 mutation) on a mixed C57Bl6/129 strain background and non-CF littermates (McCray *et al* 1999). These animals were exposed to a single dose of ~ 1 x 10^6 cfu by nebulisation. A marked BAL neutrophilia was reported in all mice, declining over 72 hours. The bacteria were shown to be rapidly cleared by 24 hours

and no significant differences were observed between the *Cftr*^{tm1Kth}/*Cftr*^{tm1Kth} mice and non-CF littermates. These studies, in conjunction with the study using *Cftr*^{tm1Unc}/*Cftr*^{tm1Unc} with induced allergic airways disease (Cressman *et al* 1998), suggest that mouse models of CF do not display increased susceptibility to pulmonary infection with *P. aeruginosa*.

These studies all attempted to model the process of initial lung infection with *P. aeruginosa* using relevant clinical strains. This approach is intended to elucidate the mechanisms underlying increased susceptibility to lung infection with this organism in CF individuals, the transition to mucoidy (see Chapter 1, section 1.4.2.4) and selection for mucoid variants in lung colonisation. Another study, using wild-type C57Bl/6J mice, reported significantly less efficient clearance of mucoid strains of *P. aeruginosa* in comparison to the parental non-mucoid strains, following challenge with aerosolised bacteria (Yu *et al* 1998). However, such observations do not provide any explanation for the predisposition to colonisation with *P. aeruginosa* and mucoid transformation in the CF lung.

The use of agar beads has been adopted as an alternative approach in two studies (van Heeckeren *et al* 1997, Gosselin *et al* 1998). This technique involves the direct instillation of *P. aeruginosa* laden agar beads into the lungs of the experimental animals. This is purported to model the colonisation of the CF lung by mucoid *P. aeruginosa*. These studies used *Cftr*^{tm1Unc}/*Cftr*^{tm1Unc} mice, on either the original mixed C57Bl/6J/129 strain (van Heeckeren *et al* 1997), or backcrossed onto a inbred C57Bl/6 strain using speed congenics (Gosselin *et al* 1998). In both cases the mice were reared on a liquid diet. In one study the dose of bacteria delivered was analysed and estimated to be ~1 x 10^5 cfu. However, such analysis is complicated by the effects of the agar.

A significantly decreased survival rate of *Cftr*^{tm1Unc}/*Cftr*^{tm1Unc} mice in response to bronchopulmonary instillation of sub-lethal doses of *P. aeruginosa* laden agar beads, in comparison to non-CF mice, was reported in both studies. No deaths were reported after exposure to sterile beads. In

addition, one study reported a significantly more severe weight loss in *Cftr*^{tm1Unc}/*Cftr*^{tm1Unc} mice treated with *P. aeruginosa* agar beads, than in non-CF mouse (van Heeckeren *et al* 1997). However the published data suggest that this differential was equally severe after inoculation with sterile beads. This would suggest that in terms of weight loss, the major difference between genotypes was in fact in response to the technique rather than the bacteria.

The bacterial load was examined at different time points after inoculation. In one study no significant difference was observed between genotypes (van Heeckeren *et al* 1997). The other study presented evidence that bacterial proliferation existed regardless of genotype, but also reported the recovery of significantly higher numbers of bacteria from the lungs of *Cftr*^{tm1Unc}/*Cftr*^{tm1Unc} mice, in comparison to non-CF littermates (Gosselin *et al* 1998). However, such analysis is notoriously difficult to interpret. The breakdown of a single bead within the lung and the consequent release and proliferation of bacteria may seriously distort such results (Govan, personal communication).

Analysis of the lung histopathology of these mice revealed severe, focal, neutrophil dominated, endobronchial inflammation, obstruction of the distal airways with agar beads and inflammatory cells and excessive mucus production. However, no significant differences were observed between *Cftr*^{tm1Unc}/*Cftr*^{tm1Unc} mice and non-CF littermates in either study.

In one study, significantly higher levels of pro-inflammatory cytokines were reported in the *Cftr*^{tm1Unc}/*Cftr*^{tm1Unc} mice, in comparison to the non-CF controls (van Heeckeren *et al* 1997). This was despite an absence of significant differences in the bacterial lung burden or pulmonary histopathology.

Thus, the primary phenotypic difference reported in these studies is an increased mortality in *Cftr*^{tm1Unc}/*Cftr*^{tm1Unc} mice in response to the instillation of *P. aeruginosa* laden agar beads. In the absence of other significant findings it is unclear what the cause of this increased mortality is. The significantly increased bacterial burden in the *Cftr*^{tm1Unc}/*Cftr*^{tm1Unc} mice reported in one study

was not observed in the other despite replicating the increased mortality phenotype. One study reported negative bacteriological analysis of kidney, spleen and liver homogenates, ruling out systemic infection (Gosselin *et al* 1998). In the other study, despite negative blood cultures, bacteria were isolated in splenic homogenates from 1 out of 10 $Cftr^{tm1Unc}/Cftr^{tm1Unc}$ mice and 2 of 12 non-CF mice. This was only assessed at day 3, before the vast majority of the deaths had been observed (van Heeckeren *et al* 1997). The small proportion of $Cftr^{tm1Unc}/Cftr^{tm1Unc}$ mice surviving to adulthood on a liquid diet have a lower body weight and demonstrate abnormalities associated with malnutrition (Ip *et al* 1996). As a result they are likely to be systemically weaker than their non-CF littermates. In addition, neither study made close examination of the intestines, despite gastointestinal disease being the sole cause of mortality in the vast majority of the $Cftr^{tm1Unc}/Cftr^{tm1Unc}$ mice. Thus, the cause of death cannot be definitively attributed to pulmonary disease.

The observation of significantly increased levels of pro-inflammatory cytokines has been the subject of a subsequent report (van Heeckeren *et al* 1999). The BAL cytokine levels were assessed in $Cftr^{tm1Unc}/Cftr^{tm1Unc}$ mice on the original mixed background strain and inbred onto the C57Bl/6J strain. In both cases, 3 days after inoculation with *P. aeruginosa* laden agar beads, significantly higher levels of pro-inflammatory cytokines (TNF-α, IL-1β, IL-6, MIP-2 and KC) were observed in the $Cftr^{tm1Unc}/Cftr^{tm1Unc}$ mice, in comparison to wild type controls. In addition, in contrast to wild type mice, the anti-inflammatory cytokine IL-10 was reported not to be measurable in $Cftr^{tm1Unc}/Cftr^{tm1Unc}$ mice. Furthermore, no significant difference was observed between the levels of IL-10 in $Cftr^{tm1Unc}/Cftr^{tm1Unc}$ mice and heterozygotes, while heterozygotes were also reported to demonstrate significantly raised levels of some proinflammatory cytokines in comparison to wild type mice. This is the first report to suggest an abnormal phenotype in mice heterozygous for mutations in *Cftr*. These studies support the theory that an inappropriate cytokine response to inflammatory stimuli may be important in the

development of CF lung disease. However, a recent study examining the innate lung defences against *P. aeruginosa* in a malnourished mouse model reported some striking similarities in mice exposed to aerosolised *P. aeruginosa* strain PAO1 after three weeks on a protein energy malnourished diet (Yu *et al* 2000). These mice displayed significantly reduced pulmonary clearance (corrected by restoration of a normal diet), TNF-α levels, and iNOS levels in comparison to controls and significantly increased levels of MIP-2 and KC. In addition, in contrast to controls, the malnourished infected mice had no detectable IL-10. This study suggests that malnutrition in the liquid-diet fed $Cftr^{tm1Unc}/Cftr^{tm1Unc}$ mice may contribute to their pulmonary phenotype in response to *P. aeruginosa* laden agar beads, independently of any direct effects of CFTR dysfunction in the lung.

The agar bead model reveals interesting phenotypic differences, despite a somewhat artificial microenvironment, and may prove effective in the study of the host response to established infection. If the development of CF lung disease were simply the consequence of a failure of mucociliary clearance, then the ability of this technique to prevent bacterial clearance may be important. However, this is not an accurate model of chronic infection with mucoid *P. aeruginosa* in CF, simply superimposing bacterial retention, in an artificial medium, on an otherwise unaffected lung. This model is unlikely to provide much information about the initiation and development of early stage CF lung disease, or the increased susceptibility to infection secondary to CFTR dysfunction. While providing an additional phenotypic endpoint for analysis of mouse models of CF, the studies described above do not provide evidence of an increased susceptibility to *P. aeruginosa*.

In conclusion, despite the evidence of several significant differences between the response of mouse models of CF and non-CF littermates to bacteria, important differences exist when compared to CF lung disease in humans. Studies such as the repeat bacterial exposure experiments described in this chapter are lengthy, labour intensive and unlikely to be

sufficient to reveal the mechanisms by which mutations in *Cftr* result in abnormal lung phenotypes. The consequent challenge is to design experiments to examine the relevance of existing hypotheses for the development of CF lung disease in humans, in the mouse models of CF. In addition, these studies should aim to establish the differences between CF related lung disease in humans and mice and the underlying mechanisms. Such studies will serve to further our understanding of the biology of the murine and human lung in health and disease.

Chapter 5

Bacterial internalisation

Chapter 5: Bacterial internalisation

5.1 Introduction

The internalisation of *P. aeruginosa* by epithelial cells has been proposed as a CFTR-dependent component of the lung defence system (see Chapter 1, section 1.5.2.2). Studies using cell lines and a wild-type neonatal mouse model have suggested that the first predicted extracellular domain (amino acids 108-117) of CFTR may act as a specific cellular receptor for the lipopolysaccharide core oligosaccharide of *P. aeruginosa* (Pier *et al* 1996, Pier *et al* 1997). Bacterial ingestion, followed by epithelial cell shedding, perhaps involving a CFTR-dependent apoptotic mechanism, has been proposed as an important mechanism in the protection of the lung from *P. aeruginosa*.

These studies have demonstrated bacterial internalisation *in vivo*, in neonatal mice, but only wild type mice were examined. The putative first extracellular domain of CFTR is well conserved between humans and mice, with 13 of the 15 amino acids identical (the two differences are D112E and V115E, human to mouse). In addition, the inoculation of a synthetic first extracellular domain peptide of human CFTR with the bacterial inoculum has been reported to reduce the internalisation of *P. aeruginosa* by dissociated mouse lung cells by > 95% (Pier et al 1997). Thus, mouse models of CF represent an ideal system in which to study the role of CFTR in bacterial internalisation by airway epithelial cells and the relevance of this process *in vivo*.

5.2 Bacterial internalisation *in vivo*

The published studies utilised a neonatal mouse model, in which 7 day old BALB/c mice were inoculated with bacteria intra-nasally and performed a gentamicin exclusion assay to assess internalisation. This method was extensively adapted and optimised for application using adult mice and is described in full in the Materials and Methods (see Chapter 2, section 2.8.1 and Figure 5.1).

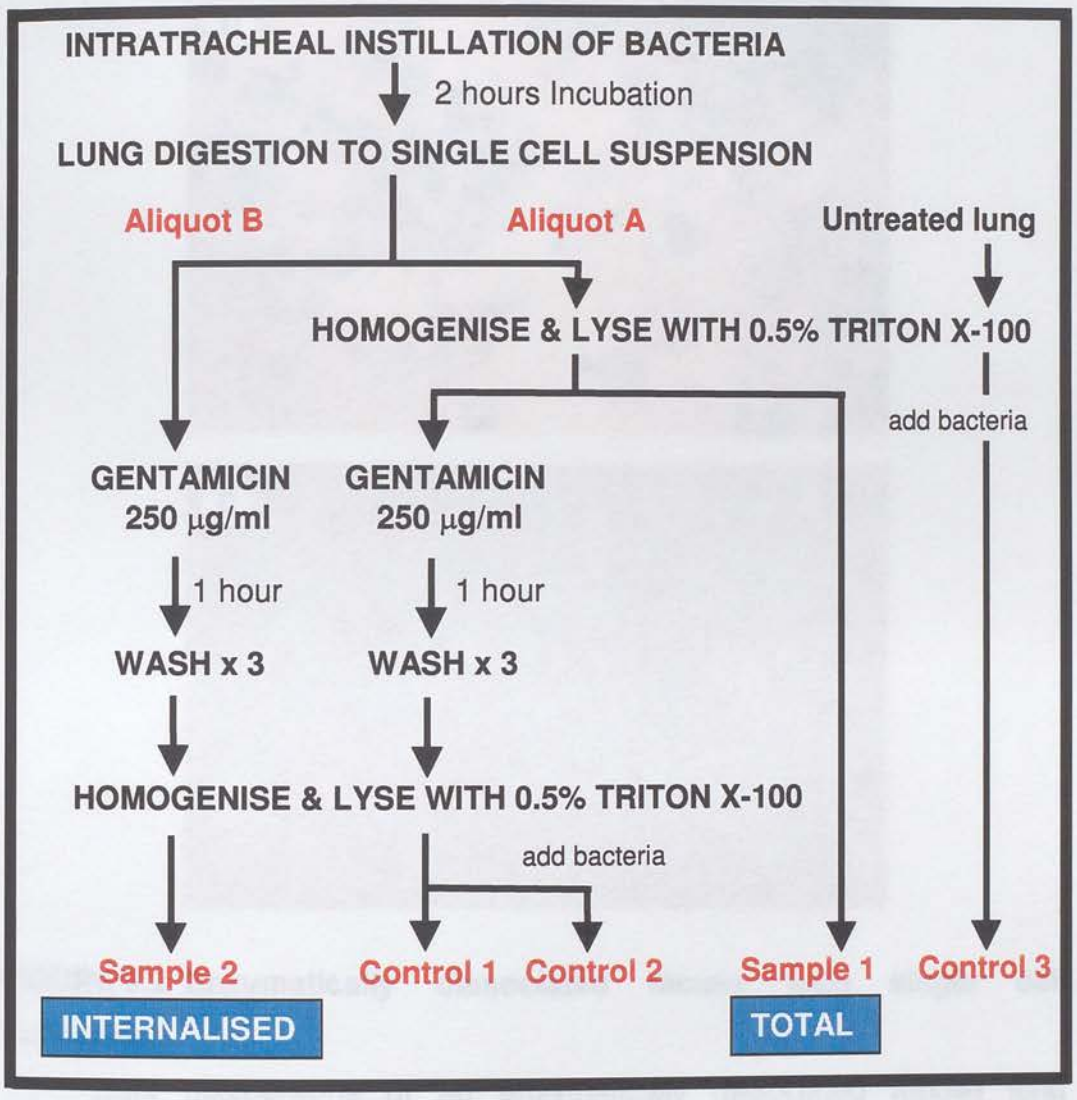

FIGURE 5.1 Assessment of bacterial internalisation

Experimental protocol to assess the *in vivo* internalisation of *P. aeruginosa* by murine lung cells.

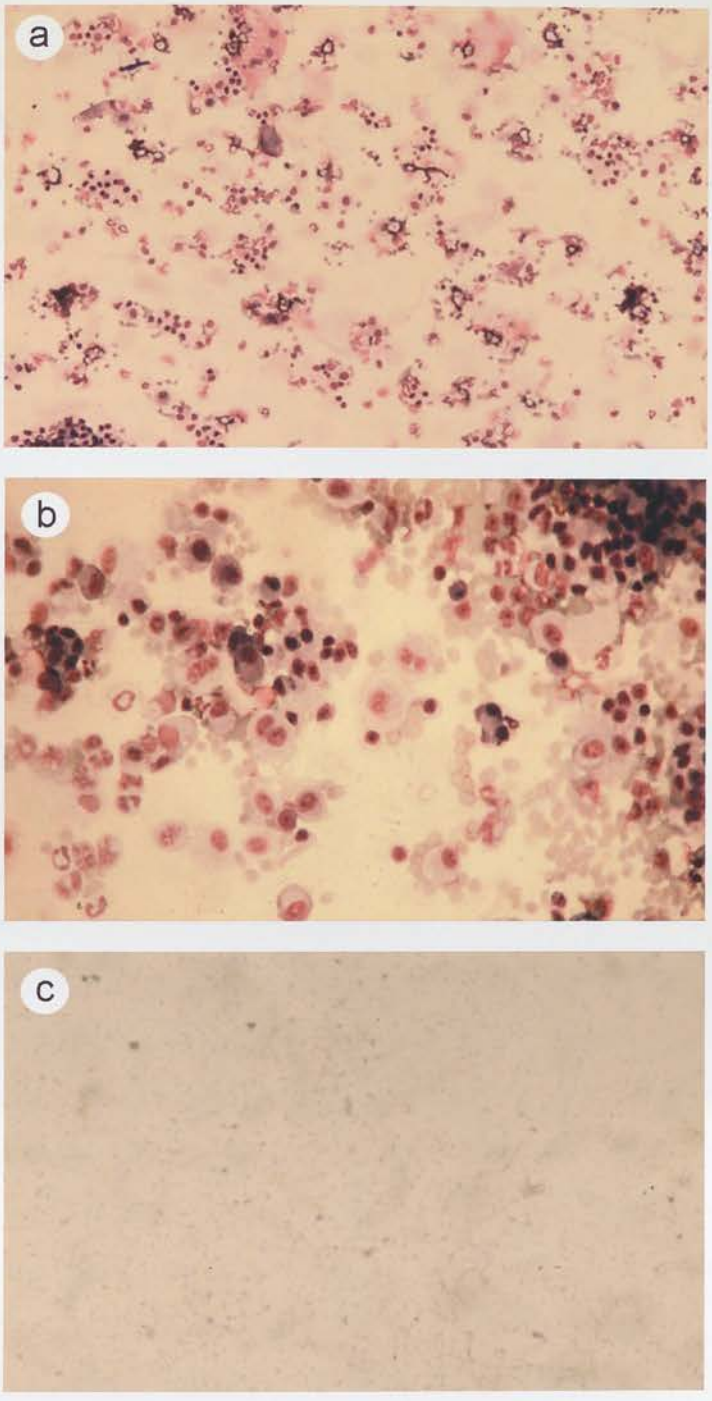

FIGURE 5.2 Enzymatically dissociated mouse lung single cell suspension

Light micrographs of an enzymatically dissociated mouse lung cytospin, stained with Diff-Quik. A single cell suspension is demonstrated at a) 100x magnification, and b) 250x magnification. c) Following homogenisation and the addition of 0.5% Triton X-100 all the cells are lysed (100x magnification).

Anaesthetised adult mice (3-6 months old) were inoculated with suspensions of fresh, overnight cultures of *P. aeruginosa* CF clinical isolate J1385 by direct intratracheal instillation (see Chapter 2, section 2.5.2 and Chapter 3, section 3.3). Bacteria were prepared by Wendy Hannant, Jayne Hughes or Cathy Doherty, Department of Medical Microbiology, University of Edinburgh. After an incubation period of two hours, the lungs and tracheae were removed and finely chopped. Enzymatic dissociation was then performed, optimised for minimal effect upon bacterial viability. The resultant single cell suspension (see Figure 5.2a and b) was then split, as illustrated in Figure 5.1. Aliquot A was homogenised and treated with 0.5% Triton X-100, to lyse all the cells (see Figure 5.2c) and release any internalised bacteria. Duplicate serial dilutions of samples were performed and plated on agar (Sample 1). This sample indicates the total number of bacteria delivered. The remains of Aliquot A and the whole of Aliquot B were treated with 250 μg/ml of gentamicin, which kills extracellular, but not intracellular bacteria (Pier *et al* 1997) and incubated for 1 hour at 37 °C. Gentamicin was demonstrated to be bactericidal for *P. aeruginosa* strain J1385 at 10 μg/ml (see Materials and Methods, Chapter 2, section 2.8.2). Gentamicin was removed by washing and the samples were homogenised and treated with 0.5% Triton X-100 to lyse the cells. Duplicate serial dilutions of samples from the gentamicin treated Aliquot A (Control 1) and Aliquot B (Sample 2) were performed and plated on agar. Sample 2 indicates the number of bacteria surviving the gentamicin treatment and is proposed to represent the internalised bacteria, released by cell lysis. Control 1 confirms the bactericidal activity of gentamicin on all the bacteria exposed to it and should not contain any viable bacteria. A dilution of the original bacterial suspension (1% of the total dose delivered to the mice) was added to the remains of the gentamicin treated Aliquot A after washing. Duplicate serial dilutions of samples were performed and plated on agar (Control 2). Control 2 confirms that the washing steps are sufficient to remove the gentamicin

and thus that any internalised bacteria released by cell lysis will not be subject to the effects of this aminoglycoside antibiotic. In addition, the lungs and trachea of an untreated mouse were removed, homogenised, treated with 0.5% Triton X-100 and a dose of bacteria equal to that delivered to the mice added. Duplicate serial dilutions of samples were performed and plated on agar (Control 3). Control 3 evaluates any antibacterial activity of the homogenised, lysed cellular material.

Initial studies were performed on wild type mice. A typical study is described below (Table 5.1 and Figure 5.3). An expected dose of 2.5×10^7 cfu of *P. aeruginosa* isolate J1385 was delivered to two anaesthetised, adult, outbred CD-1 mice by direct intratracheal instillation. After two hours incubation the mice were sacrificed, their lungs were removed and prepared as described above. The samples were plated out on agar and cfu counts performed after 24 hours incubation. Each control sample was prepared from only one mouse.

		Cfu count
Mouse A	Sample 1 - TOTAL	$7.1 \times 10^7 \pm 1.5 \times 10^7$
	Sample 2 - INTERNALISED	$1.3 \times 10^5 \pm 0.2 \times 10^5$
Mouse B	Sample 1 - TOTAL	$7.2 \times 10^7 \pm 2.9 \times 10^7$
	Sample 2 - INTERNALISED	$1.3 \times 10^5 \pm 0.3 \times 10^5$
	Control 1	$< 1.0 \times 10^2$
	Control 2 (expected 2.5×10^5)	$4.0 \times 10^5 \pm 0.3 \times 10^5$
Mouse C	Control 3	$2.8 \times 10^7 \pm 0.3 \times 10^7$
Expected dose delivered		2.5×10^7

TABLE 5.1 Internalisation of *P. aeruginosa* by wild type CD-1 mice

Assessment of the internalisation of *P. aeruginosa* by wild type CD-1 mice. Colony counts are mean ± SD, from duplicate dilutions.

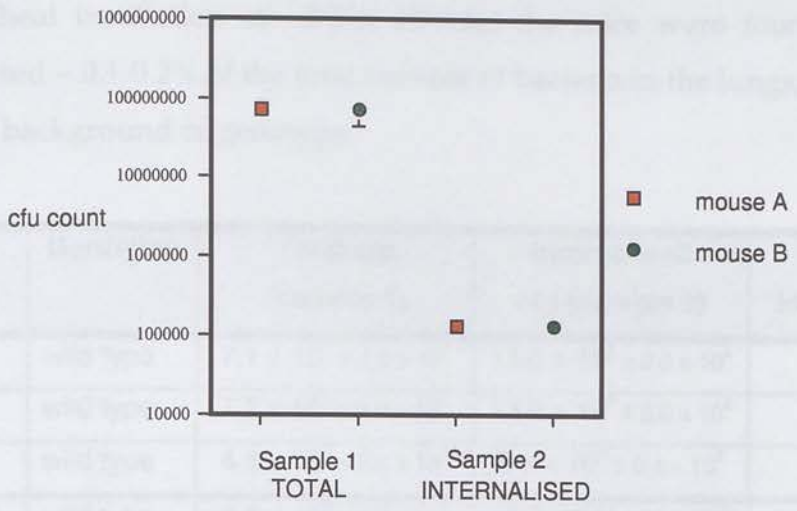

FIGURE 5.3 Internalisation of *P. aeruginosa* by wild type CD-1 mice

The internalisation of *P. aeruginosa* by wild type CD-1 mice. The points of the graph represent the two individual mice. Colony counts are mean ± SD, from duplicate dilutions.

This study demonstrates the *in vivo* internalisation of *P. aeruginosa* by mouse lung cells. Using this procedure, the number of bacteria observed to be internalised was ~ 1.3×10^5 cfu per mouse, representing 0.2% of the total pulmonary bacterial load of ~ 7×10^7 cfu. The expected total dose delivered, calculated on the basis of the quantified bacterial delivery profile for direct tracheal instillation (see Chapter 3, section 3.3.1) was ~ 2.5×10^7 cfu. Control 3, representing the delivery of this same dose to homogenised and lysed lung tissue, suggested no antibacterial effect of lysed cellular material. In both mice, sample 1, representing the total dose in the lung, was observed to be ~2–3 fold higher than expected, this suggests some bacterial proliferation prior to tissue processing. Controls 1 and 2 demonstrated the bactericidal activity of gentamicin and its effective removal by washing.

This experimental protocol was repeated using wild-type C57Bl/6N and MF1 mice and $Cftr^{tm1Hgu}/Cftr^{tm1Hgu}$ mice on a mixed, outbred MF1/129

strain background (summarised in Table 5.2). In each case, following the intratracheal instillation of ~2.5 x 10^7 cfu, the mice were found to have internalised ~ 0.1-0.2% of the total number of bacteria in the lungs, regardless of strain background or genotype.

Strain	Genotype	Total cfu (sample 1)	Internalised cfu (sample 2)	% internalised
CD-1	wild type	$7.1 \times 10^7 \pm 1.5 \times 10^7$	$13.0 \times 10^4 \pm 2.0 \times 10^4$	0.18
CD-1	wild type	$7.2 \times 10^7 \pm 2.9 \times 10^7$	$13.0 \times 10^4 \pm 3.0 \times 10^4$	0.18
CD-1	wild type	$4.8 \times 10^7 \pm 0.4 \times 10^7$	$5.0 \times 10^4 \pm 0.4 \times 10^3$	0.11
C57Bl/6N	wild type	$4.6 \times 10^7 \pm 0.2 \times 10^7$	$10.0 \times 10^4 \pm 1.0 \times 10^4$	0.22
C57Bl/6N	wild type	$4.6 \times 10^7 \pm 0.3 \times 10^6$	$9.0 \times 10^4 \pm 0.2 \times 10^5$	0.20
MF1	wild type	$1.7 \times 10^7 \pm 0.5 \times 10^6$	$1.8 \times 10^4 \pm 0.1 \times 10^4$	0.11
MF1	wild type	$2.5 \times 10^7 \pm 1.4 \times 10^7$	$4.9 \times 10^4 \pm 1.1 \times 10^4$	0.20
MF1	*Cftr^{tm1Hgu}*	$5.4 \times 10^7 \pm 1.1 \times 10^7$	$8.2 \times 10^4 \pm 0.2 \times 10^4$	0.15
MF1	*Cftr^{tm1Hgu}*	$5.0 \times 10^7 \pm 1.8 \times 10^7$	$7.4 \times 10^4 \pm 0.2 \times 10^4$	0.15

TABLE 5.2 Internalisation of *P. aeruginosa* after high dose delivery

A summary of the *in vivo* internalisation of *P. aeruginosa*, following the direct intratracheal instillation of ~2.5 x 10^7 cfu. Colony counts are mean ± SD, from duplicate dilutions.

This experimental protocol was repeated using *Cftr^{tm1Hgu}/Cftr^{tm1Hgu}* mice and non-CF littermates, backcrossed onto a C57Bl/6N inbred strain background. A lower dose of bacteria was instilled, with an expected delivery of ~ 1.3 x 10^4 cfu. The results are summarised in Table 5.3. In this study, both the total number of bacteria in the lungs and the number of bacteria internalised decreased as a result of the lower dose of bacteria delivered. However, the percentage of the total dose that was internalised increased ~ 10 fold, suggesting that this process may have been saturated when the higher dose was used. Nevertheless, the internalisation of bacteria was similar in all the mice, regardless of genotype.

Strain	Genotype	Total cfu (sample 1)	Internalised cfu (sample 2)	% internalised
C57Bl/6N	non-CF	$1.3 \times 10^5 \pm 0.5 \times 10^4$	$3.3 \times 10^3 \pm 0.0$	2.5
C57Bl/6N	non-CF	$2.4 \times 10^5 \pm 0.8 \times 10^4$	$3.9 \times 10^3 \pm 0.1 \times 10^3$	1.6
C57Bl/6N	*Cftr*^{tm1Hgu}	$1.0 \times 10^5 \pm 0.2 \times 10^4$	$2.0 \times 10^3 \pm 0.2 \times 10^3$	2.0
C57Bl/6N	*Cftr*^{tm1Hgu}	$1.2 \times 10^5 \pm 0.0$	$4.9 \times 10^3 \pm 0.3 \times 10^3$	4.1

TABLE 5.3 Internalisation of *P. aeruginosa* after low dose delivery

A summary of the *in vivo* internalisation of *P. aeruginosa* following the direct intratracheal instillation of ~2.5×10^7 cfu. Colony counts are mean ± SD, from duplicate dilutions.

5.3 Discussion

The studies described above demonstrate the successful adaptation of the gentamicin exclusion assay to assess the internalisation of bacteria by adult mouse lung cells. The results achieved using this assay represent preliminary studies utilising mouse models of CF to establish the relevance of bacterial internalisation in CF lung disease.

Published studies using transformed cell lines and a neonatal mouse model, suggest that CFTR is a cellular receptor for the binding, endocytosis and clearance of *P. aeruginosa* from the normal lung (Pier *et al* 1996, Pier *et al* 1997). In these studies, human and murine epithelial cell lines, over-expressing normal human CFTR, have both been reported to internalise 10–100 times more *P. aeruginosa* than control cells, either expressing ΔF508 CFTR or not expressing CFTR. Nevertheless, even in these control cell lines ~ 10^3 bacteria were reported to be internalised by ~10^5 transformed epithelial cells. Significant inhibition of internalisation has been reported using membranes from the CFTR expressing cell lines or purified human CFTR. However, considerable bacterial internalisation was still observed in these studies.

Inhibition has also been demonstrated in a concentration dependent manner, using either a) a monoclonal antibody specific to the first extracellular domain of CFTR, but not antibodies specific to the fourth extracellular domain or C-terminus, or b) a specific peptide corresponding to the first extracellular domain of CFTR, but not a peptide corresponding to the fourth extracellular domain, or a scrambled first extracellular domain peptide. Interestingly, in some of the inhibition studies, using the monoclonal antibody specific to the first extracellular domain of CFTR, complete inhibition of internalisation was observed. This is in contrast to all the other methods of inhibition reported. In addition to these results, the level of internalisation observed in these cell lines was demonstrated to be 10–100 fold lower for bacteria with an incomplete LPS core. These rough LPS strains of *P. aeruginosa* represent one of the phenotypic changes observed in chronic infection of the CF lung (see Chapter 1, section 1.4.2.4). Taken together, these studies have been reported to indicate that the first predicted extracellular domain of CFTR acts as a specific cellular receptor for the LPS core oligosaccharide of *P. aeruginosa*.

The use of a neonatal mouse model to assess the relevance of these observations *in vivo* was also reported. In this model ~10^8 bacteria were instilled intranasally using 7 day old BALB/c mice. A very variable number of bacteria were isolated from the lungs after 24 hours, with a range of 2×10^4 - 2×10^7 cfu (mean of 1×10^6 cfu) per gram of lung tissue. The level of internalisation reported was equally variable, with a range of 1×10^3 - 1×10^6 cfu (mean of 1×10^5 cfu) per gram of lung tissue after 24 hours. Interestingly, the number of bacteria internalised after 1 hour was reported to be unchanged at 24 hours. Inhibition of internalisation was demonstrated using the synthetic peptide corresponding to the first extracellular domain of human CFTR, but not the control peptides. This antibody inhibited 95% of the internalisation and resulted in a significantly raised bacterial load in the lungs at 24 hours after instillation. These studies suggest that intact mouse

lungs cells ingest *P. aeruginosa* using murine CFTR in a manner analogous to cell lines expressing human CFTR.

On the basis of the published studies, a significant difference in the level of internalisation of *P. aeruginosa* would be predicted between mouse models of CF and non-CF mice. An earlier study demonstrated the susceptibilty of the neonatal mouse model to infection with intranasally instilled *P. aeruginosa* and contrasted this with the considerable resistance of adult mice (Tang *et al* 1995). This increased susceptibility to infection was given as justification for the use of the neonatal mouse model in the studies addressing bacterial internalisation. Given that internalisation is proposed to be a protective mechanism it seems rather perverse to select a model on the basis of increased susceptibility to infection. Thus, for the studies described in this chapter, the assays were adapted and optimised for use in adult mice, in which resistance to lung infection with *P. aeruginosa* is reported to be greater. If internalisation plays a significant role in lung defence one would expect it to be at least as prominent in an adult mouse model. In addition, nasal instillation of bacteria, while quick and easy, was found to provide a more variable delivery, with less extensive deposition in the smaller airways than direct intratracheal instillation. Thus, the latter technique was employed.

The reported studies indicate that the LPS structure of the bacteria has a significant bearing on the level of internalisation (Pier *et al* 1996). A smooth LPS, non-mucoid, CF clinical isolate of *P. aeruginosa* (J1385), known to have undergone mucoid transformation *in vivo* (Nelson *et al* 1990), was used for the studies described in this chapter.

The level of bacterial internalisation anticipated in an adult mouse, on the basis of extrapolation from the published studies, is difficult to ascertain. The internalisation of *P. aeruginosa* by cell lines indicated approximately 1 bacteria internalised for every 10 cells. However, it seems unlikely that a lung defence strategy would involve 10% of cells engulfing bacteria, with subsequent desquamation, in response to bacterial challenge. Corneal

epithelial cells have been shown to internalise *P. aeruginosa* following physical injury, with desquamating cells engulfing many bacteria (Fleiszig *et al* 1995). The hypothesis that one "primed" cell may upregulate the level of bacterial receptors on its apical membrane (see below) and engulf numerous bacteria prior to shedding, represents a more viable model. Hence, the value of assessing the mean number of internalised bacteria per cell is unclear. In addition, the kinetics and saturation of the internalisation process are not evident. The published studies reported *in vivo* internalisation normalised as bacteria per gram of lung tissue. The weight of neonatal mouse lungs was not reported, although 1 gram of lung tissue was indicated to represent 10^6 cells. This would also suggest a level of internalisation of approximately 1 bacteria per 10 cells, although in this case the cellular population is mixed. In addition to these concerns, the studies described in this chapter were performed on adult mice with a different strain background, using an alternative delivery technique and a different strain of *P. aeruginosa*. Thus, extrapolation from the published data may not be valid. Nevertheless, in order to provide a level of comparison between studies, anticipated levels of internalisation can be estimated. In the studies detailed in this chapter the lungs of an adult mouse were found to weigh ~ 200 mg and represented ~ 10^7 cells. The proportion of these cells representing airway epithelial cells is unknown. Previous studies using rats indicate that rat lungs consist of approximately 2×10^8 cells, of which 5×10^7 (25%) are airway epithelial cells (Johnson *et al* 1990, Mercer *et al* 1994). A similar proportion may be expected in murine lungs, suggesting ~ 2.5×10^6 airway epithelial cells. This would lead to an anticipated internalisation of 2.5×10^5 cfu in an adult mouse lung. On the basis of the neonatal mouse studies, using the weight of lung tissue alone, approximately 2×10^4 internalised bacteria might be anticipated in 200 mg adult, wild type mouse lungs, after the delivery of 1×10^8 bacteria. On the basis of the inhibition studies reported, both *in vivo* and *in vitro*, the level of internalisation in mouse models of CF might be expected show a reduction of between 10% and 99%.

Despite the caveats relating to the differences between the studies described in this chapter and those reported in the literature, the level of internalisation observed was remarkably close to that anticipated, with ~ 1 x 10^4 – 1 x 10^5 cfu (mean 8.1 x 10^4 ± 3.8 x 10^4) internalised after the delivery of ~ 2.5 x 10^7 cfu, and 2 hours incubation (see table 5.2). However, no difference was observed between *Cftr*^{tm1Hgu}/*Cftr*^{tm1Hgu} mice and non-CF mice. On the basis of these preliminary results, the sample sizes required to have an 80% power to detect a 10% and 90% decrease in internalisation in mouse models of CF are n = 394 and n = 6 respectively. Although the strain variations and the small number of mice studied prevent firm conclusions being reached, the studies described in this chapter do not support the hypothesised role for CFTR in the process of bacterial internalisation. Several possible explanations for this discrepancy exist. Discrimination between these will require a series of further studies utilising this adapted technique.

The studies performed in adult mice provide supplementary evidence for the internalisation of *P. aeruginosa* by mouse lung cells *in vivo*. However, the conclusion that CFTR is responsible for this process is not supported by these experiments. Indeed, even the published studies demonstrate that significant internalisation will still occur in cell lines that do not express normal CFTR. It is possible that the process of internalisation is not primarily reliant on CFTR, but that overexpression of CFTR in cell lines used may result in interactions that influence the mechanism responsible in some undetermined manner. It is interesting to note that only the monoclonal antibody raised against the first extracellular domain of CFTR was capable of complete inhibition of internalisation (Pier *et al* 1997). This antibody has been previously demonstrated to cross react with another unknown protein (Walker *et al* 1995). This raises the possibility that this other protein may in fact be the relevant receptor for *P. aeruginosa*. Indeed, it was use of synthetic peptides corresponding to this same domain that successfully inhibited internalisation in the neonatal mouse model.

An alternative explanation might be that significant biological differences exist between mice and humans. However, the published results using murine epithelial cell lines transfected with human CFTR and the inhibition of internalisation in the neonatal mouse model bear sufficient similarity to the results using human cell lines to make this an unlikely explanation. A more probable explanation may relate to the specific mouse model of CF used in these studies reported in this chapter. The *Cftr*^{tm1Hgu}/*Cftr*^{tm1Hgu} mice have been shown to express a low level of normal wild type CFTR (Dorin *et al* 1994). Despite this they clearly demonstrate an abnormal phenotype that resembles CF in many respects (see Chapter 1, section 1.7.3 and Chapter 4). Nevertheless, it is possible that this low level of normal CFTR is sufficient to result in a normal level of internalisation of *P. aeruginosa*. It has been suggested that a considerable amount of CFTR may be subapically localised and that CFTR may play a role in the regulation of endocytosis and exocytosis (reviewed in Bradbury 1999). In this manner, CFTR may be capable of upregulating the level of its own expression at the apical membrane (see Chapter 1, section 1.3.6). Indeed, using the monoclonal antibody raised against the first extracellular domain of CFTR, a dramatic increase in the positive staining observed in the bronchial epithelial cells of mice infected with *P. aeruginosa* has been reported (Pier *et al* 1997). Thus, it is conceivable that upon stimulation with *P. aeruginosa*, subapical stores of normal CFTR could be relocated to the apical membrane of epithelial cells in the residual function *Cftr*^{tm1Hgu}/*Cftr*^{tm1Hgu} mice. This could be sufficient to confer a wild type level of internalisation despite a low level of normal CFTR production. Such a mechanism might also be expected to occur in CF individuals with residual function mutations, in whom severe lung disease and colonisation with *P. aeruginosa* are observed (The Cystic Fibrosis Genotype–Phenotype Consortium 1993). However, these CF individuals have residual function due to reduced activity of abnormal CFTR rather than a small amount of normal CFTR, perhaps with different consequences. It is unclear how internalisation of bacteria might be affected

in CF individuals with class 3 or 4 mutations, in which CFTR is correctly localised to the apical membrane but does not operate effectively as a chloride ion channel (see Chapter 1, section 1.3.3). These issues could be addressed by studying of the level of bacterial internalisation in alternative mouse models of CF (see Chapter 1, section 1.7) with less, or no CFTR (*Cftr*^{tm1Hgu}/*Cftr*^{tm1Unc} compound heterozygote mice or *Cftr*^{tm1Unc}/*Cftr*^{tm1Unc} mice) or those carrying the G551D mutation (*Cftr*^{tm1G551D}/*Cftr*^{tmG551D} mice). It is also conceivable that the process of *P. aeruginosa* internalisation by airway epithelial cells observed in human cell lines, is only accurately modelled *in vivo* in neonatal mice and/or mice with a BALB/c strain background. However, these explanations seem unlikely given the increased susceptibility of neonatal mice to infection with *P. aeruginosa* and the similar levels of internalisation observed in three different strains of mice in the preliminary studies described in this chapter.

Thus the degree of internalisation observed in mouse models of CF could be related to the specific mutation of the mouse models used and perhaps even to the age and background strain of the animals. However, subsequent reports examining the internalisation of *P. aeruginosa*, including studies utilising various mouse models of CF, have not included any data to suggest that differences in the level of internalisation can be observed *in vivo*, secondary to CFTR dysfunction (Pier *et al* 1999, Cannon *et al* 1999). Indeed, the focus of these follow-up studies has been significantly different, concentrating on *in vitro* and *in vivo* data suggestive of CFTR dependent apoptosis in airway epithelial cells. These recent reports hypothesise that the airway clearance of *P. aeruginosa* involves internalisation by epithelial cells with consequent apoptosis of those cells. The apparent inability of CF cells to internalise *P. aeruginosa* is proposed to result in the failure of CF cells to undergo apoptosis. The resultant continued presence of *P. aeruginosa* on the epithelial surface would then lead to the continued production of inflammatory mediators and inappropriate inflammatory responses. In addition, it has been suggested that the normal upregulation of apical CFTR

in response to *P. aeruginosa* may be capable of effecting a dramatic local decrease in the NaCl content of the ASL (see Chapter 1, section 1.5.1.2). This could consequently enhance the antibacterial activity of defensins and other components of the innate lung defence system (see Chapter 1, section 1.6). This response would also be impaired in the CF lung. The internalisation hypothesis initially appears to contradict the bacterial adherence hypothesis, in which increased binding of *P. aeruginosa* is observed on CF cells (see Chapter 1, section 1.5.2.1). However, it has been suggested that the initial binding of *P. aeruginosa* to the epithelial cell may not in fact be an interaction with CFTR (Pier *et al* 1997). The bacteria may initially bind to receptors such as aGM_1 before interacting with upregulated, apically localised CFTR precipitating internalisation. In this scenario, more bacteria would bind to CF cells than non-CF cells and those that did bind to non-CF cells would be internalised. In contrast, those binding to CF cells would remain at the cell surface provoking a continued inflammatory response. In this manner the role of internalisation would serve to exaggerate the differences in binding observed in EM studies of CF and non-CF cells (Davies *et al* 1997). While incorporating several of the major hypotheses proposed for the development of CF lung disease, these proposals are highly speculative and the supporting evidence for such arguments remains insubstantial at this stage. In addition, the internalisation hypothesis still fails to address the role of organisms other than *P. aeruginosa* in the development of CF lung disease and the influence of the mucus layer.

Irrespective of concerns about the role of CFTR in the process of internalisation, the adapted gentamicin exclusion assay in adult mice does demonstrate the internalisation of *P. aeruginosa* by mouse lung cells, *in vivo*. However, such studies do not reveal which cell type has internalised the bacteria. The implication in the published studies is that the similarity in inhibition of internalisation observed *in vivo* and in epithelial cell cultures suggests that epithelial cells are responsible for this process. However, phagocytosis of bacteria instilled into the murine lung would be expected

both by alveolar macrophages and by neutrophils. Studies to visualise the cellular location of *P. aeruginosa* are required, using immunohistochemical techniques or bacteria expressing green fluorescent protein. In addition, primary cultures of murine airway epithelial cells could be used to assess internalisation by a purely epithelial murine cell culture (see Chapter 7). These cultures could be established from different mouse models of CF and non-CF controls and unlike cell lines would not have been affected by immortalisation, or overexpression of human CFTR.

In addition to concerns about the cellular compartment responsible for the internalisation of *P. aeruginosa*, the biological consequences of internalisation also require careful consideration. To date there is no evidence that internalisation of *P. aeruginosa* by lung epithelial cells has a protective role. Such a mechanism has been described in protecting the bladder against infection (Orikasa and Hinman 1977, Aronson *et al* 1988). However, a previous study using the neonatal model of lung infection, reported that internalisation was seen mainly in those animals that developed more severe pneumonia (Tang *et al* 1995). Indeed, internalisation was postulated as a route to more widespread infection in the lung. Furthermore, CFTR dependent invasion of intestinal epithelial cells has been proposed as a virulence factor for *Salmonella typhi* (Pier *et al* 1998). On this basis, decreased susceptibility of CF heterozygotes to typhoid fever has been suggested as an explanation for the prevalence of CF carrier status in caucasian populations. Thus, the role of any airway epithelial cell internalisation of *P. aeruginosa* must be considered uncertain.

In conclusion, the internalisation of *P. aeruginosa* as a component of the pulmonary defence system remains a speculative and contentious hypothesis. As a result of local practical considerations only preliminary studies are described in this thesis. These studies, using an adapted gentamicin exclusion assay in adult $Cftr^{tm1Hgu}/Cftr^{tm1Hgu}$ mice and non-CF controls, do not support a role for CFTR in the process of bacterial internalisation. However, further studies are required to consolidate these

observations using increased numbers of mice, other mouse models of CF and techniques to visualise the cellular compartment responsible for the bacterial internalisation observed *in vivo*. This chapter clearly illustrates the potential value of mouse models of CF in evaluating the *in vivo* significance of hypotheses borne from studies performed exclusively in transformed cell lines.

Chapter 6

β- Defensins

Chapter 6: β- Defensins

6.1 Introduction

The discovery that the airway surface liquid, which lines the epithelial surfaces of the lung, demonstrated salt-sensitive antimicrobial activity, stimulated considerable interest in the role of the antimicrobial constituents of the ASL in the pathogenesis of CF lung disease.

The ASL produced by primary cultures of human airway epithelia, at an air/liquid interface, has been shown to have broad spectrum antibacterial activity, impaired by the addition of NaCl (Smith *et al* 1996). In contrast, the ASL from primary cultures of airway epithelia from CF individuals had impaired antibacterial activity. This activity was restored by decreasing the ionic concentration, suggesting that the antibacterial agents were present but dysfunctional in the environment of CF ASL. Subsequent studies demonstrated that the absorption of NaCl by cultured CF airway epithelia was impaired, with consequent failure to produce the hypotonic ASL environment required for effective antimicrobial activity (Zabner *et al* 1998). Although other studies provide conflicting evidence (see Chapter 1, section 1.5.1.1), this established an elegant and simple hypothesis to explain the increased susceptibility of CF individuals to lung infection.

The ASL contains an array of antimicrobial compounds, including lysozyme, lactoferrin, SLPI and defensins (see Chapter 1, section 1.6). Studies utilising a xenograft model of human airway epithelium assessed the role of human β-defensin-1 in the ASL (Goldman *et al* 1997). Ablation of *HBD-1* expression, using antisense DNA specific to the 5′ region of *HBD-1*, was shown to largely abolish the antimicrobial activity of the ASL. In addition, synthetic hBD-1 peptide was demonstrated to have salt sensitive bactericidal properties against *P. aeruginosa*. These results suggest that HBD-

1 may play a pivotal role in the salt sensitive antimicrobial activity of the ASL.

Defb1, a murine homologue of *HBD-1*, was isolated on mouse chromosome 8 (Huttner *et al* 1997, Bals *et al* 1998a, Morrison *et al* 1998). *Defb1* encodes a 69 aa prepropeptide, with 51% identity to HBD-1 at the amino acid level. It has been shown to be constitutively expressed, with the highest levels found in the kidney and trachea, but also expressed in the lung, liver, heart, reproductive tract and alveolar macrophages (see Chapter 1, Table 1.7). To assess the antibacterial profiles, salt-sensitivity and degree of functional homology between these human and mouse defensins, synthetic peptides were designed, purchased and analysed.

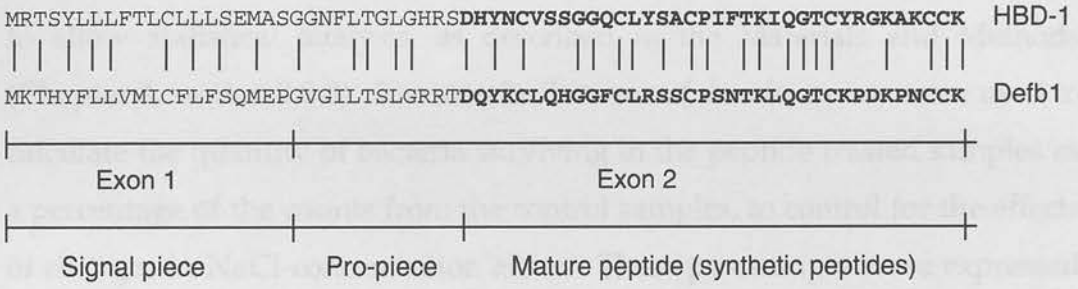

FIGURE 6.1 Comparison of HBD-1 and Defb1 peptide sequences

Vertical lines show a direct match. The peptide sequences used to produce the synthetic peptides are highlighted in bold.

6.2 The antibacterial activity of synthetic β-defensin peptides

To assess the antibacterial profiles of HBD-1 and Defb1, synthetic peptides were purchased from Albachem Ltd. These peptides were synthesised corresponding to the amino acid sequence of the proposed

mature peptide of HBD-1 and Defb1 (see Figure 6.1). The success of synthesis was analysed by Albachem Ltd., using HPLC; resulting in a single peak in both cases, and mass spectroscopy; confirming the correct molecular weight for the peptides synthesised.

The lyophilised peptides were resuspended in phosphate buffer and incubated for 30 minutes, at 37°C, with bacterial suspensions (containing ~ 5 x 10^4 cfu) in varying concentrations of NaCl, as described in the Materials and Methods (see Chapter 2, section 2.9.2). Duplicate reactions were performed, and each was plated in duplicate on the appropriate agar. The resultant cfu counts were compared to those for parallel control samples. The controls were performed without the addition of peptide to assess any contribution of the varying NaCl concentrations to the outcome. A square root transformation was applied to homogenise the variance between groups to allow statistical analysis, as described in the Materials and Methods (Chapter 2, section 2.9.3). The standard means of the cfu counts were used to calculate the quantity of bacteria surviving in the peptide treated samples as a percentage of the counts from the control samples, to control for the effects of changes in NaCl concentration alone. These percentages were expressed as "percentage killing" and the standard errors calculated. Fresh overnight cultures of clinical isolates of bacteria were supplied by Professor John Govan, prepared by Wendy Hannant, Department of Medical Microbiology, University of Edinburgh (see Chapter 2, section 2.3).

6.2.1 Synthetic hBD-1

The concentration of HBD-1 in the ASL *in vivo* is unknown, although subsequent estimates have been made (see Chapter 1, Table 1.8). The previous study assessing the anti-pseudomonal activity (Goldman *et al* 1997) of synthetic hBD-1, reported similar bacterial killing, in the presence of low

NaCl concentrations, with synthetic hBD-1 concentrations ranging from 0.06 to 0.5 mg/ml. Hence to conserve peptide stocks, a concentration of 0.05 mg/ml of synthetic hBD-1 was used.

The antibacterial activity of synthetic hBD-1 was assessed against *P. aeruginosa* (CF clinical isolate J1385 and laboratory strain PAO1), *S. aureus* (CF clinical isolate C1705), *E. coli* (clinical isolate J2408) and *B. cepacia* (CF clinical isolate, epidemic strain J2315). Studies were tested for repeatability, to reproduce the salt-sensitive antibacterial profile in a minimum of two separate studies, and representative experiments are illustrated in Figures 6.2 and 6.3.

Synthetic hBD-1 peptide, at 0.05 mg/ml, displayed significant antibacterial activity against *P. aeruginosa* CF clinical isolate J1385 in comparison to the control samples ($p < 0.001$) at all NaCl concentrations tested, over the range of 0 to 150 mM NaCl (see Figure 6.2a). A significantly greater number of bacteria survived despite the presence of synthetic hBD-1 peptide when the NaCl concentration was increased from 0mM to 30 mM, from 30 mM to 60 mM and from 60 mM to 90 mM ($p < 0.001$ in each case). However, the concentration of salt alone was observed to have an effect on bacterial viability in the control samples, in the absence of synthetic hBD-1 peptide. This deleterious effect was greatest at the highest (150 mM NaCl) and lowest (0 mM) concentrations of NaCl studied (see Figure 6.2a). To compensate for this effect, the number of bacteria surviving in the presence of synthetic hBD-1 peptide was expressed as a percentage of the number of bacteria present in the control sample at the relevant NaCl concentration. The inverse of this proportion is referred to as the percentage kill and illustrated in Figure 6.2b. This analysis demonstrates 100% killing of *P. aeruginosa* isolate J1385 at 0 mM NaCl, dropping to and stabilising at ~ 50% killing at 90-150 mM NaCl. At the extremes of NaCl concentration (0 and 150 mM) the bacterial viability in the control samples was equally impaired. These NaCl concentrations also represent the conditions under which the

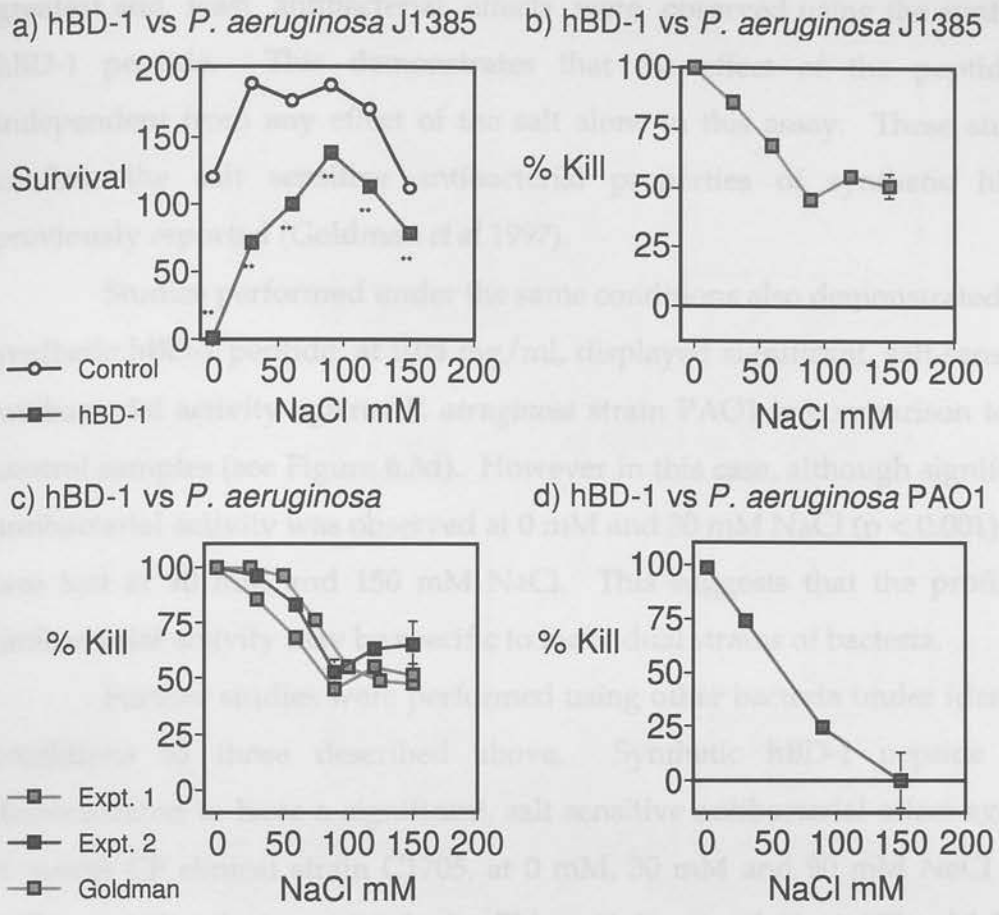

FIGURE 6.2 The antibacterial effect of synthetic hBD-1 against *P. aeruginosa*

Bacteria were incubated with synthetic hBD-1 peptide at 0.05 mg/ml, over a range of salt concentrations. Graphs a), b) and c) show hBD-1 versus *P. aeruginosa* CF clinical isolate J1385, graph d) shows hBD-1 versus *P. aeruginosa* strain PAO1. Graph a) demonstrates survival using the mean cfu count after square root transformation ± SE, for blank control samples and peptide samples, ** $p < 0.001$, * $p < 0.01$. Graphs b), c) and d) show the mean percentage kill ± SE, assessed by calculating the number of bacteria surviving in the peptide treated samples as a percentage of the counts from the buffer only control samples, to correct for the effect of NaCl alone. Graph c) shows duplicate experiments using *P. aeruginosa* CF clinical isolate J1385 and makes comparison with data published by Goldman *et al* 1997, using an alternative *P. aeruginosa* clinical isolate.

greatest and least antibacterial effects were observed using the synthetic hBD-1 peptide. This demonstrates that the effect of the peptide is independent from any effect of the salt alone in this assay. These studies confirm the salt sensitive antibacterial properties of synthetic hBD-1 previously reported (Goldman *et al* 1997).

Studies performed under the same conditions also demonstrated that synthetic hBD-1 peptide, at 0.05 mg/ml, displayed significant, salt-sensitive antibacterial activity against *P. aeruginosa* strain PAO1 in comparison to the control samples (see Figure 6.3d). However in this case, although significant antibacterial activity was observed at 0 mM and 30 mM NaCl ($p < 0.001$), this was lost at 90 mM and 150 mM NaCl. This suggests that the profile of antibacterial activity may be specific to individual strains of bacteria.

Further studies were performed using other bacteria under identical conditions to those described above. Synthetic hBD-1 peptide was demonstrated to have a significant, salt sensitive antibacterial effect against *S. aureus* CF clinical strain C1705, at 0 mM, 30 mM and 90 mM NaCl ($p < 0.001$ at each salt concentration). This activity was lost at 150 mM NaCl (Figure 6.3a and b). Synthetic hBD-1 peptide was also demonstrated to have a significant, salt sensitive antibacterial effect against *E. coli* clinical strain J2408, at 0 mM and 30 mM NaCl ($p < 0.001$ in each case). This activity was not evident in the presence of 90 mM or 150 mM NaCl (Figure 6.3c and d).

The antibacterial effect of synthetic hBD-1 was observed to be greatest against *P. aeruginosa*, with 100% killing at 0 mM NaCl and less effective against *S. aureus* and *E.coli*, with ~ 75% and ~ 50% killing respectively under optimal conditions in these studies.

In contrast to the other bacteria studied, synthetic hBD-1 peptide, at 0.05 mg/ml, was not observed to have any significant antibacterial effect on *B. cepacia* CF clinical isolate J2315 (Figure 6.3e and f). Indeed the opposite effect was observed, with a significantly greater number of bacteria present after incubation with synthetic hBD-1 peptide at 0 mM NaCl than in the

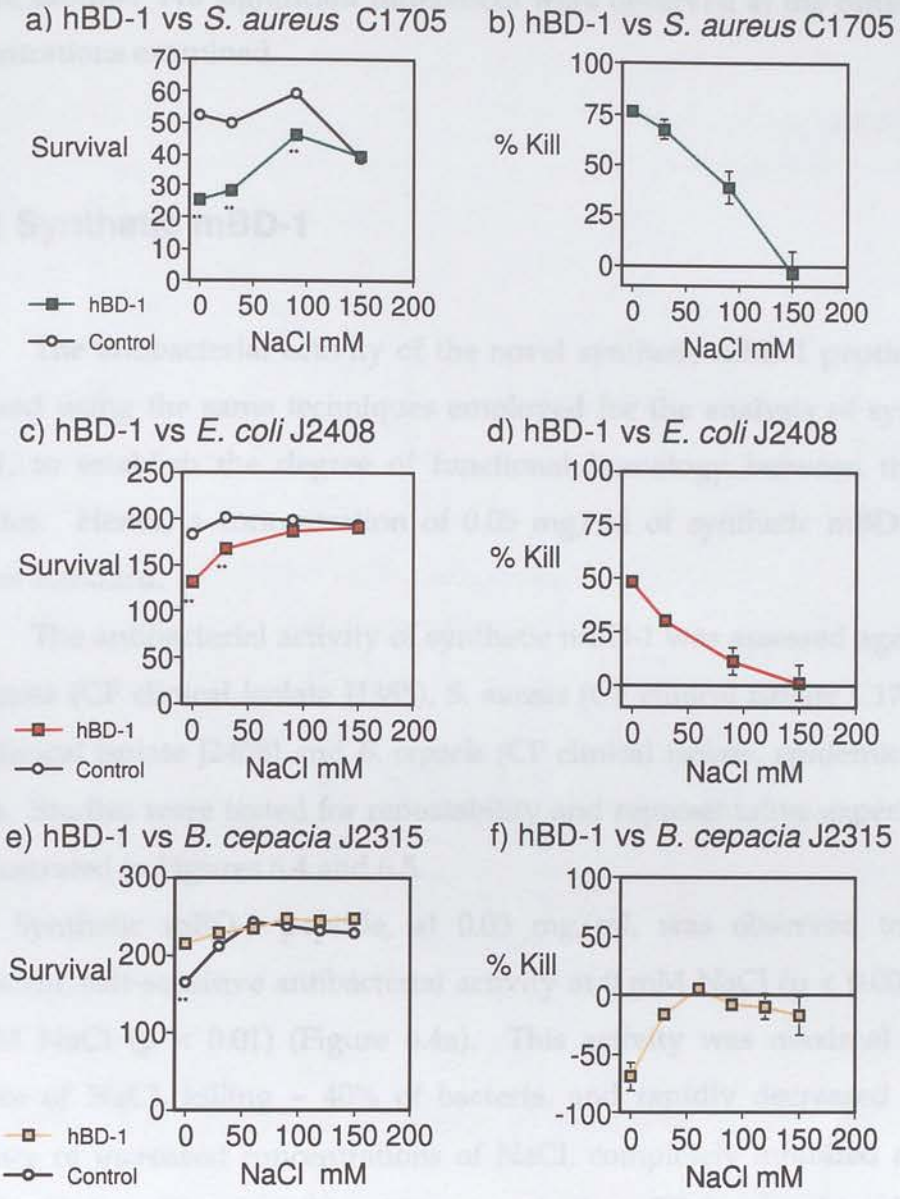

FIGURE 6.3 The antibacterial effect of synthetic hBD-1

Bacteria were incubated with synthetic hBD-1 peptide at 0.05 mg/ml, over a range of salt concentrations. A selection of bacteria were used; a) and b) *S. aureus* CF clinical isolate C1705, c) and d) *E. coli* clinical isolate J2408, e) and f) *B. cepacia* CF clinical isolate J2315. Graphs a), c) and e) demonstrate survival using the mean cfu count after square root transformation ± SE, for blank control samples and peptide samples, ** $p < 0.001$, * $p < 0.01$. Graphs b), d) and f) show the mean percentage kill ± SE, assessed by calculating the number of bacteria surviving in the peptide treated samples as a percentage of the counts from the buffer only control samples, to correct for the effect of NaCl alone.

control sample. No significant differences were observed at the other NaCl concentrations examined.

6.2.2 Synthetic mBD-1

The antibacterial activity of the novel synthetic mBD-1 peptide was analysed using the same techniques employed for the analysis of synthetic hBD-1, to establish the degree of functional homology between the two peptides. Hence, a concentration of 0.05 mg/ml of synthetic mBD-1 was used as standard.

The antibacterial activity of synthetic mBD-1 was assessed against *P. aeruginosa* (CF clinical isolate J1385), *S. aureus* (CF clinical isolate C1705), *E. coli* (clinical isolate J2408) and *B. cepacia* (CF clinical isolate, epidemic strain J2315). Studies were tested for repeatability and representative experiments are illustrated in Figures 6.4 and 6.5.

Synthetic mBD-1 peptide, at 0.05 mg/ml, was observed to have significant, salt-sensitive antibacterial activity at 0 mM NaCl ($p < 0.001$) and 30 mM NaCl ($p < 0.01$) (Figure 6.4a). This activity was maximal in the absence of NaCl, killing ~ 40% of bacteria, and rapidly decreased in the presence of increased concentrations of NaCl, completely inhibited at ≥ 90 mM NaCl (see Figure 6.4b). Thus, synthetic mBD-1 peptide exhibited considerably less antibacterial activity against *P. aeruginosa* CF clinical isolate J1385 than synthetic hBD-1 peptide, at the same concentration. An increase in the concentration of synthetic mBD-1 peptide used in otherwise identical studies resulted in a corresponding increase in the proportion of bacteria killed at each salt concentration tested (see Figure 6.4c). At a concentration of 0.5 mg/ml, synthetic mBD-1 killed ~ 80% of bacteria in the absence of NaCl. This decreased to ~ 30% in the presence of ≥ 120 mM NaCl. Thus, the profile of antibacterial activity of synthetic mBD-1 at 0.5 mg/ml was observed to be

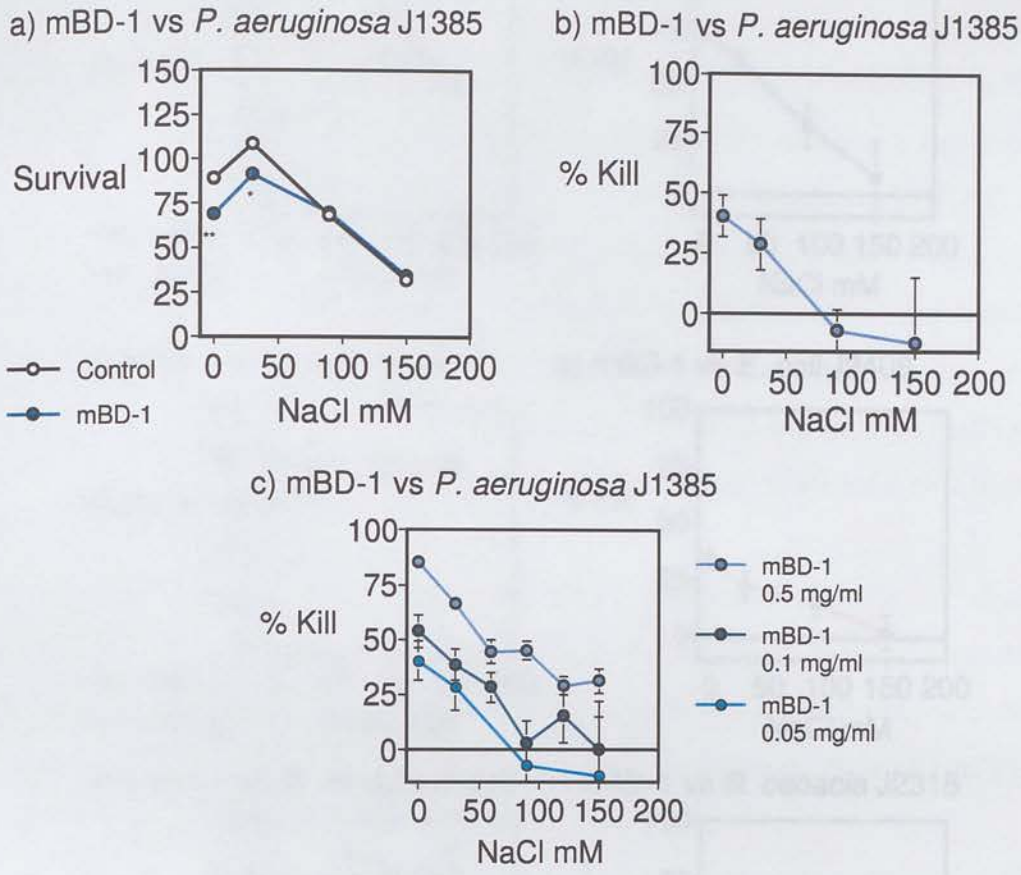

FIGURE 6.4 The antibacterial effect of synthetic mBD-1 against *P. aeruginosa*

Synthetic mBD-1 peptide was incubated with *P. aeruginosa* CF clinical isolate J1385 over a range of salt concentrations. The concentration of synthetic mBD-1 used was a) and b) 0.05 mg/ml, or c) 0.5 mg/ml, 0.1 mg/ml or 0.05 mg/ml. Graph a) demonstrates survival using the mean cfu count after square root transformation ± SE, for blank control samples and peptide samples, ** $p < 0.001$, * $p < 0.01$. Graphs b) and c) show the mean percentage kill ± SE, assessed by calculating the number of bacteria surviving in the peptide treated samples as a percentage of the counts from the buffer only control samples, to correct for the effect of NaCl alone.

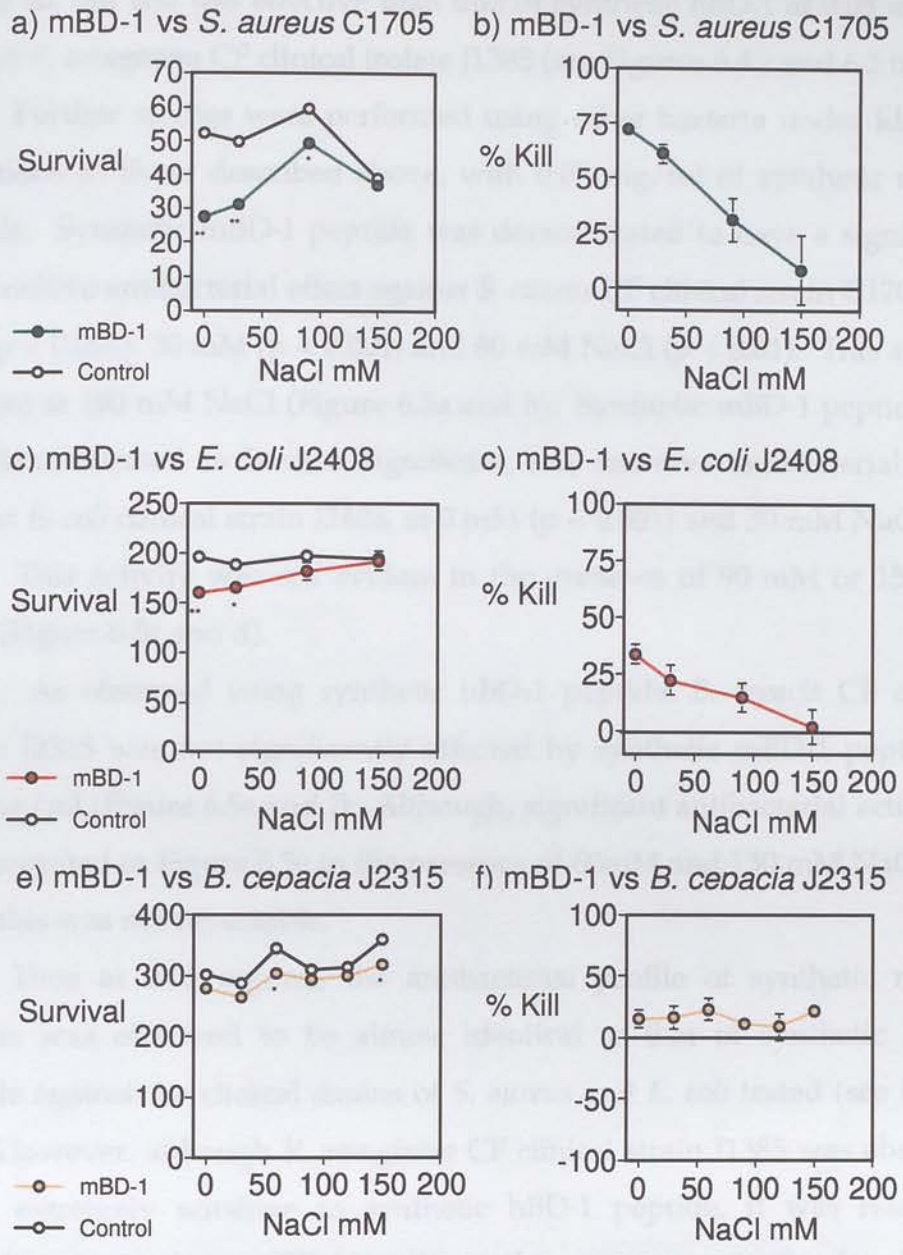

FIGURE 6.5 The antibacterial effect of synthetic mBD-1

Bacteria were incubated with synthetic mBD-1 peptide at 0.05 mg/ml, over a range of salt concentrations. A selection of bacteria were used; a) and b) *S. aureus* CF clinical isolate C1705, c) and d) *E. coli* clinical isolate J2408, e) and f) *B. cepacia* CF clinical isolate J2315. Graphs a), c) and e) demonstrate survival using the mean cfu count after square root transformation ± SE, for blank control samples and peptide samples, ** $p < 0.001$, * $p < 0.01$. Graphs b), d) and f) show the mean percentage kill ± SE, assessed by calculating the number of bacteria surviving in the peptide treated samples as a percentage of the counts from the buffer only control samples, to correct for the effect of NaCl alone.

similar to, but still less effective than that of synthetic hBD-1 at 0.05 mg/ml, against *P. aeruginosa* CF clinical isolate J1385 (see Figures 6.4 c and 6.2 b).

Further studies were performed using other bacteria under identical conditions to those described above, with 0.05 mg/ml of synthetic mBD-1 peptide. Synthetic mBD-1 peptide was demonstrated to have a significant, salt sensitive antibacterial effect against *S. aureus* CF clinical strain C1705, at 0 mM ($p < 0.001$), 30 mM ($p < 0.001$) and 90 mM NaCl ($p < 0.01$). This activity was lost at 150 mM NaCl (Figure 6.5a and b). Synthetic mBD-1 peptide was also demonstrated to have a significant, salt sensitive antibacterial effect against *E. coli* clinical strain J2408, at 0 mM ($p < 0.001$) and 30 mM NaCl ($p < 0.01$). This activity was not evident in the presence of 90 mM or 150 mM NaCl (Figure 6.5c and d).

As observed using synthetic hBD-1 peptide, *B. cepacia* CF clinical isolate J2315 was not significantly affected by synthetic mBD-1 peptide at 0.05 mg/ml (Figure 6.5e and f). Although, significant antibacterial activity is demonstrated in Figure 6.5e in the presence of 60mM and 150 mM NaCl ($p < 0.01$), this was not repeatable.

Thus at 0.05 mg/ml, the antibacterial profile of synthetic mBD-1 peptide was observed to be almost identical to that of synthetic hBD-1 peptide against the clinical strains of *S. aureus* and *E. coli* tested (see Figure 6.6). However, although *P. aeruginosa* CF clinical strain J1385 was observed to be extremely sensitive to synthetic hBD-1 peptide, it was relatively insensitive to synthetic mBD-1 peptide at the same concentration (see Figure 6.6). Synthetic hBD-1 peptide demonstrated much greater antibacterial activity against *P. aeruginosa* than any other bacteria tested. In contrast, at 0.05 mg/ml, synthetic mBD-1 peptide demonstrated greatest antibacterial activity against *S. aureus* CF clinical strain C1705. No repeatable, significant antibacterial activity was observed against *B. cepacia* CF clinical isolate J2315 using either peptide at 0.05 mg/ml.

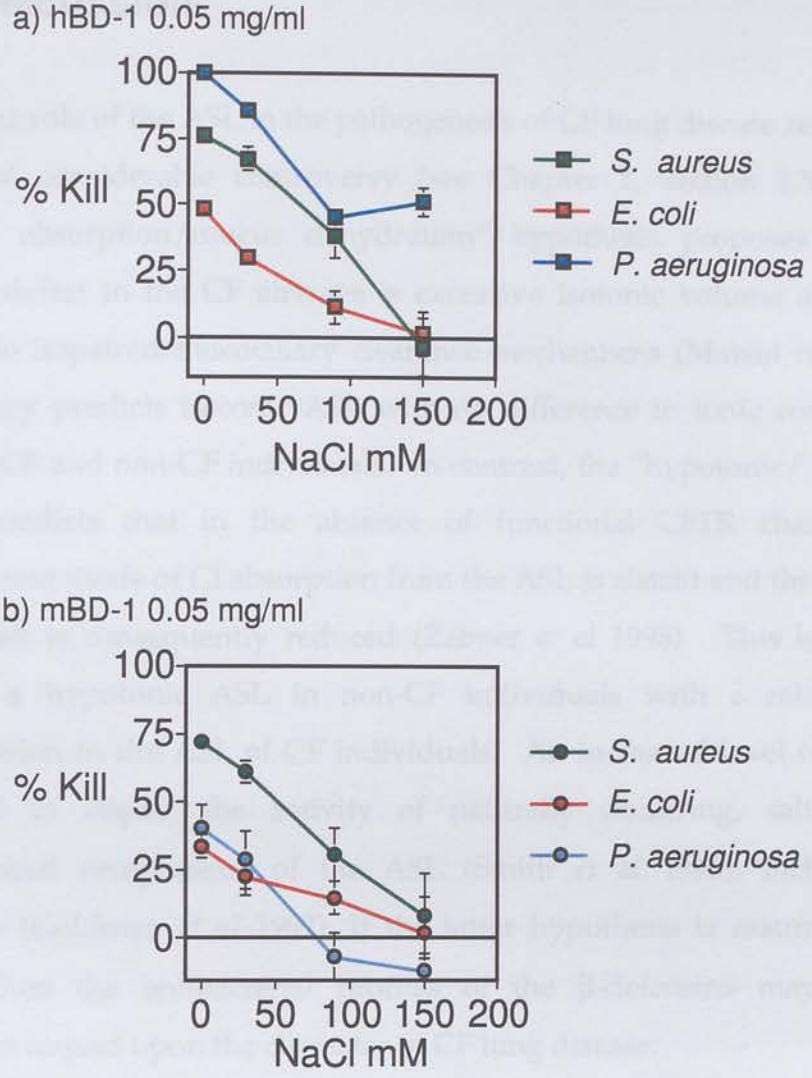

FIGURE 6.6 The antibacterial effect of synthetic hBD-1 and mBD-1

Bacteria were incubated with a) synthetic hBD-1 peptide, or b) synthetic mBD-1 peptide, at 0.05 mg/ml, over a range of salt concentrations. A selection of bacteria were used; *S. aureus* CF clinical isolate C1705, *E. coli* clinical isolate J2408 and *P. aeruginosa* CF clinical isolate J1385. Graphs show the mean percentage kill ± SE, assessed by calculating the number of bacteria surviving in the peptide treated samples as a percentage of the counts from the buffer only control samples, to correct for the effect of NaCl alone.

6.3 Discussion

The role of the ASL in the pathogenesis of CF lung disease remains the subject of considerable controversy (see Chapter 1, section 1.5.1). The "isotonic absorption/mucus dehydration" hypothesis proposes that the primary defect in the CF airways is excessive isotonic volume absorption leading to impaired mucociliary clearance mechanisms (Matsui *et al* 1998). This theory predicts isotonic ASL with no difference in ionic composition between CF and non-CF individuals. In contrast, the "hypotonic/ defensin" theory predicts that in the absence of functional CFTR channels the predominant mode of Cl absorption from the ASL is absent and the ability to absorb salt is consequently reduced (Zabner *et al* 1998). This hypothesis predicts a hypotonic ASL in non-CF individuals with a raised NaCl concentration in the ASL of CF individuals. An increased level of NaCl is proposed to impair the activity of naturally occurring, salt-sensitive antimicrobial components of the ASL (Smith *et al* 1996), including β-defensins (Goldman *et al* 1997). If the latter hypothesis is assumed to be correct then the antibacterial profiles of the β-defensins may have a significant impact upon the character of CF lung disease.

The studies described in this chapter, using synthetic β-defensin peptides, confirm the salt sensitive antibacterial properties of HBD-1 peptide *in vitro*. The previously reported study, which examined the antibacterial activity of synthetic hBD-1 peptide, did not control for the effect of salt alone on bacterial viability, nor was antibacterial activity demonstrated for organisms other than a *P. aeruginosa* clinical isolate (activity against *E. coli* was reported, but these data were not shown) (Goldman *et al* 1997). Nevertheless, illustrating the results from that study in the manner of the percentage killing graphs used in this chapter, it is clear that the synthetic hBD-1 peptides used in both studies have comparable anti-pseudomonal activity (see Figure 6.2c). The salt-sensitive antibacterial nature of HBD-1

has been further confirmed using purified recombinant HBD-1 peptides made using an insect cell/baculovirus system (Singh *et al* 1998). This study demonstrated that the antibacterial effect of HBD-1 is concentration dependent and that inhibition by increased levels of NaCl could be offset by greater concentrations of peptide. In this study, salt-sensitivity was assessed using a strain of *E. coli* containing a gene encoding a luminescence protein. Interestingly, the antibacterial activity of HBD-1 peptides reported using this luminescence assay was much greater than that observed in the studies described in this chapter, with 100% of a 10^7 cfu/ml suspension killed by 1.2 μg/ml of HBD-1 peptide in the absence of NaCl. This greater antibacterial activity against *E. coli* may relate to the assay, the bacterial strain or the method of peptide production employed.

The studies described in this chapter, using synthetic hBD-1 peptide, demonstrate much greater antibacterial activity against *P. aeruginosa* than any other bacteria tested, with 100% killing in the absence of NaCl, decreasing to ~50% (for CF clinical isolate J1385) in the presence of 90 mM NaCl. Nevertheless, significant antibacterial activity was observed against *S. aureus* CF clinical isolate C1705 and, to a lesser extent, against *E. coli* clinical isolate J2408, with ~ 75% and ~ 50% killing respectively in the absence of NaCl, but no significant effect in the presence of 90 mM NaCl. No significant antibacterial activity was observed against *B. cepacia* CF clinical strain J2315, at any concentration of NaCl. Surprisingly, in the absence of NaCl, *B. cepacia* appeared to thrive in the presence of synthetic hBD-1 peptide. It is interesting to note that a previous study has shown that this organism can actually use penicillin G as its sole source of carbon and energy (Beckman and Lessie 1979).

At a concentration of 0.05 mg/ml, synthetic mBD-1 and hBD-1 peptides were demonstrated to have very similar antibacterial profiles against *S. aureus* CF clinical isolate C1705 and *E. coli* clinical isolate J2408. However, the antibacterial activity of synthetic mBD-1 peptide against *P. aeruginosa* CF clinical strain J1385 was found to be considerably reduced in

comparison to synthetic hBD-1 peptide. This antibacterial activity was observed to be concentration dependent, consistent with previous reports using human peptides (Singh *et al* 1998). Synthetic mBD-1 peptide at 0.5 mg/ml was observed to be similar to, but still less effective than synthetic hBD-1 at 0.05 mg/ml, with the murine peptide exhibiting a comparative reduction in antibacterial activity in excess of 10 fold against this organism. A further study, using the lysates of transfected human adrenal adenocarcinoma cells expressing mBD-1, demonstrated that mBD-1 had more effective antibacterial activity against a CF clinical isolate of *S. aureus* and a strain of *E. coli*, than against a clinical isolate of *P. aeruginosa* (Bals *et al* 1998a). In this study, 100% killing of both *S. aureus* and *E. coli* was observed. However, the concentration of peptides was not quantified, nor was the presence of other factors in the lysate that may have been capable of antibacterial activity, or displaying a synergistic effect with mBD-1. Nevertheless, both these studies suggest that in contrast to HBD-1, mBD-1 displays less effective antimicrobial activity against *P. aeruginosa* than against other organisms. Synthetic mBD-1 peptide had no repeatable significant antibacterial activity against *B. cepacia*.

The "hypotonic/ defensin" theory proposes that raised levels of NaCl in the ASL result in the dysfunction of β-defensins and other salt-sensitive antimicrobial agents. The consequences of this impairment would probably be manifest as increased susceptibility to infection with the organisms against which the impaired peptide was most active. Thus, differences in the antibacterial profiles of the affected components of the ASL might influence the pulmonary phenotype observed.

Humans are normally resistant to lung infection with *P. aeruginosa*, however CF individuals are exquisitely susceptible to this organism. The results discussed above demonstrate that HBD-1 has potent anti-pseudomonal activity, *in vitro*. These results also demonstrate that HBD-1 is more active against this organism than against the other human pathogens studied. Thus, HBD-1 dysfunction in a high salt environment may result in

the affected individual being particularly susceptible to infection with *P. aeruginosa*.

In contrast, mouse models of CF are clearly not acutely susceptible to lung infection with *P. aeruginosa*. Neither studies using *Cftr*^{tm1Hgu}/*Cftr*^{tm1Hgu} mice (Larbig *et al* 1998), nor those using *Cftr*^{tm1Kth} /*Cftr*^{tm1Kth} mice, with the ΔF508 mutation (McCray *et al* 1999), have been able to see any difference between CF mutants and wild-type littermates in response to repeated nebulisation with *P. aeruginosa*. Although *Cftr*^{tm1Unc}/ *Cftr* ^{tm1Unc} mice have been reported to demonstrate significantly poorer survival rates in response to bronchopulmonary instillation of *P. aeruginosa* laden agar beads (van Heeckeren *et al* 1997, Gosselin *et al* 1998), in comparison to wild type mice, severe bronchopneumonia and evidence of bacterial proliferation existed regardless of genotype and the cause of death was not definitively attributed to pulmonary disease (see Chapter 4, section 4.7). Thus, in contrast to their human counterparts, mouse models of CF display robust resistance to airway infection with *P. aeruginosa*. However, the *in vitro* results discussed above suggest that mBD-1 does not play a significant part in this process, having little anti-pseudomonal activity in isolation. Thus, salt-induced dysfunction of mBD-1 may have little effect upon the susceptibility of mouse models of CF to *P. aeruginosa*. Alternative antimicrobial agents and/or cellular mechanisms may mediate the resistance to *P. aeruginosa* infection in the mouse lung. It is quite possible that these mechanisms are not significantly compromised by a high salt environment. In contrast to *P. aeruginosa*, mBD-1 does show marked salt-sensitive antibacterial activity against *S. aureus, in vitro*. Dysfunction of mBD-1 in a high salt environment might therefore be expected to have a more profound effect upon the susceptibility of the murine lung to infection with *S. aureus* than with *P. aeruginosa*. This may contribute to the impaired airway clearance of *S. aureus* in the *Cftr*^{tm1Hgu}/*Cftr*^{tm1Hgu} mice (Davidson et al 1995) and the development of more

severe pulmonary pathology in response to repeated nebulisation with this organism, which has been observed (see Chapter 4).

Thus, the existence of species specific differences in the antibacterial profiles of these homologous peptides may have the potential to influence the profile of bacterial susceptibility secondary to a raised NaCl concentration in the ASL. Therefore, it is possible that while the basic mechanisms underlying increased susceptibility to lung infection in CF may be conserved between mice and humans, this may not be the case for the specific profile of bacterial susceptibility.

This represents an attractive hypothesis. However, a number of critical factors must be considered in the interpretation of the results from the synthetic defensin peptide studies. These include the use of synthetic peptides, resistance of *B. cepacia*, the role of other antimicrobial agents *in vivo*, the relevant *in vivo* concentration of β-defensins and the NaCl concentration of the ASL in human and murine airways *in vivo*.

The synthetic hBD-1 peptide used for the studies described in this chapter demonstrates a profile of activity against *P. aeruginosa* identical to that previously reported for similar synthetic peptides (Goldman *et al* 1997). In addition, both human and murine synthetic β-defensin peptides displayed antibacterial profiles broadly consistent with other published studies (Bals *et al* 1998a, Singh *et al* 1998). However, purified HBD-1 produced using an insect cell/baculovirus system may have greater antimicrobial activity, at lower concentrations, than the synthetic hBD-1 used in the studies reported in this chapter (Singh *et al* 1998). This could be due to the cellular processing of the pre-propeptide to the final mature peptide. Indeed, several forms may be synthesised *in vivo*, with varying degrees of antimicrobial activity and salt sensitivity (Valore *et al* 1998). Furthermore, a recent study has described the synthesis of a novel theta defensin by the head-to-tail ligation of two truncated α-defensins in rhesus macaque leukocytes (Tang *et al* 1999). These studies highlight the potential importance of cellular processing mechanisms.

In contrast, the synthetic peptides are chemically synthesised and represent only the putative mature form of the β-defensin peptide.

The impairment of the antibacterial activity of β-defensins in a raised NaCl ASL, secondary to CFTR dysfunction, has been proposed as an explanation for the increased susceptibility of CF individuals to lung infection. However, one of the bacteria characteristic of CF lung disease is *B. cepacia* (see Chapter 1, section 1.4.2.5). The clinical isolate of *B. cepacia* used in the studies described in this chapter, demonstrated resistance to both synthetic hBD-1 and synthetic mBD-1. This is consistent with previous reports (Hancock 1997) and indicates that this hypothesis can only be, at best, a partial explanation. The susceptibility of CF individuals to *B. cepacia* must be mediated by other, as yet undetermined, consequences of CFTR dysfunction.

In the studies described in this chapter, the synthetic β-defensin peptides were studied in isolation. This is in contrast to the *in vivo* situation, where β-defensins are part of a complex mixture of antimicrobial agents present in the ASL (see Chapter 1, section 1.6). It seems probable that the antimicrobial components of the ASL interact and indeed a synergistic interaction has been demonstrated *in vitro* between β-defensins and both lysozyme and lactoferrin, at non-bacteriostatic concentrations (Bals *et al* 1998b). Furthermore, this chapter describes the analysis of synthetic hBD-1 and mBD-1, but additional β-defensins, also expressed in the airways, have since been isolated (HBD2 in humans (Harder *et al* 1997), Defb2 (Morrison *et al* 1999), mBD-3 (Bals *et al* 1999) and mBD-4 (Jia *et al* 1999) in the mouse). These additions to the β-defensin gene families are inducible by proinflammatory stimuli (Harder *et al* 1997, Bals *et al* 1998b, Liu *et al* 1998 Singh *et al* 1998, Morrison *et al* 1999, Bals *et al* 1999, Jia *et al* 1999). Purified hBD-2, made using an insect cell/baculovirus system, has been demonstrated to exhibit salt-sensitive antibacterial activity against *P. aeruginosa* strain PAO1 and a strain of *E. coli* containing a luminescence

plasmid, with the activity exceeding that of HBD-1 peptide by approximately 10 fold (Singh *et al* 1998). Purified mBD-3, made using an insect cell/baculovirus system has been reported to display antibacterial activity against strains of *P. aeruginosa* and *E. coli*, although salt-sensitivity has not been demonstrated (Bals *et al* 1999). The degree of functional overlap and redundancy between the defensins is unclear although their roles may be somewhat different. *HBD-1* is constitutively expressed and its product may form part of the primary line of lung defence, whereas the inducible β-defensins may be more important once constitutive defences have been breached and inflammatory signals are generated.

In addition to the impact of synergistic interactions with other components of the ASL and role of other β-defensins, the activity of defensins as signalling molecules should not be ignored. A recent report suggested that β-defensins in submicromolar concentrations were chemotactic for T cells and dendritic cells (Yang *et al* 1999). It is unclear whether a raised NaCl concentration may also impact upon this function. Thus, although the studies of synthetic hBD-1 and mBD-1 peptides *in vitro*, in isolation, provide interesting insights, appropriate mammalian cellular expression systems, air-interface primary culture model systems and mouse models with targeted deletions of specific β-defensins are required to confirm the results.

The reported studies of β-defensin activity all suffer from a lack of accurate quantitation of the levels of β-defensins in the ASL. Recent investigations of BAL fluid suggest levels of < 2 ng/ml for HBD-1 and 0.1 – 100 ng/ml for HBD-2 (Singh *et al* 1998, Ganz 1998). It has been suggested that this falls within the range of antimicrobial activity of HBD-2 but not HBD-1. These estimated levels are dramatically lower than the concentrations of synthetic defensin peptides used in the studies described in this chapter and much of the published work. However, the relevant local concentrations may not be accurately reflected in BAL measurements and, as

before, this is without regard for the effect of synergistic interactions or indirect roles for β-defensins in lung defence. In addition, the concentration at which antimicrobial effects have been observed *in vitro* has been demonstrated to be dependent upon the ionic environment (Singh *et al* 1998). Therefore the relevant antimicrobial concentration *in vivo* is dependent upon the NaCl concentration of the ASL. This critical factor is also unknown and the subject of considerable controversy.

A series of contradictory results have been published reporting studies of the ionic composition of the ASL *in vivo* and no conclusive results are yet available (see Chapter 1, section 1.5.1.3 and Table 1.6). Studies using human subjects are limited by technical constraints, the requirement to limit invasive procedures, the presence of infection in most of the available subjects and the lack of appropriate controls. A number of studies have circumvented some of these complicating factors by attempting to measure the ionic composition of the ASL in murine airways.

A capillary electrophoresis fluid collection technique has previously been used to demonstrate the hypotonic nature of ASL in rats (Cowley *et al* 1997b). This technique has also been performed on $Cftr^{tm1Unc}/Cftr^{tm1Unc}$ mice, backcrossed onto a C57Bl/6 strain background, and non-CF littermates (Cowley *et al* 1998). A hypotonic ASL was also reported in mice, however no difference was observed between $Cftr^{tm1Unc}/Cftr^{tm1Unc}$ mice and non-CF littermates (Table 6.1). Interestingly, despite this observation, elevated levels of Na^+ and K^+ were observed in these mice following the instillation of *P. aeruginosa* laden agar beads.

A recent study used a novel cryoprobe collection technique and x-ray microanalysis to analyse the elemental composition of the tracheal ASL in $Cftr^{tm1Hgu}/Cftr^{tm1Hgu}$ mice on a mixed outbred MF1/129 strain, and non-CF littermates (Zahm *et al* 1999). This study also reported that the ASL in mice was markedly hypotonic. However, in contrast to the previous study, a significantly increased concentration of NaCl was observed in the ASL

collected from $Cftr^{tm1Hgu}/Cftr^{tm1Hgu}$ mice in comparison to wild type mice ($p < 0.05$) (Table 6.1).

A third study used an *E. coli* luminescence assay to demonstrate the salt-sensitive antibacterial activity of wild type murine BAL fluid and confirmed the expression of *Defb1* in the murine lung (McCray *et al* 1999). An uncharacterised primary culture model of murine tracheal epithelium was then utilised and the ionic content of the ASL on these cultured cells was assessed using a radiotracer technique. This study also confirmed the hypotonic nature of the ASL but found no difference between the Cl^- concentration of ASL from primary cultures of $Cftr^{tm1Kth}/Cftr^{tm1Kth}$ mice, with the ΔF508 mutation on a mixed C57Bl/6/129 strain background, and non-CF littermates (Table 6.1).

	Mouse strain	*Cftr* mutation	I/U	Methods	Airway Surface Liquid		
					Osmolarity	Na^+	Cl^-
Cowley *et al* 1998	C57Bl/6	non-CF	U	Capillary electro-phoresis	hypotonic	87 mM	57 mM
		$Cftr^{tm1Unc}/Cftr^{tm1Unc}$	U		hypotonic	not significantly different from non-CF	
		non-CF	I		hypotonic	112 ± 17 mM	NR
Zahm *et al* 1999	MF1 /129	non-CF	U	Cryo-probe collection, x-ray analysis	hypotonic	12.0 ± 1.9 mM	8.5 ± 1.4 mM
		$Cftr^{tm1Hgu}/Cftr^{tm1Hgu}$	U		hypotonic	52.9 ± 10.3 mM	37.2 ± 7.2 mM
McCray *et al* 1999	C57Bl/6 / 129	non-CF	U	Primary culture, radio-tracer	hypotonic	NR	18.3 ± 3.1 mM
		$Cftr^{tm1Kth}/Cftr^{tm1Kth}$	U		hypotonic	NR	14.7 ± 1.6 mM

TABLE 6.1 The ionic composition of murine ASL

U = uninfected, I = infected using bronchopulmonary instillation *of P. aeruginosa* laden agar beads, NR = not reported.

The contrasting results of these studies appear to replicate the conflicting results generated by the studies of human ASL. However, the

critical factors influencing the data from the mouse model studies may be more easily addressed.

There are several possible explanations to explain the apparent contradictions between these studies. Firstly, the genetic background of the mice may be critical. The two groups that found no difference between the mouse models of CF and non-CF littermates, studied mice on a pure inbred or a mixed C57Bl/6 background. Inbred C57Bl/6 mice do not demonstrate significant CFTR function in the trachea in response to forskolin stimulation, even in wild type mice (Farley *et al* 1998). Thus, mutations in *Cftr* may not affect the NaCl content of the ASL in the tracheas of mutant mice on this genetic background. Secondly, the specific *Cftr* mutation may be important. In many of the mouse models of CF studied, upregulation of Ca^{+}-dependent Cl^{-} channels has been reported in the airway epithelia of the nose or trachea (see Chapter 1, section 1.7.3.5). This upregulation has not been observed in the $Cftr^{tm1Hgu}/Cftr^{tm1Hgu}$ mice (Smith *et al* 1995). Thus, it is possible that despite, or even as a result of the residual wild type CFTR present in this model, there is a relative absence of alternative chloride channels capable of compensating for the loss of CFTR and consequently a more severe lung phenotype. Hence, both the background strain and specific *Cftr* mutation may play a role in determining the manifestation of the CF phenotype in the murine trachea and determine the most appropriate model for human disease. The differences between mouse models of CF are potentially informative with regard to establishing the most important factors in determining the ionic content of the ASL.

In addition to the influence of mouse strain and specific *Cftr* mutation, methodological differences are likely to play a significant role in determining the values reported by these three studies for the ionic composition of murine ASL. The analysis of ASL using capillary electrophoresis requires a narrow bore polyethylene tube to be in contact with the tracheal epithelium for approximately 30 minutes, through a tracheotomy (Cowley et al 1998). It seems likely that this could act as an irritant and a response may be

provoked by the procedure. If the "hypotonic/defensin" is correct, there may not be sufficient time or epithelial contact to allow the absorption of NaCl from secretions produced in response to such stimulus, resulting in an artificially raised NaCl level. Furthermore it is quite possible that significant evaporation may occur over this time, exacerbating this effect. In contrast, the cryoprobe technique allows the rapid collection of ASL under conditions that do not induce any stimulatory, morphological or functional alterations of the airways cells that produce ASL (Bacconias *et al* 1998). However, as a result of the extremely small volume of ASL sampled, this technique is heavily dependent upon the accurate assessment of the water content of ASL measured. The alternative approach involved the use of an *in vitro* model rather than making direct *in vivo* measurements of the ASL (McCray *et al* 1999). This has the obvious caveat that the system used must be rigorously characterised to demonstrate its validity as a model of murine tracheal epithelium, but this was not performed, to the extent that the presence of CFTR was not demonstrated, either by RT-PCR or electrophsyiological analysis. This is obviously critical if *Cftr* mutation is evoked as a mechanism for determining the NaCl content of the ASL.

In addition to the different conditions of sampling, the exact site of sampling within the trachea may be significant, depending upon the role of submucosal glands in determining the composition of the ASL. It has been suggested that the submucosal glands are the primary source of hypotonic ASL (Knowles *et al* 1997). Thus, failure of salt absorption in the submucosal glands could result in abnormal tonicity of the ASL. Whilst the submucosal glands in humans extend distally into the bronchi they are restricted to the proximal region of the trachea in wild-type mice (Borthwick *et al* 1999). Hence, the exact position of the collection of ASL with respect to the position of the submucosal glands may be important in determining the ionic content measured. Interestingly, a recent study has demonstrated that $Cftr^{tm1Hgu}/Cftr^{tm1Hgu}$ mice show a significant difference in submucosal gland distribution pattern, when compared with wild-type littermates, with glands

extending more distally in the trachea (Borthwick *et al* 1999). This distal expansion of the submucosal glands in conjunction with a failure of salt absorption, secondary to the CFTR defect, may contribute to the higher ionic concentration observed in ASL collected from *Cftr*^{tm1Hgu}/*Cftr*^{tm1Hgu} mice. Furthermore, significant variation in the submucosal gland distribution has been reported in different strains of mice, with C57Bl/6N mice observed to have a relative lack of submucosal glands, concentrated in the proximal trachea (Innes and Dorin 1999). This observation may also be relevant when comparing the results of the three studies summarised in Table 6.1 and again emphasises the importance of the background strain of mice used. In addition, it is worth noting that if the submucosal glands do indeed play a critical role, studies using primary culture models, which will not contain submucosal glands, would not be expected to display a difference in the composition of the ASL produced by CF and non-CF cells.

Despite these considerable differences, all three studies indicate a hypotonic ASL, consistent with the predictions made by the "hypotonic/ defensin" theory. Although only one study demonstrated a significant difference in the NaCl content of the ASL, differences in the methodology and the strain and specific mutations of the mice studied may explain the lack of consistency between these three studies. At the increased NaCl concentration estimated for ASL collected from *Cftr*^{tm1Hgu}/*Cftr*^{tm1Hgu} mice *in vivo*, in comparison to non-CF littermates, impairment of the antibacterial activity of synthetic mBD-1 is observed. However, uncertainty about the relevant *in vivo* concentrations of mBD-1 and the effect of co-existing antimicrobial components of the ASL, preclude further extrapolation of the *in vivo* relevance of this observation.

In conclusion, synthetic hBD-1 and mBD-1 peptides display broad spectrum, salt-sensitive, antibacterial activity in isolation, *in vitro*. The antibacterial profiles of these two peptides vary significantly with respect to anti-pseudomonal activity, but are otherwise very similar. This may contribute to species specific patterns of bacterial susceptibility secondary to

CFTR dysfunction and the resistance of mouse models of CF to lung infection with *P. aeruginosa*. Raised NaCl levels in the ASL of *Cftr*^{tm1Hgu}/*Cftr*^{tm1Hgu} mice may compromise the antibacterial activity of mBD-1 *in vivo*. On the basis of *in vitro* results, this dysfunction may contribute to the abnormal pulmonary responses observed in these mice in response to lung infection with *S. aureus*. Thus, it is possible that while the basic mechanisms underlying increased susceptibility to lung infection in CF may be conserved between mice and humans, the specific profile of bacterial susceptibility may not be. Although *Cftr*^{tm1Hgu}/*Cftr*^{tm1Hgu} mice may not necessarily demonstrate an identical bacterial infection profile to humans, the pulmonary response to the classical early stage CF-related lung pathogen *S. aureus*, may provide insights into the process of initiation of CF lung disease.

The results of studies utilising synthetic β-defensin peptides provide interesting results. However, analysis of other members of the β-defensin gene families and other antimicrobial components of the ASL is required to provide a more complete understanding. In addition, analysis of the ASL in a well characterised air-interface primary culture model system and mouse models with targeted deletions of specific β-defensins are required to confirm the results of these *in vitro* studies.

Chapter 7

A primary culture model of differentiated mouse tracheal epithelium

Chapter 7: A primary culture model of differentiated mouse tracheal epithelium

7.1 Introduction

The development of robust techniques for the primary culture of airway epithelial cells from a variety of species, including humans (Yamaya *et al* 1992), rats (Chang *et al* 1995, Clark *et al* 1995), dogs (Kondo *et al* 1991), guinea pigs (Adler *et al* 1990), rabbits (Liedtke *et al* 1988) and hamsters (Whitcutt *et al* 1988), has provided invaluable *in vitro* models for the study of airway physiology in health and disease. However, the development of successful techniques for the culture of mouse airway epithelial cells has remained elusive. The most successful published techniques result in the establishment of a relatively undifferentiated epithelium, with few, if any, ciliated cells (Clarke *et al* 1992b, Kumar *et al* 1997). The failure of such models to demonstrate appropriate differentiation of murine airway epithelium in culture suggests that these will not provide a functionally equivalent system for *in vitro* studies.

Primary cultures of human airway epithelia, at an air/liquid interface, have recently been used to investigate the pathogenesis of lung disease in CF (Smith *et al* 1996, Matsui *et al* 1998, Zabner *et al*, 1998). This approach has permitted investigation of the characteristics of the ASL and suggested that it may play a key role in the development of the chronic infection and inflammation that characterise this disease (see Chapter 1, section 1.5.1). These models may lack functionally important components of the system that regulates the ASL *in vivo*, such as the submucosal glands (see Chapter 1, section 1.5.4). Nevertheless, they do provide a model system in which the ASL and airway epithelium are readily accessible for study and

manipulation and in which antimicrobial components of the ASL may be studied in relative isolation from other complicating influences.

Despite the prominent role that mouse models of CF have played in recent research into this disorder, studies to parallel and further develop these critical observations have been hampered by the absence of an acceptable primary culture model for murine airway epithelial cells.

In order to address this situation, a technique was developed for the primary culture of differentiated murine tracheal epithelium, grown at an air-liquid interface.

7.2 Establishment of a primary culture model

A technique for the isolation and primary culture of murine tracheal epithelial cells was developed by making a series of adaptations to the methods employed in the laboratory of Professor M. J. Welsh, in Iowa, for the culture of human airway epithelium. These adaptations included; a) optimisation of number of murine tracheae to be processed per tissue culture insert and the age of mice used, b) establishment of the portion of the murine trachea required to provide subsequent differentiation in culture, c) alteration of the conditions for epithelial cell isolation, from overnight at 4 °C to one hour at 37 °C, followed by gentle agitation, d) a change in the type of tissue culture insert and membrane material used, and e) an increase in the period of submerged culture, in Culture Media, from 48 to 72 hours before transfer to air/liquid interface and USG Media. This work was carried out with technical assistance from Fiona Kilanowski.

The resultant technique is described in detail in the Material and Methods section (see Chapter 2, section 2.10). Briefly, murine tracheae were dissected by incision immediately proximal to the thyroid cartilage and at the level of the bifurcation of the bronchi. A short enzymatic dissociation of

pooled tracheae was performed at 37 °C and approximately 2 x 10^5 cells were generated per trachea, with cell viability of ~ 95% as assessed by trypan blue dye exclusion. Isolated cells were seeded at high density on collagen-coated semi-permeable membranes, using the dissociated cells from two tracheae (~ 4 x 10^5 cells) per insert. Following 72 hours of submerged culture, the apical media, along with any non-adherent cells and debris, was removed to create an air/liquid interface at the apical surface of the cells. Phase contrast light microscopy demonstrated that these epithelial cultures had a smooth, "cobblestone" appearance. Consistent with this finding, high transepithelial resistance (R_t) values indicated confluency, with the formation of tight junctions, from day 4 onwards. During the second week of culture the development of beating cilia was observed with the gradual appearance of scattered foci of "cell stacking" noted over the next few weeks.

Further morphological studies were performed using scanning and transmission electron microscopy, histochemistry and immunohistochemistry. Additional characterisation was performed using RT-PCR to analyse gene expression and Ussing chamber experiments to study the electrophysiological profile of the primary cultures.

7.3 Electron Microscopic analysis

Scanning electron microscopy (SEM) was performed on primary cultures of murine tracheal epithelia on days 4, 8, 14 and 28 after seeding ($n \geq 2$ at each time point) and tracheal specimens from five week old animals (n=2) (Figure 7.1). See Materials and Methods (Chapter 2, section 2.10.4).

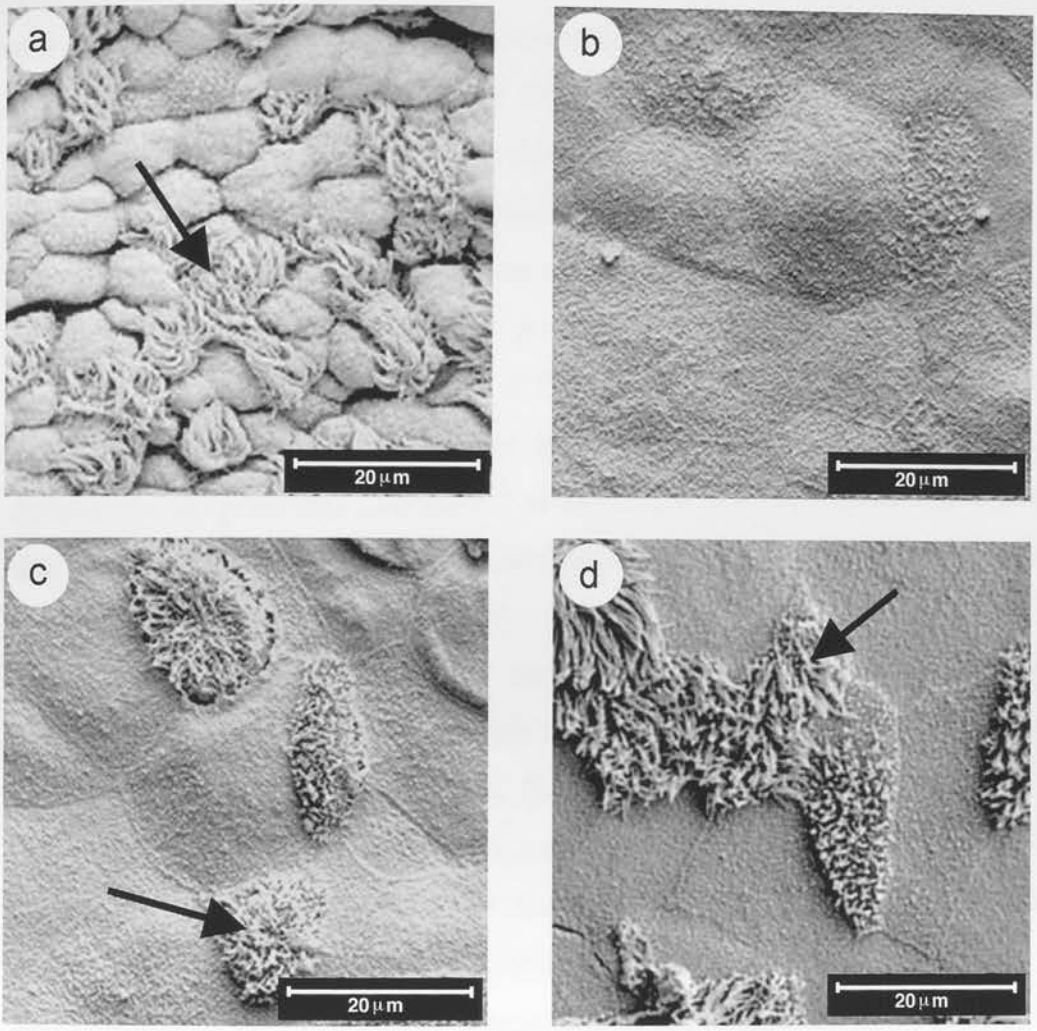

FIGURE 7.1 Scanning electron microscopy of murine trachea and primary cultures

Scanning electron micrographs of a) a 5 week old mouse trachea, and primary cultures of murine tracheal epithelia at day 4 (b), day 8 (c) and day 28 (d). Cilia are indicated (black arrow).

At day 4 a flattened epithelium was observed (Figure 7.1b), with no features of differentiated cells. This was characteristic of early stage primary culture models using other species and is described for cultured rat tracheal epithelial cells. These cells lose their cilia and secretory granules to become morphologically indistinct, poorly differentiated cells (PDC) over the first 48 hours (Chang *et al* 1995, Clark *et al* 1995). In these rat models only a small proportion of ciliated cells attached to the semi-permeable support membrane. These cells lost their cilia but were not observed to proliferate in culture (Chang *et al* 1995). The other cell types were observed to dedifferentiate into PDC cells and proliferate prior to the reappearance of differentiated cell types (Chang *et al* 1995, Clark *et al* 1995). Both basal and non-ciliated columnar cells appear to have clonogenic ability and broad differentiation potential (Randell *et al* 1991, Liu *et al* 1994). It seems likely that in our model, the mouse tracheal epithelial cells at day 4 also represent a population of undifferentiated cells.

Basic morphometric analysis was performed after immunohistiochemical staining with anti-Proliferating Cell Nuclear Antigen (PCNA) antibodies (see Figure 7.2). No positive staining was observed in the epithelial cells on sections of murine trachea. However, anti-PCNA antibodies detected 78% (± 9) of the cells in primary cultures of murine tracheal epithelia at day 4 after seeding. This suggests that the majority of cells attaching to the support membrane undergo proliferation in the first few days. The proportion of positive staining cells was observed to decrease with increasing culture age, reduced to only 25% (± 8) by day 28. These results suggest that, as in rat culture models, the majority of cells underwent dedifferentiation and proliferation, rather than the proliferation of a small subset of stem cells. Furthermore, the level of proliferation decreases as the degree of differentiation is observed to increase.

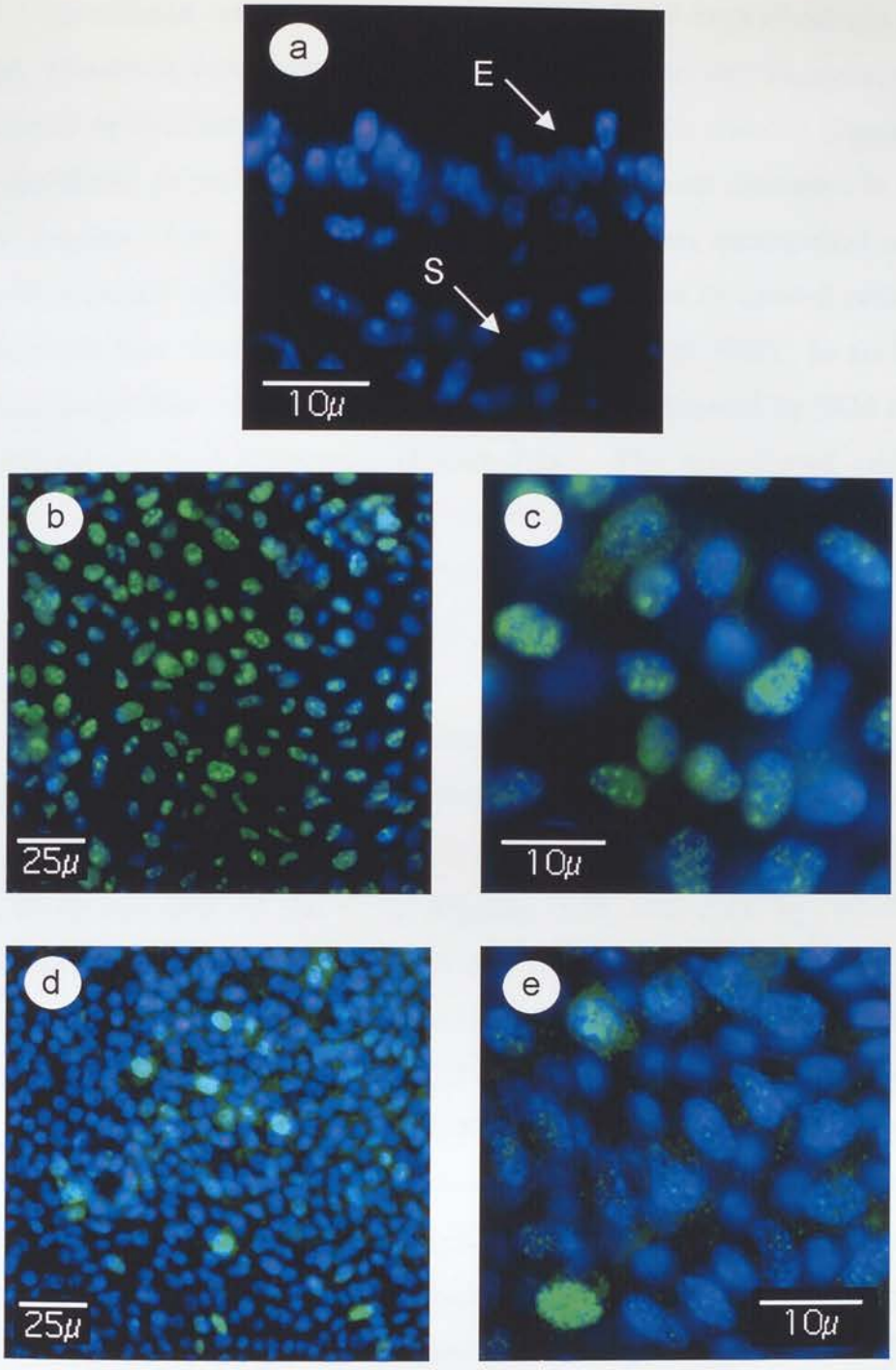

FIGURE 7.2 PCNA immunohistochemistry of murine trachea and primary cultures

Fluorescent immunohistochemical characterisation of a mouse tracheal section (a) or primary cultures of murine tracheal epithelia at day 4 (b, c) or day 28 (d, e), with PCNA antibody. Positive FITC signal is represented in green, with DAPI nuclear stain in blue. Epithelium (E) and submucosal glands (S) are indicated.

No ciliated cells were observed by SEM after 4 days of culture (Figure 7.1b). However, morphometric analyses at day 8 and day 14 revealed 16 (± 3) and 15 (± 4) ciliated cells respectively, per 100 cells counted (Figure 7.1c). By day 28 the proportion of ciliated cells in culture was estimated to be 34% (± 9) (Figure 7.1d). This is consistent with a previous quantitative study of murine tracheal epithelium, in which the proportion of ciliated cells in the epithelium was observed to be about 38% (Pack *et al* 1980). In addition, a similar proportion of ciliated cells (33% ± 5) was estimated by SEM analysis of murine tracheal specimens (Figure 7.1a). The non-ciliated cells were observed to be flatter and broader in culture in comparison to the domed appearance seen in the murine tracheal specimen (Figure 7.1a and d). These cells are assumed to be Clara cells, the predominant cell type in murine airway epithelium (Pack *et al* 1980).

Transmission electron microscopy (TEM) was performed to provide additional information about the ultrastructure of the primary cultures and the cell types present. Primary cultures of murine tracheal epithelia were processed on day 19 (n = 4) (Figures 7.3b and 7.4), by which time differentiation was evident on SEM analyses. A tracheal specimen from a five week old mouse was also processed (Figure 7.4), for comparison with published studies (Pack *et al* 1980). The preparation of TEM specimens was performed by John Findlay at King's Buildings, University of Edinburgh.

A confluent, polarised epithelium was observed in primary cultures of murine tracheal epithelium. The cultured cells were observed to be broader and shorter than native murine tracheal epithelial cells, closer to cuboidal than columnar in shape. This observation is consistent with studies of the primary culture model of guinea pig tracheal epithelium (Adler *et al* 1990). The murine epithelial cultures were comprised predominantly of a single layer of ciliated and non-ciliated cells of cuboidal morphology (Figures 7.3b and 7.4a) with apical microvilli of varying proportions. Both short, immature cilia and long mature cilia were noted, with cytoplasmic basal bodies and classical microtubule organisation. Numerous complex interdigitations of

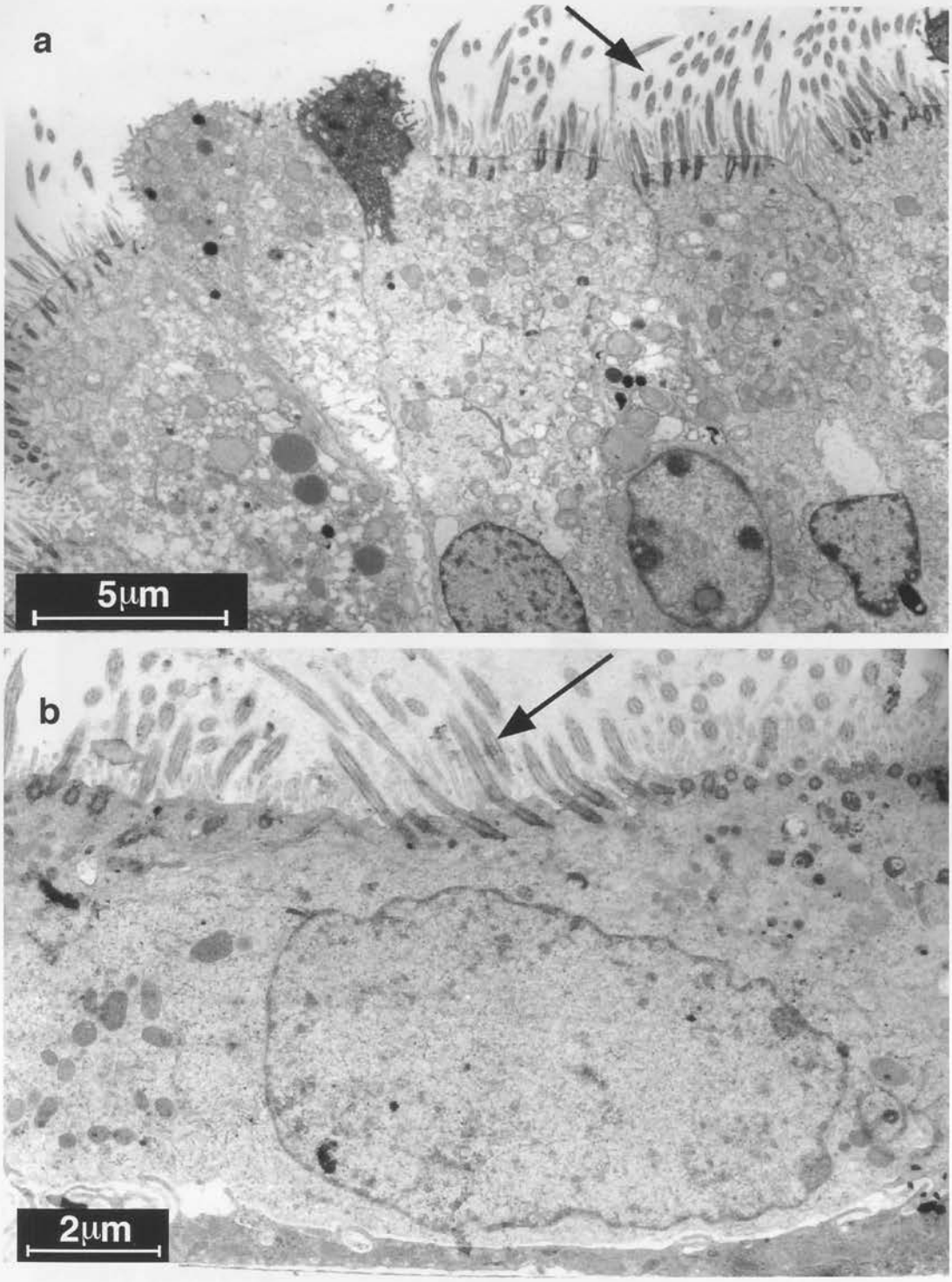

FIGURE 7.3 Transmission electron microscopy of murine trachea and primary cultures 1

Transmission electron micrographs of a) a 5 week old mouse trachea and b) primary cultures of murine tracheal epithelia at day 19. Sections through cilia, identified at the apical surface of the cells by electron dense basal bodies, are indicated (black arrow), interspersed with microvilli.

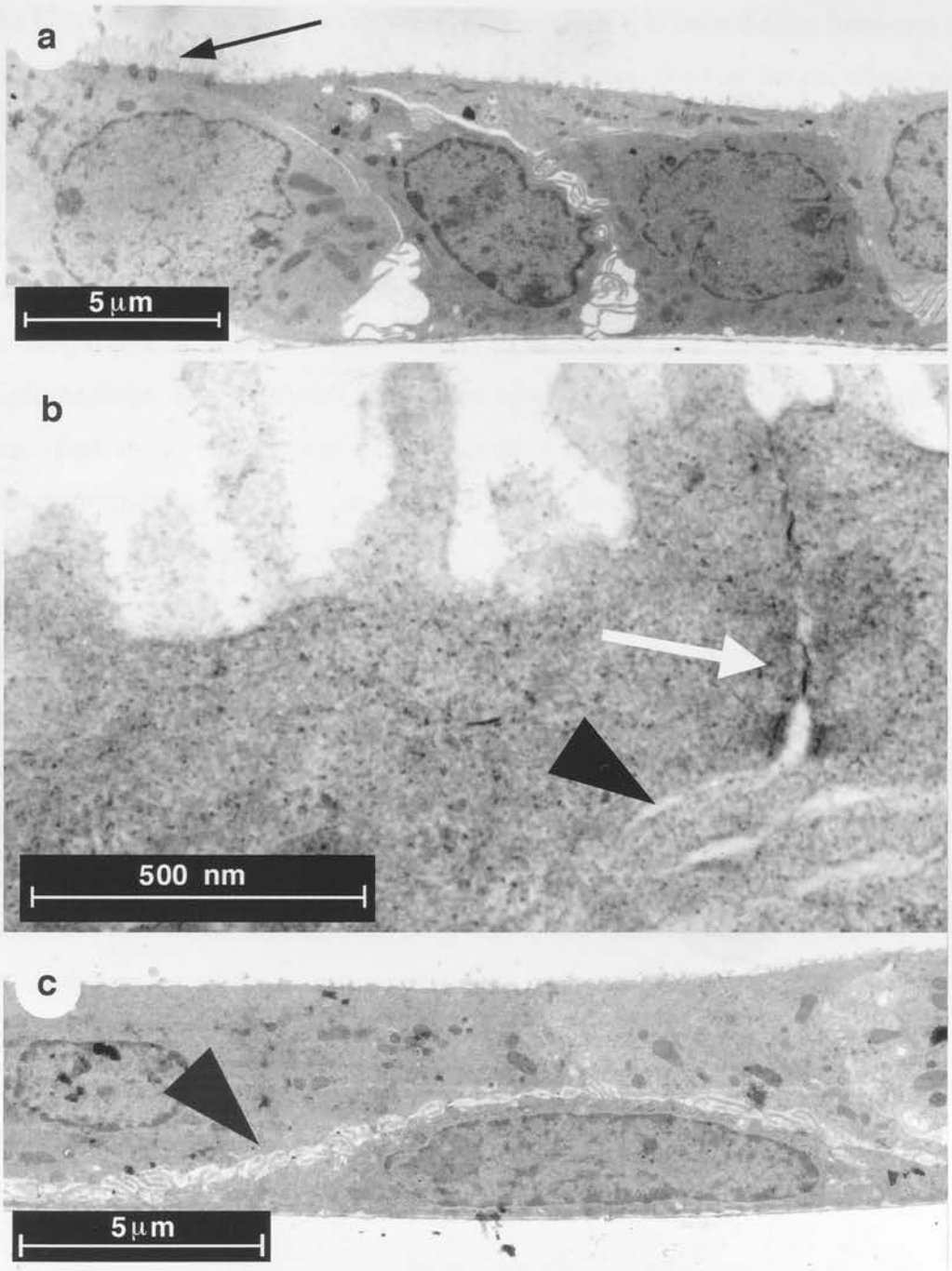

FIGURE 7.4 Transmission electron microscopy of murine trachea and primary cultures 2

Transmission electron micrographs of primary cultures of murine tracheal epithelia at day 19, demonstrating a) a layer of cuboidal epithelial cells, b) an apical junctional complex and basolateral interdigitations and c) a flattened "basal-like" cell underlying non-ciliated epithelial cells. Microvilli and several cilia (black arrow), a desmosome at the apical junction between two epithelial cells (white arrow) and lateral interdigitations between the basolateral membranes (large black arrowheads) are indicated.

the basolateral cell membrane were observed at the boundaries between the cells (Figure 7.4b). These have previously been shown to correlate with improved cellular differentiation and ion transport properties in human airway cultures (Yamaya *et al* 1992). Many apical junctional complexes, containing tight junctions and desmosomes were noted (Figure 7.4b). Larger, flattened cells, with a more squamous morphology, were also observed underlying this cuboidal epithelium. These cells had large oval nuclei, a high nucleus to cytoplasm ratio and long projections (lamellipodiae) that extended over the surface of the insert and provided multiple points of attachment beneath the other cells (Figure 7.4c). These cells may represent basal cells within this model system. The tall columnar epithelial cells seen in native mouse trachea (Figure 7.3a) were not observed in culture. However, the morphology described above is similar to that observed in 11 day old rat tracheal primary cultures (Kaartinen *et al* 1993), which later develop a morphology that more closely resembles native rat tracheal epithelium. No goblet cells were observed in the primary cultures by TEM.

Thus, electron microscopic analysis of primary cultures of murine tracheal epithelia demonstrates the presence of ciliated and non-ciliated cells, in similar proportions to native epithelia, and putative basal cells. However, the ultrastructure of these cultured cells remains significantly altered from native murine tracheal epithelial cells. As such, important differences in the differentiated state and function of these cells cannot be excluded.

7.4 Histochemical characterisation

Analysis of primary cultures of murine tracheal epithelium by TEM did not demonstrate the presence of any secretory cells. However, this form of analysis was not suited to examining large numbers of cells. Thus, histochemical analysis was performed on segments of cultured

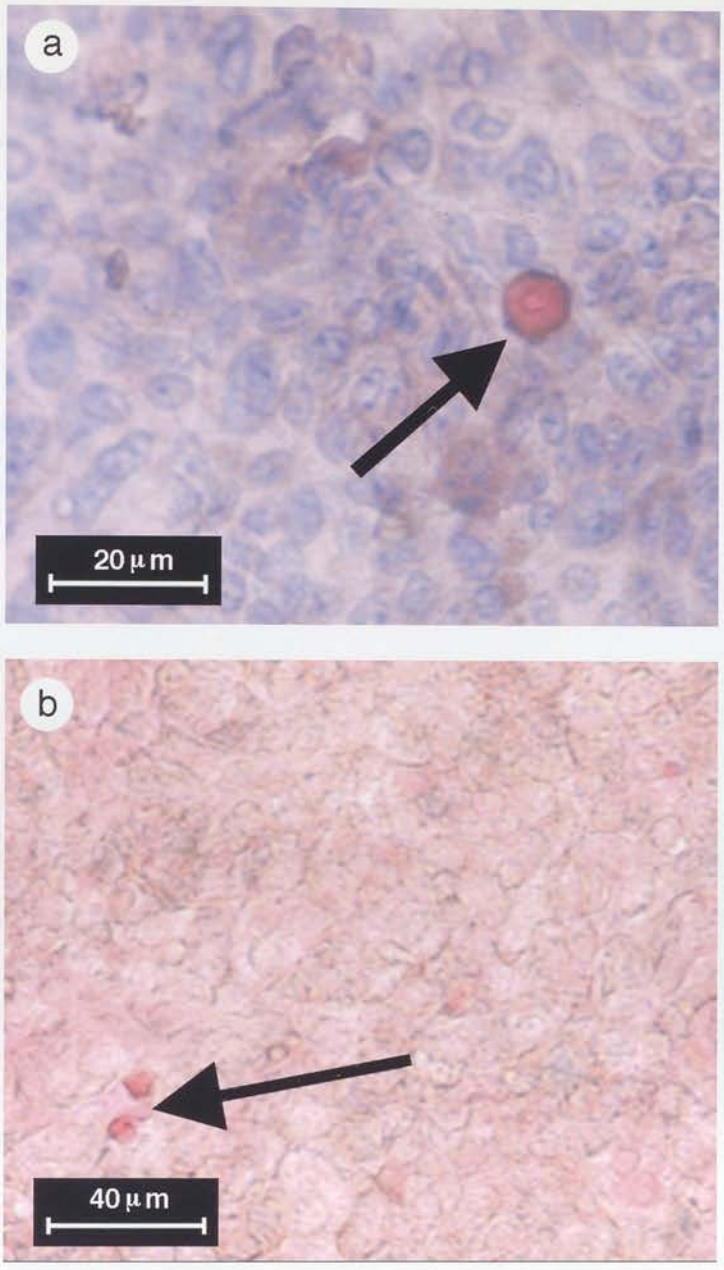

FIGURE 7.5 Periodic Acid-Schiff's stain of primary cultures of murine tracheal epithelia

Histochemical characterisation of primary cultures of murine tracheal epithelia using a Periodic Acid – Schiff's stain. a) Bright field light micrograph with haematoxylin counter stain, b) phase contrast micrograph, without counterstain. Magenta staining, PAS positive cells are indicated (black arrow).

epithelia on semi-permeable membranes. A Periodic Acid - Schiff's (PAS) stain was performed at day 4, 8, 14 and 28 after seeding ($n \geq 4$ at each time point). This stain revealed occasional PAS positive, magenta stained cells, suggesting the presence of mucus producing goblet cells (Figure 7.5). These cells were not always present and were variable in number, with no pattern observed on the basis of culture age. The reason for this irregularity is not clear. Given the scarcity of these cells in the primary cultures it is perhaps not surprising that they were not detected by TEM. This minimal presence of goblet cells reflects their paucity in the native tracheal epithelium of healthy mice (Pack *et al* 1980).

7.5 Immunohistochemical characterisation

To characterise the cell types that constituted the primary cultures of murine tracheal epithelia, immunohistochemical analysis was performed at days 4, 8, 14 and 28 ($n \geq 3$ for each antibody at each time point), using a panel of antibodies, and compared to murine tracheal sections ($n \geq 3$ specimens for each antibody) (Figures 7.6 and 7.7). Morphometric analyses were performed as described in Materials and Methods (see Chapter 2, section 2.10.6).

The density of cells in primary cultures of murine airway epithelium was observed to undergo a 2-3 fold increase between day 4 and day 28. The average number of cells estimated per field of view at day 4, 8, 14 and 28 were 51 (± 11), 112 (± 17), 123(± 26) and 150 (± 30) respectively. Thus, proliferation of the cells within the primary cultures is greatest at the earlier stages, in keeping with the observations using anti-PCNA antibodies (see section 7.3).

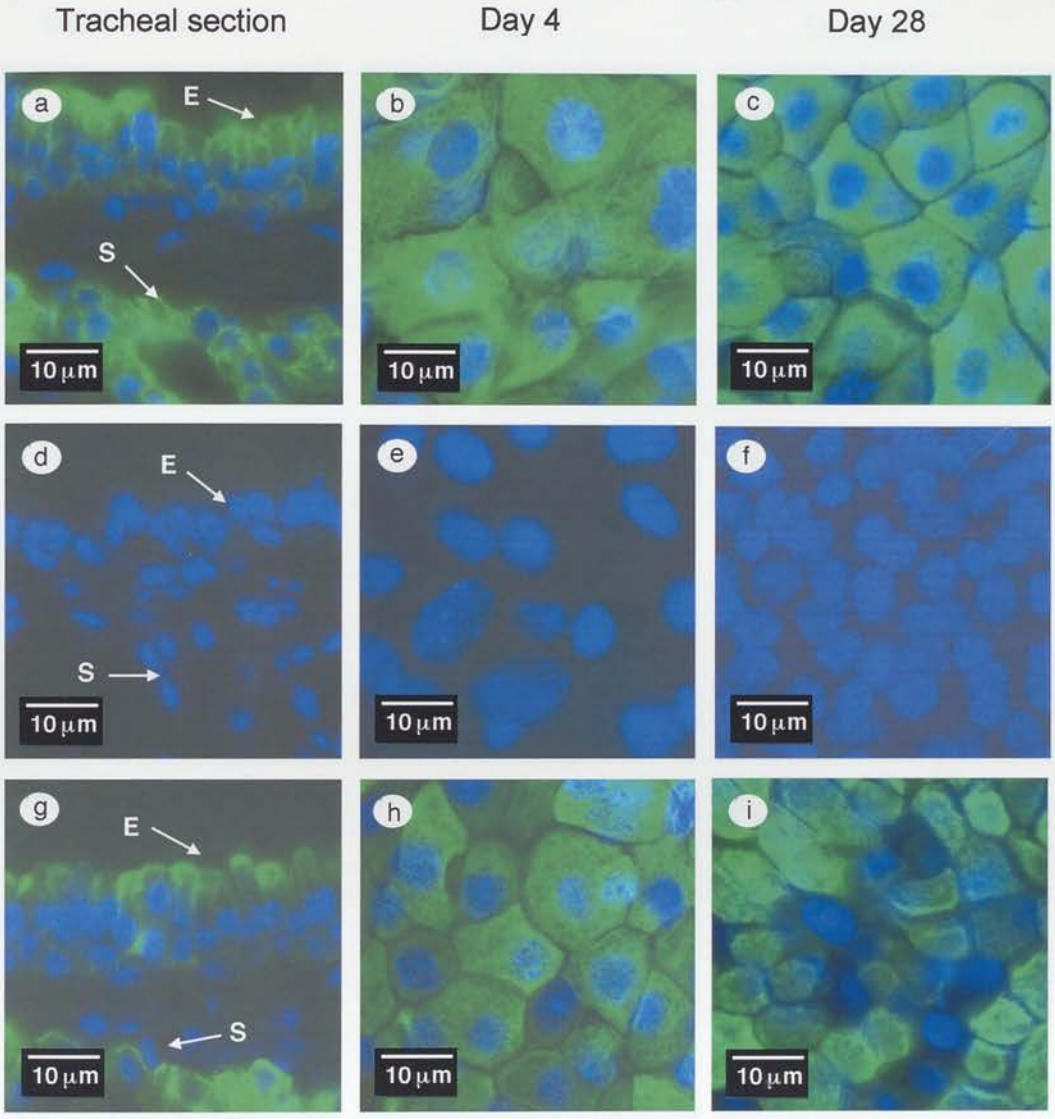

FIGURE 7.6 Immunohistochemical characterisation of murine trachea and primary cultures 1

Fluorescent immunohistochemical characterisation of mouse tracheal sections (a, d, g) or primary cultures of murine tracheal epithelia at day 4 (b, e, h) or day 28 (c, f, i), with anti-human pan cytokeratin antibody (a, b, c), no primary antibody (negative control) (d, e, f), or anti-mouse cytokeratin 18 antibody (g, h, i). Positive FITC signal is represented in green with DAPI nuclear stain in blue. Epithelium (E) and submucosal glands (S) are indicated.

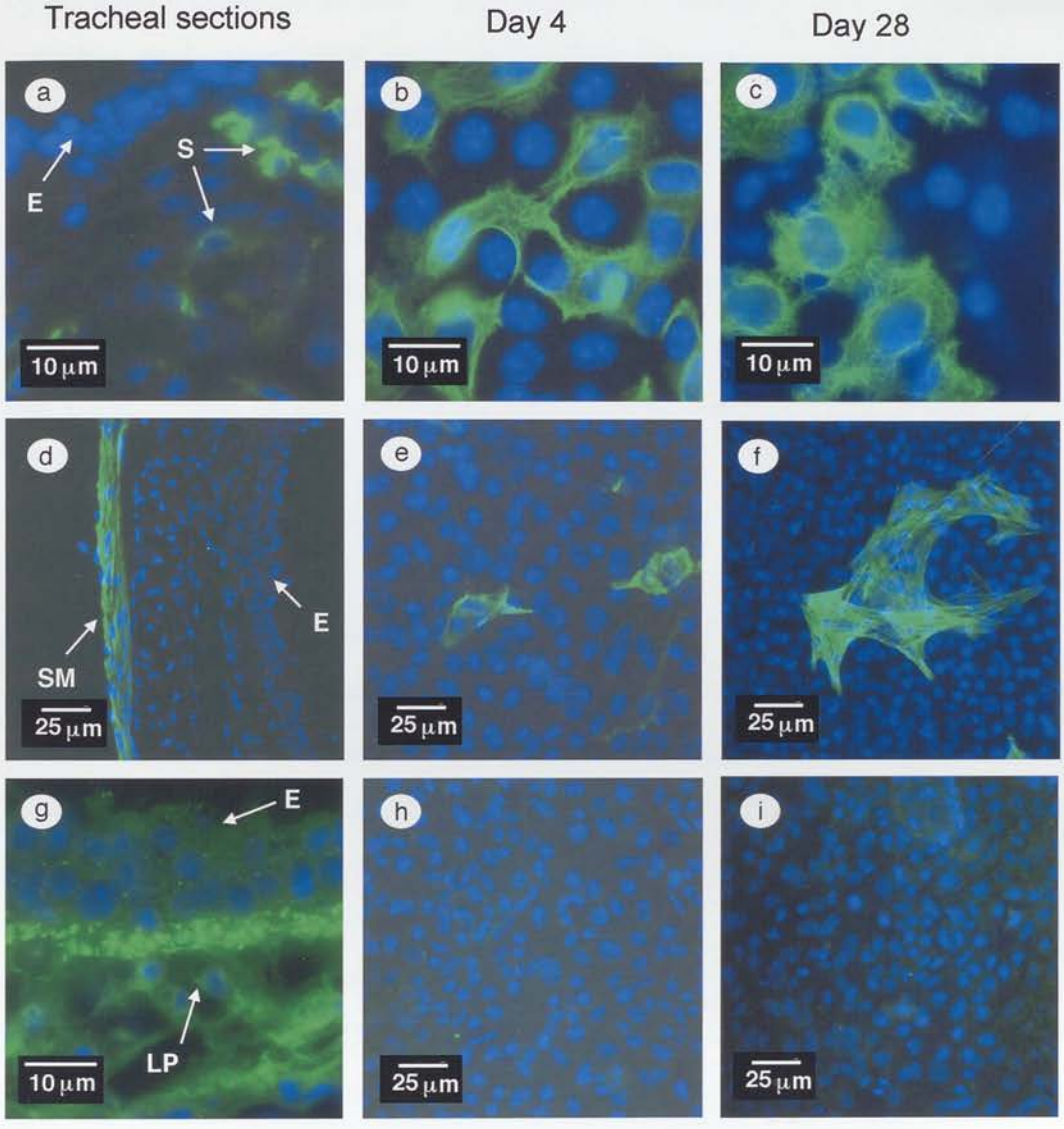

FIGURE 7.7 Immunohistochemical characterisation of murine trachea and primary cultures 2

Fluorescent immunohistochemical characterisation of mouse tracheal sections (a, d, g) or primary cultures of murine tracheal epithelia at day 4 (b, e, h) or day 28 (c, f, i), with anti-mouse cytokeratin 14 antibody (a, b, c), anti-human α-smooth muscle actin antibody (d, e, f) or anti-human vimentin antibody (g, h, i). Positive FITC signal is represented in green with DAPI nuclear stain in blue. Epithelium (E), submucosal glands (S), smooth muscle (SM) and lamina propria (LP) are indicated.

Epithelial cells were characterised using antibodies raised against different cytokeratins, a family of intermediate filaments involved in the cytoskeleton of epithelial cells. The expression profile of these cytokeratins is variable and dependent upon epithelial cell subtype and the stage of differentiation (reviewed in Fuchs *et al* 1987). However, these expression patterns can be altered in wound healing, influenced by extracellular factors and affected by cell culture (reviewed in Guin *et al* 1987). Antibodies raised against α-smooth muscle actin (expressed in smooth muscle cells) and vimentin (expressed in cells of mesenchymal origin) were used to establish the contribution of non-epithelial cells to the primary cultures of murine tracheal epithelia.

The anti-human pan cytokeratin antibody (raised against cytokeratins 1, 4, 5, 6, 8, 10, 13, 18 and 19) detected all the cells of the tracheal epithelia and submucosal gland epithelia in sections of mouse trachea (Figure 7.6a). This antibody was used to demonstrate the epithelial nature of the confluent primary cultures, with all the culture cells apparently detected, at all time points (Figure 7.6b and c). Some variation in the intensity of staining was observed in different cells within the same cultures. Small patches of intensely stained cells, on a focal plane above the majority of the cells, were observed with greater frequency in the older cultures.

Subtypes of epithelial cells were demonstrated in mouse tracheal sections using antibodies raised against the murine homologues of human cytokeratins 18 (Figure 7.6g, h and i) and 14 (Figure 7.7a, b and c).

Cytokeratin 18 was detected in the ciliated and non-ciliated columnar cells in the tracheal epithelia and acinar epithelial cells in the submucosal glands in sections of mouse trachea (Figure 7.6g). The anti-cytokeratin 18 antibody detected 91% (± 4) of the cells in primary cultures at day 4. Estimation of the proportion of cytokeratin 18 positive cells in primary cultures at later time points was complicated by the increased cell density and high proportion of positive staining cells. However, no gross alteration was observed. A range of intensities of positive signal was observed in

different cell within the same culture at all time points (Figure 7.6h and i). These cells were observed to have a largely confluent "cobblestone" appearance similar to the staining apparent with the anti-pan cytokeratin antibody, although "gaps", representing unstained cells, were observed.

No significant alteration was seen in the staining pattern of cytokeratin 18 positive cells during the poorly differentiated stage, or at the time of cellular differentiation to produce ciliated cells. This was in contrast to the tracheal xenograft model of rat airway epithelium. This model system involves re-population of a denuded rat tracheal graft with isolated rat epithelial cells (Shimizu *et al* 1992) and closely parallels rat tracheal cell primary culture on coated support membranes. In xenografts, the PDC cells initially maintain their original cytokeratin 18 and 14 expression patterns when other markers of differentiated cell type are lost. However, at day 3, regardless of their original profile, all PDC cells express cytokeratin 14, but not cytokeratin 18 (Liu *et al* 1994). The expression of cytokeratin 18 is not restored until the second week, coincident with the first evidence of ciliary and secretory differentiation of columnar cells (Shimizu *et al* 1992). The mouse tracheal cells in our culture system did not show such dramatic dedifferentiation in the process of establishing a model epithelium. The reason for this difference is unclear.

Cytokeratin 14 was detected in the myoepithelial cells and cuboidal epithelial cells of the proximal duct of the submucosal glands, and in less than 5% of basal cells in the tracheal epithelium, with an irregular distribution pattern, in murine tracheal sections (Figure 7.7a). In primary cultures the anti-cytokeratin 14 antibody detected 24% (±8) of cells at day 4. The proportion of cytokeratin 14 positive cells remained constant, with 23% (±8), 23% (±10) and 23% (±7) estimated at day 8, 14 and 28 respectively. These cells were observed to have a fairly scattered distribution with less contact between positive staining cells than the cytokeratin 18 positive cells (Figure 7.7b and c). They were observed to have an irregular shape with fine cytoplasmic protrusions and to lie in a focal plane below the majority of the

epithelial cells. It is possible that these represent the flat, underlying, "basal-like" cells observed by TEM. Although basal cells only constitute 5-10% of the native murine tracheal epithelium (Pack *et al* 1980), an enrichment of basal cells may have occurred if only a small proportion of ciliated cells were able to attach to the support membrane, as observed in the rat culture model (Chang *et al* 1995).

The origin of these cytokeratin 14 positive cells remains unclear. The great majority of the cells detected by the anti-cytokeratin 14 antibody in mouse tracheal sections were, in fact, of submucosal gland origin, both myoepithelial and ductal cells. However, immunohistochemical analysis of tracheal "husks" remaining after the dissociation of cells for culture, demonstrated disruption, but minimal dissociation, of submucosal gland cells as a result of this procedure. Thus, it is unlikely that a large proportion of the cultured cells originate from the submucosal glands. Nonetheless, it is worth noting that in preliminary studies, removal of the most proximal portion of the tracheae (to which the thyroid gland is adherent) before epithelial cell dissociation resulted in a failure to differentiate and produce ciliated cells in culture, despite the standard number of cells being seeded. This suggests that cells from the proximal trachea (the main site of murine submucosal glands (Borthwick *et al* 1999)) are important in the development of a fully differentiated primary culture of murine tracheal epithelium. Furthermore, recent studies have demonstrated that the ciliated duct of murine submucosal glands may be a specific niche for airway stem cells (Borthwick *et al* 1998).

The studies using these anti-cytokeratin antibodies demonstrate the existence of distinct subgroups of epithelial cells within the primary cultures. However, the alteration of cytokeratin expression patterns in epithelial cells under culture conditions necessitates caution in making direct comparison between the expression profiles of specific cell subtypes in native tracheal epithelium and those in the primary cultures of murine tracheal epithelia on the basis of these results. In addition, it is clear from the estimates of cells

staining positive for cytokeratin 14 and cytokeratin 18 that either some cells exhibit dual staining or cytokeratin 18 negative cells were obscured for the purposes of morphometric analysis, perhaps underlying positive staining cells. Thus the main conclusion must be that these primary cultures of murine tracheal epithelium are indeed primarily epithelial in nature and that different subtypes of epithelial cells exist. These subtypes may represent columnar and basal cell groups.

The anti-human α-smooth muscle actin antibody was shown to detect smooth muscle, but not epithelial cells, in mouse tracheal sections (Figure 7.7d). In day 4 primary cultures of murine tracheal epithelia this antibody demonstrated the presence of a variable number (< 1% of cells) of scattered, individual, positive staining cells (Figure 7.7e). These cells were observed to lie in a focal plane below the majority of cultured cells. These α-smooth muscle actin positive cells were observed to proliferate gradually, with larger clumps of cells detected by day 28 (Figure 7.7f), suggesting outgrowth from the single cells contaminating the original cell preparation. The proportion of these contaminating cells was variable and largely dependent upon the length of the dissociation step and the vigour with which tracheal suspensions were agitated. Primary cultures prepared from dissociated cell suspensions with large numbers of contaminating cells progressively developed lower R_t and lost ability to maintain an air/liquid interface. This suggests that growth of these cells may eventually disrupt and "puncture" the confluent epithelial membrane when initial contamination is excessive.

The anti-human vimentin antibody detected connective tissue cells of the lamina propria in mouse tracheal sections, but also a slight punctate background staining of the epithelial cells (Figure 7.7g). Immunostaining of primary cultures demonstrated the same slight background staining throughout, but no evidence of genuine positive signal at any time point (Figure 7.7h and i). This indicated that there was no contamination with vimentin positive cell types in the primary cultures.

These results provide confirmation of the almost exclusively epithelial nature of these primary cultures of murine tracheal epithelium.

No positive staining was observed in negative controls, treated in an identical manner to the other samples but omitting the primary antibodies (Figure 7.6d, e and f).

7.6 Gene Expression

Recent investigations of the pathogenesis of CF lung disease have focused on the characteristics of the ASL and its role in mucociliary clearance and the innate lung defences, as previously discussed. The analysis of ASL *in vivo* has proven to be extremely difficult technically and has produced conflicting results (see Chapter 1, section 1.5.1.3). Consequently, key studies addressing the ionic composition and antibacterial activity of the ASL have been performed in primary cultures of human airway epithelia. To maximise the opportunities presented by the availability of mouse models of CF, it has been critical to develop a primary culture model for murine airway epithelial cells. However, in addition to demonstrating morphological equivalence between this model system and native murine trachea, it is critical that the cultured epithelial cells should express *Cftr* and murine β-defensins.

Primary cultures of murine tracheal epithelia at day 12-13 ($n \geq 3$ for each condition described) were characterised, using RT-PCR, to establish the expression of *Cftr*, *Defb-1* and *Defb-2*, as described in Materials and Methods (Chapter 2, sections 2.10.7 to 2.10.11). *Defb-2* expression is upregulated in response to pro-inflammatory stimuli *in vivo* (Morrison *et al* 1999), hence these studies were performed using cultures both with and without exposure to either *E. Coli* LPS or *P. aeruginosa* CF clinical isolate J1385, in PBS. Untreated cultures were exposed to PBS

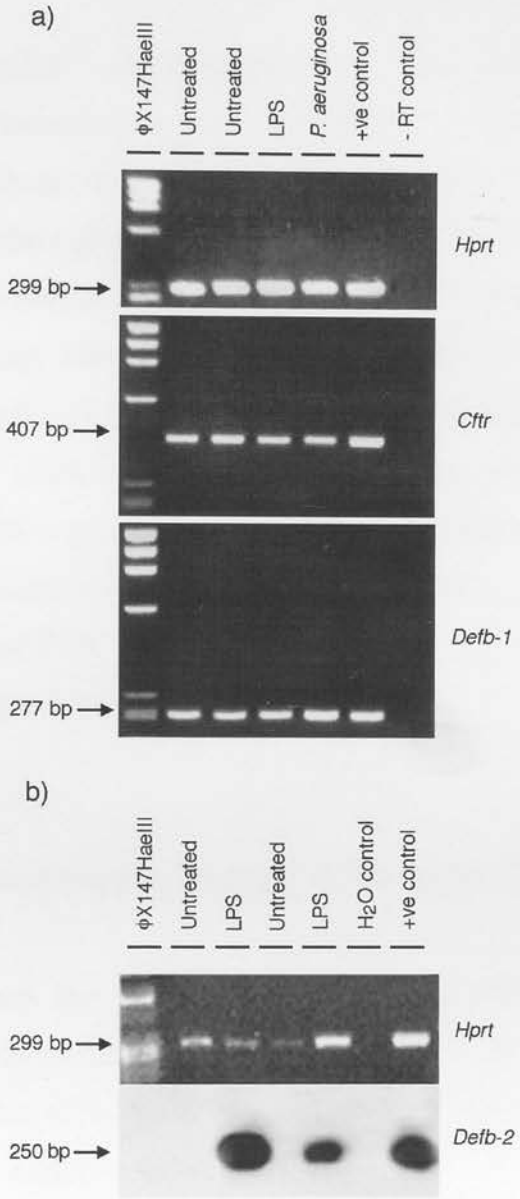

FIGURE 7.8 RT-PCR analysis of murine tracheal primary cultures

RT-PCR of a) *Hprt*, *Cftr* and *Defb-1*, and b) *Hprt* and *Defb-2*, from primary cultures of murine tracheal epithelia. Cultures were utilised after 30 minutes exposure to either LPS or *P. aeruginosa*, in PBS. Untreated cultures were exposed to PBS alone. Amplified products were analysed on a 2% agarose gel, with a ΦX147HaeIII marker, amplified plasmid positive controls and negative controls, using either heat-inactivated reverse transcriptase (-RT) or distilled water substituted for RNA during cDNA synthesis. *Defb-2* PCR products were observed only after hybridisation to a *Defb-2* internal probe.

alone. Parallel amplification of the murine hypoxanthine phosphoribosyltransferase gene (*Hprt*) was performed as a control (Figure 7.8). These studies demonstrated that the expression pattern of these genes in the cultured cells replicated the *in vivo* situation (Morrison *et al* 1997, Morrison *et al* 1999). *Cftr* and *Defb-1* were both constitutively expressed (Figure 7.8a) whereas *Defb2* was induced by exposure to pro-inflammatory stimuli (Figure 7.8b). *Defb2* expression was not observed without prior stimulation (n = 3), but was repeatedly observed in response to LPS exposure (n = 4). As *in vivo*, the level of expression of *Defb2* after induction was too low to be observed on a stained agarose gel after 34 cycles of PCR. However, it was observed after hybridisation with an internal oligonucleotide.

7.7 Electrophysiological characterisation

To assess the confluency of primary cultures of murine tracheal epithelia, R_t was monitored at days 4, 8, 14 and 28. Table 7.1 shows that the maximum value of R_t, (28.4 kΩ cm^{-2}), was measured on day 4, immediately following the establishment of an air / liquid interface. Subsequently, R_t values decreased to ~12 kΩ cm^{-2} by day 14, after which they remained stable at about this value (Table 7.1). These values of R_t are markedly higher than those reported for cultures of airway epithelia from other species including human (200-3000 Ω cm^{-2} (Yamaya *et al* 1992)) and dog tracheal epithelia (200-400 Ω cm^{-2} (Kondo *et al* 1991)). They also greatly exceed those reported for poorly differentiated primary cultures of murine tracheal epithelia (~ 400 Ω cm^{-2} (Clarke *et al* 1992b)). Interestingly, primary cultures of murine tracheal epithelia that failed to achieve elevated values of R_t were able to maintain an air/liquid interface, but did not develop ciliated epithelial cells.

In contrast to the primary cultures of murine tracheal epithelia, confluent Human Bronchial Epithelial (HBE) cell lines, cultured on identical collagen coated membranes, failed to maintain an air-liquid interface and demonstrated a mean R_t value of 525 ± 81 Ω cm^{-2} (n = 6), stable from day 7 after seeding onwards.

Time (days)	R_t (kΩ cm^{-2})	n
Day 4	28.4 ± 7.6	40
Day 8	20.3 ± 4.5	31
Day 14	11.6 ± 3.6	21
Day 28	12.1 ± 5.1	16

TABLE 7.1 Transepithelial resistance (R_t) of primary cultures of murine tracheal epithelium

Values are means ± SD; n, total number of cultures tested.

To investigate the epithelial ion transport properties of primary cultures of murine tracheal epithelia, day 28 primary cultures were mounted in modified Ussing chambers and I_{sc} and R_t were recorded. Under baseline conditions, R_t was 14.3 ± 1.7 kΩ cm^{-2} (n = 6) and I_{sc} was 12.9 ± 1.0 μA cm^{-2} (n = 6). Figure 7.9 demonstrates that the addition of amiloride (10 μM) to the apical solution inhibited I_{sc} ($P < 0.001$). Subsequent addition of cAMP agonists (10 μM forskolin, 100 μM IBMX and 500 μM CPT-cAMP) stimulated I_{sc} ($P < 0.001$; Figure 7.9). Finally, addition of bumetanide (100 μM) to the basolateral solution inhibited I_{sc} ($P < 0.001$; Figure 7.9). These data are consistent with studies of native murine epithelia (Smith *et al* 1992). The results suggest the presence of amiloride-sensitive sodium channels and cAMP-stimulated CFTR chloride channels. However, further studies are

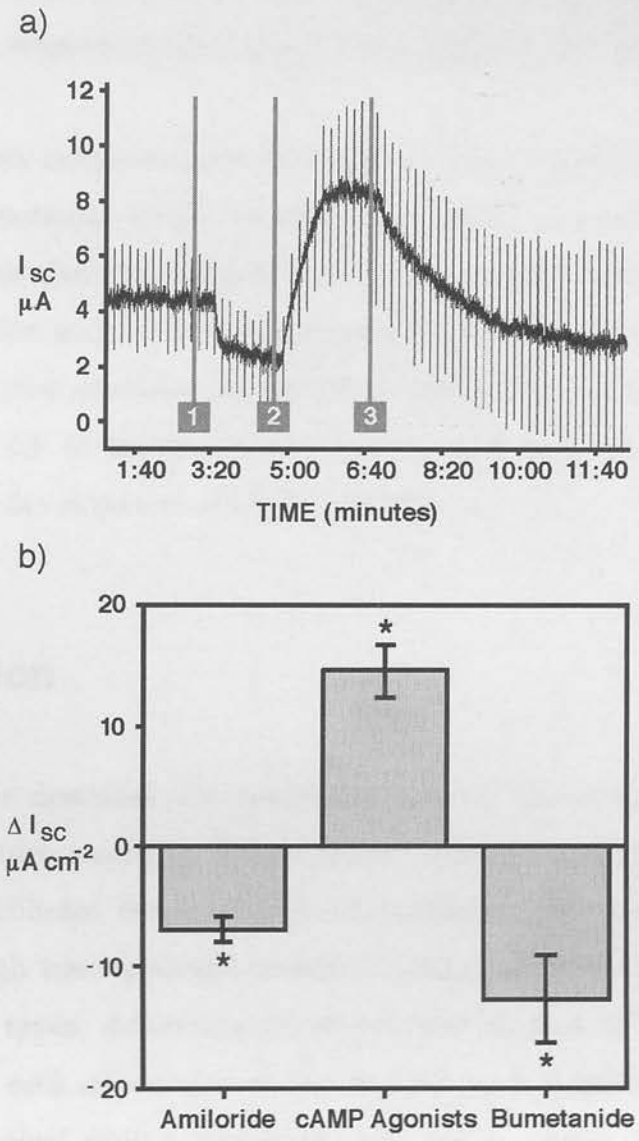

FIGURE 7.9 Ussing chamber analysis of primary cultures of murine tracheal epithelia

I_{sc} measurements in primary cultures of murine tracheal epithelia, a) representative recording of I_{sc}. Amiloride (10 μM), cAMP agonists (10 μM forskolin, 100 μM IBMX and 500 μM CPT-cAMP) and bumetanide (100 μM) were added as indicated at time points 1, 2 and 3 respectively. b) magnitude of changes in I_{sc} (ΔI_{sc}) stimulated by amiloride, cAMP agonists and bumetanide. ΔI_{sc} was calculated as current measured at the peak of the response (~ 2 minutes after the addition of amiloride or cAMP agonists and ~7 minutes after the addition of bumetanide) minus current immediately before agonist addition. Values are mean ± SD (n = 6). Asterisks indicate a significant change in I_{sc} in response to treatment ($p < 0.001$).

necessary to confirm these conclusions, in particular to exclude the possibility that the response to forskolin was mediated by Ca^{2+}-dependent Cl^- channels.

Thus, primary cultures established from the tracheae of mouse models of CF, lacking functional CFTR, would be expected to demonstrate the consequences of this channel dysfunction and any resultant abnormalities in the ionic composition and antibacterial activity of the ASL. This will enable complementary *in vitro* studies to be performed using cultured tracheae from mouse models of CF to investigate the role of ASL and its antibacterial components in the development of CF lung disease.

7.8 Discussion

This chapter describes the establishment and characterisation of a novel primary culture model of differentiated murine tracheal epithelium. This technique facilitates the formation of confluent, polarised epithelial cultures with a high transepithelial resistance, minimal contamination with non-epithelial cell types, differentiation to produce ciliated cells and small numbers of goblet cells, expression of *Cftr* and mouse β-defensin genes and an electrophysiological profile consistent with the presence of amiloride-sensitive sodium channels and cAMP-stimulated CFTR chloride channels. Thus, this model demonstrates important features of native murine tracheal epithelia, particularly with respect to the study of mouse models of CF.

Further characterisation is required to rigorously demonstrate the equivalence of this model and native murine tracheal epithelium. Such studies include a) an extension of TEM investigations to provide quantitation and analysis at later time points, b) further studies of the secretory cell population observed and the factors regulating their presence and quantity, c) additional gene expression studies to establish the expression of the

recently described murine β-defensin genes; *mBD-3* (Bals *et al* 1999) and *mBD-4* (Jia *et al* 1999), and other components of the innate lung defence system, such as lysozyme, and d) further electrophysiological studies to confirm the ion channel basis for the observations presented above and examine the role of Ca^{2+}-dependent Cl^- channels. In addition, the exceptionally high transepithelial resistances displayed by the primary cultures of murine tracheal epithelia, in comparison to native murine tracheal epithelia, must be considered in any studies of the ASL.

Despite these reservations, this primary culture system facilitates novel approaches for the study of lung disease in mouse models of CF. Primary cultures of tracheal epithelium from mouse models of CF should now be established and characterised in the manor described above for wild type animals. Such cultures can then be compared to those prepared from non-CF littermates in a series of studies to evaluate the consequences CFTR dysfunction in the relative isolation of this model system. These investigations should be designed to complement *in vivo* studies using mouse models of CF and studies performed with human airway primary cultures. In the former scenario, the absence of many of the "complicating factors" present *in vivo* should facilitate these investigations. However, the possible importance of these factors should not be forgotten. Such studies should include; a) the analysis of the ionic composition and volume control dynamics of murine ASL, b) the antibacterial properties of murine ASL and the key components of this response, particularly in β-defensin knockout mice, c) further studies on the internalisation of *P. aeruginosa*, in a system only incorporating epithelial cells, and d) investigation of the adherence of CF related pathogens to murine airway epithelial cells, both established and regenerating. In the latter case experimental design should a) take advantage of the opportunities afforded by inbred strains of mice (see Chapter 1, section 1.7.4) to study genetic modifiers, b) establish data that confirms or refutes the results of human studies and further investigate the key similarities and differences between mice and humans.

In addition to the study of CF, this model system may be valuable in the study of the growth and differentiation dynamics of mouse tracheal epithelium, the pathophysiology of other airway diseases for which mouse models exist and the evaluation of novel therapies.

Chapter 8

Summary and Future Prospects

Chapter 8: Summary and Future Prospects

The studies described in this thesis characterise an abnormal lung phenotype in *Cftr*^{tm1Hgu}/*Cftr*^{tm1Hgu} mice in response to aerosolised *Staphylococcus aureus* and assess the factors contributing to the variability of this phenotype. The contributions of bacterial internalisation and the dysfunction of β-defensins to lung disease in mouse models of CF are examined and the establishment and characterisation of a primary culture model of differentiated murine tracheal epithelium is described.

Techniques for the delivery of bacteria to the lungs of experimental mice were developed, optimised and quantified. Bacterial nebulisation chambers were designed and characterised. This technique demonstrated moderate dose, reproducible, easily repeatable, minimally invasive delivery, throughout the airways and lung parenchyma. The technique was subsequently used to characterise the response of mouse models of CF to aerosolised bacteria. Tracheal intubation and direct intratracheal instillation techniques were optimised and characterised, demonstrating reproducible high dose delivery. This technique was subsequently utilised in the assessment of bacterial internalisation by epithelial cells.

Previous studies had demonstrated that *Cftr*^{tm1Hgu}/*Cftr*^{tm1Hgu} mice, on a mixed outbred MF1/129 background strain, were impaired in their ability to clear aerosolised *S. aureus* from their lungs and developed more severe, pathogen specific, lung pathology in response to aerosolised CF related lung pathogens, than non-CF littermates. Studies were performed to examine the sources of variation in this lung phenotype following repeated exposure to aerosolised *S. aureus*. *Cftr*^{tm1Hgu}/*Cftr*^{tm1Hgu} mice and *Cftr*^{tm1Hgu}/*Cftr*^{tm1Unc} mice, backcrossed onto a C57Bl/6N background were observed to develop lung pathology in response to repeated exposure to aerosolised *S. aureus*. The characteristics of this pathology were similar to that observed in the outbred mice. Moreover, as observed in studies using the outbred mice, significantly

more severe pathology was observed in mouse models of CF in comparison to non-CF littermate controls. The spectrum of disease in response to bacterial exposure was narrowed in the C57Bl/6N mice, in comparison to the mixed, outbred background strain. However, the predominant effect appeared to be an increased severity of disease in the inbred wild type mice, suggesting increased predisposition to lung disease in this background strain. No difference was observed between the severity of disease observed in *Cftr*^{tm1Hgu}/*Cftr*^{tm1Unc} compound heterozygote mice in comparison to *Cftr*^{tm1Hgu}/*Cftr*^{tm1Hgu} mice on the same inbred background, despite an expected decrease of ~ 50% in the background level of normal *Cftr* expression. This observation suggests that an abnormal pulmonary phenotype may be manifest when the level of functional CFTR falls below a minimum threshold level, but will not be exacerbated by further decreases. Although more severe lung pathology was evident in mice repeatedly exposed to bacteria than control mice, regardless of genotype, variable levels of background lung disease were observed. Thus the phenotype variability observed in outbred mice was concluded to be related primarily to independently segregating genes in the outbred strain and variation in the degree of pre-existing lung pathology in the mice. Differences between individual *Cftr*^{tm1Hgu}/*Cftr*^{tm1Hgu} mice in the level of residual CFTR function are less likely to have had a significant effect. The future use of congenic mice (including C57Bl/6N, BALB/c and FVB) born and raised in SPF facilities should enhance the prospects of more clearly defined lung phenotypes in *Cftr*^{tm1Hgu}/*Cftr*^{tm1Hgu} mice. This may be particularly true of mice congenic for the *Cftr*^{tm1Hgu} mutation on a BALB/c background, a strain demonstrated to be less susceptible to lung infection and to have more significant levels of CFTR activity in the trachea, as assessed by electrophysiology. Such phenotypes may be used as pathophysiological endpoints for the testing of novel therapies and for the isolation of genetic modifiers. Further studies might also include analysis of the BALF levels of IL-10, MIP-2 and KC in infected mice, the effect of malnourishment on the susceptibility of *Cftr*^{tm1Hgu}/*Cftr*^{tm1Hgu} mice to lung

infection, the use of other mouse models of CF, such as the ΔF508, G551D and G480C models and the use of an alginate bead model as a more acceptable alternative to the use of agar beads. The future availability of gene expression array technologies may also prove illuminating in studying the basis for the differences observed in the pulmonary response to bacterial exposure between mouse models of CF and non-CF littermates.

Histopathological assessment of the lungs of mice repeatedly exposed to *S. aureus* revealed a significant difference between the mouse models of CF and non-CF controls. This was consistently demonstrated when assessment was performed using the total score, but not for the scores assigned to the five features from which it was comprised. Thus, the total score assigned for severity of pathology was more closely correlated with genotype than any individual component part of that score. This suggests an exaggerated normal response in these mice, rather than abnormality in any one aspect of this response. This would be compatible with a general impairment of the antimicrobial properties of the murine tracheal ASL, a mucociliary clearance defect or any other mechanism that would have resulted in the prolonged presence of bacteria in the lungs of mouse models of CF. To further dissect the mechanisms underlying the pathogenesis of the lung pathology observed, alternative approaches were adopted, examining specific hypotheses for the development of CF lung disease.

The internalisation of *P. aeruginosa* by epithelial cells has been proposed as a CFTR-dependent component of the lung defence system. A gentamicin exclusion assay was adapted and optimised to assess the internalisation of bacteria by adult mouse lung cells. Preliminary studies, in adult $Cftr^{tm1Hgu}/Cftr^{tm1Hgu}$ mice and non-CF controls, demonstrated internalisation of a non-mucoid clinical strain of *P. aeruginosa*, but did not support a role for CFTR in this process. Further studies are required to visualise the cellular compartment responsible for the bacterial internalisation observed *in vivo*, to determine whether these observations extend to other mouse models of CF (including mice carrying the G551D and

ΔF508 mutations in *Cftr*) and to determine the effect of different background strains. These studies illustrate the potential value of mouse models of CF in evaluating the *in vivo* significance of hypotheses borne from studies performed in transformed cell lines.

The role of the ASL in the pathogenesis of CF lung disease remains the subject of considerable controversy. Impairment of the salt–sensitive antimicrobial activity of β-defensins in ASL with a raised concentration of NaCl, secondary to CFTR dysfunction, has been proposed to explain the development of CF lung disease. The antibacterial profiles of synthetic β-defensins peptides were studied, representing the products of homologous human and murine β-defensin genes. Synthetic hBD-1 and mBD-1 peptides displayed broad spectrum, salt-sensitive, antibacterial activity in isolation, *in vitro*. The antibacterial profiles of these two peptides were demonstrated to vary significantly with respect to anti-pseudomonal activity, but were otherwise very similar. This may contribute to species specific patterns of bacterial susceptibility secondary to CFTR dysfunction and the resistance of mouse models of CF to lung infection with *P. aeruginosa*. Raised NaCl levels in the ASL of $Cftr^{tm1Hgu}/Cftr^{tm1Hgu}$ mice are likely to compromise the antibacterial activity of mBD-1 *in vivo*. This dysfunction may contribute to the abnormal pulmonary responses observed in these mice in response to lung infection with *S. aureus*, but have little effect upon the response to *P. aeruginosa*. Thus, it is possible that while the basic mechanisms underlying increased susceptibility to lung infection in CF may be conserved between mice and humans, this may not extend to the specific profile of bacterial susceptibility. Although $Cftr^{tm1Hgu}/Cftr^{tm1Hgu}$ mice may not necessarily demonstrate an identical bacterial infection profile to humans, the pulmonary response to the classical early stage CF-related lung pathogen *S. aureus*, may provide insights into the process of initiation of CF lung disease.

Further studies are required to build upon these results, including further analysis of other members of the β-defensin gene families and other

antimicrobial components of the ASL. In addition, analysis of the ASL in a well characterised air-interface primary culture model system and mouse models with targeted deletions of specific β-defensins are required to confirm the results of these *in vitro* studies. Additional studies might include complete characterisation of the *Defcr* locus and the development of mammalian expression systems in which to analyse biologically synthesised and processed β-defensins. A more complete understanding of the antibacterial activity of defensins and of the functional consequences of the species-specific variations observed in these molecules may prove to be of great value in the design of novel, antibacterial compounds active against multiple antibiotic resistant organisms. The use of gene expression arrays, based on the fully sequenced genome of *P. aeruginosa*, may provide interesting insights into the mechanism of bacterial killing employed by defensins and possible bacterial defence strategies.

Finally, a novel primary culture model of differentiated murine tracheal epithelium was established and characterised. This technique was demonstrated to facilitate the formation of confluent, polarised epithelial cultures with a high transepithelial resistance. Differentiation to produce ciliated cells and small numbers of goblet cells was demonstrated, with minimal contamination by non-epithelial cell types. The cultured cells were shown to express *Cftr* and murine β-defensin genes and to have an electrophysiological profile consistent with the presence of amiloride-sensitive sodium channels and cAMP-stimulated CFTR chloride channels. This model demonstrates important features of native murine tracheal epithelia, particularly with respect to the study of mouse models of CF. The model system will be of value in the future analysis of a) the ionic composition and volume control dynamics of murine ASL, b) the antibacterial properties of murine ASL and the key components of this response and c) in studies of the internalisation and adherence of CF related pathogens to murine airway epithelial cells. Such studies should be

performed using selected mouse models of CF and β-defensin knockout mice, on different background strains.

In conclusion, the studies presented in this thesis demonstrate and characterise a phenotype of abnormal pulmonary response to bacteria in mice secondary to mutations in *Cftr*. Important differences between the lung disease observed in mouse models of CF to date and human CF lung disease were recognised and possible explanations for such differences have been studied and discussed. While these species differences may prevent mouse models of CF from accurately reproducing all aspects of CF lung disease in humans, they may prove as illuminating as the similarities. Rather than exclusively pursuing the development of all aspects of classical human CF lung disease in mouse models, studies should specifically address the effects of *Cftr* mutation upon the lung pathophysiology of mice. In this manner the consequence of *Cftr* mutation in the mouse lung can be addressed and the underlying mechanisms evaluated. By recognising the key similarities and differences, mouse models of CF may provide ideal systems for the analysis of specific aspects of CF lung disease, such as the initial predisposition to infection with *S. aureus*. In this manner the validity of specific hypotheses may be examined in an *in vivo* model. Extrapolation to human disease processes can then be performed, recognising both the similarities and the differences between mice and humans. Furthermore, the contrasting phenotypes observed in different mouse models of CF, particularly between different background strains, are an important strength. Using such observations it may be possible to more clearly define the critical factors required for the development of CF lung disease in humans. By adopting such an approach, mouse models of CF can provide valuable contributions to our understanding of this disease process and support efforts towards organ-based treatment for CF patients.

References

Adler, K. B., Cheng, P.-W., and Kim, K. C. 1990 Characterization of guinea pig tracheal epithelial cells maintained in biphasic organotypic culture: cellular composition and biochemical analysis of released glycoconjugates. *Am. J. Respir. Cell Mol. Biol.* **2**; 145-154

Afzelius, B. A. 1997 Ciliary dysfunction. In *The Lung; Scientific Foundations 2nd Edition.* (ed. Crystal, R. G., West, J. B., Weibel, E. R., Barnes, P. J.) 2573-2578

Alton, E. W. F. W., Currie, D., Logan-Sinclair, R., Warner, J. O., Hodson, M. E., and Geddes, D. M. 1990 Nasal potential difference: a clinical diagnostic test for cystic fibrosis. *Eur. Respir. J.* **3**; 922-926

Alton, E. W. F. W., Middleton, P. G., Caplen, N. J., Smith, S. N., Steel, D. M., Munkonge, F. M., Jeffery, P. K., Geddes, D. M., Hart, S. L., Williamson, R., Fasold, K. I., Miller, A. D., Dickinson, P., Stevenson, B. J., McLachlan, G., Dorin, J. R., and Porteous, D. J. 1993 Non-invasive liposome-mediated gene delivery can correct the ion transport defect in cystic fibrosis mutant mice. *Nat. Gen.* **5**; 135-142

Andersen, D. H. 1938 Cystic fibrosis of the pancreas and its relation to celiac disease: a clinical and pathological study. *Am. J. Dis. Child.* **56**; 344-399

Anderson, M. P., Gregory, R. J., Thompson, S., Souza, D. W., Paul, S., Mulligan, R. C., Smith, A. E., and Welsh, M. J. 1991a Demonstration that CFTR is a chloride channel by alteration of its anion selectivity. *Science* **253**; 202-205

Anderson, M. P., Berger, H. A., Rich, D. P., Gregory, R. J., Smith, A. E., and Welsh, M. J. 1991b Nucleoside triphosphates are required to open the CFTR chloride channel. *Cell* **67**; 775-784

Anderson, M. P., Sheppard, D. N., Berger, H. A., and Welsh, M. J. 1992 Chloride channels in the apical membrane of normal and cystic fibrosis airway and intestinal epithelia. *Am. J.Physiol.* **263**; L1-L14

Armstrong, D. S., Grimwood, K., Carlin, J. B., Carzino, R., Gutierrez, J. P., Hull, J., Olinsky, A., Phelan, E. M., Robertson, C. F., and Phelan, P. D. 1997 Lower airway inflammation in infants and young children with cystic fibrosis. *Am. J. Respir. Crit. Care Med.* **156**; 1197-1204

Armstrong, D., Grimwood, K., Carlin, J. B., Carzino, R., Hull, J., Olinsky, A., and Phelan, P. D. 1998 Severe viral respiratory infections in infants with cystic fibrosis. *Pediatr. Pulmonol.* **26**; 371-379

Aronson, M., Medalia, O., Amichay, D., and Nativ, O. 1988 Endotoxin-induced shedding of viable uroepithelial cells is an antimicrobial defence mechanism. *Infect. Immun.* **56** (6); 1615-1617

Baconnais, S., Zahm, J.-M., Killian, L., Bonhomme, P., Gobillard, D., Perchet, A., Puchelle, E., and Balossier, G. 1998. X-ray microanalysis of native airway surface liquid collected by cryotechnique. *J. Microsc.* **191**; 311-319

Ballard, S. T., Fountain, J. D., Inglis, S. K., Corboz, M. R., and Taylor, A. E. 1995 Chloride secretion across distal airway epithelium: relationship to submucosal gland distribution. *Am. J. Physiol.* **268**; L526-L531

Bals, R., Goldman, M. J., and Wilson, J. M. 1998a Mouse beta-defensin 1 is a salt-sensitive antimicrobial peptide present in epithelia of the lung and urogenital tract. *Infect. Immun.* **66** (3); 1225-32

Bals, R., Wang, X., Wu, Z., Freeman, T., Bafna, V., Zasloff, M., and Wilson, J. M. 1998b Human β-defensin 2 is a salt-sensitive peptide antibiotic expressed in human lung. *J. Clin. Invest.* **102** (5); 874-880

Bals, R., Wang, X., Zasloff, M., and Wilson, J. M. 1998c The peptide antibiotic LL-37/hCAP-18 is expressed in epithelia of the human lung where it has broad antimicrobial activity at the airway surface. *Proc. Natl. Acad. Sci. USA* **95** (16); 9541-9546

Bals, R., Wang, X., Meegalla, R. L., Wattler, S., Weiner, D., Nehls, M. C., and Wilson, J. M. 1999 Mouse β-defensin 3 is an inducible antimicrobial peptide expressed in the epithelia of multiple organs. *Infect. Immun.* **67** (7); 3542-3547

Barasch, J., Kiss, B., Prince, A., Saiman, L., Gruenert, D., and Al-Awqati, Q. 1991 Defective acidification of intracellular organelles in cystic fibrosis. *Nature* **352**; 70-73

Bear, C. E., Li, C. H., Kartner, N., Bridges, R. J., Jensen, T. J., Ramjeesingh, M., and Riordan, J. R. 1992 Purification and functional reconstitution of the cystic fibrosis transmembrane conductance regulator (CFTR). *Cell* **68**; 809-818

Beckman, W. and Lessie, T. G. 1979 Response of *Pseudomonas cepacia* to β-lactam antibiotics: utilisation of penicillin G as the carbon source. *J. Bacteriol.* **140** (3); 1126-1128

Bensch, K. W., Raida, M., Mägert, H.-J., Schulz-Knappe, P., and Forssmann, W.-G. 1995 hBD-1: a novel β-defensin from human plasma. *FEBS Letters* **368**; 331-335

Berger, J., Sorensen, R. U., Tosi, M. F., Dearbron, D. G., and Döring, G. 1989 Complement receptor expression on neutrophils at an inflammatory site, the *Pseudomonas* infected lung in cystic fibrosis. *J. Clin. Invest.* **84**; 1302-1313

Birrer, P., McElvaney, N. G., Rüdeberg, A., Wirz Sommer, C., Liechti-Gallati, S., Kraemer, R., Hubbard, R., and Crystal, R. G. 1994 Protease-antiprotease imbalance in the lungs of children with cystic fibrosis. *Am. J. Respir. Crit. Care Med.* **150**; 207-213

Bliss, C. I. 1967 Provisionally normal distributions. In *Statistics in biology* (ed. Bliss, C. I.) McGraw-Hill Inc., New York; 152-155

Boat, T. J., Welsh, M. J., and Beaudet, A. L. 1989 Cystic Fibrosis. In *The metabolic basis of inherited disease Vol II.* (ed Scriver, C. R., Beaudet, A. L., Sly, W. S., and Valle, D.) McGraw-Hill Inc, New York; 2649-2682

Bonfield, T. L., Panuska, J. R., Konstan, M. W., Hilliard, K. A., Hilliard, J. B., Ghniam, H., and Berger, M. 1995 Inflammatory cytokines in cystic fibrosis lungs. *Am. J. Respir. Crit. Care Med.* **152**; 2111-2118

Bonfield, T. L., Konstan, M. W., and Berger, M. 1999 Altered respiratory epithelial cell cytokine production in cystic fibrosis. *J. Allergy Clin. Immunol.* **104**; 72-78

Borthwick, D. W., Krantz, T., Dorin, J. R., and Randell, S. H. 1998 A potential stem cell niche in the ciliated ducts of murine submucosal glands. *Pediatr. Pulmonol.* (Suppl. 17); 283

Borthwick, D. W., West, J. D., Keighren, M. A., Flockhart, J. H., Innes, B. A., and Dorin, J. R. 1999 Murine submucosal glands are clonally derived and show a *Cftr* dependent distribution pattern. *Am. J. Respir. Cell Mol. Biol.* **20**; 1181-1189

Boucher, J. C., Yu, H., Mudd, M. H., and Deretic, V. 1997 Mucoid *Pseudomonas aeruginosa* in cystic fibrosis: characterisation of *muc* mutations in clinical isolates and analysis of clearance in a mouse model of respiratory infection. *Infect. Immun.* **65** (9); 3838-3846

Boucher, R. C. 1994 Human airway ion transport (Part one). *Am. J. Respir. Crit. Care Med.* **150**; 271-281

Boucher, R. C. 1999 Status of gene therapy for cystic fibrosis. *J. Clin. Invest.* **103** (4); 441-445

Bradbury, N. A., Jilling, T., Berta, G., Sorscher, E. J., Bridges, R. J., and Kirk, K. L. 1992 Regulation of plasma membrane recycling by CFTR. *Science* **256**; 530-532

Bradbury, N. A. 1999 Intracellular CFTR: localisation and function. *Phys. Rev.* **79** (Suppl.1); S175-S191

Bronsveld, I., Bijman, J., Mekus, F., Laabs, U., Ballmann, M., Ellemunter, H., Mastella, G., Thomas, S., Veeze, H., and Tümmler, B. 1998 European cystic fibrosis twin and sibling study: intrapair and interpair comparison of

electrophysiological properties in airways and intestinal tissue. *Pediatr. Pulmonol.* (Suppl. 17); 247

Burkholder, W. H. 1950 Sour skin, a bacterial rot of onion bulbs. *Phytopath.* **40**; 115-117

Cannon, C. L., Stopak, K., and Pier, G. B. 1999 Defective apoptosis of lung cells expressing mutant CFTR after infection with *Pseudomonas aeruginosa*. *Pediatr. Pulmonol.* (Suppl. 19); 322

Carroll, T. P., Morales, M. M., Fulmer, S. B., Allen, S. S., Flotte, T. R., Cutting, G. R., and Guggino, W. B. 1995 Alternate translation initiation codons can create functional forms of cystic fibrosis transmembrane conductance regulator. *J. Biol.Chem.* **270**; 11941-11946

Chandy, G., Moore, H. P., and Machen, T. E. 1999 Regulation of golgi pH in human respiratory epithelial cells measured with targeted GFP. *Pediatr. Pulmonol.* (Suppl. 17); 249

Chang, L.-Y., Wu, R., and Nettesheim, P. 1995 Morphological changes in rat tracheal cells during the adaptive and early growth phase in primary cell culture. *J. Cell Sci.* **74**; 283-301

Cheng, S. H., Gregory, R. J., Marshall, J., Paul, S., Souza, D. W., White, G. A., O'Riordan, C. R., and Smith, A. E. 1990 Defective intracellular transport and processing of CFTR is the molecular basis of most cystic fibrosis. *Cell* **63**; 827-834

Chmiel, J. F., Konstan, M. W., Knesebeck, J. E., Hilliard, J. B., Bonfield, T. L., Dawson, D. V., and Berger, M. 1999 IL-10 attenuates excessive inflammation

in chronic *Pseudomonas* infection in mice. *Am. J. Respir. Crit. Care Med.* **160**; 2040-2047

Chu, C. S., Trapnell, B. C., Curristin, S. M., Cutting, G. R., and Crystal, R. G. 1992 Extensive post-transcriptional deletion of the coding sequences for part of nucleotide-binding fold-1 in respiratory epithelial messenger-RNA transcripts of the cystic fibrosis transmembrane conductance regulator gene is not associated with the clinical manifestations of cystic fibrosis. *J. Clin. Invest.* **90**; 785-790

Clark, A. B., Randell, S. H., Nettesheim, P., Gray, T. E., Bagnell, B., and Ostrowski, L. E. 1995 Regulation of ciliated cell differentiation in cultures of rat tracheal epithelial cells. *Am. J. Respir. Cell Mol. Biol.* **12**; 329-338

Clarke, L. L., Grubb, B. R., Gabriel, S. E., Smithies, O., Koller, B. H., and Boucher, R. C. 1992a Defective epithelial chloride transport in a gene targeted mouse model of cystic fibrosis. *Science* **257**; 1125-1128

Clarke, L. L., Burns, K. A., Bayle, J.-Y., Boucher, R. C., and Van Scott, M. R. 1992b Sodium- and chloride-conductive pathways in cultured mouse tracheal epithelium. *Am. J. Physiol.* **263**; L519-L525

Clarke, L. L., Grubb, B. R., Yankaskas, J. R., Cotton, C. U., McKenzie, A. and Boucher, R. C. 1994 Relationship of a non-CFTR mediated chloride conductance to organ level disease in cftr (-/-) mice. *Proc. Natl. Acad. Sci. USA* **91**; 479-483

Cohn, J. A. 1994 CFTR localisation: implications for cell and tissue pathophysiology. In *CF - Current Topics, Volume 2.* (ed, Dodge, J. A., Brock, D. J. H., and Widdicombe, J. H.); 173-191

Colledge, W. H., Abella, B. S., Southern, K. W., Ratcliff, R., Jiang, C. W., Cheng, S. H., Macvinish, L. J., Anderson, J. R., Cuthbert, A. W., and Evans, M. J. 1995 Generation and characterisation of a delta-F508 cystic fibrosis mouse model. *Nature Genetics* **10**; 445-452

Cowley, E. A., Wang, C.-G., Gosselin, D., Radzioch, D., and Eidelman, D. H. 1997a Mucociliary clearance in cystic fibrosis knockout mice infected with *Pseudomonas aeruginosa*. *Eur. Respr. J.* **10**; 2312-2318

Cowley, E. A., Govindaraju, K., Lloyd, D. K., and Eidelman, D. H. 1997b Airway surface fluid composition in the rat determined by capillary electrophoresis. *Am. J. Physiol.* **273**; L895-L899

Cowley, E. A., Govindaraju, K., Radzioch, D., and Eidelman, D. H. 1998 ASF composition in CFTR knockout mice. *Pediatr. Pulmonol.* (Suppl. 17); 237

Cressman, V. L., Hicks, E. M., Funkhouser, W. K., Backlund, D. C., and Koller, B. H. 1998 The relationship of chronic mucin secretion to airway disease in normal and CFTR-deficient mice. *Am. J. Respir. Cell Mol. Biol.* **19** (6); 853-66

Dankert-Roelse, J. E., and Te Meerman G. J. 1997 Screening for cystic fibrosis – time to change our position. *New Eng. J. Med.* **337** (14); 997-998

Davidson, D. J., Dorin, J. R., McLachlan, G., Ranaldi, V., Lamb, D., Doherty, C., Govan, J. R. W., and Porteous, D. J. 1995 Lung disease in the cystic fibrosis mouse exposed to bacterial pathogens. *Nature Genetics* **9**; 351-357

Davidson, D. J., and Porteous, D. J. 1998 The genetics of cystic fibrosis lung disease. *Thorax* **53** (5); 389-397

Davies, J. C., Stern, M., Dewar, A., Caplen, N. J., Munkonge, F. M., Pitt, T., Sorgi, F., Huang, L., Bush, A., Geddes, D. M., and Alton, E. W. F. W. 1997 CFTR gene transfer reduces the binding of *Pseudomonas aeruginosa* to cystic fibrosis respiratory epithelium. *Am. J. Respir. Cell Mol. Biol.* **16**; 657-663

Davies, J. C., Dewar, A., Bush, A., Pitt, T., Gruenert, D., Geddes, D. M., and Alton, E. W. F. W. 1999 Reduction in the adherence of *Pseudomonas aeruginosa* to native cystic fibrosis epithelium with anti-asialoGM1 antibody and neuraminidase inhibition. *Eur. Respir. J.* **13**; 565-570

Davies, D. G., Parsek, M. R., Pearson, J. P., Iglewski, B. H., Costerton, J. W., and Greenberg, E. P. 1998 The involvement of cell-to-cell signals in the development of a bacterial biofilm. *Science* **280**; 295-298

DeBentzmann, S., Roger, P., Dupuit, F., Bajoletlaudinat, O., Fuchey, C., Plotkowski, M. C., and Puchelle, E. 1996 AsialoGM1 is a receptor for *Pseudomonas aeruginosa* adherence to regenerating respiratory epithelial cells. *Infect. Immun.* **64**; 1582-1588

Delaney, S. J., Alton, E. W. F. W., Smith, S. N., Lunn, D. P., Farley, R., Lovelock, P. K., Thomson, S. A., Hume, D. A., Lamb, D., Porteous, D. J., Dorin, J. R., Wainwright, B. J. 1996 Cystic fibrosis mice carrying the missense mutation G551D replicate human genotype-phenotype correlations. *Embo Journal* **15**; 955-963

DeLisle, R. C. 1995 Increased expression of sulfated gp300 and acinar tissue pathology in Cftr (-/-) mice. *Am. J. Physiol.* **268**; G717-G723

Denning, G. M., Anderson, M. P., Amara, J. F., Marshall, J., Smith, A. E., and Welsh, M. J. 1992 Processing of mutant cystic fibrosis transmembrane conductance regulator is temperature-sensitive. *Nature* **358**; 761-764

Devidas, S., and Guggino, W. B. 1997 The cystic fibrosis transmembrane conductance regulator and ATP. *Curr. Opin. Cell Biol.* **9**; 547-552

Dickinson, P., Kilanowski, F., Kimber, W., Webb, S., Taylor, M. S., Porteous, D. J., and Dorin, J. R. 1998 Generation of a CF mutant mouse possessing the G480C mutation. *22nd European CF conference Berlin Book of Abstracts*, PS7.14; 143

Di Sant'Agnese, P. A., and Anderson, D. L. 1946 Celiac Syndrome: chemotherapy of infections of the respiratory tract associated with cystic fibrosis of the pancreas; observations with penicillin and drugs of the sulphonamide groups, with special reference to penicillin aerosol. *Am. J. Dis. Child* **72**; 17-61

Dodge, J. A. 1999 Why screen for cystic fibrosis? A clinician's view. *Acta Paediatr.* (Suppl 432); 28-32

Dorin, J. R., Dickinson, P., Alton, E. W. F. W., Smith, S. N., Geddes, D. M., Stevenson, B. J., Kimber, W. L., Fleming, S., Clarke, A. R., Hooper, M. L., Anderson, L., Beddington, R. S. P., and Porteous, D. P. 1992 Cystic fibrosis in the mouse by targeted insertional mutagenesis. *Nature* **359**; 211-215

Dorin, J. R., Stevenson, B. J., Fleming, S., Alton, E. W. F. W., Dickinson, P., and Porteous, D. J. 1994 Long term survival of the exon 10 insertional cystic fibrosis mutant mouse is a consequence of low level residual wild type *Cftr* gene expression. *Mamm. Genet.* **5**; 465-472

Dorin, J. R., Farley, R., Webb, S., Smith, S. N., Farini, E., Delaney, S. J., Wainwright, B. J., Alton, E. W. F. W., and Porteous, D. J. 1996 A demonstration using mouse models that successful gene therapy for cystic fibrosis requires only partial gene correction. *Gene Therapy* **3**; 797-801

Dorin, J. R., Davidson, D. J., Innes, B. A., Webb, S., Farley, R., Smith, S. N., and Alton, E. W. F. W. 1997 Respiratory tract phenotype in different inbred and congenic CF mice strains. *Pediatr. Pulmonol.* (Suppl. 14); 182

Döring, G. 1999 Serine proteinase inhibitor therapy in α_1-antitrypsin inhibitor deficiency and cystic fibrosis. *Pediatr. Pulmonol.* **28**; 363-375

Drittanti, L., Masciovecchio, M. V., Gabbarini, J., and Vega, M. 1997 Cystic fibrosis: gene therapy or preventive gene transfer? *Gene Therapy* **4**; 1001-1003

Drumm, M. 1999 What happens to ΔF508 in vivo? *J. Clin. Invest.* **103** (10); 1369–1370

Durie, P. R., Ahmed, N., Corey, M., Zielenski, J., Ellis, L., Tullis, E., and Tsui, L.-C. 1999 CFTR gene mutations and the pancreatic phenotype. *Pediatr. Pulmonol.* (Suppl. 19); 127

Eisenhauer, P. B. and Lehrer, R. I. 1992 Mouse neutrophils lack defensins. *Infect. Immun.* **60** (8); 3446-3447

Ellsworth, R. E., Jamison, D. C., Touchman, J. W., Chissoe, S. L., Braden Maduro, V. V., Bouffard, G. G., Dietrich, N. L., Beckstrom-Sternberg, S. M., Iyer, L. M., Weintraub, L. A., Cotton, M., Courtney, L., Edwards, J., Maupin, R., Ozersky, P., Rohlfing, T., Wohldmann, P., Miner, T., Kemp, K., Kramer, J., Korf, I., Pepin, K., Antonacci-Fulton, L., Fulton, R. S., Minx, P., and Hillier, L.

W. 2000 Comparative genomic sequence analysis of the human and mouse cystic fibrosis transmembrane conductance regulator genes. *Proc. Natl. Acad. Sci. USA* **97** (3); 1172-1177

Engelhardt, J. F., Yankaskas, J. R., Ernst, S. A., Yang, Y., Marino, C. R., Boucher, R. C., Cohn, J. A., and Wilson, J. M. 1992 Submucosal glands are the predominant site of CFTR expression in the human bronchus. *Nat. Genet.* **2**; 240-247

Esterly, J. R., and Oppenheimer, E. H. 1968 Cystic fibrosis of the pancreas: structural changes in peripheral airways. *Thorax* **23**; 670-675

Estivill, X. 1996 Complexity in a monogenic disease. *Nat. Genet.* **12**; 348-350

Farley, R., Smith, S. N., Innes, B., Webb, S., Alton, E. W. F. W., and Dorin, J. R. 1998 Mouse models for modifier genes in cystic fibrosis. *Pediatr. Pulmonol.* (Suppl. 17); 304

Farrell, P. M., Kosorok M. R., Laxova, A., Shen, G., Koscik, R. E., Bruns, W. T., Splaingard, M., and Mischler, E. H. 1997 Nutritional benefits of neonatal screening for cystic fibrosis. *New Engl. J. Med.* **337**; 963-969

Feinberg, A. P., and Vogelstein, B. 1983 A technique for radiolabelling DNA restriction endonuclease fragments to high specific activity. *Anal. Biochem.* **132** (1); 6-13

Figarella, C. and Carrere, J. 1994 The evolution of pancreatic disease in cystic fibrosis. In *Cystic Fibrosis - Current topics, Volume 2.* (ed. Dodge, J. A., Brock, D. J. H., Widdicombe, J. H.) John Wiley and Sons Ltd. Chichester, UK; 255-275

Fleiszig, S. M. J., Zaidi, T. S., and Pier, G. B. 1995 *Pseudomonas aeruginosa* invasion of and multiplication within corneal epithelial cells *in vitro*. *Infect. Immun.* **63**; 4072-4077

Freedman, S. D., Katz, M. H., Parker, E. M., Laposata, M., Urman, M. Y. and Alvarez, J. G. 1999 A membrane lipid imbalance plays a role in the phenotypic expression of cystic fibrosis in *cftr*$^{-/-}$ mice. *Proc. Natl. Acad. Sci. USA* **96**; 13995-14000

Fuchs, E., Tyner, A. L., Giudice, G. J., Marchuk, D., RayChaudhury, A., and Rosenberg, M. 1987 The human keratin genes and their differential expression. *Curr. Top. Dev. Biol.* **22**; 5-34

Gadsby, D. C., and Nairn, A. C. 1999 Control of CFTR channel gating by phosphorylation and nucleotide hydrolysis. *Physiol. Rev.* **79** (Suppl. 1); S77-S107

Ganz, T. and Lehrer, R. I. 1995 Defensins. *Pharm. Ther.* **66**; 191-205

Ganz, T. 1998 Defensins are not the principal antimicrobial substances in ASL. *Pediatr. Pulmonol.* (Suppl. 17); 130

Ganz, T. 1999 Defensins and host defence. *Science* **286**; 420-421

Ganz, T., and Lehrer, R. I. 1999 Antibiotic peptides from higher eukaryotes: biology and applications. *Mol. Med. Today* **5**; 292-297

Garred, P., Pressler, T., Madsen, H., O., Frederiksen, B., Svejgaard, A., Høiby, Schwartz, M., and Koch, C. 1999 Association of mannose-binding lectin gene heterogeneity with severity of lung disease and survival in cystic fibrosis. *J. Clin. Invest.* **104** (4); 431-437

Gilligan, P. H. 1991 Microbiology of airway disease in patients with cystic fibrosis. *Clin. Micro. Rev.* **4** (1); 35-51

Gilljam, H., Ellin, A. and Strandvik, B. 1989 Increased bronchial chloride concentration in cystic fibrosis. *Scand. J. Clin. Lab. Invest.* **49**; 121-124

Goldman, M. J., Anderson, G. M., Stolzenberg, E. D., Kari, U. P., Zasloff, M., and Wilson, J. M. 1997 Human beta-defensin-1 is a salt-sensitive antibiotic in lung that is inactivated in cystic fibrosis. *Cell* **88** (4); 553-560

Gosselin, D., DeSanctis, J., Boule, M., Skamene, E., Matouk, C., and Radzioch, D. 1995, Role of tumour necrosis factor alpha in innate resistance to mouse pulmonary infection with *Pseudomonas aeruginosa*. *Infect. Immun.* **63** (9); 3272-3278

Gosselin, D., Stevenson, M. M., Cowley, E. A., Griesenbach, U., Eidelman, D. H., Boulé, M., Tam, M. F., Kent, G., Skamene, E., Tsui, L.-C., and Radzioch, D. 1998. Impaired ability of *Cftr* knockout mice to control lung infection with *Pseudomonas aeruginosa*. *Am. J. Respir. Crit. Care Med.* **157**; 1253-1262

Govan, J. R. W., and Harris, G. S. 1986 *Pseudomonas aeruginosa* and cystic fibrosis: unusual bacterial adaptation and pathogenesis. *Micro. Sciences* **3** (10); 302-308

Govan, J. R. W., and Nelson, J. W. 1992 Microbiology of lung infection in cystic fibrosis. *Brit. Med. Bulletin* **48**; 912-930

Govan, J. R. W., Brown, P. H., Maddison, J., Doherty, C. J., Nelson, J. W., Dodd, M., Greening, A. P., and Webb, A. K. 1993 Evidence for the

transmission of *Pseudomonas cepacia* by social contact in cystic fibrosis. *Lancet* **342**; 15-19

Govan, J. R. W. and Deretic, V. 1996 Microbial pathogenesis in cystic fibrosis: mucoid *Pseudomonas aeruginosa* and *Burkholderia cepacia*. *Microbiological Reviews* **60** (3); 539-574

Grasemann, H., and Ratjen, F. 1999 Cystic fibrosis lung disease: the role of nitric oxide. *Pediatr. Pulmonol.* **28**; 441-448

Gray, M. A., Winpenny, J. P., Verdon, B., McAlroy, H., and Argent, B. E. 1995 Chloride channels and cystic fibrosis of the pancreas. *Bioscience Reports* **15** (6); 531-541

Grimwood, K., Armstrong, D., Carlin, J., Carzino, R., Kyd, J., Moore, R., and Olinsky, A. 1997 Acquisition of *Pseudomonas aeruginosa* in young infants. *Pediatr. Pulmonol.* (Suppl. 14); 133

Grubb, B. R., Vick, R. N., and Boucher, R. C. 1994a Hyperabsorption of Na^+ and raised Ca^{2+}-mediated Cl^- secretion in nasal epithelia of CF mice. *Am. J. Physiol.* **266**; C1478-C1483

Grubb, B. R., Paradiso, A. M., and Boucher, R. C. 1994b Anomolies in ion transport in CF mouse tracheal epithelium. *Am. J. Physiol.* **267**; C293-C300

Grubb, B. R. and Boucher, R. C. 1999 Gene-targeted mouse models for cystic fibrosis. *Physiol. Rev.* **79** (Suppl. 1); S193-S214

Guggino, W. B. 1999 Cystic fibrosis and the salt controversy. *Cell* **96**; 607-610

Guin, W. M. O., Galvin, S., Schermer, A., and Sun, T.-T. 1987 Patterns of keratin expression define distinct pathways of epithelial development and differentiation. *Curr. Top. Dev. Biol.* **22**; 97-127

Hamosh A., King, T. M., Rosenstein, B. J., Corey, M., Levison, H., Durie, P., Tsui, L.-C., McIntosh, I., Keston, M., Brock ,D. J., Macek Jr., M., Zemkova, D., Krasniconova, H., Vavrova, V., Macek Sr., M., Golder, G., Schwarz, M. J., Super, M., Watson, E. K., Williams, C., Bush, A., O'Mahoney, S. M., Humphries, P., DeArce, M. A., Reis, A., Burger, J., Stuhrmann, M., Schmidtke, J., Wulbrand, U., Dork, T., Tummler, B., and Cutting, G. 1992 Cystic fibrosis patients bearing both the common missense mutation Gly-Asp at codon 551 and the delta F508 mutation are clinically indistinguishable from delta F508 homozygotes, except for decreased risk of meconium ileus. *Am. J. Hum. Genet.* **51** (2); 245-50

Hancock, R. E. W. 1997 Peptide antibiotics. *Lancet* **349**; 418-422

Hancock, R. E. W. 1998 Resistance mechanisms in *Pseudomonas aeruginosa* and other nonfermentative gram-negative bacteria. *Clin. Infect. Dis.* **27**, (Suppl. 1); S93-S99

Hancock, R. E. W., and Chapple D. S. 1999 Peptide antibiotics. *Antimicrob. Agents. Chemo.* **43** (6); 1317-1323

Harder, J., Bartels, J., Christophers, E., and Schröeder, J.-M. 1997 A peptide antibiotic from human skin. *Nature* **387**; 861

Haston, C. K., McKerlie, C., Corey, M., Budisin, B., Samanta, T., Kent, G., Tsui, L.-C., and Rozmahel, R. 1999. *Pediatr. Pulmonol.* (Suppl. 19); 217

Hasty, P., Ramirezsolis, R., Krumlauf, R., and Bradley, A. 1991 Introduction of a subtle mutation into the hox-2.6 locus in embryonic stem-cells. *Nature* **350**; 243-246

Hasty, P., O'Neal, W. K., Liu, K. Q., Morris, A. P., Bebok, Z., Shumyatsky, G. B., Jilling, T., Sorscher, E. J., Bradley, A., and Beaudet, A. L. 1995 Severe phenotype in mice with termination mutation in exon 2 of cystic fibrosis gene. *Som. Cell Mol. Genet.* **21**; 177-187

Hiemstra, P. S., Maassen, R. J., Stolk, J., Heinzel-Wieland, R., Steffens, G. J., and Dijkman, J. H. 1996 Antibacterial activity of antileukoprotease. *Infect. Immun.* **64** (11); 4520-4524

Ho, L.-P., Innes, J. A., and Greening, A. P. 1998 Exhaled nitric oxide is not elevated in the inflammatory airways diseases of cystic fibrosis and bronchiectasis. *Eur. Respir. J.* **12**; 1290-1294

Ho, W. and Furst, A. 1973 Intratracheal instillation method for mouse lungs. *Oncology* **27**; 385-393

Hull, J., Skinner, W., Roberston, C., and Phelan, P. 1998 Elemental content of airway surface liquid from infants with cystic fibrosis. *Am. J. Respir. Crit. Care Med.* **157**; 10-14

Hutchison, M. L., and Govan, J. R. W. 1999 Pathogenicity of microbes associated with cystic fibrosis. *Microbes and Infection* **1**; 1005-1014

Hutchison, M. L., Bonell, E. C., Poxton, I. R., and Govan, J. R. W. 2000 Endotoxic activity of lipopolysaccharides isolated from emergent potential cystic fibrosis pathogens. *FEMS Immunol. Med. Micro.* **27**; 73-77

Huttner, K. M., Kozak, C. A., and Bevins, C. L. 1997 The mouse genome encodes a single homolog of the antimicrobial peptide human beta-defensin 1. *FEBS Letters* **413**; 45-49

Huttner, K. M. and Bevins, C. L. 1999 Antimicrobial peptides as mediators of epithelial host defense. *Pediatr. Res.* **45** (6); 785-794

Hyde, S. C., Gill, D. R., Higgins, C. F., Trezise, A. E. O., MacVinish, L. J., Cuthbert, A. W., Ratcliff, R., Evans, M. J., and Colledge, W. H. 1993 Correction of the ion transport defect in cystic fibrosis transgenic mice by gene therapy. *Nature* **362**; 250-255

Imundo, L., Barasch, J., Prince, A., and Al-Awqati, Q. 1995 Cystic fibrosis epithelial cells have a receptor for pathogenic bacteria on their apical surface. *Proc. Natl. Acad. Sci. USA* **92**; 3019-3023

Innes, B. A., and Dorin, J. R. 1999 QTL mapping identifies loci associated with submucosal gland distribution in mice. *Pediatr. Pulmonol.* (Suppl. 19); 217

Ip, W. F., Bronsveld, I., Kent, G., Corey, M., and Durie, P. 1996 Exocrine pancreatic alteration in long-lived surviving cystic fibrosis mice. *Pediatr. Res.* **40** (2); 242-249

Isles, A., Maclusky, I., Corey, M., Gold, R., Prober, C., Fleming, P., and Levison, H. 1984 *Pseudomonas cepacia* infection in cystic fibrosis: an emerging problem. *J. Pediatr.* **104** (2); 206-210

Ismailov, I. I., Awayada, M. S., Jovov, B., Berdiev, B. K., Fuller, C. M., Dedman, J. R., Kaetzel, M. A., and Benos, D. J. 1996 Regulation of epithelial

sodium channels by the cystic fibrosis transmembrane conductance regulator. *J. Biol. Chem.* **271** (9); 4725-4732

Jia, H. P., Schutte, B. C., Tack, B. F., Bevins, C. L., and McCray, P. B. 1999 Cloning and characterisation of a murine β-defensin homologue. *Pediatr. Pulmonol.* (Suppl. 19); 323

Johnson, L. G., Olsen, J. C., Sarkadi, B., Moore, K. L., Swanstrom, R., and Boucher, R. C. 1992 Efficiency of gene transfer for restoration of normal airway epithelial function in cystic fibrosis. *Nat. Genet.* **2**; 21-25

Johnson, N. F., Wilson, J. S., Habbersett, R., Thomassen, D. G., Shopp, G. M., and Smith, D. M. 1990 Separation and characterisation of basal and secretory cells from the rat trachea by flow cytometry. *Cytometry* **11** (3); 395-405

Joris, L., and Quinton, P. M. 1992 Filter paper equilibration as a novel technique for *in vitro* studies of the composition of airway surface fluid. *Am. J. Physiol.* **263**; L243-L248

Joris, L., Dab, I., and Quinton, P. M. 1993 Elemental composition of human airway surface fluid in healthy and diseased airways. *Am. Rev. Respir. Dis.* **148**; 1633-1637

Kälin, N., Claaß, A., Sommer, M., Puchelle, E., and Tümmler, B. 1999 ΔF508 CFTR protein expression in tissues from patients with cystic fibrosis. *J. Clin. Invest.* **103** (10); 1379-1389

Kaartinen, L., Nettesheim, P., Adler, K. B., and Randell, S. H. 1993 Rat tracheal epithelial cell differentiation in vitro. *In Vitro Cell. Dev. Biol.* **29A**; 481-492

Kartner, N., Augustinas, O., Jensen, T. J., Naismith, L., and Riordan, J. R. 1992 Mislocalization of ΔF508 CFTR in cystic fibrosis sweat gland. *Nat. Genet.* **1**; 321-327

Kelley, T. J., and Drumm, M. L. 1998 Inducible nitric oxide synthase expression is reduced in cystic fibrosis murine and human airway epithelial cells. *J. Clin. Invest.* **102** (6); 1200-1207

Kelly, F. J. 1999 Glutathione: in defence of the lung. *Food Chem. Tox.* **37**; 963-966

Kent, G., Oliver, J. K., Foskett, H., Frndova, H., Durie, P., Forstner, J., Forstner, G. G., Riordan, J. R., Percy, D., and Buchwald, M. 1996 Phenotypic abnormalities in long-term surviving cystic fibrosis mice. *Pediatr. Res.* **40**(2); 233-241

Kent, G., Iles, R., Bear, C. E., Huan, L. J., Griesenbach, U., McKerlie, C., Frndova, H., Ackerley, C., Gosselin, D., Radzioch, D., O'Brodovich, H., Tsui, L.-C., Buchwald, M., Tanswell, A. K. 1997 Lung disease in mice with cystic fibrosis. *J. Clin. Invest.* **100** (12); 3060-9

Kerem, B. S., Rommens, J. M., Riordan, J. A., Markiewicz, D., Cox, T. K., Chakravarti, A., Buchwald, M., and Tsui, L.-C. 1989 Identification of the cystic fibrosis gene – genetic analysis. *Science* **245**; 1073-1080

Kerem, E., and Kerem, B. 1995 The relationship between genotype and phenotype in cystic fibrosis. *Curr. Opin. Pulmon. Med.* **1**; 450-456

Kerem, B. and Kerem, E. 1996 The molecular basis for disease variability in cystic fibrosis. *Eur. J. Hum. Genet.* **4**; 65-73

Kerem, E., Bistrizer, T., Hanukoglu, A., Maclaughlin, E., Boucher, R., and Knowles, M. 1997 Respiratory disease in patients with the systemic form of pseudohypoaldosteronism type I. *Pediatr. Pulmonol.* (Suppl. 14); 78

Khan, T. Z., Wagener, J. S., Bost, T., Martinez, J., Accurso, F. J., and Riches, D. W. H. 1995 Early pulmonary inflammation in infants with cystic fibrosis. *Am. J. Respir. Crit. Care Med.* **151**; 1075-1082

Knowles, M., Gatzy, J., and Boucher, R. 1981 Increased bioelectric potential difference across respiratory epithelia in cystic fibrosis. *N. Engl. J. Med.* **305**(25); 1489-1495

Knowles, M. R., Robinson, J. M., Wood, R. E., Pue, C. A., Mentz, W. M., Wager, G. C., Gatzy, J. T., and Boucher, R. C. 1997 Ion composition of airway surface liquid of patients with cystic fibrosis as compared with normal and disease-control subjects. *J. Clin. Invest.* **100**; 2588-2595

Kondo, M., Finkbeiner, W. E., and Widdicombe, J. H. 1991 Simple technique for culture of highly differentiated cells from dog tracheal epithelium. *Am. J. Physiol.* **261**; L106-L117

Konstan, M. W. and Berger, M. 1993 Infection and inflammation of the lung in cystic fibrosis. In *Cystic Fibrosis, Lung Biology in Health and Disease* (ed. Davis, P. B.) Dekker, New York; 219-275

Kopito, R. R. 1999 Biosynthesis and degradation of CFTR. *Phys. Rev.* **79**, (Suppl. 1); S167-S174

Kubesh, P., Dörk, T., Wulbrand, U, Kälin, N., Neumann, T., Wulf, B., Geerlings, H., Weißbrodt, H., von der Hardt, H., and Tümmler, B. 1993

Genetic determinants of airways' colonisation with *Pseudomonas aeruginosa* in cystic fibrosis. *Lancet* **341**; 189-193

Kumar, R. K., Maronese, S. E., and O'Grady, R. 1997 Serum-free culture of mouse tracheal epithelial cells. *Exp. Lung Res.* **23**; 427-440

Kunzelman, K., Kiser, G. L., Schreiber, R., and Riordan, J. R. 1997 Inhibition of epithelial Na^+ currents by intracellular domains of the cystic fibrosis transmembrane conductance regulator. *FEBS Letters* **400**; 341-344

Lanng, S., Schwartz, M, Thorsteinsson, B and Koch, C. 1991 Endocrine and exocrine pancreatic function and the ΔF508 mutation in cystic fibrosis. *Clin. Genet.* **40**; 345-348

Larbig, M., Steinmetz, I., Reganzerowski, A., Tschernig, T., Bellmann, B., Berhard, W., Dorin, J. R., Jansen, S., Porteous, D. J., and Tümmler, B. 1998 *Pseudomonas aeruginosa* infection in cystic fibrosis: animal model of the transgenic *cftr*^{m1HGU} mouse. *22nd European CF conference Berlin Book of Abstracts*, PS7.3; 140

Le Grys, V. A., Burritt, M. F., Gibson, L. E., Hammond, K. B., Kraft, K., and Rosenstein, B. J. 1994 Sweat Testing: Guide to a sample collection and quantitative analysis - approved guide, NCCLS Document C34-A. Villanova, PA: National Committee on Clinical Laboratory Standards; 1-45

Lehrer, R.I. and Ganz, T. 1999 Antimicrobial peptides in mammalian and insect host defence. *Curr. Opin. Immunol.* **11**; 23-27

LeVine, A.-M., Kurak, K. E., Bruno, M. D., Stark, J. M., Whitsett, J. A., and Korfhagen, T. R. 1998 Surfactant protein-A-deficient mice are susceptible to *Pseudomonas aeruginosa* infection. *Am. J. Respir. Cell Mol. Biol.* **19** (4); 700-708

Li, C., Ramjeesingh, M., Reyes, E., Jensen, T., Chang, X., Rommens, J. M., and Bear, C. E. 1993 The cystic fibrosis mutation (ΔF508) does not influence the chloride channel activity of CFTR. *Nat. Genet.* **3**; 311-316

Li, C., Ramjeesingh, M., and Bear, C. E. 1996 Purified cystic fibrosis transmembrane conductance regulator (CFTR) does not function as an ATP channel. *J. Biol. Chem.* **271** (20); 11623-11626

Li, J. D., Dohrman, A. F., Gallup, M., Miyata, S., Gum, J. R., Kim, Y. S., Nadel, J. A., Prince, A., and Basbaum, C. B. 1997 Transcriptional activation of mucin by *Pseudomonas aeruginosa* lipopolysaccharide in the pathogenesis of cystic fibrosis lung disease. *Proc. Natl. Acad. Sci. USA* **94**; 967-972

Liedtke, C. M. 1988 Differentiated properties of rabbit tracheal epithelial cells in primary culture. *Am. J. Physiol.* **255**; C760-770

Linsdell, P., and Hanrahan, J. W. 1998 Glutathione permeability of CFTR. *Am. J. Physiol.* **275**; C323-C326

Linzmeier, R., Ho, C. H., Hoang, B. V., and Ganz, T. 1999 A 450-kb contig of defensin genes on human chromosome 8p23. *Gene* **233**; 205-211

Liu, J. Y., Nettesheim, P., and Randell, S. H. 1994 Growth and differentiation of tracheal epithelial progenitor cells. *Am. J. Physiol.* **266**; L296-L307

Liu, L., Zhao, C., Heng, H. H. Q., and Ganz, T. 1997 the human β-defensin-1 and α-defensins are encoded by adjacent genes: two peptide families with differing disulfide topology share a common ancestry. *Genomics* **43**; 316-320

Liu, L., Wang, W., Jia, H. P., Zhao, C., Heng, H. H. Q., Schutte, B. C., McCray, P. B., and Ganz, T. 1998 Structure and mapping of the human β-defensin-2 HBD-2 gene and its expression at sites of inflammation. *Gene* **222**; 237-244

MacMicking, J. D., Nathan, C., Hom, G., Chartrain, N., Fletcher, D. S., Trumbauer, M., Stevens, K., Xie, Q.-W., Sokol, K., Hutchinson, N., Chen, H., and Mudgett, J. S. 1995 Altered response to bacterial infection and endotoxic shock in mice lacking inducible nitric oxide synthase. *Cell* **81**; 641-650

MacVinish, L. J., Gill, D. R., Hyde, S. C., Mofford, K. A., Evans, M. J., Higgins, C. F., Colledge, W. H., Huang, L., Sorgi, F., Ratcliff, R., Cuthbert, A. W. 1997 Chloride secretion in the trachea of null cystic fibrosis mice: the effects of transfection with pTrial10-CFTR2. *J. Physiol. (Lond.)* **499** (3); 677-687

Mahenthiralingham, E., Coenye, T., Chung, J. W., Speert, D. P., Govan, J. R. W., Taylor, P., and Vandamme, P. 2000 Diagnostically and experimentally useful panel of strains from the *Burkholderia cepacia* complex. *J. Clin. Micro.* **38** (2); 910-913

Mak, V., Jarvi, K. A., Zielenski, J., Durie, P., and Tsui, L.-C. 1997 Higher proportion of intact exon 9 CFTR mRNA in nasal epithelium compared with vas deferens. *Hum. Mol. Genet.* **6**; 2099-2107

Marino, C. R., Matovcik, L. M., Gorelick, F. S., and Cohn, J. A. 1991 localisation of the cystic fibrosis transmembrane conductance regulator in the pancreas. *J. Clin. Invest.* **88**; 712-716

Martin, D. W., Schurr, M. J., Mudd, M. H., Govan, J. R. W., Holloway, B. W., and Deretic, V. 1993 Mechanism of conversion to mucoidy in *Pseudomonas aeruginosa* infecting cystic fibrosis patients. *Proc. Natl. Acad. Sci. USA* **90** (18); 8377-8381

Mathee, K., Ciofu, O., Sternberg, C., Lindum, P. W., Campbell, J. I., Jensen, P., Johnsen, A. H., Givskov, M., Ohman, D. E., Molin, S., Höiby, N., and Kharazmi, A. 1999 Mucoid conversion of *Pseudomonas aeruginosa* by hydrogen peroxide: a mechanism for virulence activation in the cystic fibrosis lung. *Microbiology* **143**; 1349-1357

Matsui, H., Grubb, B. R., Tarran, R., Randell, S. H., Gatzy, J. T., Davis, C. W., and Boucher, R. C. 1998. Evidence for periciliary liquid layer depletion, not abnormal ion composition, in the pathogenesis of cystic fibrosis airways disease. *Cell* **95**; 1005-1015

McCray, P. B., and Bentley, L. 1997 Human airway epithelia express a β-defensin. *Am. J. Respir. Cell Mol. Biol.* **16**; 343-349

McCray, P. B., Zabner, J., Jia, H. P., Welsh, M. J., and Thorne, P. S. 1999 Efficient killing of inhaled bacteria in ΔF508 mice: role of airway surface liquid composition. *Am. J. Physiol.* **277**; L183-L190

McPherson, M. A., Dormer, R. L., Bradbury, N. A., Dodge, J. A., and Goodchild, M. C. 1986 Defective β-adrenergic secretory responses in submandibular acinar cells from cystic fibrosis patients. *Lancet* **2** (8514); 1007-1008

Ménache, M. G., Miller, F. J., and Raabe, O. G. 1995 Particle inhalability curves for humans and small laboratory animals. *Ann. Occup. Hyg.* **39** (3); 317-328

Meng, Q.-H., Springall, D. R., Bishop, A. E., Morgan, K., Evans, T. E., Habib, S., Gruenert, D. C., Gyi, K. M., Hodson, M. E., Yacoub, M., and Polak, J. M. 1998 Lack of inducible nitric oxide synthase in bronchial epithelium: a possible mechanism of susceptibility to infection in cystic fibrosis. *J. Path.* **184**; 323-331

Mercer, R. R., Russell, M. L., Roggli, V. L., and Crapo, J. D. 1994 Cell number and distribution in human and rat airways. *Am. J. Respir. Cell Mol. Biol.*, **10** (6); 613-624

Merrill, M. C., Steagall, W. K., Hazel, M., Gretter, B., Kelley, T. J., and Drumm, M. L. 1998 Comparison and characterisation of four different murine CFTR alleles. *Pediatr. Pulmonol.* (Suppl. 17); 304

Meyrick, B., Sturgess, J., and Reid, L. 1969 Reconstruction of the duct system and secretory tubules of the human bronchial submucosal gland. *Thorax* **24**; 729-736

Mills, C. L., Dorin, J. R., Davidson, D. J., Porteous, D. J., Alton, E. W. F. W., Dormer, R. L., and McPherson, M. A. 1995 Decreased β-adrenergic stimulation of glycoprotein secretion in CF mice submandibular glands: reversal by the methylxanthine, IBMX. *Biochem. Biophys. Res. Commun.* **215**; 674-681

Molin, S., Sternberg, C., Christensen, B. B., Heydorn, A., and Givskov, M. 1999 Determinations of growth and gene activities in microbial biofilms. *Clin. Microbiol. Infect.* **5**; 5S4-5S5

Morrison, G. M., Davidson, D. J., Kilanowski, F. M., Borthwick, D. W., Crook, K., Maxwell, A. I., Govan, J. R. W., and Dorin, J. R. Mouse Beta Defensin-1 is a functional homologue of Human Beta Defensin-1. *Mamm. Genome* **9**; 453-457

Morrison, G. M., Davidson, D. J., Dorin, J. R. 1999a A novel mouse beta defensin, *Defb2*, which is upregulated in the airways by lipopolysaccharide. *FEBS Letters* **442** (1); 112-116

Morrison, G. M. 1999b Analysis of the pulmonary inflammatory phenotype of the CF mutant mouse. University of Edinburgh PhD Thesis

Naren, A. P., Cormet-Boyaka, E., Fu, J., Villain, M., Blalock, J. E., Quick, M. W., Kirk, K. L. 1999 CFTR chloride channel regulation by an interdomain interaction. *Science* **286** (5439); 544-548

National Institutes of health Consensus Development Conference Statement on Genetic Testing for Cystic Fibrosis. 1999 Genetic testing for cystic fibrosis. *Arch. Intern. Med.* **159**; 1529-1539

Nelson, J. W., Tredgett, M. W., Sheehan, J. K., Thornton, J. K., Notman, D., and Govan, J. R. W. 1990 Mucinophilic and chemotactic properties of *Pseudomonas aeruginosa* in relation to pulmonary colonisation in cystic fibrosis. *Infect. Immun.* **58**; 1489-1495

O'Neal, W. K., Hasty, P., McCray, P. B., Casey, B., Riveraperez, J., Welsh, M. J., Beaudet, A. L., and Bradley, A. 1993 A severe phenotype in mice with a duplication of exon 3 in the cystic fibrosis locus. *Hum. Mol. Genet.* **2**; 1561-1569

Oppenheimer, E. H. 1981 Similarity of the tracheobronchial mucous glands and epithelium in infants with and without cystic fibrosis. *Hum. Path.* **12**; 36-48

Oppenheimer, E. H., and Esterly, J. R. 1975 Pathology of cystic fibrosis; review of the literature and comparison with 146 autopsied cases. *Perspect. Pediatr. Pathol.* **2**; 241-278

Orikasa, S, and Hinman, F. 1977 Reaction of the vesical wall to bacterial penetration: resistance to attachment, desquamation, and leukocytic activity. *Invest. Urol.* **15** (3); 185-193

Ornoy, A., Arnon, J., Katznelson, D., Granat, M., Sacpi, B., and Chemke, J. 1987 Pathological confirmation of cystic fibrosis in the foetus following prenatal diagnosis. *Am. J. Med. Genet.* **28**; 935-947

Osika, E., Cavaillon, J.-M., Chadelat, K., Boule, M., Fitting, C., Tournier, G., and Clement, A. 1999 Distinct sputum cytokine profiles in cystic fibrosis and other chronic inflammatory airway disease. *Eur. Respir. J.* **14**; 339-346

Ostedgaard, L. S. and Welsh, M. J. 1992 Partial purification of the cystic fibrosis transmembrane conductance regulator. *J. Biol. Chem.*, **267** (36); 26142-26149

Pack, R. J., Layla, H., Ugaily, A., Morris, G., and Widdicombe, J. G. 1980 The distribution and structure of cells in the tracheal epithelium of the mouse. *Cell Tissue Res.* **208**; 65-84

Pack, R. J., Layla, H., Ugaily, A., and Morris, G. 1981 The cells of the tracheobronchial epithelium of the mouse: a quantitative light and electron microscopic study. *J. Anat.* **132** (1); 71-84

Parad, R. B., Gerard, C. J., Zurakowski, D., Nichols, D. P., and Pier, G. B. Pulmonary outcome in cystic fibrosis is influenced primarily by mucoid *Pseudomonas aeruginosa* infection and immune status and only modestly by genotype. 1999 *Infect. Immun.* **67** (9); 4744-4750

Pier, G. B., Grout, M., Zaidi, T. S., Olsen, J. C., Johnson, L. G., Yankaskas, J. R., and Goldberg, J. B. 1996 Role of mutant CFTR in hypersusceptibility of cystic fibrosis patients to lung infections. *Science* **271**; 64-67

Pier, G. B., Grout, M., and Zaidi, T. S. 1997 Cystic fibrosis transmembrane conductance regulator is an epithelial cell receptor for clearance of *Pseudomonas aeruginosa* from the lung. *Proc. Natl. Acad. Sci. USA* **94**; 12088-12093.

Pier, G. B., Grout, M., Zaidi, T. S., Meluleni, G., Mueschenborn, S. S., Banting, G., Ratcliff, R., Evans, M. J., and Colledge, W. H. 1998 *Salmonella typhi* uses CFTR to enter intestinal epithelial cells. *Nature* **393**; 79-82

Pier, G. B., Cannon, C. L., Stopak, K., Schroeder, T. H., and Zaidi, T. 1999 Role of the cystic fibrosis transmembrane conductance regulator (CFTR) protein in susceptibility and resistance to *Pseudomonas aeruginosa* lung infection. *Clin. Microbiol. Infect.* **5**; 5S22-5S23

Pilewski, J. M., and Frizzell, R. A. 1999 Role of CFTR in airway disease. *Physiol. Rev.* **79** (Suppl. 1); S 215-S255

Porteous, D. J., and Innes, J. A. 1999 Gene therapy for cystic fibrosis. In *Gene Therapy*. (ed. Blankenstein, T.); 137-149

Prince, A. 1999 Pulmonary pathogens activate Ca^{2+}-dependent MAPK expression in respiratory epithelial cells. *Ped. Pulmonol.* (Suppl. 19); 100-101

Puchelle, E., Jacquot, J., Beck, G., Zahm, J.-M., and Galabert, C. 1985 Rheological and transport properties of airway secretions in cystic fibrosis relationships with the degree of infection and severity of the disease. *Eur. J. Clin. Invest* **15**; 389-94

Quinton, P. M. Choride impermeability in cystic fibrosis. 1983 *Nature* **302**; 421-422

Quinton, P.M. 1999 Physiological basis of cystic fibrosis: a historical perspective. *Physiol. Rev.* **79** (Suppl. 1); S3-S22

Raabe, O. G., Al-Bayati, M. A., Teague, S. V., and Rasolt, A. 1988 Regional deposition of inhaled monodisperse coarse and fine aerosol particles in small laboratory animals. *Ann. Occup. Hyg.* **32** (Supplement 1); 53-63

Ramsay, B. W. 1996 Management of pulmonary disease in patients with cystic fibrosis. *New Eng. J. Med.* **355** (3); 179-188

Randell, S. H., Comment, C. E., Ramaekers, F. C. S., and Nettesheim, P. 1991 Properties of rat tracheal epithelial cells separated based on the expression of cell surface α-galactosyl end groups. *Am. J. Respir. Cell Mol. Biol.* **4**; 544-554

Ratcliff, R., Evans, M. J., Cuthbert, A. W., Macvinish, L. J., Foster, D., Anderson, J. R., and Colledge, W. H. 1993 Production of a severe cystic-fibrosis mutation in mice by gene targeting. *Nat. Genet.* **4**; 35-41

Rave-Harel, N., Kerem, E., Nissim-Rafinia, M., Madjar, I., Goshen, R. Augarten, A., Rahat, A., Hurwitz, A., Darvasi, A., and Kerem, B. 1997 The molecular basis of partial penetrance of splicing mutations in cystic fibrosis. *Am. J. Hum. Genet.* **60**; 87-94

Reddy, M. M., Light, M. J., and Quinton, P. M. 1999 Activation of the epithelial Na^+ channel (ENaC) requires CFTR Cl^- channel function. *Nature* **402**; 301-303

Regnis, J. A., Robinson, M., Bailey, D. L., Cook, P., Hooper, P., Chan, H. K., Gonda, I., Bautovich, G., and Bye, P. T. P. 1994 Mucociliary clearance in patients with cystic-fibrosis and in normal subjects. *Am. J. Respir. Crit. Care Med.* **150**; 66-71

Riordan, J. A., Rommens, J. M., Kerem, B. S., Alon, N., Rozmahel, R., Grzelczak, Z., Zielenski, J., Lok, S., Plavsic, N., Chou, J. L., Drumm, M. L., Iannuzzi, M. C., Collins, F. S., and Tsui, L.-C. 1989 Identification of the cystic fibrosis gene – cloning and characterisation of complementary DNA. *Science* **245**; 1066-1072

Robbins, S. L., and Kumar, V. 1987 Genetic Diseases. In *Basic Pathology (4th Edition)*. (ed. Robbins, S. L., and Kumar, V.) W. B. Saunders Company, Philadelphia, P.A.; 106-108

Römling, U., Fiedler, B., Bosshammer, J., Grothues, D., Greipel, J., von der Hardt, H., and Tümmler, B. 1994 Epidemiology of chronic *Pseudomonas aeruginosa* infections in cystic fibrosis. *J. Infect. Dis.* **170**; 1616-1621

Rommens, J. M., Iannuzzi, M. C., Kerem, B., Drumm, M. L., Melmer, G., Dean, M., Rozmahel, R., Cole, J. L., Kennedy, D., Hidaka, N., Zsiga, M., Buchwald, M., Riordan, J. R., Tsui, L.-C., and Collins, F. 1989 Identification of the cystic fibrosis gene: chromosome walking and jumping *Science* **245**:1059-1065

Ross, M. H., and Reith, E. J. 1985 Respiratory system. In *Histology, a text and atlas*. (ed. Ross, M. H., and Reith, E. J.) Harper and Row, J. B. Lippincott Company, New York; 504-527

Rozmahel, R., Wilschanski, M., Matin, A., Plyte, S., Oliver, M., Auerbach, W., Moore, A., Forstner, J., Durie, P., Nadeau, J., Bear, C., and Tsui, L.-C. 1996 Modulation of disease severity in cystic fibrosis transmembrane conductance regulator deficient mice by a secondary genetic factor. *Nat. Genet.* **12**; 280-287

Russell, J. P., Diamond, G., Tarver, A. P., Scanlin, T. F., and Bevins, C. L. 1996 Coordinate induction of two antibiotic genes in tracheal epithelial cells exposed to the inflammatory mediators lipopolysaccharide and tumour necrosis factor α. *Infect. Immun.* **64**; 1565-1568

Saiki, R. K., Gelfand, D. H., Stoffel, S., Scharf, S. J., Higuchi, R., Horn, G. T., Mullis, K. B., and Erlich, H. A. 1988 Primer directed enzymatic amplification of DNA with a thermostable DNA polymerase. *Science* **239** (4839); 487-491

Saiman, L., Cacalano, G., Gruenert, D., and Prince, A. 1992 Comparison of adherence of *Pseudomonas aeruginosa* to respiratory epithelial cells from cystic fibrosis patients and healthy subjects. *Infect. Immun.* **60** (7); 2808-2814

Saiman, L., and Prince, A. 1993 *Pseudomonas aeruginosa* pili bind to asialoGM1 which is increased on the surface of cystic fibrosis epithelial cells. *J. Clin. Invest.* **92**; 1875-1880

Sajjan, U. S., Sun, L., Goldstein, R., and Forstner, J. F. 1995 Cable (*cbl*) type-II pili of cystic fibrosis associated *Burkholderia (Pseudomonas) cepacia* – Nucleotide sequence of the *cbl*A major subunit pilin gene and novel morphology of the assembled appendage fibers. *J. Bacteriol.* **177**; 1030-1038

Sanders, A., and Crystal, R. G. 1997 Consequences to the lung of specific deficiencies in host defence. In *The Lung; Scientific Foundations 2nd Edition.* (ed. Crystal, R. G., West, J. B., Weibel, E. R., and Barnes, P. J.) Lippincott-Raven, New York; 2367-2370

Schnapp, D. and Harris, A. 1998 Antibacterial peptides in bronchoalveolar lavage fluid. *Am. J. Respir. Cell Mol. Biol.* **19**; 352-356

Schwiebert, E. M., Benos, D. J., Egan, M. E., Stutts, M. J., and Guggino, W. B. 1999 CFTR is a conductance regulator as well as a chloride channel. *Phys. Rev.* **79** (Suppl. 1); S145-S166

Seksek, O., Biwersi, J., Verkman, A. S. 1996 Evidence against defective trans-Golgi acidification in cystic fibrosis. *J. Biol. Chem.* **271**(26); 15542-15548

Shelhammer, J. H. 1997 Effects of bacterial products and inflammatory mediators on mucin secretion. *Pediatr. Pulmonol.* (Suppl. 14), 104

Sheppard, D. N., Rich, D. P., Ostedgaard, L. S., Gregory, R. J., Smith, A. E., and Welsh, M. J. 1993 Mutations in *CFTR* associated with mild disease form. *Nature* **362**; 160-164

Sheppard, D. N. and Ostedgaard, L. S. 1996 Understanding how cystic fibrosis mutations cause a loss of Cl^- channel function. *Mol. Med. Today* **2**; 290-297

Sheppard, D. N., and Welsh, M. J. 1999 Structure and function of the CFTR chloride channel. *Phys. Rev.* **79** (Suppl. 1); S23-S45

Shimizu, T., Nettesheim, P., Ramaekers, F. C. S., and Randell, S. H. 1992 Expression of "cell-type-specific" markers during rat tracheal epithelial regeneration. *Am. J. Respir. Cell Mol. Biol.* **7**; 30-41

Simpson, A. J., Maxwell, A. I., Govan, J. R. W., Haslett, C., and Sallenave, J.-M. 1999 Elafin (elastase-specific inhibitor) has anti-microbial activity against gram-positive and gram-negative respiratory pathogens. *FEBS Letters* 452; 309-313

Singh, P., and Welsh, M. J. 1997 Components of airway surface fluid have syngergistic antimicrobial activity. *Pediatr. Pulmonol.* (Suppl. 14); 323

Singh, P. K., Jia, H. P., Wiles, K., Hesselberth, J., Liu, L., Conway, B. A., Greenberg, E. P., Valore, E. V., Welsh, M. J., Ganz, T., Tack, B. F., and McCray, P. B. 1998 Production of beta-defensins by human airway epithelia. *Proc. Natl. Acad. Sci. U S A* **95** (25); 14961-14966

Singh, P. K., Parsek, M. R., Costerton, J. W., Greenberg, E. P., and Welsh, M. J. 1999 *Pseudomonas aeruginosa* biofilms are resistant to killing by airway surface liquid antimicrobial factors. *Pediatr. Pulmonol.* (Suppl. 17), 322

Smit, L. S., Strong, T.V., Wilkinson, D. J., Macek, M. Jr, Mansoura, M. K., Wood, D. L., Cole, J. L., Cutting, G. R., Cohn, J. A., Dawson, D. C., and Collins, F., S. 1995 Missense mutation (G480C) in the CFTR gene associated with protein mislocalization but normal chloride channel activity. *Hum. Mol. Genet.* **4** (2); 269-73

Smith, J. J., Travis, S. M., Greenberg, E. P., and Welsh, M. J. 1996 Cystic fibrosis airway epithelia fail to kill bacteria because of abnormal airway surface fluid. *Cell* **85**; 229-236

Smith, S. N., Alton, E. W. F. W., and Geddes, D. M. 1992 Ion transport characteristics of the murine trachea and caecum. *Clin. Sci.* **82**; 667-672

Smith, S. N., Steel, D. M., Middleton, P. G., Munkonge, F. M., Geddes, D. M., Caplen, N. J., Porteous, D. J., Dorin, J. R., and Alton, E. W. F. W. 1995 Bioelectric characteristics of exon 10 insertional cystic fibrosis mouse: comparison with humans. *Am. J. Physiol.* **268**; C297-C307

Snouwaert, J. N., Brigman, K. K., Latour, A. M., Malouf, N. N., Boucher, R. C., Smithies, O., and Koller, B. H. 1992 An animal model for cystic fibrosis made by gene targeting. *Science* **257**; 1083-1088

Stevenson, M. M., Kondratieva, T. K., Apt, A. S., Tam, M. F., and Skamene, E. 1995 *In vitro* and *in vivo* T cell responses in mice during bronchopulmonary infection with mucoid *Pseudomonas aeruginosa*. *Clin. Exp. Immunol.* **99**; 98-105

Strong, T. V., Boehm, K., and Collins, F. S. 1994 Localisation of cystic fibrosis transmembrane conductance regulator mRNA in the human gastrointestinal tract by *in situ* hybridisation. *J. Clin. Invest.* **93**; 347-354

Sturgess, J. M., and Imrie, J. R. 1981 The development of the exocrine pancreas in cystic fibrosis. In *Approaches to cystic fibrosis.* (ed. Kaiser, D.) Berlin; 175-188

Stutts, M. J., Canessa, C. M., Olsen, J. C., Hamrick, M., Cohn, J. A., Rossier, B. C., and Boucher, R. C. 1995 CFTR as a cAMP-dependent regulator of sodium channels. *Science* **269**; 847-850

Tang, H., Kays, M., and Prince, A. 1995 Role of *Pseudomonas aeruginosa* pili in acute pulmonary infection. *Infect. Immun.* **63**; 1278-1285

Tang, Y.-Q., Yuan, J. Ösapay, G., Ösapay, K.,Tran, D., Miller, C. J., Ouellette, A. J., and Selsted, M. E. 1999 A cyclic antimicrobial peptide produced in primate leukocytes by the ligation of two truncated α-defensins. *Science* **286**; 498-502

Tata, F., Stanier, P., Wicking, C., Halford, S., Kruyer, H., Lench, N. J., Scambler, P. J., Hansen, C., Braman, J. C., Williamson, R., and Wainwright, B. J. 1991 Cloning the mouse homolog of the human cystic-fibrosis transmembrane conductance regulator gene. *Genomics* **10**; 301-307

The Cystic Fibrosis Genotype-Phenotype Consortium. 1993 Correlation between genotype and phenotype in patients with cystic fibrosis. *N. Engl. J. Med.* **329** (18); 1308-1313

Tivier, D., Houdret, N., Courcol, R. J., Lamblin, G., Roussel, P. and Davril, M. 1997 The binding of surface proteins from *Staphylococcus aureus* to human bronchial mucins. *Eur. Respir. J.* **10**; 804-810

Travis, S. M., Forsyth, W. R., Anderson, N. N., Singh, P. K., Jia, H. P., Starner, T. D., Greenberg, E. P., McCray, P. B., Welsh, M. J., and Tack, B. F. 1999a Cathelicidin-derived bactericidal peptides: airway expression and antipseudomonal activity. *Pediatr. Pulmonol.* (Suppl. 19); 260

Travis, S. M., Conway, B.-D. A., Zabner, J., Smith, J. J., Anderson, N. A., Singh, P. K., Greenberg, P., and Welsh, M. J. 1999b Activity of abundant antimicrobials of the human airway. *Am. J. Respir. Cell Mol. Biol.* **20**; 872-879

Trezise, A. E. O., and Buchwald, M. 1991 *In vivo* cell-specific expression of the CFTR. *Nature* **353**; 434-437

Tsui, L.-C., Markiewicz, D., Zielinski, J., Corey, M., and Durie, P. 1992 Mutation analysis in cystic fibrosis. In *Cystic Fibrosis Current Topics.* (ed. Dodge, J. A., Brock, D. J. H., Widdicombe, J. H.) J. Wiley & Sons, Chichester; 27-44

Tümmler, B., and Kiewitz, C. 1999 Cystic Fibrosis: an inherited susceptibility to bacterial respiratory infections. *Mol. Med. Today*. **5**; 351-358

Ulrich, M., Herbert, S., Berger, J., Bellon, G., Louis, D., Münker, G. and Döring, G. 1999 Localisation of *Staphylococcus aureus* in infected airways of

patients with cystic fibrosis and in a cell culture model of *S. aureus* adherence. *Am. J. Respir. Cell Mol. Biol.* **19**; 83-91

Uyekubo, S. N., Fischer, H., Maminishkis, A., Illek, B., Miller, S. S., and Widdicombe, J. H. 1998 cAMP-dependent absorption of chloride across airway epithelium. *Am. J. Physiol.* **275**; L1219-L1227

Valore, E. V., Martin, E., and Ganz, T. 1994 the anionic propiece of HNP-1 is an activation peptide. *Clinical Res.* **42**; 151A

Valore, E. V., Park, C. H., Quayle, A. J., Wiles, K. R., McCray, P. B., and Ganz, T. 1998 Human β-defensin-1: an antimicrobial peptide of the urogenital tissues. *J. Clin. Invest.* **101** (8); 1633-1642

van Doorninck, J. H., French, P. J., Verbeek, E., Peters, R. H. P. C., Morreau, H., Bijman, J., and Scholte, B. J. 1995 A mouse model for the cystic fibrosis delta-F508 mutation. *Embo Journal* **14**; 4403-4411

van Heeckeren, A., Walenga, R., Konstan, M. W., Bonfield, T., Davis, P. B., and Ferkol, T. 1997 Excessive inflammatory response of cystic fibrosis mice to bronchopulmonary infection with *Pseudomonas aeruginosa*. *J. Clin. Invest* **100** (11); 2810-2815

van Heeckeren, A., Bonfield, T., Berger, M., Davis, P. B., and Ferkol, T. 1999 Response to bronchopulmonary infection with *Pseudomonas aeruginosa* in mice heterozygous for the cystic fibrosis transmembrane conductance regulator. *Pediatr. Pulmonol.* (Suppl. 19); 318

van Wetering, S., Sterk, P. J., Rabe, K. F., and Hiemstra, P. S. 1999 Defensins: key players or bystanders in infection, injury and repair in the lung? *J. Allergy Clin. Immunol.* **104** (6); 1131-1138

van Wetering, S., van der Linden, A. C., van Sterkenberg, M. A., de Boer, W. I., Kuijpers, A. L., Schalkwijk, J., and Hiemstra, P. S. 2000 Regulation of SLPI and elafin release from bronchial epithelial cells by neutrophil defensins. *Am. J. Physiol.* **278**; L51-L58

Vandamme, P., Holmes, B., Vancanneyt, M., Coenye, T., Hoste, B., Coopman, R., Revets, H., Lauwers, S., Gillis, M., Kersters, K., and Govan, J. R. W. 1997 Occurrence of multiple genomovars of *Burkholderia cepacia* in cystic fibrosis patients and proposal of a *Burkholderia multivorans* sp. Nov. *Int. J. Syst. Bacteriol.* **47** (4); 1188-1200

Walker J., Watson, J., Holmes, C., Edelman, A., and Banting, G. 1995 Production and characterisation of monoclonal and polyclonal antibodies to different regions of the cystic fibrosis transmembrane conductance regulator (CFTR): detection of immunologically related proteins. *J. Cell Sci.* **108**; 2433-2444

Walter, S., Gudowius, P., Boßhammer, J., Römling, U., Weißbrodt, H., Schürmann, W., von der Hardt, H., and Tümmler, B. 1997 Epidemiology of chronic *Pseudomonas aeruginosa* infections in the airways of lung transplant recipients with cystic fibrosis. *Thorax* **52**; 318-321

Welsh, M. J. 1996 Cystic Fibrosis. In *Molecular biology of membrane transport disorders* (ed. Schultz, S. G.); 605-623

Welsh, M. J. 1999 Gene transfer for cystic fibrosis. *J. Clin. Invest.* **104** (9); 1165-1166

Whitcutt, M. J., Adler, K. B., and Wu, R. 1988 A biphasic chamber system for maintaining polarity of differentiation of cultured respiratory tract epithelial cells. *In Vitro Cell. Dev. Biol.* **24**; 420-428

Whitsett, J. A. 1999 Role of collectins in the modulation of pulmonary host defence and inflammation. *Pediatr. Pulmonol.* (Suppl. 19); 154

Wilschanski, M. A., Rozmahel, R., Beharry, S., Kent, G., Li, C., Tsui, L.-C., Durie, P., and Bear, C. E. 1996 *In vivo* measurements of ion transport in long-living CF mice. *Biochem. Biophys. Res. Comm.* **219**; 753-759

Wilson, C. L., Ouellette, A. J., Satchell, D. P., Ayabe, T., Lopez-Boado, Y. S., Stratman, J. L., Hultgren, S. J., Matrisian, L. M., and Parks, W. C. 1999 Regulation of intestinal alpha-defensin activation by the metalloproteinase matrilysin in innate host defence. *Science* **286** (5437); 113-117

Wine, J. 1999 The genesis of cystic fibrosis lung disease. *J. Clin. Invest.* **103**; 309-312

Yamaya, M., Finkbeiner, W. E., Chun, S. Y., and Widdicombe, J. H. 1992 Differentiated structure and function of cultures from human tracheal epithelium. *Am. J. Physiol.* **262**; L713-L724

Yang, D., Chertov, O., Bykovskaia, S. N., Chen, Q., Buffo, M. J., Shogan, J., Anderson, M., Schroder, J. M., Wang, J. M., Howard, O. M. Z., and Oppenheim, J. J. 1999 β-defensins: linking innate and adaptive immunity through dendritic and T cell CCR6. *Science* **286**; 525-528

Yeates, D. B., Sturgess, J. M., Kahn, S. R., Levison, H., and Aspin, N. 1976 Mucociliary transport in trachea of patients with cystic fibrosis. *Arch. Dis. Child.* **51**; 28-33

Yu, H., Hanes, M., Chrisp, C. E., Boucher, J. C., and Deretic, V. 1998 Microbial pathogenesis in cystic fibrosis: pulmonary clearance of mucoid *Pseudomonas aeruginosa* and inflammation in a mouse model of repeated respiratory challenge. *Infect. Immun.* **66**(1); 280-288

Yu, H., Nasr, S. Z., and Deretic, V. 2000 Innate lung defences and compromised *Pseudomonas aeruginosa* clearance in the malnourished mouse model of respiratory infections in cystic fibrosis. *Infect. Immun.* **68**(4); 2142-2147

Zabner J., Smith, J. J., Karp, P. H., Widdicombe, J. H., and Welsh, M. J. 1998 Loss of CFTR chloride channels alters salt absorption by cystic fibrosis airway epithelia in vitro. *Mol. Cell* **2**; 397-403

Zahm, J. M., Gaillard, D., Dupuit, F., Hinnrasky, J., Porteous, D. J., Dorin, J. R., and Puchelle, E. 1997 Early alterations in airway mucociliary clearance and inflammation of the lamina propria in CF mice. *Am. J. Physiol.* **41**; C853-C859

Zahm, J.-M., Baconnais, S., Davidson, D. J., Webb, S., Bonnet, N., Balossier, G., Dorin, J. and Puchelle, E. 1999 NaCl in airway surface liquid from cystic fibrosis mice is elevated. *Pediatr. Pulmonol.* (Suppl. 19); 221

Zapp, K. G., and Drumm, M. L. Genetic control of nasal epithelial ion transport in mice. *Pediatr. Pulmonol.* (Suppl. 17); 303

Zar, H., Saiman, L., Quittell, L., and Prince, A. 1995 Binding of *Pseudomonas aeruginosa* to respiratory epithelial cells from patients with various mutations in the cystic fibrosis transmembrane regulator. *J. Pediatr.* **126**; 230-233

Zeiher, B. G., Eichwald, E., Zabner, J., Smith, J. J., Puga, A. P., McCray, P. B., Capecchi, M. R., Welsh, M. J., and Thomas, K. R. 1995 A mouse model for the delta-F508 allele of cystic-fibrosis. *J. Clin. Invest.* **96**; 2051-2064

Zeitlin, P. L. 1999 Novel pharmacological therapies for cystic fibrosis. *J. Clin. Invest.* **103** (4); 447-452

Zerhusen, B., Zhao, J., Xie, J., Davis, P. B., and Ma, J. 1999 A single conductance pore for chloride ions formed by two cystic fibrosis transmembrane conductance regulator molecules. *J. Biol. Chem.*, **274** (12); 7627-7630

Zhang, Y. and Engelhardt, J. F. 1999 Airway surface fluid volume and Cl content in cystic fibrosis and normal bronchial xenografts. *Am. J. Physiol.* **276**; C469-C476

Zhao, C., Wang, I., and Lehrer, R. I. 1996 Widespread expression of beta-defensin hBD-1 in human secretory glands and epithelial cells. *FEBS Letters* **396**; 319-322

Zhou, L., Dey, C. R., Wert, S. E., Duvall, M. D., Frizzell, R. A., and Whitsett, J. A. 1994 Correction of lethal intestinal defect in a mouse model of cystic fibrosis by human CFTR. *Science* **266**; 1705-1708

Zielenski, J., Corey, M., Rozmahel, R., Markiewicz, D.,Aznarez, I., Casals, T., Larriba, S., Mercier, B., Cutting, G. R., Krebsova, A., Macek, M., Langfelder-

Schwind, E., Marshall, B. C., DeCelie-Germana, J., Claustres, M., Palacio, A., Bal, J., Nowakowska, A., Ferec, C., Estivill, X., Durie, P., and Tsui, L.-C. 1999 Detection of a cystic fibrosis modifier locus for meconium ileus on human chromosome 19q13. *Nat. Genet.* **22**; 128-129